Technische Universität München
Zentrum Mathematik
Mathematische Modellierung

Modelling quorum sensing evolutionary dynamics in spatially structured bacterial populations

Anne Mund

Vollständiger Abdruck der von der Fakultät für Mathematik der Technischen Universität München zur Erlangung des akademischen Grades eines

Doktors der Naturwissenschaften (Dr. rer. nat.)

genehmigten Dissertation.

Vorsitzender:		Prof. Dr. Johannes Müller
Prüfer der Dissertation:	1.	Univ.-Prof. Dr. Christina Kuttler
	2.	Birmingham Fellow Sara Jabbari, Ph.D. University of Birmingham, UK

Die Dissertation wurde am 01.06.2017 bei der Technischen Universität München eingereicht und durch die Fakultät für Mathematik am 04.09.2017 angenommen.

Abstract

Quorum sensing is a mechanism that guides cooperative group behaviour in bacteria and as such is vulnerable to exploitation by non-cooperative individuals. We employ the G-function ansatz to model evolutionary dynamics in order to find evolutionary stable strategies. We discuss different model differential equations, with a focus on how spatial structure can be taken into account and how it influences the long-term outcome. For all utilized models the existence and uniqueness of solutions are proven. Numerical simulations corroborate the analytical results as well as serving to visualize the arising dynamics. We also performed and present experiments using the bacterium *P. aeruginosa* that investigate these dynamics.

Als Mechanismus zur Steuerung von Gruppenverhalten in Bakterien ist Quorum Sensing anfällig gegenüber Ausbeutung durch nicht kooperierende Individuen. Wir verwenden den G-Funktionsansatz zur Modellierung der evolutionären Kräfte, um evolutionär stabile Strategien zu finden. Mit Fokus auf den Einfluss räumlicher Strukturen und ihrer Langzeitwirkung untersuchen wir unterschiedliche Modellgleichungen und zeigen auch die Existenz und Eindeutigkeit von Lösungen für alle verwendeten Modelle. Numerische Simulationen untermauern die analytischen Erkenntnisse und zeigen die entstehende Dynamik auf, welche ebenfalls in Experimenten mit Bakterien vom Typ *P. aeruginosa* untersucht werden.

Contents

Frequently occuring variables

Variable	Meaning
α	Baseline production rate
b	Amount of bacteria in a population, an n-dimensional vector
b_i	Amount of bacteria in one subpopulation
β	Production rate in induced state
γ	Degradation rate
D	Diffusion rate
e	Quorum sensing enzyme concentration
ε	Time scaling factor for evolution equation
μ	Population-dependent death rate
s	Quorum sensing signal concentration
τ	Activation threshold
v	Strategy vector or matrix of all bacterial subpopulations
v_i	Strategy of one bacterial subpopulation

As humans, we have invented lots of useful kinds of lie. As well as lies-to-children ('as much as they can understand') there are lies-to-bosses ('as much as they need to know') lies-to-patients ('they won't worry about what they don't know') and, for all sorts of reasons, lies-to-ourselves. Lies-to-children is simply a prevalent and necessary kind of lie. Universities are very familiar with bright, qualified school-leavers who arrive and then go into shock on finding that biology or physics isn't quite what they've been taught so far. 'Yes, but you needed to understand that,'they are told, 'so that now we can tell you why it isn't exactly true.'Discworld teachers know this, and use it to demonstrate why universities are truly storehouses of knowledge: students arrive from school confident that they know very nearly everything, and they leave years later certain that they know practically nothing. Where did the knowledge go in the meantime? Into the university, of course, where it is carefully dried and stored.

TERRY PRATCHETT, THE SCIENCE OF DISCWORLD

Chapter 1

Introduction

Bacteria are pervasive and influence our daily lives in a myriad of ways, some beneficial, some detrimental. We use them in sewage treatment and for manufacturing many different chemicals, we carry them in our gut flora and on the skin. At the same time, there are bacterial pathogens that kill millions of people per year. It is imperative that we gain more understanding about the underlying mechanisms of bacterial behaviour, especially with the progressing antibiotics resistance. Mathematical models can help us gain insight into these mechanisms and discern focus points for future experiments.

1.1 Biological Background

For a long time, bacteria were thought to live relatively independent of each other. This viewpoint has changed with the discovery of quorum sensing (QS) in 1977 [HN77]. Nowadays we know that cooperation between bacteria seems to be the rule rather than the exception. One important process to guide such cooperation is QS, a regulation mechanism for group behaviour. It is, among others, employed by *Pseudomonas aeruginosa* (*P. aeruginosa*), an important pathogen and one of the model organisms for QS which we introduce in section 1.1.2.

1.1.1 Quorum sensing

> *The importance of accurate demographic information is reflected in the United States Constitution, Article 1, which provides for a decennial census of this country's human population. Bacteria also conduct a census of their population and do so more frequently, more efficiently, and as far we know, with little if any of the political contentiousness caused by human demographers.* *[FWG96]*

Bacterial QS is a cell-to-cell signalling mechanism that coordinates a range of behaviours at the population level [Sch+13; RB12]. It occurs in a wide range of living conditions, from soil and water (where QS-regulated genes influence nutrient cycling) to animal hosts (where QS-regulated genes determine pathogen virulence).

Figure 1.1 shows the basic mechanism of QS in Gram-negative bacteria by means of the *las* cycle of *P. aeruginosa*. As is the case for most communication systems, it includes a sender, a message, and a receiver. By way of a signal synthase (the "sender", here: LasI), a small signal molecule (the "message", here: N-3-oxo-dodecanoyl-l-homoserine lactone (3-oxo-C12-HSL)) is produced and secreted by the bacterium. For small molecules such as 3-oxo-C12-HSL, this secretion is a passive diffusion through the cell wall. At the same time, signal from the extracellular space is (re-)absorbed by the bacterium. A receptor molecule (the "receiver", here: LasR) is produced that can bind to the intracellular signal. If this happens, the receptor molecule can then bind to operators on the bacterial DNA to allow transcription, thus facilitating the production of proteins on these DNA strands. In this way, every bacterium can sense its own signal molecule as well as that produced by others, leading to the term *autoinducer*. Two of the various proteins under this QS control in *P. aeruginosa* are exemplarily shown in figure 1.1: nucleoside hydrolase (Nuh), a protein which degrades inosine to hypoxanthine plus ribose (this metabolic pathway is shown in greater detail in figure 5.1 on page 97) and elastase, a protein that is secreted into the surrounding media to break down cytokines as well as a number of other substrates. Additionally, a receptor with bound signal molecule also enhances the production of signal synthase, leading to a positive feedback loop [SPI95].

Through the signal molecules bacteria can sense the cell density in the surrounding media, leading to the term quorum sensing [NPH70; FWG94]. As the signal molecule underlies diffusion, some have argued that the bacteria employ it mainly to sense the diffusivity of the media [Red02]. Hense et al. [Hen+07] coined the term *efficiency sensing* for the mixed scenario, where both quorum and diffusion sensing is possible. In both ways, QS helps ensure that bacteria only turn on costly behaviour such as producing and secreting proteins when the cost to benefit ratio is reasonable.

In turn, QS, like any other social behaviour, opens up the possibility of cheaters. It involves two levels of cooperation: at the signalling level as well as on the level of QS-controlled target genes. Both are prone to cheater mutants. In *P. aeruginosa*, *lasI* mutants are unable to produce signal molecules and are thus called signal cheaters, while *lasR* mutants are unable to respond to signal because they lack the receptor molecule and are often called signal blind.

Once any kind of molecule is secreted, it is available to all bacteria in the local environment. For this reason, they are often called public goods (PGs).

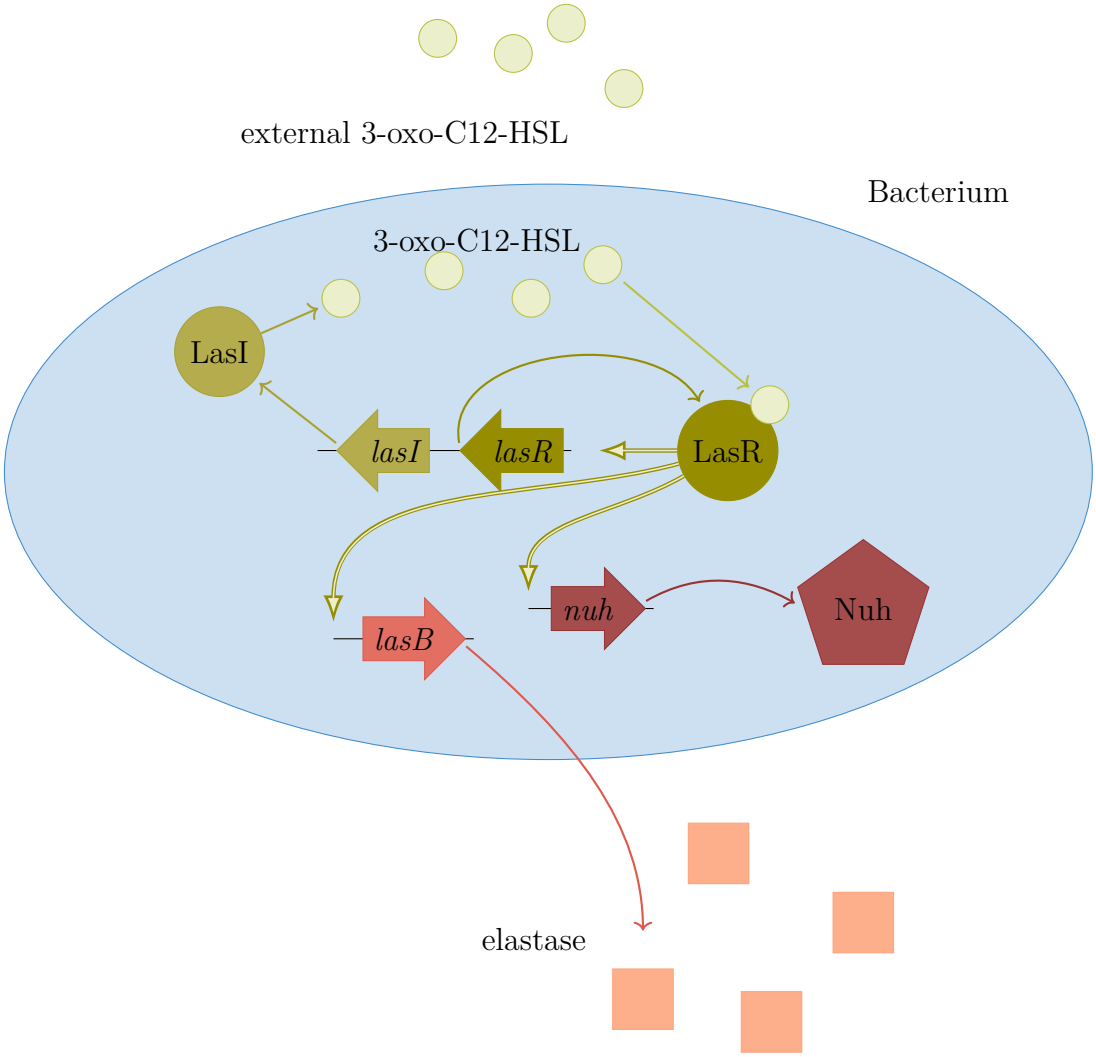

Figure 1.1: Schematic depiction of QS in a bacterial cell, by means of the *las* system of *P. aeruginosa*. Block arrows indicate genes, other shapes transcribed or produced molecules. The two-coloured arrows symbolise the activation through bound receptor molecule.

Cheaters can thus reap the benefits of PG production if a producer is nearby, without paying the associated metabolic costs [BJ01; Dig+07; Rum+09; SMS07]. This serves to destabilise QS in the long term. Once cheaters arise (e.g. through loss-of-function mutation), they should theoretically outgrow the producers as they have more resources available to invest in cell division. Cheaters have been shown to outcompete producers both *in vitro* and *in vivo*, but QS seems to be evolutionary stable in natural systems nevertheless.

Several mechanisms, such as kin selection [BB08] and policing [Wan+15], have been described that could explain the evolutionary stability of cooperation and QS despite the advantages cheaters have in such a system [see e.g. KRG14]. We will take a closer look at two of them: assortment and private goods.

Assortment

Spatial structuring of populations is a fundamental principle allowing for assortment in bacteria. Such separation could serve to stabilise cooperation in combination with population bottlenecks [Bro07]. Spatial structuring can be caused by environmental heterogeneities, but also by self-organisation via bacterial interactions [FR11]. In biofilms, for example, producers and cheaters tend to grow in clusters [NFX10]. Both theoretical and experimental studies [CMF12; CRL09; Mel+10; Rum+12] showed that under certain conditions, cyclic separations of the whole population into small subpopulations and subsequent re-mixing events can protect cooperative behaviour from being completely outcompeted. Even if only parts of the population undergo cyclic separation and growth in colonies, cooperation can remain evolutionary stable [Mun+16].

All in all, it is important to take spatial relations between bacteria into account when modelling QS. We will discuss methods to do so using ordinary differential equations (ODEs) (see chapter 3) as well as modelling spatial coordinates explicitly with partial differential equations (PDEs) (see chapter 4).

Private goods

In contrast to the afore mentioned public goods, private goods are only accessible to the producing cell itself. They are hence innately protected from cheaters and provide their benefit exclusively for cells with a functioning QS system.

Apart from extracellular molecules, QS also controls the production of proteins which act within the cell. In *P. aeruginosa*, one such protein is Nuh. As Nuh is involved in metabolising adenosine, only bacteria with intact signal receptors can digest this carbon source. In this way cooperation via QS provides a private fitness benefit to cooperating cells if adenosine is available as carbon source [DCG12].

But even extracellular molecules do not provide benefit indiscriminately, but

are limited by diffusion and habitat structure. Kümmerli et al. [Küm+14] found a negative correlation between habitat structure and water solubility of siderophores, a class of secreted enzymes under QS control in a wide range of bacteria. For highly structured environments such as animal tissues, water solubility of siderophores is high, while microstructures in the environment naturally limit the resulting diffusion. Conversely, water solubility of siderophores is low in unstructured environments such as water habitats. This leads to siderophores clinging to each other as well as to lipid membranes. In this way a fraction of the siderophores stay with their producer (see also figure 2.5) and provide some private benefit. As *P. aeruginosa* is found in freshwater and soil as well as hosts, Kümmerli et al. [Küm+14] rank its habitat structure as average (3.3 on a scale of 1 to 5). Following this line of thought, one can consider every PG to have both a private and a public benefit.

For the QS signal a similar mechanism has been proposed. Given that signal synthesis as well as binding to the receptor both happen within the cell, the binding strength of the receptor and the diffusivity of the membrane (amongst other factors) regulate the degree of self– versus neighbour sensing [FS13; YL14; MY15]. A low receptor binding strength paired with high diffusivity will favour secretion (and subsequent absorption) of signal, while a cell membrane with low diffusion coefficient will favour intracellular aggregation of signal molecules (see also figure 2.6). Consequently, we can think of the QS signal as having a private and a public part. We will come back to this hypothesis in section 2.2.3.

All in all, when we develop a mathematical model of QS in the following, we need to take both levels of cooperation into account. In order to keep the model at a manageable size regardless, we will make some modelling simplifications on the complex process of QS.

We can make a quasi steady state assumption for the concentration of signal synthase if we assume that its production is on a slower time scale than the subsequent production of signal molecules themselves. This can be rationalised if one notes that signal synthase is the product of a lengthy translational and transciptional process, while signal molecules are relatively small and assembled by one enzymatic reaction. Indeed, it has been verified experimentally that concentration of signal synthase and signal itself is approximately proportional (e.g., in the *las* system of *P. aeruginosa* by Duan and Surette [DS07]). Hence we can focus only on signal quantity when modelling later on, omitting the intermediate step of producing the signal synthase LasI. In a similar fashion, we will leave out the process of transcription and translation as well as the synthases for QS controlled proteins.

1.1.2 *Pseudomonas aeruginosa*

P. aeruginosa is an opportunistic human pathogen that causes serious illnesses in immunocompromised hosts, especially in individuals with cystic fibrosis or

traumatic burn wounds. It is Gram-negative, rod-shaped and found in many different habitats, from soil to animal or plant hosts [Red].

Of particular importance for clinical applications are its intrinsically low antibiotic susceptibility [Poo04] as well as its ability to form enduring biofilms [HCB10]. Both make it a bacterium commonly found in hospitals and on medical equipment. *P. aeruginosa* infection of immunocompromised hosts often leads to potentially fatal infections - Horino et al. [Hor+12] give a 30-day mortality rate of 20.9 %. While exact numbers vary from study to study, it is a problem not to be underestimated.

In addition to its low intrinsic antibiotic susceptibility, *P. aeruginosa* can also rapidly develop new resistances to multiple classes of antibacterials, even during therapy, mostly through plasmid acquisition or mutation [LWH09]. For all of these reasons one is looking for alternative ways to treat *P. aeruginosa* infections. One such way could be through the QS system. Many virulence factors in *P. aeruginosa* are under control of QS, including for example the well-studied iron-scavenging siderophores [WB03]. As such, QS is fundamental for the success of *P. aeruginosa* infections. This has been confirmed by studies in mice, with mice infected by QS-mutant strains having a lower mortality rate [Rum+09].

Brown et al. [Bro+09] make some suggestions on how one could go about using mutant strains to reduce virulence. Besides using QS-deficient mutants directly, other methods include *quorum quenching* to disrupt the QS ability of wild-type bacteria [Sio+06]. But all of these methods rely on the ability of cheating strains to outcompete wild-type producers. It is thus of great interest to gain a better understanding of the relations between producing and non-producing bacteria and the evolutionary pressures that they underlie in order to better estimate the chances and risks of these kind of therapies.

Up until now, studies have found four different QS systems in *P. aeruginosa*, called the *las*, *rhl*, *Pseudomonas quorum sensing (pqs)* and *integrated quorum sensing (iqs)* system [WDS11; Lee+13]. Their respective signal molecules are shown in figure 1.2.

We will focus on the *las* system of *P. aeruginosa*, as it is one of its two main QS systems, the other being the *rhl* system. In fact, the *rhl* and *las* system have a hierarchical structure, with the *las* system dominating [PPI97].

For a more comprehensive review of the QS mechanisms of *P. aeruginosa* as well as its response to antibiotics, see Rasamiravaka and El Jaziri [REJ16] and the references therein.

1.2 Mathematical modelling

Mathematical models are very versatile tools that have been used to analyse data, understand biological concepts and to predict behaviour. The exact mathematical

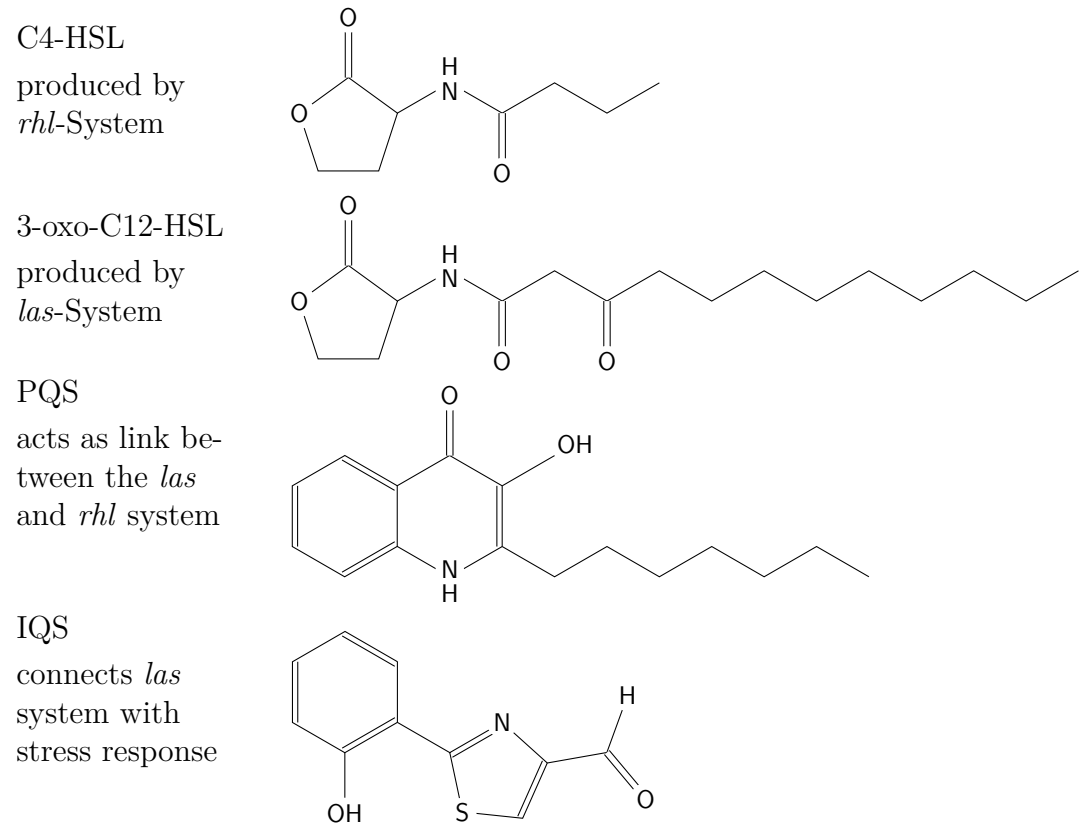

Figure 1.2: Chemical structure of QS molecules of *P. aeruginosa* [WDS11; Lee+13].

tools involved vary as much as the purpose.

1.2.1 Modelling approaches for population growth

Maybe the most fundamental class of models for population growth is the discrete population model

$$N_{t+1} = f(N_t),$$

with a function $f : \mathbb{R}_+ \to \mathbb{R}_+$, where N_t signifies the amount of individuals at time $t \in \mathbb{N}$. Discrete population models are well-suited for populations with a common generation time such as insect life cycles [see e.g. EK04]. In the case of bacteria, cells will divide continuously. A model with continuous time is therefore better suited.

Ordinary differential equations (ODEs) are the classical way to include such a continuous time scale. In general, a first-order ODE model for one population reads

$$\frac{\mathrm{d}N(t)}{\mathrm{d}t} = f\Big(t, N(t)\Big),$$

where N again signifies the amount or density of individuals at time $t \in \mathbb{R}_+$. One concrete example is the Verhulst equation

$$\frac{\mathrm{d}N(t)}{\mathrm{d}t} = rN(t)\left(1 - \frac{N(t)}{K}\right).$$

It was first introduced by Pierre-François Verhulst, but rediscovered by McKendrick and Pai [MP12], who used the equation in order to model the population dynamics of bacteria in test tubes. The two occurring parameters are r, the intrinsic growth rate, and K, the so-called carrying capacity. The carrying capacity is the maximal number of individuals that can survive in the population. A higher number of individuals than K cannot be sustained by the environment. The exact reasons vary dependent on the biological background of the model, but can include a limited abundance of food or space as well as accumulation of toxins. By defining $\mu := \frac{r}{K}$ we can reformulate the Verhulst equation to

$$\frac{\mathrm{d}N(t)}{\mathrm{d}t} = N(t)\left(r - \mu N(t)\right).$$

In this version, instead of a capacity K, one has a population-dependent death rate $\mu N(t)$. Like the capacity, it models the natural limit of the population size, shifting focus towards the rivalry for resources between individuals.

If two populations are considered (or the population consists of two subpopulations), this rivalry can be modelled more explicitly. One example that arises from the Verhulst equation are Lotka-Volterra-type equations:

$$\frac{\mathrm{d}N_1(t)}{\mathrm{d}t} = r_1 N_1(t)\left(1 - \frac{N_1(t) + \alpha_{12}N_2(t)}{K_1}\right),$$
$$\frac{\mathrm{d}N_2(t)}{\mathrm{d}t} = r_2 N_2(t)\left(1 - \frac{N_2(t) + \alpha_{21}N_1(t)}{K_2}\right).$$

In addition to the afore mentioned growth rate and carrying capacity we consider α_{ij}, the interaction coefficient between species i and j. If $\alpha_{ij} > 0$, population j has a negative impact on population i, e.g. through competition or predation. Conversely, if $\alpha_{ij} < 0$, population j has a positive impact on population i. Thus if α_{ij} and $\alpha_{ji} < 0$, the populations have a mutually beneficial relationship. Cooperator-cheater interactions are marked by $\alpha_{ij} < 0$, $\alpha_{ji} > 0$ if j is the cooperator subpopulation. For n (sub-)populations, the model reads

$$\frac{\mathrm{d}N_i(t)}{\mathrm{d}t} = r_i N_i(t)\left(1 - \frac{\sum_{j=1}^{n} \alpha_{ij}N_j(t)}{K_i}\right),$$

where we define $\alpha_{ii} = 1$. ODEs such as these have been used in modelling QS cooperator–cheat relationships in the past [Fra10].

When modelling with ODEs, one usually assumes a homogeneous population. Spatial inhomogeneities in a population are not directly reflected in such a model, as there is only one independent variable (the time t) and the equation is independent of spatial variables. If explicit spatial dependence is needed, one can use partial differential equations (PDEs) to also gain continuous space dimensions. The general form of a second-order PDE for one population is

$$\frac{\partial N(t,x)}{\partial t} = f\left(t, x, N(t,x), \frac{\partial N(t,x)}{\partial x_i}, \frac{\partial^2 N(t,x)}{\partial x_{ij}^2}\right),$$

where x denotes the spatial coordinates and ∂x_{ij} the derivatives with respect to the different coordinates of x. Chopp et al. [Cho+02] used such a model for the *las* system of *P. aeruginosa* and its influence on biofilm growth, while Koerber et al. [Koe+02] employed it in the context of burn wound infection. Jabbari, King, and Williams [JKW12], on the other hand, modelled interaction between two bacterial strains via a combination of ODEs and PDEs.

Both ODE and PDE models will be discussed later on, in chapter 3 and chapter 4, respectively. Apart from them, there are many more viable modelling approaches, such as partial integro-differential equations [BJ01], graph-based modelling [PK15] and individual-based modelling [CMF12; GBDM14]. For a more in-depth review of the history of mathematical models for QS, the reader is referred to Pérez-Velázquez, Gölgeli, and García-Contreras [PVGGC16].

1.2.2 Modelling approaches for evolution

As mentioned in section 1.1.2, *P. aeruginosa* has the ability to gain immunity to antimicrobials even during an ongoing therapy. This means that we can see evolution already on short time scales. It is thus imperative that one takes mutations and evolutionary pressure into consideration when modelling growth of *P. aeruginosa*.

There are several ways one can model evolution. One important method is the use of *adaptive dynamics*, a method developed by Geritz et al. [Ger+97], which is introduced nicely in Brännström, Johansson, and Festenberg [BJF13]. In its basic form, it assumes two populations, a resident population N_r and a mutant population N_m. We can write down the population dynamics as before, using a formulation with population-dependent death rate instead of explicit capacity:

$$\begin{aligned}\frac{\mathrm{d}N_r(t)}{\mathrm{d}t} &= N_r(t)\left(r_r - \mu\left(N_r(t) + N_m(t)\right)\right),\\ \frac{\mathrm{d}N_m(t)}{\mathrm{d}t} &= N_m(t)\left(r_m - \mu\left(N_r(t) + N_m(t)\right)\right).\end{aligned}$$

The particular idea of adaptive dynamics is to assume that mutants are so rare initially ($N_m \ll N_r$), that we can assume $N_r + N_m = N_r$ and N_r itself to be at its equilibrium value ($N_r = {}^{r_r}/_{\mu}$). We call the growth of the rare mutant an *invasion* of the resident population. The outcome of such an invasion is dependent on the reproductive success of the mutant, also called its *fitness*. One can then define invasion fitness $s_r(m)$ of a mutant to be its per capita growth rate:

$$s_r(m) = \frac{{}^{\mathrm{d}N_m(t)}/_{\mathrm{d}t}}{N_m(t)} = r_m - \mu N_r(t) = r_m - r_r.$$

It is imperative that the mutant population size N_m does not appear in this expression, since we just assumed that it is negligibly small. It must also hold that $s_r(r) = 0$, signifying that the resident population cannot invade itself. We can then find the selection gradient as the derivative of $s_r(m)$ with respect to m. In our simple example, it would hold that $s_r'(m) = 1$, and thus the trait would evolve to ever increasing values. For (realistic) natural systems, there is always some kind of trade-off that prevents such explosions and one can find values of $\bar{r}$ for which $s_{\bar{r}}'(\bar{r}) = 0$. Such values for $\bar{r}$, or strategies, are called evolutionary singular strategies and can be divided into fitness minima and fitness maxima (and a third degenerate case, a saddle point, which is without biological significance). As the name already suggests, strategies in a fitness maximum maximise the fitness of the population and as such are evolutionary stable, while evolutionary branching can occur in fitness minima.

One generalisation of adaptive dynamics is the idea of G-functions, where one defines a general growth function for all populations that depends directly on the

trait value of that population. This allows one to consider the evolution of an arbitrary number of populations as well as their population dynamics simultaneously. It will be discussed in depth in chapter 2.

The slightly different approach of Cohen and Galiano [CG13] employs methods of PDEs by considering the trait, or strategy, of a population as another continuous independent variable next to t. If we denote the strategy value by v, one could for example write

$$\partial_t N(v,t) = r\left(N(v,t) + \frac{\varepsilon^2}{2}\partial_{vv}N(v,t)\right) - s\left(N(v,t),v\right)N(v,t).$$

The function s embodies the natural selection in this scenario while ε gives a measure of the mutation rate. Additionally, the equation must be supplemented with biologically meaningful boundary conditions.

Again, the models shown here are but a few in a wide range of possibilities. Depending on the nature of the population model considered, different ways to depict evolution are appropriate.

1.2.3 Evolutionary stable strategies and equilibria

The terms evolutionary stable strategy (ESS) and evolutionary stable equilibrium (ESE) are essential to dealing with evolving populations. While we will define them mathematically later on, the concepts can also be expressed in a biological context. To that end, we use the definitions coined by Smith [Smi82] and Vincent, Van, and Goh [VVG96]:

> An ESS is a strategy such that, if all members of a population adopt it, then no mutant strategy could invade the population under the influence of natural selection.

> Individuals in a biological community will be at an ESE if fixing the strategies used by the individuals results in stable population densities subject to perturbations in those densities.

Thus, an ESS is stable with respect to changes in *strategy* values, while an ESE is stable with respect to (small) perturbations in *population* densities.

Additionally, there might also be unstable equilibria. Eventually, small stochastic variances will drive the biological systems from these points. In the case of strategy values, we call such a process *divergent evolution*, or *speciation* [Met+95].

1.3 Overview

This thesis is structured as follows: We will start out by taking a detailed look at the G-function ansatz in chapter 2 and describing different functional terms that represent different biological assumptions and theories. Both versions, with and without abiotic components, are considered with regards to their long-term behaviour.

Chapters 3 and 4 analyse a number of frameworks that allow us to consider the role of both time and spatial distribution in QS. While chapter 3 focuses on ODEs and different ways to introduce spatial dependence therein, chapter 4 introduces several different PDE systems. Existence and uniqueness of solutions are considered for all introduced PDE systems, as well as their asymptotic behaviour.

Before comparing all of these frameworks in chapter 6, we show some experimental results for *P. aeruginosa* in chapter 5. In order to explain the evolutionary stability of QS, experiments have traditionally focussed on signal-blind cheaters [WDS11; Pop+12; Pol+14], but Ruparell et al. [Rup+16] and Keller and Surette [KS06] have shown that there is also a metabolic cost associated with the production of QS signals. We provide experimental proof that *lasI* mutants indeed show cheating behaviour whose pay-off depends on the diffusivity of the environment.

The data from these experiments is used to set parameters for numerical simulations in chapter 6. Apart from replicating experimental results, we compare both different G-functions introduced in chapter 2 as well as different equation systems from chapters 3 and 4 before summarising the results in chapter 7.

Chapter 2

G-Function

The basic idea of the G-functions as introduced by [CVB99] is to define a *growth function* G for a population b, which can then be universally applied to all individuals or groups b_i within this population. In order to do that, one defines a *strategy* v_i for every group b_i. The strategy can describe any behaviour of interest, assigning a real-valued number to it. It might also be vector-valued if one is looking at multiple behavioural rules. Examples for strategies include diverse behaviour such as number of offspring, habitat choice, and time of nesting for birds. How exactly the mapping of biological observations to scalar representation is done depends on the context of the particular problem.

In the context of quorum sensing, we will be looking at *signalling strength* v_i^s and *response strength* v_i^e of a subpopulation of bacteria. This means $v_i = (v_i^s, v_i^e)^T \in \mathbb{R}^2$ is a measure for the cooperativeness of a bacterial subpopulation. In the presented context, we will assume a normalised value of 0 to indicate no participation and a value of 1 to be normal wild-type level cooperation.

In order to derive equations from these fundamental principles, we start out with a very basic population model describing the population growth of a population b_i reproducing with a constant growth rate G:

$$\dot{b}_i(t) = G \cdot b_i(t). \tag{2.0.1}$$

This equation should hold for all subpopulations $b_i, i \in \{1, \ldots, n\}$ that make up the total population considered, b. b is thus the vector of all subpopulations, i.e. $b(t) \in \mathbb{R}^n$. Similarly, we define v to be the matrix of all strategy values, such that if $v_i(t) \in \mathbb{R}^m$, $v(t) \in \mathbb{R}^{n \times m}$. G remains the same for all subpopulations as per assumption.

It is quite clear that such an equation with a constant G cannot properly model the population dynamics at hand. We proceed to recognise that the growth rate G of a subpopulation will be mainly influenced by three factors: its own strategy v_i,

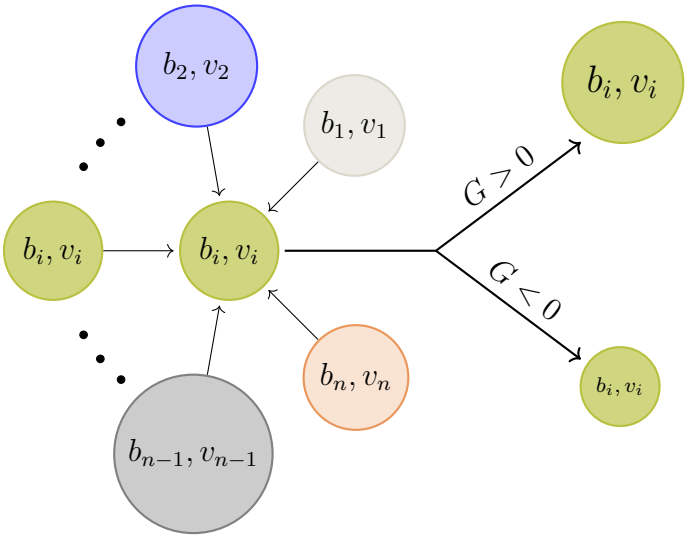

Figure 2.1: Schematic representation of influences on the growth rate of a population.

the environment defined by the complete strategy set v and the whole population b (see figure 2.1).

It follows that G should be a function dependent on v_i, v and b, so equation (2.0.1) can more accurately be written as

$$\dot{b_i}(t) = G(v_i(t), v(t), b(t)) \cdot b_i(t). \tag{2.0.2}$$

In this way, G can be interpreted as the per-capita-growth. Following the arguments in [VCB93], we assume that the strategy distribution remains approximately Gaussian and the variance is small [Bul+80]. Then for scalar strategies the strategy v_i of subpopulation b_i changes according to

$$\dot{v_i}(t) = \varepsilon \frac{\partial}{\partial u} G(u, v(t), b(t))|_{u=v_i(t)}. \tag{2.0.3}$$

We can interpret this as a move in strategy towards higher per-capita-growth. This move happens on a slower time scale than the population dynamics, $\varepsilon \ll 1$. This time scale difference actually depends on the heritability coefficient h and the genetic variance σ^2, such that $\varepsilon = h\sigma^2$.

An equivalent equation holds true for vector-valued strategies $v_i \in R^m$:

$$\begin{pmatrix} \dot{v}_i^1(t) \\ \vdots \\ \dot{v}_i^m(t) \end{pmatrix} = \varepsilon \begin{pmatrix} \frac{\partial}{\partial u_1} G\Big((u_1(t), \ldots, u_n(t)), v(t), b(t)\Big)|_{u=v_i(t)} \\ \vdots \\ \frac{\partial}{\partial u_m} G\Big((u_1(t), \ldots, u_n(t)), v(t), b(t)\Big)|_{u=v_i(t)}. \end{pmatrix} \tag{2.0.4}$$

In order to simplify notation, we will use equation (2.0.3) for scalar as well as vector-valued strategies, as well as write ∂_1 to signify derivation with respect to the first argument of a function. We then get a system of equations describing both the population and strategy dynamics.

$$\dot{b_i}(t) = G(v_i(t), v(t), b(t)) \cdot b_i(t) \tag{2.0.5a}$$
$$\dot{v_i}(t) = \varepsilon \partial_1 G(v_i(t), v(t), b(t)) \tag{2.0.5b}$$

With this framework, we can define the following necessary conditions for an evolutionary stable equilibrium (ESE) (v^*, b^*):

$$\left.\begin{aligned} G(v_i^*, v^*, b^*) &= 0 \\ \partial_1 G(v_i^*, v^*, b^*) &= 0 \\ \partial_1^2 G(v_i^*, v^*, b^*) &\leq 0 \end{aligned}\right\} \quad \forall v_i^* \in \{v_i^* | b_i^* \neq 0\} \tag{2.0.6}$$

Essentially, we require the population to be in equilibrium with respect to population dynamics. This can be achieved either through $G(v_i^*, v^*, b^*) = 0$ or $b_i^* = 0$. If $b_i^* = 0$, the subpopulation has died out, hence the associated strategy dynamic can be disregarded. If $b_i^* \neq 0$, there needs to be equilibrium with respect to strategy dynamics as well, resulting in the second equation of (2.0.6). The third equation is a necessary condition on the derivative of G for there to be a *fitness maximum* at the ESE — a minimum would lead to divergent evolution [CVB99]. As usual, a strict inequality would be a sufficient condition for a (fitness) maximum and therefore for an ESE.

2.1 Assumptions

From here onwards, we will assume some basic properties of the G-function. All of these are of biological relevance.

2.1.1 General assumptions on G

We make some regularity assumptions on G and its derivative in order to simplify mathematical analysis later on. These do not restrict the possibilities for biological applications, as most model growth functions do not include discontinuous behaviour and are smooth.

(I) $G(v_i, v, b)$ is Lipschitz continuous in all variables.

(II) $\partial_1 G(v_i, v, b)$ is Lipschitz continuous in $(v, b)^T$.

Additionally, we make some assumptions on G from the biological background.

(III) $G(v_i, v, b)$ has a (direct or indirect) negative feedback loop in b_i.

(IV) $\exists\, \overline{u} : \partial_1 G(v_i, v, b) \leq 0 \quad \forall v_i > \overline{u}$.

(V) $\exists\, \underline{u} < \overline{u} : \partial_1 G(\underline{u}, v, b) = 0$.

If one of these assumptions is violated, equation (2.0.5) will exhibit divergent behaviour ($v \to \infty$ and/or $b \to \infty$), which is not biologically plausible. If e.g. $\partial_1 G(v_i, v, b) \geq \gamma > 0\ \forall v_i$, then $c + \lambda t$ with $\lambda = \gamma \cdot \varepsilon$ is a lower solution of equation (2.0.5b), as

$$\varepsilon \partial_1 G(\lambda t + c, v, b) - \lambda \geq 0.$$

It follows that $v_i \geq c + \lambda t$ and thus $v_i \to \infty$. This would mean ever-increasing strategy values without some kind of trade-off, which we do not find in nature.

In the special case of quorum sensing (QS), we will take $\underline{u}$ to be 0, requiring $\partial_1 G(0, v, b) = 0$. This keeps v from leaving the biologically meaningful parameter-range $\mathbb{R}_0^+$ (production cannot be lower than 0).

In assumption (I) we only require Lipschitz continuity of $G(v_i, v, b)$, but the right-hand side of equation (2.0.5a) consists of $G(v_i, v, b) \cdot b_i$. We thus prove a small lemma that guarantees the Lipschitz continuity of the whole right-hand side.

Lemma 2.1. *If $G(v_i, v, b)$ is a Lipschitz continuous function in (v, b) and $(v, b) \in V \times B$ with B a bounded set, then $G(v_i, v, b) \cdot b_i$ is a Lipschitz continuous function in (v, b).*

Proof. We set K_i as the Lipschitz constant of $G(v_i, v, b)$ and take two vectors $(\overline{v}, \overline{b})$ and $(\underline{v}, \underline{b}) \in V \times B$.

$$\begin{aligned}
&\|G(\overline{v}_i, \overline{v}, \overline{b}) \cdot \overline{b}_i - G(\underline{v}_i, \underline{v}, \underline{b}) \cdot \underline{b}_i\| \\
&\qquad = \left\|G(\overline{v}_i, \overline{v}, \overline{b}) \cdot \overline{b}_i - G(\overline{v}_i, \overline{v}, \overline{b}) \cdot \underline{b}_i + G(\overline{v}_i, \overline{v}, \overline{b}) \cdot \underline{b}_i - G(\underline{v}_i, \underline{v}, \underline{b}) \cdot \underline{b}_i\right\| \\
&\qquad \leq \left\|G(\overline{v}_i, \overline{v}, \overline{b})\right\| \cdot \left\|\overline{b}_i - \underline{b}_i\right\| + \left\|G(\overline{v}_i, \overline{v}, \overline{b}) - G(\underline{v}_i, \underline{v}, \underline{b})\right\| \cdot \|\underline{b}_i\| \\
&\qquad \leq \left\|G(\overline{v}_i, \overline{v}, \overline{b})\right\| \cdot \left\|\overline{b}_i - \underline{b}_i\right\| + K_i \left\|\begin{pmatrix}\overline{b}\\ \overline{v}\end{pmatrix} - \begin{pmatrix}\underline{b}\\ \underline{v}\end{pmatrix}\right\| \cdot \|\underline{b}_i\| \\
&\qquad \leq \left\|G(\overline{v}_i, \overline{v}, \overline{b})\right\| \cdot \left\|\begin{pmatrix}\overline{b}\\ \overline{v}\end{pmatrix} - \begin{pmatrix}\underline{b}\\ \underline{v}\end{pmatrix}\right\| + K_i \left\|\begin{pmatrix}\overline{b}\\ \overline{v}\end{pmatrix} - \begin{pmatrix}\underline{b}\\ \underline{v}\end{pmatrix}\right\| \cdot \|\underline{b}_i\| \\
&\qquad = \left(\left\|G(\overline{v}_i, \overline{v}, \overline{b})\right\| + K_i \cdot \|\underline{b}_i\|\right) \cdot \left\|\begin{pmatrix}\overline{b}\\ \overline{v}\end{pmatrix} - \begin{pmatrix}\underline{b}\\ \underline{v}\end{pmatrix}\right\|
\end{aligned}$$

This shows that $G(v_i, v, b) \cdot b_i$ is Lipschitz continuous with (maximal) Lipschitz constant $G_{\max} + K_i \cdot \sup_{b \in B} \|b\|$. □

2.1.2 Dividing G into growth and benefit terms

In order to model the G-function for QS, one of the avenues we can take is to divide the impact of v_i, v, and b into two parts: a growth term influenced by v_i and a benefit provided by v, b, and possibly also v_i. This reflects the fact that production of QS molecules is costly to the individual, while the resulting factors are public goods (PGs) and therefore provide benefit to all bacteria. The additional dependence on v_i can be seen as a form of private benefit and will be discussed in detail when it occurs.

Growth term

One important thing to note is that the growth term is actually *reduced* with rising v_i, as increased PG production incurs increased metabolic costs. In this way, less energy is retained for reproduction. We denote the term by $C : \mathbb{R}^2 \to \mathbb{R}_+$, and make the following assumptions:

1. As PG production is costly, C is strictly monotonically decreasing in v_i^s and v_i^e in the positive quadrant.

2. When producing PGs, the growth rate is reduced by a certain factor,

$$0 < C(v_i) < 1 \quad \text{for } v_i \neq (0,0), \qquad C(0,0) = 1. \tag{2.1.1}$$

3. Producing signal is less expensive than responding,

$$\partial_1 C(v_i^s, v_i^e) < \partial_2 C(v_i^s, v_i^e) \text{ if } v_i^s = v_i^e. \tag{2.1.2}$$

While the first item is clear from our assumptions on QS, the other two are not as immediately clear. We introduce equation (2.1.1) because we will use this factor multiplicatively for G. Thus a value of 1 would signify unimpeded growth, while a value between 0 and 1 reduces growth. In this way, we assume that QS costs alone do not lead to negative growth rates. Inequality (2.1.2) incorporates the biological assumption that signalling is less expensive than actually producing the QS-controlled proteins. If both are produced equally, changing signal production has less impact on the growth rate than changing signal response has. Note that this need not hold for unequal production values.

One term that has all required properties and will be used whenever a more detailed view of G is required would be

$$C(v_i) = \exp\left(-K_e(v_i^e)^2 - K_s(v_i^s)^2\right), \tag{2.1.3}$$

with $K_e > K_s$ being the costs for production. We use quadratic terms instead of linear ones to emphasise the self-enhancing aspect of QS.

Benefit term

The benefit of QS is provided by secreting extracellular proteins. We denote it by $B : \mathbb{R}^{m\times 2} \times \mathbb{R}^m \to \mathbb{R}_+$ and make two main assumptions here:

1. There is a limit to how much benefit can be obtained,

$$\lim_{v_s, v_e \to \infty} B(v, b) = B_{\max}. \tag{2.1.4}$$

2. There is no benefit if no PGs are produced,

$$B(v, b) = 0, \quad \text{if } b = 0, \sum_i b_i v_{i_s} = 0 \text{ or } \sum_i b_i v_{i_e} = 0. \tag{2.1.5}$$

Equation (2.1.4) models a saturation behaviour for the benefit — even if the cells were producing an infinite amount of extracellular protein, the benefit that can be derived is still capped through saturation of enzymes or similar phenomena. Equation (2.1.5) ensures that there is no benefit from QS when there are no living bacteria, or all of them have stopped either signalling or responding to signal, as PGs are only produced when there is both signalling and responding happening (though not necessarily by the same subpopulation).

A similar thought spawns the idea that v_i^s and v_i^e could be coupled in a multiplicative way, giving the most benefit when both are roughly equal as opposed to overproduction in one part of QS while neglecting the other. In order to calculate how much the bacteria benefit through the production, we compare the total amount produced ($\sum_i b_i v_{i_s}$ or $\sum_i b_i v_{i_e}$, respectively) with the total amount of bacteria in the population ($\sum_i b_i$). Hill terms of order 2 then ensure that the terms are bounded from above as well as below and exhibit a sharp increase around the threshold parameter, which we set to half the total amount of bacteria. As such, a first idea for a benefit term could be

$$B(v, b) = B_{\max} \cdot \frac{(\sum_i b_i v_i^s)^2}{(\sum_i b_i v_i^s)^2 + (\frac{1}{2}\sum_i b_i)^2} \cdot \frac{(\sum_i b_i v_i^e)^2}{(\sum_i b_i v_i^e)^2 + (\frac{1}{2}\sum_i b_i)^2}.$$

Note that this term does not satisfy assumption (2.1.5). In order to see this, set $b = \varepsilon\vec{1}$. The term then simplifies to

$$\begin{aligned} B(v, b) &= B_{\max} \cdot \frac{(\varepsilon \sum_i v_i^s)^2}{(\varepsilon \sum_i v_i^s)^2 + (\frac{1}{2}\varepsilon n)^2} \cdot \frac{(\varepsilon \sum_i v_i^e)^2}{(\varepsilon \sum_i v_i^e)^2 + (\frac{1}{2}\varepsilon n)^2} \\ &= B_{\max} \cdot \frac{(\sum_i v_i^s)^2}{(\sum_i v_i^s)^2 + (\frac{1}{2}n)^2} \cdot \frac{(\sum_i v_i^e)^2}{(\sum_i v_i^e)^2 + (\frac{1}{2}n)^2}, \end{aligned}$$

which is unequal to zero even if $\varepsilon \to 0$. This is due to the fact that the amount of enzyme or signal production needed scales with the total amount of bacteria in the population. Such a scaling makes sense, as a large population needs more enzymes to derive the same benefit per individual. But a proportional scaling such as this means that an infinitely small population needs an infinitely small amount of producers, which does not hold from experiments.

Stepping back to the biological problem, we recognise that there are two main ways in which a population loses QS-factors, namely decay and diffusion. While the decay rate stays the same for small and large populations, the loss of molecules through diffusion is governed by the ratio of surface area to volume. This means large populations lose proportionally fewer molecules through diffusion, as surface area increases more slowly than volume. This effect is what keeps small populations from immediately gaining full QS benefit, even if all of them are cooperating.

We can adjust the proposed term by exchanging $(\frac{1}{2}\sum_i b_i)^2$ for a term that grows on a slower scale. One possibility is to use $(\frac{1}{2})^2 \sum_i b_i$, or, to be more flexible, $\tau \sum_i b_i$. This gives an example term as

$$B(v,b) = \begin{cases} B_{\max} \cdot \dfrac{(\sum_i b_i v_i^s)^2}{(\sum_i b_i v_i^s)^2 + \tau \sum_i b_i} \cdot \dfrac{(\sum_i b_i v_i^e)^2}{(\sum_i b_i v_i^e)^2 + \tau \sum_i b_i} & \text{if } \sum_i b_i \neq 0 \\ 0 & \text{if } \sum_i b_i = 0 \end{cases} \tag{2.1.6}$$

We take another look at the limit behaviour of this term. We can prove the following:

Theorem 2.2. *The benefit term defined in equation* (2.1.6) *exhibits the following properties:*

1. $0 \leq B(v,b) \leq B_{\max}$.

2. $B(v,b)$ *is differentiable in* b *and* v.

3. $\lim\limits_{|v|\to 0} B(v,b) = 0$.

4. $\lim\limits_{|v|\to\infty} B(v,b) = B_{\max}$, *if* $\exists j,k : b_j, b_k \neq 0, v_j^s, v_k^e \to \infty$.

5. $\lim\limits_{|b|\to\infty} B(v,b) = c$,

where c *is any number between 0 and* $B_{\max}$. *Indeed, for every such* c *there exist* v *and a sequence* $(b_k)_{k\in\mathbb{N}}$ *with* $|b_k| \to \infty$ *s.t.* $B(v,b_k) \to c$ *for* $k \to \infty$.

Proof. Properties 1, 3 and 4 are trivial. For property 2 we first show that $B(v,b)$ is continuous at $b=0$. We take $\overline{v} := \max_{i=1,\dots,n}\{v_i^s, v_i^e\}$ for an arbitrary but fixed v. It holds that

$$\frac{(\sum_i b_i v_i^s)^2}{(\sum_i b_i v_i^s)^2 + \tau \sum_i b_i} \leq \frac{(\sum_i b_i \overline{v})^2}{\tau \sum_i b_i} = \frac{\overline{v}^2 (\sum_i b_i)^2}{\tau \sum_i b_i} = \frac{\overline{v}^2}{\tau} \cdot \sum_i b_i.$$

The right-hand side now clearly converges to 0 as $|b| \to 0$. At the same time, the original term is non-negative as $b_i \geq 0 \quad \forall i$. It follows that

$$\lim_{|b|\to 0} \frac{(\sum_i b_i v_i^s)^2}{(\sum_i b_i v_i^s)^2 + \tau \sum_i b_i} = 0. \tag{2.1.7}$$

The same statement can be derived for v_i^e. That proves the continuity for b and fulfils our original assumption (2.1.5). $B(v,b)$ is clearly continuous as well as differentiable in v, so it only remains to prove that $B(v,b)$ is differentiable in b. We will prove that $\partial_{b_j} B(v,b)$ exists for all $j \in \{1,\dots,n\}$ and that these partial derivatives are continuous.

$$\partial_{b_j}\left(\frac{(\sum_i b_i v_i^s)^2}{(\sum_i b_i v_i^s)^2 + \tau \sum_i b_i}\right) = \frac{(\sum_i b_i v_i^s)\tau\left(2v_j^s \sum_i b_i - \sum_i b_i v_i^s\right)}{\left((\sum_i b_i v_i^s)^2 + \tau \sum_i b_i\right)^2}$$

An equivalent statement holds for the v_i^e-term. This leads to

$$\begin{aligned}\partial_{b_j} B(v,b) = {} & B_{\max} \cdot \frac{(\sum_i b_i v_i^s)^2}{(\sum_i b_i v_i^s)^2 + \tau \sum_i b_i} \cdot \frac{(\sum_i b_i v_i^e)\tau\left(2v_j^e \sum_i b_i - \sum_i b_i v_i^e\right)}{\left((\sum_i b_i v_i^e)^2 + \tau \sum_i b_i\right)^2} \\ & + B_{\max} \cdot \frac{(\sum_i b_i v_i^e)^2}{(\sum_i b_i v_i^e)^2 + \tau \sum_i b_i} \cdot \frac{(\sum_i b_i v_i^s)\tau\left(2v_j^s \sum_i b_i - \sum_i b_i v_i^s\right)}{\left((\sum_i b_i v_i^s)^2 + \tau \sum_i b_i\right)^2}\end{aligned}$$

We already know from equation (2.1.7), that part of the summands will tend to zero. It remains to show that the other fraction does not go to infinity.

$$\begin{aligned}\frac{(\sum_i b_i v_i^e)\tau\left(2v_j^e \sum_i b_i - \sum_i b_i v_i^e\right)}{\left((\sum_i b_i v_i^e)^2 + \tau \sum_i b_i\right)^2} &\leq \frac{(\sum_i b_i \overline{v})\tau 2v_j^e \sum_i b_i}{\left(\tau \sum_i b_i\right)^2} \\ &= \frac{\overline{v}(\sum_i b_i)^2 \tau 2v_j^e}{\tau^2 \left(\sum_i b_i\right)^2} \\ &= \frac{\overline{v}}{\tau} \cdot 2v_j^e,\end{aligned}$$

and also

$$\begin{aligned}\frac{(\sum_i b_i v_i^e)\tau\left(2v_j^e\sum_i b_i - \sum_i b_i v_i^e\right)}{\left((\sum_i b_i v_i^e)^2 + \tau\sum_i b_i\right)^2} &\geq \frac{(\sum_i b_i\overline{v})\tau\left(-\sum_i b_i\overline{v}\right)}{\left(\tau\sum_i b_i\right)^2}\\ &= \frac{-\overline{v}^2(\sum_i b_i)^2\tau}{\tau^2\left(\sum_i b_i\right)^2}\\ &= \frac{-\overline{v}^2}{\tau}.\end{aligned}$$

This fraction is therefore bounded from above by a constant. As it is also bounded from below, we can conclude (after a similar calculation for v_i^s) that

$$\lim_{|b|\to 0}\partial_{b_j}B(v,b) = 0 \quad \forall j \in \{1,\dots,n\},$$

which in turn shows the continuity of all partial derivatives in 0.

For property 5 we first look at the cases $c = 0$ or $B_{\max}$. We can take $b_1 \to \infty$ and $b_i = 0$ for $i = 2,\dots,n$ to make things simpler. If $v_1 = 0$, e.g. $v_1^s = v_1^e = 0$ we get $B(v,b) = 0$ and thus $\lim_{|b|\to\infty} B(v,b) = 0$. Taking $v_1 = 1$, on the other hand, results in

$$\begin{aligned}B(v,b)(v,b) &= B_{\max}\cdot\frac{(b_1\cdot 1)^2}{(b_1\cdot 1)^2+\tau b_1}\cdot\frac{(b_1\cdot 1)^2}{(b_1\cdot 1)^2+\tau b_1}\\ &= B_{\max}\left(\frac{1}{1+\frac{\tau}{b_1}}\right)^2\\ &\to B_{\max}.\end{aligned}$$

For a limit of $0 < c < B_{\max}$, set $b_2 = Cb_1^2, b_i = 0\,\forall i > 2$ as well as $v_1 = 1, v_2 = 0$.

$$\begin{aligned}B(v,b)(v,b) &= B_{\max}\cdot\frac{b_1^2}{b_1^2+\tau(b_1+b_2)}\cdot\frac{b_1^2}{b_1^2+\tau(b_1+b_2)}\\ &= B_{\max}\cdot\left(\frac{b_1^2}{b_1^2+\tau Cb_1^2+\tau b_1)}\right)^2\\ &= B_{\max}\left(\frac{1}{1+C+\frac{\tau}{b_1}}\right)^2\\ &\to B_{\max}\left(\frac{1}{1+C}\right)^2.\end{aligned}$$

A short calculation now shows that for a limit of c, we need to set $C = \frac{1-\sqrt{c/B_{\max}}}{\tau\sqrt{c/B_{\max}}}$. This term is positive and well-defined, as $0 < c < B_{\max}$.

□

This gives us a good idea of what behaviour we can expect from $B(v, b)$. While it fulfils all assumptions made so far, it is not monotone in b, and indeed can not be from our requirements. That makes the QS-model a mixed competition/mutualism model.

Note that we will add the minimal growth rate $B_{\min}$ the bacteria experience in the absence of QS to the benefit for ease of writing later on. Additionally, we will sometimes write $\|b\|_1$ instead of $\sum_i b_i$.

2.2 Different G-Function versions

Now that we have some preliminary ideas about general behaviour that the G-function should exhibit for our kind of application, we will look more closely upon some modelling possibilities.

2.2.1 G-Function without abiotic components

Models without abiotic components infer benefit directly from the exhibited strategies, as opposed to explicitly modelling signal and enzymes involved. As such, they are more compact than their counterparts, but also more abstract.

Public Benefit only: $\boldsymbol{G(v_i, v, b) = B(v, b) \cdot C(v_i) - \mu\|b\|_1}$

This basic model builds on the assumption that PG production is costly to the individual, thus modifying growth by a multiplicative factor $C(v_i)$ which fulfils the assumption proposed in section 2.1.2. At the same time, the total amount of PGs produced depends on the strategies and population densities of all subpopulations, v and b. Thus, the benefit B depends on these quantities. Additionally, there is a competition term μ, limiting the total amount of bacteria that can exist at one place. As such, the term for G is

$$G(v_i, v, b) = B(v, b) \cdot C(v_i) - \mu\|b\|_1. \tag{2.2.1}$$

For a formulation with carrying capacity instead of population-dependent death rate, we can transform this equation to

$$G(v_i, v, b) = B(v, b)C(v_i)\left(1 - \frac{\mu\|b\|_1}{B(v, b)C(v_i)}\right), \tag{2.2.2}$$

which gives us $\frac{B(v,b)C(v_i)}{\mu}$ as the capacity for the population. We can now look at the derivative of G with respect to v_i. Here, we will for a moment assume scalar v_i for ease of notation.

$$\partial_1 G(v_i, v, b) = B(v, b) \cdot C'(v_i). \tag{2.2.3}$$

We know from section 2.1.2 that $C(v_i)$ is strictly monotonically decreasing for positive v_i. Together with the assumptions made in section 2.1 we have $C'(v_i) < 0 \, \forall v_i > 0$, $C'(0) = 0$ and there exists only $v_i = 0$ as an evolutionary stable strategy (ESS).

Private Benefit: $\boldsymbol{G(v_i, v, b) = (B(v, b) + B(v_i)) \cdot C(v_i) - \mu \|b\|_1}$

This idea is based on the *private goods*-hypothesis explained in 1.1.1, that there is a private benefit associated with producing the PGs, e.g. a small percentage of the produced enzymes may cling to the producing bacteria. We will model this by adding a term $B(v_i)$, that means a benefit term that is solely dependent on the strategy of the subpopulation itself. This $B(v_i)$ should fulfil similar assumptions to those we made of $B(v, b)$, which is why we choose the same letter to denote it. All in all, we can write for G:

$$G(v_i, v, b) = (B(v, b) + B(v_i)) \cdot C(v_i) - \mu \|b\|_1. \tag{2.2.4}$$

Again, we can choose to write this equation with a capacity term instead of a population-dependent death rate, if we so wish. The derivative of G can be calculated as

$$\partial_1 G(v_i, v, b) = (B(v, b) + B(v_i)) \cdot C'(v_i) + B'(v_i) \cdot C(v_i), \tag{2.2.5}$$

hence for an ESS it must hold that

$$-C'(v_i) \, (B(v, b) + B(v_i)) = B'(v_i) C(v_i). \tag{2.2.6}$$

The left-hand-side of this equation has a value of 0 for $v_i = 0$, whereas the right-hand-side has a value ≥ 0 for $v_i = 0$. That means there could be any number of stable strategies (or none).

In order to get a better idea of the behaviour, we will use the growth function we proposed at the end of section 2.1.2 in equation (2.1.3). Again, we will assume scalar v_i for ease of notation, simplifying the term to $C(v_i) = \exp(-K v_i^2)$. Plugging this into (2.2.6) leads to the equation

$$\begin{aligned} 2K v_i \exp\left(-K v_i^2\right) (B(v, b) + B(v_i)) &= B'(v_i) \exp\left(-K v_i^2\right) \\ 2K v_i \, (B(v, b) + B(v_i)) &= B'(v_i) \end{aligned} \tag{2.2.7}$$

with the second derivative

$$\begin{aligned} \partial_1^2 G(v_i, v, b) = \mathrm{e}^{-K v_i^2} \Big(& (B(v, b) + B(v_i)) \left(-2K + 4K^2 v_i^2\right) \\ & + 2B'(v_i)(-2K) v_i + B''(v_i) \Big). \end{aligned} \tag{2.2.8}$$

General discussion First we observe that if $B'(0) = 0$, then $\bar{v}_i = 0$ will be a stationary solution. Before we discuss the existence of further positive solutions, we take a look at the stability of the zero solution, keeping in mind that $B(0) = 0$:

$$\partial_1^2 G(0, v, b) = -2KB(v, b) + B''(0).$$

It follows that $\bar{v}_i = 0$ is an ESS if

$$B''(0) < 2KB(v, b). \tag{2.2.9}$$

In the following, we continue to assume that $B'(0) = 0$. Then a positive solution exists if we can solve

$$(B(v, b) + B(\bar{v}_i))\,(2K) = \frac{B'(\bar{v}_i)}{\bar{v}_i}. \tag{2.2.10}$$

We know that the left hand side is monotonically increasing and for many interesting cases (e.g. both concrete examples below as well as all concave functions satisfying $B(0) = 0, B(\infty) = \bar{B} > 0$) the right hand side is monotonically decreasing (a potential $B(v_i)$ where this is not the case is discussed in section 2.2.1 later on). We also know that $B(v_i)$ should exhibit a saturation for $v_i \to \infty$, forcing

$$\lim_{v_i \to \infty} \frac{B'(v_i)}{v_i} = 0. \tag{2.2.11}$$

We take a look at the limiting values at 0:

$$\lim_{v_i \to 0} (B(v, b) + B(v_i))\,(2K) = 2KB(v, b) =: B_0,$$
$$\lim_{v_i \to 0} \frac{B'(v_i)}{v_i} \overset{l'H.}{=} \lim_{v_i \to 0} B''(v_i) = B''(0).$$

So for the cases with monotonically decreasing right hand side, there exists a positive stationary $\bar{v}_i$ if and only if $B''(0) > 2KB(v, b)$ (see also figure 2.2), which corresponds nicely with the stability of the zero solution.

If we take $B'(0)$ to be non-zero, there will always exist exactly one equilibrium solution, which is positive. This results from the same arguments as above, with the noted difference that

$$\lim_{v_i \to 0} \frac{B'(v_i)}{v_i} = +\infty,$$

due to $B'(0) > 0$. If $B'(0)$ were negative, the assumption of $B(v_i) \geq 0$ for $v_i > 0$ would be violated.

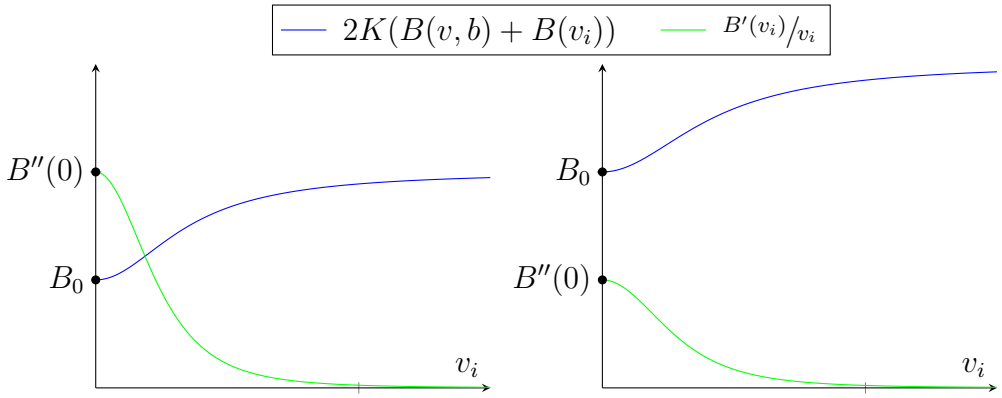

(a) $B''(0) > 2KB(v,b)$ (b) $B''(0) < 2KB(v,b)$

Figure 2.2: Graphical representation of the argument for the existence or non-existence of positive equilibrium points v_i.

Last but not least, we take a look at the stability of this positive equilibrium. Dividing equation (2.2.8) by $e^{-Kv_i^2}$, we have a stable equilibrium if

$$0 > (B(v,b)+B(\bar{v}_i))\left(-2K+4K^2\bar{v}_i^2\right)+2B'(\bar{v}_i)(-2K)\bar{v}_i+B''(\bar{v}_i).$$

We know that for $\bar{v}_i$ equation (2.2.7) must hold, leading to

$$\begin{aligned} 0 &> \frac{B'(\bar{v}_i)}{2K\bar{v}_i}\left(-2K+4K^2\bar{v}_i^2\right)+2B'(\bar{v}_i)(-2K)\bar{v}_i+B''(\bar{v}_i) \\ &= -\frac{B'(\bar{v}_i)}{\bar{v}_i}-2K\bar{v}_iB'(\bar{v}_i)+B''(\bar{v}_i) \\ &= -\left(\frac{1}{\bar{v}_i}+2K\bar{v}_i\right)B'(\bar{v}_i)+B''(\bar{v}_i). \end{aligned} \tag{2.2.12}$$

We can immediately conclude that equation (2.2.12) holds for all concave $B(v_i)$, as $B'(v_i) > 0$ as discussed before, while $B''(v_i) < 0$.

$\boldsymbol{B(v_i) = \frac{v_i^2}{v_i^2+a^2}}$ This term is quite close to the proposed term of $B(v,b)$ (equation (2.1.6)), with the difference that the value at which the strategy has half its maximum effect is now fixed to a constant a. In contrast to the situation for PGs, the private good is always just used by one bacteria, so there is no increased threshold.

In order to take a closer look at the behaviour, we first calculate the derivatives:

$$B'(v_i) = \frac{2v_ia^2}{(v_i^2+a^2)^2}, \qquad B''(v_i) = \frac{2a^4-6a^2v_i^2}{(v_i^2+a^2)^3}.$$

We note that

$$\frac{B'(v_i)}{v_i} = \frac{2a^2}{(v_i^2 + a^2)^2}$$

is a monotonically decreasing function, so we can reuse all observations made before about existence and stability of stationary solutions. In order to get a better idea of just where the positive equilibrium will be, we plug $B'(v_i)$ into equation (2.2.7) and simplify:

$$2Kv_i\left(B(v,b) + \frac{v_i^2}{v_i^2 + a^2}\right) = \frac{2v_i a^2}{\left(v_i^2 + a^2\right)^2}$$
$$2Kv_i^5(B(v,b)+1) + 2Kv_i^3a^2(2B(v,b)+1) + 2Ka^4v_iB(v,b) = 2v_ia^2.$$

So one possible solution is $v_i = 0$, as expected. Dividing by v_i allows us to keep on looking for non-zero solutions

$$2Kv_i^4(B(v,b)+1) + 2Kv_i^2a^2(2B(v,b)+1) + 2Ka^4B(v,b) - 2a^2 = 0. \quad (2.2.13)$$

The last equation is bi-quadratic, so we take $w := v_i^2$ and solve for w:

$$\begin{aligned} w_{1/2} &= \frac{-2Ka^2(2B(v,b)+1) \pm \sqrt{D}}{4K(1+B(v,b))} \\ D &= 4K^2a^2\left(a^2(2B(v,b)+1)^2 - 2(1+B(v,b))\cdot 2(a^2B(v,b) - \frac{1}{K})\right) \\ &= 4K^2a^2\left(a^2 + \frac{4}{K} + \frac{4B(v,b)}{K}\right) \\ &> 0. \end{aligned}$$

That means there will be real solutions for w; one of them will be negative, the sign of the other is still to be determined. It would be positive, if

$$\begin{aligned} 2Ka\sqrt{a^2 + \frac{4}{K} + \frac{4B(v,b)}{K}} &> 2Ka^2(2B(v,b)+1) \\ a^2 + \frac{4}{K} + \frac{4B(v,b)}{K} &> a^2(4B(v,b)^2 + 4B(v,b) + 1) \\ 1 + B(v,b) &> Ka^2B(v,b)(B(v,b)+1) \\ 1 &> Ka^2B(v,b). \end{aligned} \quad (2.2.14)$$

So only under condition (2.2.14) do we get a positive solution for w, and in turn two real solutions for v_i, one of which will be positive. All in all, if $1 > Ka^2B(v,b)$, there will be two stationary solutions for v_i: 0 and a $\bar{v}_i > 0$. This result corresponds

nicely to the results in the last paragraph, as $B''(0) = 2/a^2$. The next step is to take a look at the stability of these strategies, e.g. $\partial_1^2 G(v_i, v, b)$. We already know from equation (2.2.9) that $\bar{v}_i = 0$ will be stable if

$$\begin{aligned} & B''(0) < 2KB(v,b) \\ \Rightarrow \quad & \frac{2a^4}{a^6} < 2KB(v,b), \end{aligned}$$

which is fulfilled, if $1 < Ka^2B(v,b)$ and violated, if $1 > Ka^2B(v,b)$. So $\bar{v}_i = 0$ is an ESS only as long as the parameter constellation does not allow for a positive stationary solution. For the calculation for $\bar{v}_i > 0$ we recall equation (2.2.8).

$$\begin{aligned} \partial_1^2 G(v_i, v, b) = \mathrm{e}^{-Kv_i^2} \Big(& (B(v,b) + B(v_i)) \left(-2K + 4K^2 v_i^2\right) \\ & + 2B'(v_i)(-2K)v_i + B''(v_i) \Big). \\ = \Big(& \frac{\bar{v}_i^2}{\bar{v}_i^2 + a^2}(-2K + 4K^2\bar{v}_i^2) + 2\frac{2\bar{v}_i a^2}{(\bar{v}_i^2 + a^2)^2}(-2K)\bar{v}_i \\ & + \frac{2a^2(\bar{v}_i^2 + a^2) - 8a^2\bar{v}_i^2}{(\bar{v}_i^2 + a^2)^3} + B(v,b)(4K^2\bar{v}_i^2 - 2K) \Big) \mathrm{e}^{-K\bar{v}_i^2}. \end{aligned}$$

As we want the stability in a stationary point, we can directly use equation (2.2.12):

$$0 > -\frac{2a^2}{(\bar{v}_i + a^2)^2} - 2K\frac{2\bar{v}_i^2 a^2}{(\bar{v}_i + a^2)^2} + \frac{2a^4 - 6a^2\bar{v}_i^2}{(\bar{v}_i + a^2)^3}.$$

We can multiply this equation by $(\bar{v}_i + a^2)^3$ without change of sign

$$\begin{aligned} 0 &> -2a^2(\bar{v}_i^2 + a^2) - 4K\bar{v}_i^2 a^2(\bar{v}_i^2 + a^2) + 2a^4 - 6a^2\bar{v}_i^2 \\ &= -2a^2\bar{v}_i^2 - 2a^4 - 4K\bar{v}_i^4 a^2 - 4K\bar{v}_i^2 a^4 + 2a^4 - 6a^2\bar{v}_i^2 \\ &= -8a^2\bar{v}_i^2 - 4K\bar{v}_i^4 a^2 - 4K\bar{v}_i^2 a^4 \\ &= -4\bar{v}_i^2 a^2(K\bar{v}_i^2 + Ka^2 + 2). \end{aligned}$$

So $\bar{v}_i$ is stable for all possible parameter values (as long as it exists, i.e. $\bar{v}_i \in \mathbb{R}$).

$B(v_i) = -\mathrm{e}^{-\omega v_i^2} + 1$ Another way to achieve the desired behaviour with a completely different function is to use the exponential function. The parameter ω can be seen as a measure for the benefit of the strategy — the higher ω, the more benefit is gained from the same strategy. Again, we calculate the derivatives:

$$B'(v_i) = 2\omega v_i \mathrm{e}^{-\omega v_i^2}, \qquad B''(v_i) = 2\omega \mathrm{e}^{-\omega v_i^2} - 4\omega^2 v_i^2 \mathrm{e}^{-\omega v_i^2}.$$

Like before, we note that

$$\frac{B'(v_i)}{v_i} = 2\omega \mathrm{e}^{-\omega v_i^2}$$

is a monotonically decreasing function. We calculate the stationary solutions by plugging $B'(v_i)$ into equation (2.2.7) and simplifying.

$$\begin{aligned} (2Kv_i)(B(v,b) - \mathrm{e}^{-\omega v_i^2} + 1) &= 2\omega v_i \mathrm{e}^{-\omega v_i^2} \\ \Rightarrow \qquad \bar{v}_i = 0 \qquad \vee \qquad \bar{v}_i^2 &= \ln\left(\frac{K(B(v,b)+1)}{K+\omega}\right) \cdot \left(-\frac{1}{\omega}\right). \end{aligned} \tag{2.2.15}$$

The second term produces positive solutions if and only if $KB(v,b) < \omega$, which corresponds to equation (2.2.9) and also gives a condition for the stability of $\bar{v}_i = 0$. We can use equation (2.2.12) to check the stability of the positive solution.

$$\begin{aligned} 0 &> -\left(\frac{1}{\bar{v}_i} + 2K\bar{v}_i\right) 2\omega \bar{v}_i \mathrm{e}^{-\omega \bar{v}_i^2} + 2\omega \mathrm{e}^{-\omega \bar{v}_i^2} - 4\omega^2 \bar{v}_i^2 \mathrm{e}^{-\omega \bar{v}_i^2} \\ 0 &> -4\omega \bar{v}_i^2 (K+\omega) \mathrm{e}^{-\omega \bar{v}_i^2} \end{aligned}$$

Like in the last paragraph we can see that 0 is stable as long as no positive stationary solution exists ($KB(v,b) > \omega$) and unstable afterwards. The positive stationary solution $\bar{v}_i$ is stable if it exists (i.e. $\bar{v}_i \in \mathbb{R}$).

$\boldsymbol{B(v_i) = \frac{v_i^h}{v_i^h + a^h}}$ We have already discussed two special cases of this general term: for $h = 1$, $B(v_i)$ is a concave function for which all the results from the general discussion hold. The case $h = 2$ was also analysed before. Thus, we want to focus on $h \geq 3$ from here on. We start out by recalling the derivatives of this general Hill function.

$$B'(v_i) = \frac{h a^h v_i^{h-1}}{(v_i^h + a^h)^2}, \qquad B''(v_i) = \frac{h a^h v_i^{h-2} \left(-(h+1)v_i^h + (h-1)a^h\right)}{(v_i^h + a^h)^3}.$$

So now we want to take a look at the long-time behaviour of v_i for $h \geq 3$. We can reuse some of our prior observations and state that since $B'(0) = 0$, $v_i = 0$ is a

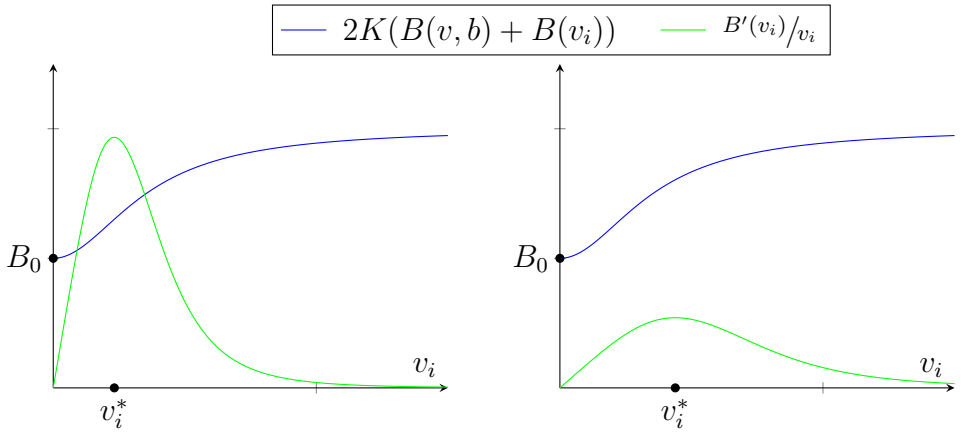

(a) $R(v_i^*) > 2K\Big(B(v,b) + B(v_i^*)\Big)$ (b) $R(v_i^*) < 2K\Big(B(v,b) + B(v_i^*)\Big)$

Figure 2.3: Graphical representation of the argument for the existence or non-existence of positive equilibria points v_i if $B_0 > 0$.

candidate ESS. If we are looking for positive solutions, the important thing to note is that the right-hand side of equation (2.2.10) is not monotonically decreasing for $h \geq 3$.

$$R(v_i) := \frac{B'(v_i)}{v_i} = \frac{ha^h v_i^{h-2}}{(v_i^h + a^h)^2} \tag{2.2.16}$$

Instead, $R(v_i)$ has the following properties:

1. $R(0) = 0$.
2. $\lim\limits_{v_i \to \infty} R(v_i) = 0$.
3. $R(v_i) \geq 0 \quad \forall v_i \geq 0$, with $R(v_i) > 0$ if $v_i > 0$.
4. $R(v_i)$ has exactly one maximum.
5. $R^{(n)}(v_i) = \frac{v_i^{h-(n+2)} f(v_i)}{(v_i^h + a^h)^{n+2}}$ for $n \leq h-2$, with a function $f(v_i)$ for which $f(0) > 0$.

A sample plot of the resulting shape of $R(v_i)$ is given in figure 2.3. While the first items are easy to see from equation (2.2.16), we will prove that $R(v_i)$ has exactly one maximum as well as calculate its maximal value. To that end, we take

the derivative of R

$$R'(v_i) = \frac{a^h h v_i^{h-3}\left(-(h+2)v_i^h + (h-2)a^h\right)}{\left(v_i^h + a^h\right)^3} \tag{2.2.17}$$

and search for critical points

$$0 = a^h h v_i^{h-3}\left(-(h+2)v_i^h + (h-2)a^h\right). \tag{2.2.18}$$

For $h > 3$ there exists a critical point at $v_i = 0$. But, since $R(0) = 0$ and $R(v_i) > 0$ for $v_i > 0$, this critical point is clearly a minimum on the bounded space $v_i \in \mathbb{R}_0^+$. The other critical point satisfies

$$v_i^* = \sqrt[h]{\frac{h-2}{h+2}} \cdot a$$

and is thus unique in $\mathbb{R}_0^+$. It remains to show that v_i^* is indeed a maximum. But knowing that $R(0) = 0$ and $\lim_{v_i \to \infty} R(v_i) = 0$, we can conclude that it can only be a maximum.

We assume for a moment that $B(v, b) > 0$. If we can now show that $R(v_i^*) > 2K(B(v, b) + B(v_i^*))$, two positive stationary solutions v_i to equation (2.2.6) exist. We have

$$R(v_i^*) = \frac{h \cdot \left(\frac{h-2}{h+2}\right)^{\frac{h-2}{h}}}{a^2 \cdot \left(\frac{2h}{h+2}\right)^2}, \qquad B(v_i^*) = \frac{h-2}{2h}.$$

In that way, $2K(B(v, b) + B(v_i^*)) < R(v_i^*)$ is equivalent to the condition

$$\begin{aligned} &(B(v,b)4h + 2(h-2))\, 2Ka^2 < (h-2)^{\frac{h-2}{h}}(h+2)^{\frac{2}{h}} \\ \Rightarrow \quad &Ka^2 < \frac{(h-2)^{\frac{h-2}{h}}(h+2)^{\frac{2}{h}}}{4(B(v,b)2h + h - 2)}, \end{aligned} \tag{2.2.19}$$

which unfortunately cannot be simplified much further, without assumptions on the parameters K and a. We remind ourselves that K is the cost of cooperation, while a denotes the amount of signalling necessary to gain half of the maximal (private) benefits. Equation (2.2.19) thus gives upper limits to these terms, dependent on the steepness of the activation curve h as well as the public benefit $B(v, b)$. A larger public benefit is actually detrimental to the existence of positive stationary strategies v_i.

At the same time, there cannot be more than two intersections in $[0, +\infty)$ by Rolle's theorem (Theorem A.8), since

$$\begin{aligned}(2KB(v,b) + B(v_i))' - R'(v_i) &= 2KB'(v_i) - R'(v_i) \\ &= \frac{a^h h v_i^{h-3}}{(v_i^h + a^h)^3}\left(2Kv_i^2(v_i^h + a^h) + (h+2)v_i^h - (h-2)a^h\right) \\ &= \frac{a^h h v_i^{h-3}}{(v_i^h + a^h)^3}\left(2Kv_i^{h+2} + (h+2)v_i^h + 2Ka^h v_i^2 - (h-2)a^h\right), \quad (2.2.20)\end{aligned}$$

where the term in parenthesis is strictly monotonically increasing and the equation therefore only has one $\xi \in (0, +\infty)$ for which $(2KB(v,b) + B(\xi))' - R'(\xi) = 0$.

It remains to check the stability of these equilibrium solutions. We know from equation (2.2.9) that $v_i = 0$ is stable if $B''(0) < 2KB(v,b)$. We also know that for $h \geq 3$ it holds that $B''(0) = 0$. Hence $v_i = 0$ is an ESS regardless of parameter values.

A positive stationary solution $\bar{v}_i$ is stable, if equation (2.2.12) holds, that is

$$\begin{aligned}& 0 > -\left(\frac{1}{\bar{v}_i} + 2K\bar{v}_i\right)B'(\bar{v}_i) + B''(\bar{v}_i) \\ \Rightarrow \quad & 0 > -\left(\frac{1}{\bar{v}_i} + 2K\bar{v}_i\right)\frac{ha^h\bar{v}_i^{h-1}}{(\bar{v}_i^h + a^h)^2} + \frac{ha^h\bar{v}_i^{h-2}\left(-(h+1)\bar{v}_i^h + (h-1)a^h\right)}{(\bar{v}_i^h + a^h)^3} \\ \Rightarrow \quad & 0 > -\left(\frac{1}{\bar{v}_i} + 2K\bar{v}_i\right)\bar{v}_i(\bar{v}_i^h + a^h) - (h+1)\bar{v}_i^h + (h-1)a^h.\end{aligned}$$

We can rearrange this inequality to

$$\left(\frac{1}{\bar{v}_i} + 2K\bar{v}_i\right)\bar{v}_i(\bar{v}_i^h + a^h) + (h+1)\bar{v}_i^h > (h-1)a^h. \quad (2.2.21)$$

The larger of both positive stationary solutions fulfils $\bar{v}_i > v_i^* = \sqrt[h]{\frac{h-2}{h+2}} \cdot a$, if it exists. It follows that

$$\begin{aligned}&\left(\frac{1}{\bar{v}_i} + 2K\bar{v}_i\right)\bar{v}_i(\bar{v}_i^h + a^h) + (h+1)\bar{v}_i^h \\ &\qquad > \left(1 + 2K\bar{v}_i^2\right)\left(\frac{h-2}{h+2} \cdot a^h + a^h\right) + (h+1) \cdot \frac{h-2}{h+2} \cdot a^h \\ &\qquad > \frac{2h}{h+2} \cdot a^h + \frac{(h+1)(h-2)}{h+2} \cdot a^h \\ &\qquad = \frac{2h + h^2 - h - 2}{h+2} \cdot a^h \\ &\qquad = (h-1) \cdot a^h.\end{aligned}$$

Hence the larger of both positive solutions is always stable, if it exists. It follows immediately from the stability of the zero solution that the smaller of both positive solutions must be unstable.

If $B(v,b)=0$, which occurs if for example the existing subpopulations do not engage in QS, the situation is different. As both $R(0)=0$ and $2KB(v,b)+B(0)=0$, there can only be one positive intersection. By using property 5, we show that $R(v_i)$ is increasing faster than $2KB(v,b)+B(v_i)$ for v_i small. First of all, we prove property 5 by induction.

Proof. **base case** We know from equation (2.2.17), that

$$\begin{aligned} R'(v_i) &= \frac{a^h h v_i^{h-3}\left(-(h+2)v_i^h+(h-2)a^h\right)}{\left(v_i^h+a^h\right)^3} \\ &= \frac{v_i^{h-(1+2)}f(v_i)}{\left(v_i^h+a^h\right)^{1+2}}, \end{aligned}$$

where $f(v_i)=a^h h\left(-(h+2)v_i^h+(h-2)a^h\right)$ and thus $f(0)=ha^{2h}(h-2)>0$.

inductive step Assuming that the statement holds for $R^{(n)}(v_i)$ and that $n+1\leq h-2$, we have

$$\begin{aligned} R^{(n+1)}(v_i) = \Big(&(v_i^h+a^h)^{n+2}(h-(2+n))v_i^{h-(n+3)}f(v_i) \\ &+(v_i^h+a^h)^{n+2}f'(v_i)v_i^{h-(n+2)} \\ &-(n+2)h(v_i^h+a^h)^{n+1}f(v_i)v_i^{2h-(n+3)}\Big)/\left(v_i^h+a^h\right)^{2n+4} \\ = &\frac{v_i^{h-(n+1+2)}g(v_i)}{(v_i^h+a^h)^{n+1+2}}, \end{aligned}$$

where

$$g(v_i)=(v_i^h+a^h)\Big((h-(2+n))f(v_i)+f'(v_i)v_i\Big)-(n+2)hf(v_i)v_i^h.$$

and thus $g(0)=a^h(h-(2+n))f(0)>0$ since $n<h-2$ and $f(0)>0$.

□

It follows that $R^{(n)}(0)=0$ for $n<h-2$ and $R^{(h-2)}(0)>0$. At the same time, a similar argument shows that

$$\Big(2K(B(v,b)+B(v_i))\Big)^{(n)}=2KB^{(n)}(v_i)=\frac{v_i^{h-n}2Kf(v_i)}{(v_i^h+a^h)^{1+n}}.$$

Table 2.1: Existence and stability of stationary solutions for v_i for private benefit with term $B(v_i) = v_i^h/v_i^h + a^h$.

	$Ka^2 > \frac{(h-2)^{\frac{h-2}{h}}(h+2)^{\frac{2}{h}}}{4(B(v,b)2h+h-2)}$	$Ka^2 < \frac{(h-2)^{\frac{h-2}{h}}(h+2)^{\frac{2}{h}}}{4(B(v,b)2h+h-2)}$
$B(v,b) \neq 0$	$\exists \underset{\text{stable}}{\bar{v}_i = 0} \quad \nexists \bar{v}_i > 0$	$\exists \underset{\text{stable}}{\bar{v}_i = 0} \quad \exists \underset{\text{stable}}{\bar{v}_i > 0}$
$B(v,b) = 0$	$\exists \underset{\text{unstable}}{\bar{v}_i = 0} \quad \exists \underset{\text{stable}}{\bar{v}_i > 0}$	

As such, $\Big(2K(B(v,b) + B(v_i))\Big)^{(n)} = 0$ for $n < h$. Taken together, these findings show that for v_i small, $R(v_i) > 2K(B(v,b) + B(v_i))$ and thus a positive intersection exists. As we know that for $B(v,b) = 0$ there is an intersection at $v_i = 0$ and from equation (2.2.20) that there can only be two intersections in $[0, +\infty)$, there can be no other positive intersection.

In order to investigate the stability, we first note that both $B''(0) = 0$ and $B(v,b) = 0$, which means we cannot gain insight into the stability of the zero solution through equation (2.2.12). But we know that for $\varepsilon > 0$ small enough $R(\varepsilon) > 2KB(\varepsilon)$ and that there exists only one positive ξ for which $2KB'(\xi) = R'(\xi)$. Additionally, we know that ξ lies in the open interval between zero and the positive intersection $\bar{v}_i$ and as such is unequal to $\bar{v}_i$. We can thus follow that

$$
\begin{aligned}
R'(\bar{v}_i) &< 2KB'(\bar{v}_i) \\
R'(\bar{v}_i) = \left(\frac{B'(\bar{v}_i)}{\bar{v}_i}\right)' &= \frac{B''(\bar{v}_i)}{\bar{v}_i} - \frac{B'(\bar{v}_i)}{\bar{v}_i^2} \\
\Rightarrow \quad \frac{B''(\bar{v}_i)}{\bar{v}_i} - \frac{B'(\bar{v}_i)}{\bar{v}_i^2} &< 2KB'(\bar{v}_i) \\
-2KB'(\bar{v}_i)\bar{v}_i - \frac{B'(\bar{v}_i)}{\bar{v}_i} + B''(\bar{v}_i) &< 0,
\end{aligned}
$$

which is exactly the condition for stability from equation (2.2.12). For $B(v,b) = 0$ we have thus an unstable zero solution and a stable positive strategy. The behaviour is summarised in table 2.1

In biological terms, our results indicate that the surrounding subpopulations have a profound impact on the evolution of cooperativity. If one of the subpopulations is cooperating ($B(v,b) \neq 0$), the others will experience bistable behaviour — they might cooperate themselves or not participate in QS, depending on starting strategy. If, on the other hand, all of the subpopulations do not cooperate at first ($B(v,b) = 0$), then the evolutionary pressure will drive them towards the positive

ESS, meaning they pick up QS with time.

Reduction in death rate: $G(v_i, v, b) = B(v, b) \cdot C(v_i) - \mu(v_i)\|b\|_1$

There have been some proposals that QS is involved in antimicrobial resistance against antibiotics, limiting the damage to the bacteria by regulating the production of certain factors [Lih+13]. We propose a model where this means that the strategy directly influences the death rate of the producing bacteria, while QS also still provides the public growth benefit.

For this to work, $\mu(v_i)$ should be a positive, monotonically decreasing function in v_i, with a limit larger than 0. Sadly, not much insight can be gained from this general form, so we choose one possible function for $\mu(v_i)$ in order to analyse the behaviour of this type of G-function.

$\boldsymbol{\mu(v_i) = (\mu_{max} - \mu_{min})e^{-dv_i^2} + \mu_{min}}$ If we take this $\mu(v_i)$, which fulfils the above assumptions, and use our standard cost-function $C(v_i) = e^{-Kv_i^2}$, we get the following condition for an ESS:

$$\begin{aligned}\partial_1 G(v_i, v, b) &= B(v, b)C'(v_i) - \mu'(v_i)\|b\|_1 \\ 0 &= B(v, b)(-2K\bar{v}_i)e^{-K\bar{v}_i^2} - (\mu_{\max} - \mu_{\min})(-2d\bar{v}_i)e^{-d\bar{v}_i^2}\|b\|_1\end{aligned}$$

Again, one solution is $v_i = 0$. We divide by v_i and carry on, denoting $\mu_{\max} - \mu_{\min}$ as $\Delta\mu$.

$$e^{-K\bar{v}_i^2 + d\bar{v}_i^2} = \frac{\Delta\mu d\|b\|_1}{B(v, b)K} \tag{2.2.22}$$

$$v_i^2 = \ln\left(\frac{\Delta\mu d\|b\|_1}{B(v, b)K}\right) \cdot \frac{1}{d - K}. \tag{2.2.23}$$

There exists one positive, real solution for v_i if and only if $\Delta\mu d\|b\|_1 > B(v, b)K$ and $d > K$ or $\Delta\mu d\|b\|_1 < B(v, b)K$ and $d < K$. We take a look at the stability:

$$\begin{aligned}\partial_1^2 G(v_i, v, b) &= B(v, b)C''(v_i) - \mu''(v_i)\|b\|_1 \\ &= B(v, b)(-2K + 4K^2 v_i^2)e^{-Kv_i^2} - \Delta\mu(-2d + 4d^2 v_i^2)e^{-dv_i^2}\|b\|_1 \\ \partial_1^2 G(0, v, b) &= B(v, b)(-2K) - \Delta\mu(-2d)\|b\|_1 \\ &= (-2)\left(KB(v, b) - \Delta\mu d\|b\|_1\right).\end{aligned}$$

Table 2.2: Existence and stability of stationary solutions for v_i for strategy-dependent mortality rates.

	$\frac{B(v,b)}{\|b\|_1} < \frac{\Delta\mu d}{K}$		$\frac{B(v,b)}{\|b\|_1} > \frac{\Delta\mu d}{K}$	
$K < d$	$\exists \bar{v}_i = 0$ unstable	$\exists \bar{v}_i > 0$ stable	$\exists \bar{v}_i = 0$ stable	$\nexists \bar{v}_i > 0$
$K > d$	$\exists \bar{v}_i = 0$ unstable	$\nexists \bar{v}_i > 0$	$\exists \bar{v}_i = 0$ stable	$\exists \bar{v}_i > 0$ unstable

As was the case in the last section, the stability of the zero solution is closely linked to the existence of a positive real solution (see table 2.2). For the positive solution $\bar{v}_i$, we use equation (2.2.22) and substitute for $B(v,b)$.

$$\begin{aligned}\partial_1^2 G(\bar{v}_i, v, b) &= \frac{\Delta\mu d\|b\|_1}{K} \mathrm{e}^{K\bar{v}_i^2 - d\bar{v}_i^2}(-2K + 4K^2\bar{v}_i^2)\mathrm{e}^{-K\bar{v}_i^2} \\ &\quad - \Delta\mu(-2d + 4d^2 v_i^2)\mathrm{e}^{-dv_i^2}\|b\|_1 \\ &= \Delta\mu d\|b\|_1 \left(-2 + 4K\bar{v}_i^2 + 2 - 4d\bar{v}_i^2\right)\mathrm{e}^{-d\bar{v}_i^2} \\ &= \Delta\mu d\|b\|_1 (K-d)\, 4\bar{v}_i^2 \mathrm{e}^{-d\bar{v}_i^2}.\end{aligned}$$

So if $d > K$, $\bar{v}_i$ is stable, otherwise it is unstable. But such an instability is in contrast to one of our general assumptions about $\partial_1 G$, namely that there exists a $\overline{u}$ such that $\partial_1 G(v_i, v, b) < 0\ \forall v_i > \overline{u}$. In particular, we have that

$$\partial_1 G(v_i, v, b) = 2d\Delta\mu\|b\|_1 v_i \mathrm{e}^{-dv_i^2} - 2KB(v,b)v_i\mathrm{e}^{-Kv_i^2},$$

so for $KB(v,b) < \Delta\mu d\|b\|_1$ and $d < K$

$$\partial_1 G(v_i, v, b) > 2KB(v,b)v_i\left(\mathrm{e}^{-dv_i^2} - \mathrm{e}^{-Kv_i^2}\right) > 0 \quad \forall v_i > 0.$$

If, on the other hand, $KB(v,b) \geq \Delta\mu d\|b\|_1$ and $d < K$ it holds that

$$\begin{aligned} v_i^2 &> \ln\left(\frac{\Delta\mu d\|b\|_1}{B(v,b)K}\right)\cdot\frac{1}{d-K} \quad \forall v_i > \bar{v}_i \\ \Rightarrow \quad & \frac{d\Delta\mu\|b\|_1}{KB(v,b)}\cdot\mathrm{e}^{-dv_i^2} > e^{-Kv_i^2}, \end{aligned}$$

from which we gather that for all $v_i > \bar{v}_i$

$$\partial_1 G(v_i, v, b) = 2KB(v,b)v_i\left(\frac{d\Delta\mu\|b\|_1}{KB(v,b)}\cdot\mathrm{e}^{-dv_i^2} - e^{-Kv_i^2}\right) > 0.$$

Altogether, $\partial_1 G$ does not exhibit a saturation behaviour in the case of $K > d$. But as mentioned before, such a saturation behaviour makes sense from a biological point of view, since there is no biological strategy without its drawbacks and no such feature can grow to infinity. But for practical purposes, one might still consider the case $K > d$, $KB(v, b) > \Delta\mu d\|b\|_1$ as long as the starting value $v_i(x, 0) < \bar{v}_i$.

The existence and stability of stationary solutions for v_i is summarised in table 2.2, while figure 2.4 recaps the asymptotic behaviour for the different G-functions considered until now.

2.2.2 G-Function with abiotic components

The different versions for the G-function discussed in the previous section nicely display the range of possibilities one has when using this ansatz, but feature quite a lot of abstraction when modelling the benefit in the different cases. As the benefit for QS is provided by secreted proteins, we could also turn to a model that takes the amount of produced proteins directly into account.

In order to achieve this, we will expand upon our model to include some abiotic component y:

$$\dot{b_i} = G(v_i, v, \begin{pmatrix} y \\ b \end{pmatrix}).$$

This basic form was proposed by Cohen, Pastor, and Vincent [CPV00]. In our case, after adding in spatial dependence and diffusion in the biotic and abiotic compartment, such a model will thus read

$$\begin{aligned} \dot{y_i} &= F_i(v, \begin{pmatrix} y \\ b \end{pmatrix}) + D_{y_i} \triangle y_i \\ \dot{b_i} &= G(v_i, v, \begin{pmatrix} y \\ b \end{pmatrix}) \cdot b_i + D_b \triangle b_i \\ \dot{v_i} &= \varepsilon \partial_1 G(v_i, v, \begin{pmatrix} y \\ b \end{pmatrix}). \end{aligned}$$

We note that the abiotic compartment influences the biotic compartment and is in turn influenced by it. The main dividing point between biotic and abiotic compartment is the existence of strategies only in the biotic case — while y is influenced by v, it does not have its own strategy, nor does it evolve.

In the context of QS in *Pseudomonas aeruginosa* (*P. aeruginosa*), the abiotic compartment should include protein and signal production. As a large amount of different proteins are secreted under control of QS, here we will only focus on enzymes that make nutrients available to the bacteria, e.g. siderophores, in order

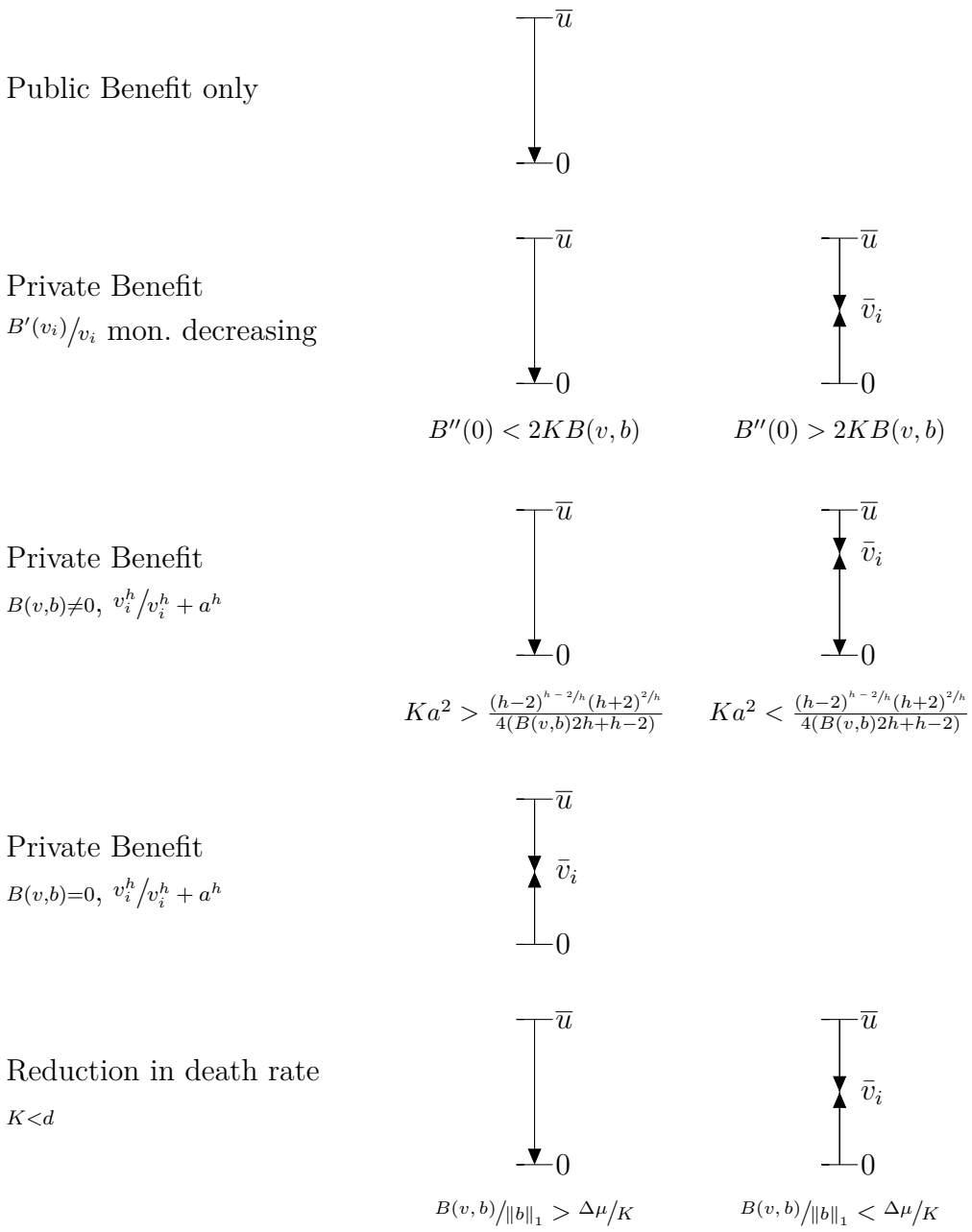

Figure 2.4: Existence and stability of ESS for different G-functions explored in this section.

to avoid making the model too complicated. Denoting the QS-signal concentration by s and the enzyme concentration by e, we get a basic model of

$$\begin{aligned}
\dot{s} &= F_s(v,(s,e,b)^T) + D_s \triangle s \\
\dot{e} &= F_e(v,(s,e,b)^T) + D_e \triangle e \\
\dot{b_i} &= G(v_i,v,(s,e,b)^T)\cdot b_i + D_b \triangle b_i \\
\dot{v_i} &= \varepsilon \partial_1 G(v_i,v,(s,e,b)^T),
\end{aligned}$$

where F_s, F_e are classically defined with Hill terms as activation coefficients, such as

$$F_s(v,(s,e,b)^T) = \alpha_s \cdot \sum_j b_j v_j^s + \beta_s \cdot \frac{s^2}{s^2+\tau^2} \cdot \sum_j b_j v_j^s - \gamma_s s \tag{2.2.24}$$

$$F_e(v,(s,e,b)^T) = \beta_e \cdot \frac{s^2}{s^2+\tau^2} \cdot \sum_j b_j v_j^e - \gamma_e e, \tag{2.2.25}$$

where α is a baseline production and β production in induced state, while γ is a degradation rate. τ denotes the concentration of signal molecules that leads to half-maximal production. All variables can also be found on page 9.

We rewrite the system to include only variables that really have an influence in the functions. For the G-function itself we assume a dependence only on v_i (influencing the growth rate through production costs), the amount of bacteria (competing for nutrients) and on e, as the enzymes themselves provide the benefit to the bacteria in this scenario. The condensed system can then be written as

$$\dot{s} = F_s(v,s,b) + D_s \triangle s \tag{2.2.26a}$$

$$\dot{e} = F_e(v,s,e,b) + D_e \triangle e \tag{2.2.26b}$$

$$\dot{b_i} = G(v_i,e,b)\cdot b_i + D_b \triangle b_i \tag{2.2.26c}$$

$$\dot{v_i} = \varepsilon \partial_1 G(v_i,e,b). \tag{2.2.26d}$$

As v_i is used to model the costs for participating in QS, while the benefits are imparted through e, we get the condition that $G(v_i,e,b)$ is monotonically decreasing in v_i. It follows that the long-time behaviour of these equations does not differ from the model without explicit abiotic components described in section 2.2.1. However, it gives a more realistic impression of the transient behaviour of this biological system.

2.2.3 G-Function with internal compartments

We have seen that a basic model with abiotic compartments behaves like the basic model without abiotic compartments. At the same time, we have seen in section 2.2.1

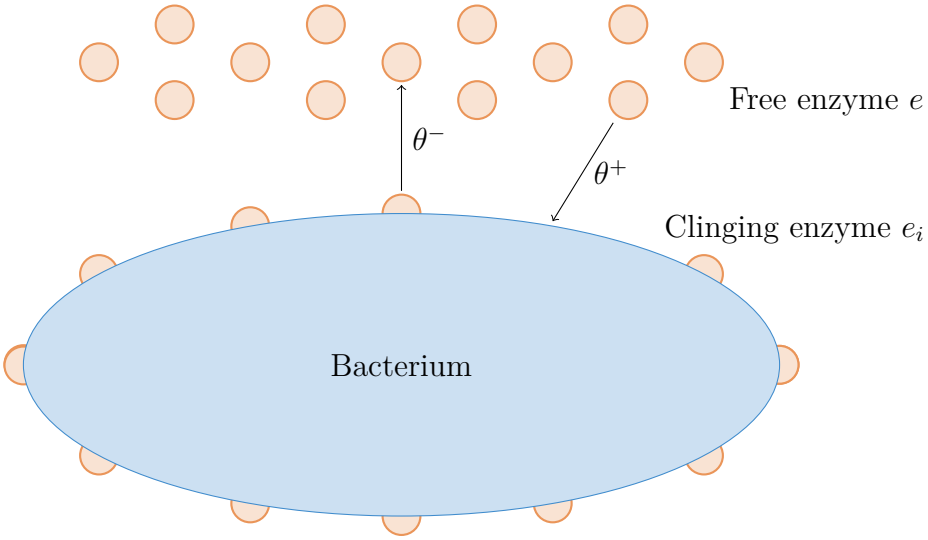

Figure 2.5: Schematic representation of attachment and release of enzymes from cell membrane.

how a model behaves if we consider some private benefit for QS, a scenario which, as discussed in section 1.1.1, is also biologically relevant. Hence, we want to combine the idea of private goods with a model including explicit terms for signal and enzyme concentrations. To that end, we build on equation (2.2.26), adding biologically motivated internal compartments for signal and enzyme. As these are on a very small spatial scale, we can assume them to be spatially homogeneous and that they can therefore be described through ordinary differential equations.

Internal compartment for enzyme

We start out considering the biological situation: if a bacterium produces enzyme in response to QS signal, the enzyme will actually cling to the outside of this bacterium before diffusing into inter-cellular space (see also figure 2.5). Given the right circumstances, this clinging phase might last longer and lead to the positive effects of the enzyme benefiting only the producing bacteria. We also consider a small reattachment rate in this model. All in all, if we denote the concentration of clinging enzyme that is experienced by subpopulation b_i by e_i, we can write the dynamics as

$$\dot{e}_i = \beta_e v_i^e \frac{s^2}{s^2 + \tau^2} - \theta^- e_i + \theta^+ e - \gamma_e e_i, \tag{2.2.27}$$

where θ^+ and θ^- are the re-attachment and disassociation rates, β_e is a production rate and γ_e the degradation rate of the enzyme as before. The freely diffusing enzyme concentration will then be

$$\dot{e} = \lambda \sum_i \left(b_i \left(\theta^- e_i - \theta^+ e \right) \right) + D_e \triangle e - \gamma_e e. \tag{2.2.28}$$

In this term, λ is a measure for the relation between internal and intercellular volume, and in this way responsible for converting internal to external concentration.

In order to see the benefit of the enzyme more clearly, we set up equations for the nutrients provided. We can split these into three groups: $\bar{n}$ will denote the undigested nutrients in the environment, which will replenish with a rate n_0. The produced enzymes will convert those with a rate c_1 into usable nutrients, n and n_i, where the former are available to all and the later just to the bacteria having clinging enzymes e_i. The bacteria then digest these nutrients with a rate c_2. Additionally, nutrients are degraded in an abiotic way as well. The equations then read

$$\dot{\bar{n}} = -c_1 \left(e + \sum_j (b_j e_j) \right) \bar{n} + n_0 - \gamma_n \bar{n} \tag{2.2.29a}$$

$$\dot{n} = c_1 e \bar{n} - c_2 n \|b\|_1 - \gamma_n n \tag{2.2.29b}$$

$$\dot{n}_i = c_1 e_i \bar{n} - c_2 n_i - \gamma_n n_i. \tag{2.2.29c}$$

We can assume that the digestion of nutrients happens on a faster time-scale than the population dynamics, so equation (2.2.29) can be assumed to be in steady state. Taking the left-hand-side to zero, we can solve for n and n_i:

$$n = \frac{c_1 e}{c_2 \|b\|_1 + \gamma_n} \cdot \frac{n_0}{c_1 \left(e + \sum_j (b_j e_j) \right) + \gamma_n}, \tag{2.2.30a}$$

$$n_i = \frac{c_1 e_i}{c_2 + \gamma_n} \cdot \frac{n_0}{c_1 \left(e + \sum_j (b_j e_j) \right) + \gamma_n}. \tag{2.2.30b}$$

We make the same steady-state assumption for equation (2.2.27) and obtain:

$$e_i = \underbrace{\frac{\beta_e}{\theta^- + \gamma_e}}_{\bar{\beta}} \cdot v_i^e \cdot \frac{s^2}{s^2 + \tau^2} + \underbrace{\frac{\theta^+}{\theta^- + \gamma_e}}_{\bar{\theta}} \cdot e =: E(v_i^e, s, e), \tag{2.2.31}$$

$$\Rightarrow \quad n(v_i^e, s, e, b) = \left(\frac{c_1 e}{c_2 \|b\|_1 + \gamma_n} + \frac{c_1 E(v_i^e, s, e)}{c_2 + \gamma_n} \right) \cdot \frac{n_0}{c_1 \left(e + \sum_j (b_j E(v_j^e, s, e)) \right) + \gamma_n}. \tag{2.2.32}$$

At this point we have defined all necessary terms and as such can state the complete model (as a reminder all variable meanings are listed on page 9).

$$\dot{s} = F_s(v, s, b) + D_s \triangle s \tag{2.2.33a}$$

$$\dot{e} = \lambda \sum_i \left(b_i \left(\theta^- e_i - \theta^+ e \right) \right) + D_e \triangle e - \gamma_e e \tag{2.2.33b}$$

$$\dot{b_i} = \underbrace{\left((r_{\min} + r_n n(v_i^e, s, e, b))\, C(v_i) - \mu \|b\|_1 \right)}_{G(v_i, s, e, b)} \cdot b_i + D_b \triangle b_i \tag{2.2.33c}$$

$$\dot{v_i} = \varepsilon \partial_1 G(v_i, s, e, b). \tag{2.2.33d}$$

As this model is quite close to the one described in equation (2.2.26), we take a closer look at $\partial_1 G(v_i, s, e, b)$ in order to compare these two. In doing so, we will concentrate on v_i^e (the QS response strength), as this is where the two models differ from each other. We will also use our usual cost function, $C(v_i) = \exp(-K_s(v_i^s)^2 - K_e(v_i^e)^2)$. It holds that

$$\begin{aligned}
\dot{v}_i^e &= \frac{\partial}{\partial u_2} G\left((u_1, u_2), s, e, b)\right)|_{u=v_i} \\
&= \mathrm{e}^{-K_s(v_i^s)^2 - K_e(v_i^e)^2} \Big(-2K_e v_i^e r_{\min} - 2K_e v_i^e r_n n(v_i^e, s, e, b) + r_n \partial_1 n(v_i^e, s, e, b) \Big) \\
&= \mathrm{e}^{-K_s(v_i^s)^2 - K_e(v_i^e)^2} \Bigg(-2K_e v_i^e r_{\min} \\
&\quad - 2K_e v_i^e r_n \left(\frac{c_1 E(v_i^e, s, e)}{c_2 + \gamma_n} + \frac{c_1 e}{c_2 \|b\|_1 + \gamma_n} \right) \cdot \frac{n_0}{c_1 \left(e + \sum_j (b_j E(v_j^e, s, e)) \right) + \gamma_n} \\
&\quad + r_n \frac{c_1 \partial_1 E(v_i^e, s, e)}{c_2 + \gamma_n} \cdot \frac{n_0}{c_1 \left(e + \sum_j (b_j E(v_j^e, s, e)) \right) + \gamma_n} \Bigg)
\end{aligned}$$

$$= \mathrm{e}^{-K_s(v_i^s)^2 - K_e(v_i^e)^2} \Bigg(-2K_e v_i^e r_{\min}$$
$$- 2K_e v_i^e r_n \frac{c_1 e}{c_2 \|b\|_1 + \gamma_n} \cdot \frac{n_0}{c_1 \left(e + \sum_j (b_j E(v_j^e, s, e)) \right) + \gamma_n}$$
$$+ \frac{r_n c_1}{c_2 + \gamma_n} \cdot \frac{n_0(-2K_e v_i^e E(v_i^e, s, e) + \partial_1 E(v_i^e, s, e))}{c_1 \left(e + \sum_j (b_j E(v_j^e, s, e)) \right) + \gamma_n} \Bigg).$$

In order to look for ESSs, we will take $r_{\min} = 0$, as this allows us to get rid of some constant terms that we know to be non-zero

$$0 = -2K_e v_i^e \frac{c_1 e}{c_2 \|b\|_1 + \gamma_n} + \frac{c_1}{c_2 + \gamma_n} \cdot (-2K_e v_i^e E(v_i^e, s, e) + \partial_1 E(v_i^e, s, e)) .$$

Using equation (2.2.31) and its derivative

$$0 = -2K_e v_i^e \frac{c_1 e}{c_2 \|b\|_1 + \gamma_n} + \frac{c_1}{c_2 + \gamma_n} \cdot (-2K_e v_i^e (\bar{\beta} v_i^e \cdot \frac{s^2}{s^2 + \tau^2} + \bar{\theta} e) + \bar{\beta} \frac{s^2}{s^2 + \tau^2})$$
$$0 = -2K_e \frac{(c_2 + \gamma_n) e}{c_2 \|b\|_1 + \gamma_n} \cdot v_i^e - 2K_e \bar{\theta} e v_i^e - 2K \bar{\beta} \cdot \frac{s^2}{s^2 + \tau^2} (v_i^e)^2 + \bar{\beta} \frac{s^2}{s^2 + \tau^2} .$$

The resulting equation is a quadratic equation in v_i^e and as such we can determine the existence of positive solutions by looking at the discriminant:

$$D = \left(-2K_e \frac{(c_2 + \gamma_n) e}{c_2 \|b\|_1 + \gamma_n} - 2K_e \bar{\theta} e \right)^2$$
$$- 4 \left(-2K \bar{\beta} \cdot \frac{s^2}{s^2 + \tau^2} \right) \left(\bar{\beta} \frac{s^2}{s^2 + \tau^2} \right)$$
$$= 4K_e^2 e^2 \left(\frac{(c_2 + \gamma_n) e}{c_2 \|b\|_1 + \gamma_n} + \bar{\theta} \right)^2 + 8K_e \bar{\beta}^2 \left(\frac{s^2}{s^2 + \tau^2} \right)^2 .$$

We can conclude that there will always be two ESSs as long as $s \neq 0$, and exactly one in the biologically meaningful positive parameter range, as $\sqrt{D}$ is larger than the linear coefficient of the equation.

Internal compartment for signal

In order to find equations for an internal signal compartment, we consider the fact that production as well as binding of QS signal molecules happens within the

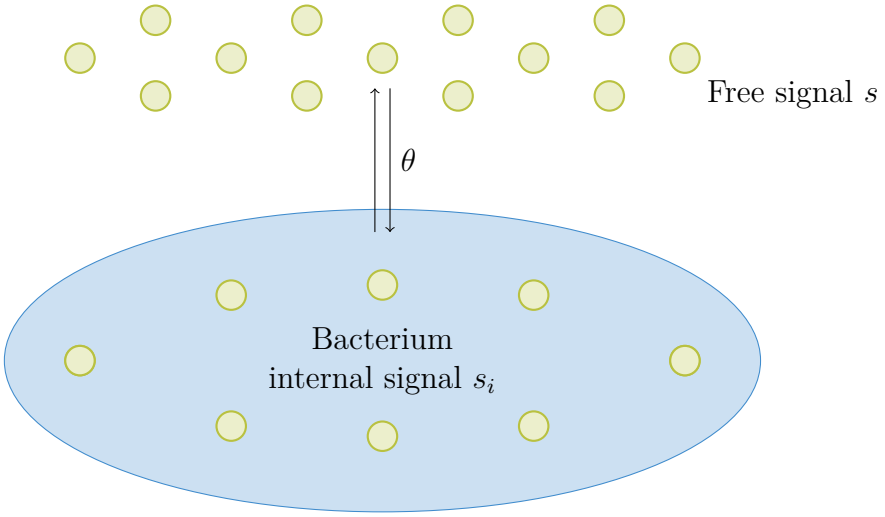

Figure 2.6: Schematic representation of signal diffusion through cell membrane.

cell itself, while transmission and therefore group interaction is achieved trough secreted signal molecules. For small signalling molecules as used by *P. aeruginosa*, this transport through the cell membrane is passive. As such, we use one rate θ that determines the exchange between inside and outside of the bacterial cell. Including a baseline production α_s, an induced production rate of β_s as well as an abiotic degradation rate γ_s, we find the equation

$$\dot{s}_i = \alpha_s v_i^s + \beta_s v_i^s \cdot \frac{s_i^2}{s_i^2 + \tau^2} + \theta(s - s_i) - \gamma_s s_i, \tag{2.2.34}$$

which is a variation of the one introduced in Dockery and Keener [DK01]. The equation for external signal concentration s is then given by

$$\dot{s} = \lambda\theta \cdot \sum_j (b_j(s_j - s)) + D_s \triangle s - \gamma_s s. \tag{2.2.35}$$

As before, λ signifies the ratio of inter- to intracellular volume. We proceed by assuming that the internal signal concentration is in a quasi steady state. This leads to

$$\begin{aligned} 0 &= \alpha_s v_i^s + \beta_s v_i^s \cdot \frac{s_i^2}{s_i^2 + \tau^2} + \theta(s - s_i) - \gamma_s s_i \\ 0 &= -s_i^3(1 + \gamma_s\theta^{-1}) + \Big((\alpha_s + \beta_s)\omega + s\Big)s_i^2 - \tau^2(1 + \gamma_s\theta^{-1})s_i + \Big(\alpha_s\omega + s\Big)\tau^2, \end{aligned} \tag{2.2.36}$$

a cubic equation in s_i, where $\omega := {}^{v_i^s}/_{\theta}$. While there is a solution formula for cubic equations, it is too complex to be of help in evaluating the influence of the parameters. As such, we will leave these equations for now but return back to them again in chapter 6.

Chapter 3

Modelling with ordinary differential equations

Modelling biological processes with ordinary differential equations (ODEs) has a long history, ranging back to the population model of Benjamin Gompertz from 1825 and further. There are many cases for which they are the appropriate choice in the biological context and their application covers the full gamut of possibilities. In the context of QS, they have for example been used successfully to model the QS systems in *P. aeruginosa* by Dockery and Keener [DK01] as well as reaction to QS-dampening drugs [Ang+04].

An ODE is normally used in a biological context where the particles under scrutiny can be considered well-mixed. But there are a number of ways to simulate spatial structures even with ODEs, without resorting to explicit spatial coordinates and therefore partial differential equations (PDEs). In this chapter, we will explicitly take a closer look at models with an external influx term (section 3.2) and ones including a mixing term (section 3.3).

3.1 ODE without additions

We first consider an ODE model without any special additions. The general case we will be looking at is equation (2.0.5). For ease of reference, we repeat it here:

$$\dot{b_i}(t) = G(v_i(t), v(t), b(t)) \cdot b_i(t) \qquad \text{(2.0.5a revisited)}$$

$$\dot{v_i}(t) = \varepsilon \partial_1 G(v_i(t), v(t), b(t)) \qquad \text{(2.0.5b revisited)}$$

The discussion in section 2.2 has shown how different versions of G affect the long-term behaviour of v_i. We can now concern ourselves with the long-term behaviour of b_i. b_i is in equilibrium if either

$$b_i = 0 \qquad \text{or} \qquad G(v_i(t), v(t), b(t)) = 0.$$

As we always assumed any kind of benefit function to be equal to zero for zero strategies, we can immediately conclude that for G-functions having only 0 as ESS, $b = 0$ will be the only stationary solution.

If there are multiple ESS candidates, we distinguish between subpopulations that are present with a strictly positive amount of associated bacteria ($b_i > 0$) and subpopulations that have a stable strategy, but have died out ($b_i = 0$). Without loss of generality we can assume the population vector b to be sorted in the way that the first r subpopulations are the ones with positive population count while for the other subpopulations $b_i = 0 \, \forall i > r$. The Jacobian for system (2.0.5a) then has the form

$$\begin{pmatrix} (\partial_{b_1} B(v,b)C(v_1) - \mu)b_1 & \cdots & (\partial_{b_n} B(v,b)C(v_1) - \mu)b_1 \\ \vdots & \ddots & \vdots \\ (\partial_{b_1} B(v,b)C(v_r) - \mu)b_r & \cdots & (\partial_{b_n} B(v,b)C(v_r) - \mu)b_r \\ \mathbf{0} & & \operatorname{diag}\left(B(v,b)C(v_i) - \mu\|b\|_1\right) \end{pmatrix},$$

where we assume that $\mathbf{0} \in \mathbb{R}^{(m-r)\times r}$ and

$$\operatorname{diag}\left(B(v,b)C(v_i) - \mu\|b\|_1\right) = \begin{pmatrix} B(v,b)C(v_1) - \mu\|b\|_1 & & \\ & \ddots & \\ & & B(v,b)C(v_r) - \mu\|b\|_1 \end{pmatrix}.$$

If we then consider the elements in rows $r+1$ to m and the respective minors, we can immediately see that a stable equilibrium needs to fulfil

$$B(v,b)C(v_i) - \mu\|b\|_1 < 0 \quad \forall i > r. \tag{3.1.1}$$

Condition (3.1.1) ensures that extinct subpopulations have a negative potential growth rate and thus remain extinct even under perturbations. It remains to determine the eigenvalues of

$$\begin{pmatrix} (\partial_{b_1} B(v,b)C(v_1) - \mu)b_1 & \cdots & (\partial_{b_r} B(v,b)C(v_1) - \mu)b_1 \\ \vdots & \ddots & \vdots \\ (\partial_{b_1} B(v,b)C(v_r) - \mu)b_r & \cdots & (\partial_{b_r} B(v,b)C(v_r) - \mu)b_r \end{pmatrix}$$

in order to determine conditions for the stability of surviving subpopulations. We will take a look at the conditions for a coalition of two, with two surviving subpopulations $b_1, b_2 > 0$.

$$\begin{aligned} J &= \begin{pmatrix} (\partial_{b_1} B(v,b)C(v_1) - \mu)b_1 & (\partial_{b_2} B(v,b)C(v_1) - \mu)b_1 \\ (\partial_{b_1} B(v,b)C(v_2) - \mu)b_2 & (\partial_{b_2} B(v,b)C(v_2) - \mu)b_2 \end{pmatrix} \\ \operatorname{tr}(J) &= (\partial_{b_1} B(v,b)C(v_1) - \mu)b_1 + (\partial_{b_2} B(v,b)C(v_2) - \mu)b_2 \\ |J| &= b_1 b_2 \mu \left(\partial_{b_1} B(v,b) - \partial_{b_2} B(v,b)\right)\left(C(v_2) - C(v_1)\right) \end{aligned}$$

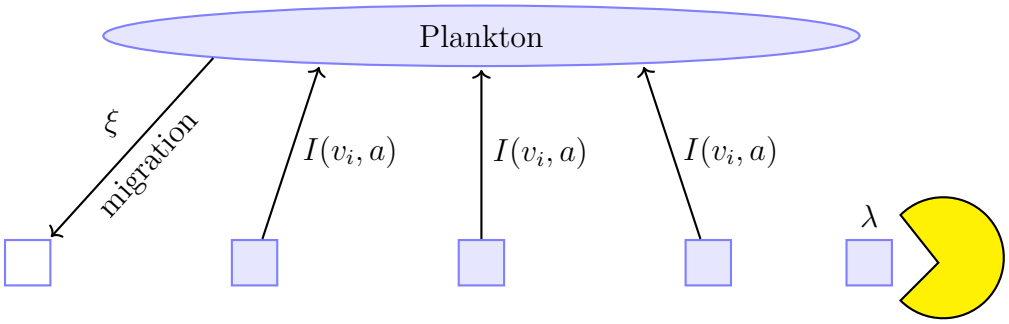

Figure 3.1: Schematic representation of external influences to a population, as happens for example when the bacteria switch between a planktonic lifestyle and growth in microcolonies.

For a 2×2 matrix the eigenvalues have negative real part if and only if $\operatorname{tr}(J) < 0$ and $|J| > 0$. We can assume without loss of generality that $v_1 > v_2$ (which implies $C(v_1) < C(v_2)$) and recover the conditions

$$\operatorname{tr}(J) < 0 \quad \Leftrightarrow \quad \partial_{b_1} B(v,b) C(v_1) b_1 + \partial_{b_2} B(v,b) C(v_2) b_2 < \mu \left(b_1 + b_2\right), \tag{3.1.2a}$$

$$|J| > 0 \quad \Leftrightarrow \quad \partial_{b_1} B(v,b) - \partial_{b_2} B(v,b) > 0. \tag{3.1.2b}$$

We can interpret condition (3.1.2a) as limiting the overall populations growth: the accumulated changes in growth rate are less than the additional death rate through overpopulation. In contrast condition (3.1.2b) states that the subpopulation with higher investment ($C(v_1) < C(v_2)$) also has the higher return ($\partial_{b_1} B(v,b) > \partial_{b_2} B(v,b)$).

In the special case of B as in equation (2.1.6), we can show that this later condition makes sense biologically, as we have

$$\partial_{b_j} B(v,b) = B_{\max} \tau \left(\sum b_i v_i\right) \cdot \frac{2 v_j \sum b_i - \sum b_i v_i}{\left(\left(\sum b_i v_i\right)^2 + \tau \sum b_i\right)^2}$$

$$\partial_{b_1} B(v,b) - \partial_{b_2} B(v,b) = \frac{B_{\max} \tau \left(\sum b_i v_i\right)}{\left(\left(\sum b_i v_i\right)^2 + \tau \sum b_i\right)^2} \cdot 2 \left(\sum b_i\right) (v_1 - v_2).$$

Since we assumed $v_1 > v_2$, condition (3.1.2b) is always fulfilled.

3.2 External influx

We take a look at models with external influx terms, such as the one considered in Mund et al. [Mun+16]. These models assume that a part of the bacteria live in a well-mixed planktonic state, while others separate themselves in order to live in

microcolonies. A fraction of the bacteria from these microcolonies re-migrate into the plankton. A schematic representation of these migrations is given in figure 3.1. If we focus on the planktonic bacteria, we can describe the population with an ODE model that contains an external influx term I signifying the re-migrating bacteria.

$$\begin{aligned} \dot{b_i} &= \left(B(v,b)C(v_i) - \mu\|b\|_1\right) b_i + I(v_i) \cdot \frac{b_i}{\|b\|_1} \\ \Rightarrow \quad G(v_i, v, b) &= B(v,b)C(v_i) - \mu\|b\|_1 + \frac{I(v_i)}{\|b\|_1} \end{aligned}$$

The influx term is dependent on the strategy v_i, as we assume that microcolonies are founded by exactly one bacterium. The development of such a microcolony, and thus the influx term, is then only dependent on its age a and the type (i.e. strategy) of its founding bacterium. As the total influx can be calculated by

$$I(v_i) = \int_0^\infty I(v_i, a)\,\mathrm{d}a,$$

we recover an influx function only dependent on the strategy of its founding bacterium. The influx is then scaled by $\frac{b_i}{\|b\|_1}$, which is the fraction of bacteria in the plankton with strategy v_i. This fraction determines how many bacteria with strategy v_i will separate themselves in order to found microcolonies.

For our purpose, it is enough to know that the influx term is a positive, monotonously increasing function only dependent on v_i. The monotony is given by the fact that a colonies lifespan is normally quite short compared to the mutation timespan. A colony can therefore be considered to contain only bacteria with the founding strategy value. As such, colonies founded by a bacterium with a larger strategy value will grow faster and to higher numbers than colonies with lower strategy values, leading to higher influx terms. Further details on this influx term can be found in Mund et al. [Mun+16]. We take a look at $\partial_1 G$ for this case:

$$\partial_1 G(v_i, v, b) = \begin{pmatrix} \partial_{v_i^s} C(v_i) \cdot B(v,b) + \frac{\partial_{v_i^s} I(v_i)}{\|b\|_1} \\ \partial_{v_i^e} C(v_i) \cdot B(v,b) + \frac{\partial_{v_i^e} I(v_i)}{\|b\|_1} \end{pmatrix}.$$

In order to determine the existence of ESSs, we need to look for roots of $\partial_1 G$. To this end we will again use the cost function proposed in equation (2.1.3), $C(v_i) = \exp\left(-K_e(v_i^e)^2 - K_s(v_i^s)^2\right)$. We find that

$$2K_s v_i^s \exp\left(-K_e(v_i^e)^2 - K_s(v_i^s)^2\right) \cdot B(v,b) = \frac{\partial_{v_i^s} I(v_i)}{\|b\|_1}, \tag{3.2.1}$$

with an equivalent equation for v_i^e. We know that $I(v_i)$ is monotonously increasing in both v_i^s and v_i^e. As such, the left hand side as well as the right hand side of equation (3.2.1) are positive. Whether a stationary point exists is therefore dependent on the exact shape of $I(v_i)$. We determine the Hessian matrix $\partial_1^2 G$:

$$\partial_1^2 G(v_i, v, b) = \begin{pmatrix} H_{1,1} & H_{1,2} \\ H_{1,2} & H_{2,2} \end{pmatrix}$$

with

$$\begin{aligned}
H_{1,1} &= 2K_s \exp\left(-K_e(v_i^e)^2 - K_s(v_i^s)^2\right) \cdot B(v,b)\left(2K_s(v_i^s)^2 - 1\right) + \frac{\partial_{v_i^s}^2 I(v_i)}{\|b\|_1}, \\
H_{1,2} &= 4K_s K_e v_i^s v_i^e \exp\left(-K_e(v_i^e)^2 - K_s(v_i^s)^2\right) \cdot B(v,b) + \frac{\partial_{v_i^s}\partial_{v_i^e} I(v_i)}{\|b\|_1}, \\
H_{2,2} &= 2K_e \exp\left(-K_e(v_i^e)^2 - K_s(v_i^s)^2\right) \cdot B(v,b)\left(2K_e(v_i^e)^2 - 1\right) + \frac{\partial_{v_i^e}^2 I(v_i)}{\|b\|_1}.
\end{aligned}$$

We aim to apply the trace-determinant criterion to determine stability of possible stationary points.

$$\begin{aligned}
|\partial_1^2 G| &= 4K_s K_e C(v_i)^2 B(v,b)^2 \left(1 - 2K_e(v_i^e)^2 - 2K_s(v_i^s)^2\right) \\
&\quad + \frac{2C(v_i)B(v,b)}{\|b\|_1} \cdot \Big(\partial_{v_i^s}^2 I(v_i) K_e(2K_e(v_i^e)^2 - 1) + \partial_{v_i^e}^2 I(v_i) K_s(2K_s(v_i^s)^2 - 1) \\
&\quad - 4K_s K_e v_i^s v_i^e \partial_{v_i^s}\partial_{v_i^e} I(v_i)\Big) \\
&\quad + \frac{1}{\|b\|_1^2}\left(\partial_{v_i^s}^2 I(v_i) \cdot \partial_{v_i^e}^2 I(v_i) - (\partial_{v_i^s}\partial_{v_i^e} I(v_i))^2\right) \\
\operatorname{tr}(\partial_1^2 G) &= 2C(v_i)B(v,b)\left(K_s(2K_s(v_i^s)^2 - 1) + K_e(2K_e(v_i^s)^2 - 1)\right) \\
&\quad + \frac{\partial_{v_i^s}^2 I(v_i) + \partial_{v_i^e}^2 I(v_i)}{\|b\|_1}
\end{aligned}$$

Sadly, it is not possible to determine concrete conditions for $\operatorname{tr}(\partial_1^2 G) < 0$ and $|\partial_1^2 G| > 0$ without choosing a specific functional term for $I(v_i)$.

If one needs to choose a functional term for $I(v_i)$, a good starting point is the equation modelling the growth in microcolonies. We have already reasoned that we can safely ignore mutation in these microcolonies because of the short lifespan. As such, based on equation (2.0.5a) we have for $b(a, v_i)$, the amount of bacteria in a colony of age a and strategy v_i

$$\partial_a b(a, v_i) = \Big(\underbrace{B_{\max} \cdot \frac{v_i^2}{v_i^2 + \tau} \cdot C(v_i)}_{=:f(v_i)} - \mu b\Big) b. \tag{3.2.2}$$

We can solve equation (3.2.2) through separation of variables, getting

$$b(a, v_i) = f(v_i) \exp\left(f(v_i)a\right) \left(\mu \exp\left(f(v_i)a\right) + \frac{f(v_i) - \mu b_0}{b_0}\right)^{-1}. \tag{3.2.3a}$$

Because $f(0) = 0$, $b(a, 0)$ is undefined. But we can calculate the limit for $v_i \to 0$ and define the continuous extension by setting

$$b(a, 0) = \lim_{v_i \to 0} b(a, v_i) = \frac{1}{a\mu + \frac{1}{b_0}}, \tag{3.2.3b}$$

which is a term declining in a, as we have set $B_{\min} = 0$ and thus made growth without QS impossible.

In addition to the population $b(a, v_i)$ in a microcolony, we need to take their lifespan into account. If we assume that the extinction events underlie a Poisson process, then the probability of a microcolony surviving until age a is $\exp(-\lambda a)$, where $\lambda = {}^1/_{\text{Average colony lifespan}}$. We also include a parameter p, which incorporates both the amount of microcolonies as well as the percentage of bacteria that migrate from them, and a parameter ξ that denotes the resettling rate for empty microcolonies. All in all, the influx term is given as

$$I(t, v_i) = \frac{\|b\|_1}{1 + \xi\lambda^{-1}\|b\|_1} \int_0^t \xi p \exp(-\lambda a) b(a, v_i)\, \mathrm{d}v_i. \tag{3.2.4}$$

The upper limit of integration is t, as we assume that there are no colonies at $t = 0$ and thus no colonies with age $a > t$. The pre-factor here is inspired by calculations from Mund et al. [Mun+16]. In order to find the derivative with respect to v_i, we need to derive $b(a, v_i)$:

$$\begin{aligned}\partial_{v_i} b(a, v_i) = f'(v_i) \exp\left(f(v_i)a\right) \left(\mu \exp\left(f(v_i)a\right) + \frac{f(v_i) - \mu b_0}{b_0}\right)^{-1} \\ \cdot \left(-f(v_i)\left(\mu a \exp(f(v_i)a) + \frac{1}{b_0}\right)\left(\mu \exp\left(f(v_i)a\right) + \frac{f(v_i) - \mu b_0}{b_0}\right)^{-1} + 1 + a f(v_i)\right).\end{aligned} \tag{3.2.5a}$$

Again, we find that $\partial_{v_i} b(a, 0)$ is undefined and define it by

$$\partial_{v_i} b(a, 0) = \lim_{v_i \to 0} \partial_{v_i} b(a, v_i) = 0. \tag{3.2.5b}$$

The zero solution is hence a stationary point regardless of parameter values, while there might be any number of additional stationary points. We will come back to these functions in section 6.6.3, where the resulting population dynamics are considered.

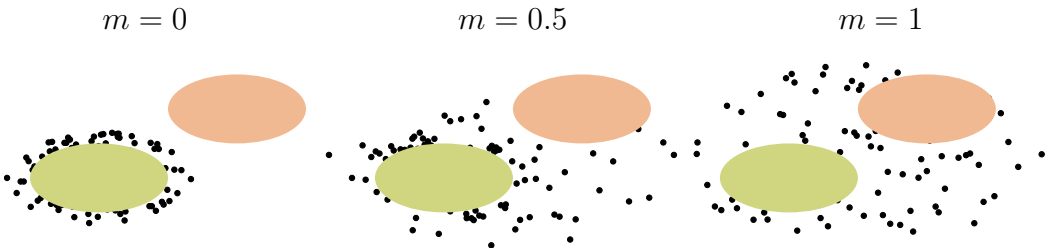

Figure 3.2: Schematic representation how the mixing parameter m influences relations between producing (green) and non-producing (red) bacteria. Black dots signify exoproducts.

3.3 Mixing

Another method to include spatial dependencies in ODEs is to introduce a mixing parameter m. m determines the ratio of external influence on a bacterium versus the self-sensing of bacteria in a fixed matrix, depicted in figure 3.2. A mixing parameter of 1 would signify a completely well-mixed system whose behaviour should resemble section 3.1. In contrast, a mixing parameter of 0 would signify a completely "unmixed", that is separated, system, where each bacterium perceives only its own QS behaviour. In reality, a mixing factor of $m \in (0, 1)$ is more likely than either of the extremes.

We can write the mixed system as

$$G(v_i, v, b) = \left(m \cdot B(v, b) + (1 - m)B(v_i, 1)\right) C(v_i) - \mu \|b\|_1,$$

with our standard terms for B,

$$B(v, b) = B_{\max} \cdot \frac{(\sum_i b_i v_i^s)^2}{(\sum_i b_i v_i^s)^2 + \tau \|b\|_1} \cdot \frac{(\sum_i b_i v_i^e)^2}{(\sum_i b_i v_i^e)^2 + \tau \|b\|_1},$$
$$B(v_i, 1) = B_{\max} \cdot \frac{(v_i^s)^2}{(v_i^s)^2 + \tau} \cdot \frac{(v_i^e)^2}{(v_i^e)^2 + \tau}.$$

As before, we take derivatives with respect to v_i^s in order to find ESSs.

$$\begin{aligned}
\partial_{v_i^s} G(v_i, v, b) &= \left(mB(v, b) + (1 - m)B(v_i, 1)\right)(-2K_s v_i^s) C(v_i) \\
&\quad + (1 - m) B_{max} \cdot \frac{2v_i^s((v_i^s)^2 + \tau) - 2v_i^s (v_i^s)^2}{((v_i^s)^2 + \tau)^2} \cdot \frac{(v_i^e)^2}{(v_i^e)^2 + \tau} C(v_i) \\
&= \left((1 - m) \left(\frac{2v_i^s \tau - 2K_s (v_i^s)^3 ((v_i^s)^2 + \tau)}{((v_i^s)^2 + \tau)^2} \right) \cdot \frac{(v_i^e)^2}{(v_i^e)^2 + \tau} \right. \\
&\quad \left. - 2mK_s v_i^s \cdot \frac{B(v, b)}{B_{max}} \right) \cdot B_{max} C(v_i),
\end{aligned}$$

with an equivalent term for v_i^e. It is clear that $v_i^s = 0$ and $v_i^e = 0$ are stationary solutions. For the sake of readability, we continue our search for positive solutions v_i^s without the term for v_i^e and set $v_i = v_i^s$. This leads to

$$\begin{aligned} 0 &= -2Km \cdot \underbrace{\frac{B(v,b)}{B_{max}}}_{=:\mathcal{B}(v,b)} \cdot \left(v_i^2 + \tau\right)^2 + (1-m)\left(2\tau - 2Kv_i^2(v_i^2+\tau)\right) \\ &= -2Km \cdot \mathcal{B}(v,b) \cdot \left(v_i^4 + 2v_i^2\tau + \tau^2\right) + (1-m)\left(2\tau - 2Kv_i^4 - 2Kv_i^2\tau\right). \end{aligned}$$

Substituting $v_i^2 =: w$ and rearranging results in

$$\begin{aligned} 0 = w^2 &\left(-2K(m\mathcal{B}(v,b) + 1 - m)\right) + w\left(-2K\tau\left(2m\mathcal{B}(v,b) + 1 - m\right)\right) \\ &+ 2\tau\left(-Km\tau\mathcal{B}(v,b) + 1 - m\right) \end{aligned}$$

The discriminant of this equation is

$$D = 4K\tau(1-m)\left(4m\mathcal{B}(v,b) + (1-m)(K\tau+4)\right).$$

We can take a look at the corner cases, $m = 0$ and $m = 1$. For $m = 0$, the "unmixed" state, solutions $w_{1/2}$ are given by

$$w_{1/2} = \frac{2K\tau \pm \sqrt{4K^2\tau^2 + 16K\tau}}{-4K} = \frac{-K\tau \mp \sqrt{K^2\tau^2 + 4K\tau}}{2K}.$$

Hence there always exists exactly one positive solution for w, and thus exactly one positive solution v_i^*, namely $\sqrt{w_2}$. It holds that

$$w_2 < \frac{-K\tau + \sqrt{K^2\tau^2 + 4K\tau + 4}}{2K} = \frac{-K\tau + (K\tau+2)}{2K} = \frac{1}{K},$$

from which we have $0 < v_i^* < \sqrt{1/K}$. A similar calculation for $m = 1$ leads to

$$w_{1/2} = \frac{2K\tau(2\mathcal{B}(v,b)) \pm \sqrt{0}}{-2K\mathcal{B}(v,b)} = -\tau,$$

which means that independently from the parameter values, there can never be a positive stationary point if $m = 1$. As the mixing model with $m = 1$ reverts back to the ODE model without additions, this fits in with our observations from section 3.1.

For $m \in (0,1)$ whether or not positive stationary points exist depends on the exact parameter values. Appel [App16] has analysed this problem in greater depth and shown that there exist stable non-zero strategies for every $0 \leq m < 1$. The

absolute value of these ESSs is dependent on the mixing factor, as can be expected. With lower m, the strategies converge to a higher stable value, while a larger m leads to lower strategy values. m also affects the survival rate of non-producers. In well-mixed conditions, non-producers can thrive on exoproducts of other subpopulations and even outgrow these in the process. In contrast, non-producers are driven to extinction in separated systems.

Chapter 4

Modelling with partial differential equations

In this chapter, we will focus on a biological model for G-functions with PDEs. In contrast to ODEs, PDEs allow us to explicitly model the spatial distribution of bacteria and their QS products. To this end, we introduce a spatial variable x in addition to the time t. As this makes notation more complex, we first fix some notation standards.

From here on, $\Omega \in \mathbb{R}^n$ will denote an open, bounded set, with $S = \partial\Omega$ as its boundary. Ω will be the set from which x is taken, while $t \in [0, T]$. We will call $\Omega \times (0, T) =: Q_T$. Hence $Q_T \in \mathbb{R}^{n+1}$ is also an open and bounded set. Equivalently, we denote $S_T = S \times (0, T)$. The remaining boundaries of Q_T are $\overline{\Omega} \times \{0\} =: B$ as well as $\overline{\Omega} \times \{T\} =: B_T$. $S + B$ is frequently called the normal boundary and contains the initial values (B) as well as the boundary values (S).

We mostly work with Robin boundary conditions where boundary conditions are needed. They are a general form of insulating boundary conditions when working with convection-diffusion equations and can additionally be easily converted to both Dirichlet and Neumann boundary conditions if the biological application calls for those.

Throughout this chapter, we will assume that $\mathcal{L}$ is an operator defined as

$$\mathcal{L} = \frac{\partial}{\partial t} - \sum_{i,j=1}^{n} a_{ij}(x,t)\frac{\partial^2}{\partial x_i \partial x_j} - \sum_{i=1}^{n} b_i(x,t)\frac{\partial}{\partial x_i} - c(x,t), \tag{4.0.1a}$$

where we require that

$$\sum_{i,j}^{n} a_{ij}(x,t)\xi_i\xi_j > 0 \qquad \forall \xi \in \mathbb{R}^n \setminus \{0\}, \forall (x,t) \in Q_T. \tag{4.0.1b}$$

Such an operator is called parabolic in Q_T. Furthermore, we will often assume that the coefficients of $\mathcal{L}$ are continuous functions in Q_T and that for all $(x, t) \in Q_T$

$$|a_{ij}(x,t) - a_{ij}(x^0,t^0)| \leq A\left(|x-x^0|^\delta + |t-t^0|^{\frac{\delta}{2}}\right), \tag{4.0.2a}$$

$$|b_i(x,t) - b_i(x^0,t)| \leq A|x-x^0|^\delta, \tag{4.0.2b}$$

$$|c(x,t) - c(x^0,t)| \leq A|x-x^0|^\delta, \tag{4.0.2c}$$

with $\delta \in (0,1)$. This implies that $\mathcal{L}$ is uniformly parabolic in Q_T, i.e. there exist positive constants $\hat{\mu}, \mu$ independent of (x,t) such that

$$\hat{\mu}|\xi|^2 \leq \sum_{i,j}^{n} a_{ij}(x,t)\xi_i\xi_j \leq \mu|\xi|^2 \qquad \forall \xi \in \mathbb{R}^n.$$

The G-function model with explicit spatial variables can then be written as

$$\mathcal{L}_b b(t,x) = G(v_i, v, b) \cdot b_i, \tag{4.0.3a}$$

$$\mathcal{L}_v v(t,x) = \varepsilon \partial_1 G(v_i, v, b), \tag{4.0.3b}$$

where ε is the time-scaling factor introduced in equation (2.0.3). In order to keep things simple, we will often consider the concrete cases

$$\mathcal{L}_b = \frac{\partial}{\partial t} - D_b \triangle \tag{4.0.4}$$

and

$$\mathcal{L}_v = \frac{\partial}{\partial t} - D_v \triangle, \tag{4.0.5a}$$

$$\mathcal{L}'_v = \frac{\partial}{\partial t}, \tag{4.0.5b}$$

with D_b and D_v positive constants.

All of these operators concentrate on growth, evolution and diffusion, omitting other spatial effects like chemotaxis. We will call a model consisting of operators (4.0.4) and (4.0.5a) a fully parabolic model, as both equation parts contain parabolic operators, and discuss it further in section 4.1. If we instead combine (4.0.4) with (4.0.5b), we call the resulting system a coupled ODE-PDE system. The operator $\mathcal{L}'_v$ is not parabolic and equation (4.0.3b) reverts back to an ODE. This sort of system is investigated in section 4.2.

4.1 Fully parabolic case

For the fully parabolic model, we assume that both bacteria and strategies underlie diffusion with positive constants D_b and D_v and thus use (4.0.4) and (4.0.5a) for

the operators $\mathcal{L}_b$ and L_v. If we take $\varepsilon' := \varepsilon \cdot D_v$, we can drop the subscript for D_b in order to simplify notation. The system then reads

$$\partial_t b_i(x,t) = G\Big(v_i(x,t), v(x,t), b(x,t)\Big) \cdot b_i(x,t) + D \triangle b_i(x,t), \tag{4.1.1a}$$

$$\partial_t v_i(x,t) = \varepsilon \partial_1 G\Big(v_i(x,t), v(x,t), b(x,t)\Big) + \varepsilon' \triangle v_i(x,t). \tag{4.1.1b}$$

A slightly more complex version has been proposed by Kronik and Cohen [KC09]:

$$\partial_t b_i(x,t) = G\Big(v_i(x,t), v(x,t), b(x,t)\Big) \cdot b_i(x,t) + D \triangle b_i(x,t), \tag{4.1.2a}$$

$$\partial_t v_i(x,t) = \varepsilon \partial_1 G\Big(v_i(x,t), v(x,t), b(x,t)\Big) + D \triangle v_i(x,t) + \frac{2D \nabla b_i(x,t) \cdot \nabla v_i(x,t)}{b_i(x,t)}. \tag{4.1.2b}$$

It is based on the assumption that it is not the strategies themselves that undergo changes, but rather the frequency with which they are employed. To that end Kronik and Cohen fix a set of N_i phenotypes j of subpopulation i and call the corresponding constant strategy v_{ij}, with population density b_{ij}. They then recover the overall strategy of subpopulation i as the weighted average of the phenotypes:

$$b_i(x,t) = \sum_{j=1}^{N_i} b_{ij}(x,t), \qquad v_i(x,t) = \sum_{j=1}^{N_i} \frac{b_{ij}(x,t) v_{ij}}{b_i(x,t)}.$$

Equation (4.1.2) is the result of differentiating these equations.

4.1.1 Coupled upper-lower-solutions

We concern ourselves with existence and uniqueness of solutions to systems (4.1.1) and (4.1.2), as well as the more general system (4.0.3).

In order to prove existence of smooth solutions to our parabolic systems, we will employ the method of upper-lower-solutions. But there is the added difficulty of the G-function not being monotonous, since bacterial subpopulations can have both a helpful, symbiotic effect on each other through QS as well as a competitive and therefore negative effect by using up resources.

Abudiab, Ahn, and Li have introduced the concept of *coupled* upper-lower-solutions for non-monotonous cases in [AAL11]. We will follow their definition, but extend it to account for dependencies on the gradients.

In the following, we will often talk about a vector of the form

$$(v_1, \ldots, v_{i-1}, u_i, v_{i+1}, \ldots, v_m, \nabla v_1, \ldots, \nabla v_{i-1}, \nabla u_i, \nabla v_{i+1}, \ldots, \nabla v_m). \tag{4.1.3}$$

In order to shorten notation, we will abbreviate equation (4.1.3) by

$$(v[u_i], D_x v[D_x u_i]),$$

while $(v, D_x v)$ denotes the "homogeneous" vector $(v_1, \dots, v_m, \nabla v_1, \dots, \nabla v_m)$. A definition of the norm $\|\cdot\|_{2+\delta, Q_T}$ can be found in definition A.2. When it is possible to do so without confusion, we will omit the Q_T and write $\|\cdot\|_{2+\delta}$.

Definition 4.1. *Two functions $\overline{u}_i, \underline{u}_i \in C^{2+\delta, 1+\delta/2}(\overline{\Omega} \times [0,T])$, with $\Omega \subset \mathbb{R}^n$, $\delta \in (0,1)$ and $\|\overline{u}_i\|_{2+\delta}, \|\underline{u}_i\|_{2+\delta} \leq K$ for a positive constant K, are called **coupled upper-lower-solutions** of the parabolic system*

$$\mathcal{L}_i u_i := \partial_t u_i - d_i \triangle u_i = f_i(u_1, \dots, u_m, \nabla u_1, \dots, \nabla u_m, x) \quad \text{in } Q_T \tag{4.1.4a}$$

$$\alpha_i u_i + \beta_i \frac{\partial u_i}{\partial n} = \psi_i(u_1, \dots, u_{i-1}, u_{i+1}, \dots, u_m, x) \quad \text{in } S_T \tag{4.1.4b}$$

$$u_i(x,0) = u_i^0(x) \quad \text{in } \Omega \tag{4.1.4c}$$

with $\alpha_i, \beta_i \in C^{1+\delta,(1+\delta)/2}(\overline{S}_T)$, $\beta_i > 0$, $f_i \in C^\delta([\inf \underline{u}, \sup \overline{u}] \times B_{m\cdot n, K}(0) \times \overline{\Omega}, \mathbb{R})$, $\psi \in C^{1+\delta}(B_{(m-1),K}(0) \times \overline{\Omega})$, $u_i^0 \in C^{2+\delta}(\overline{\Omega})$, if for all $i \in [m]$ it holds that:

(i) $\overline{u}_i \geq \underline{u}_i$

(ii) $\mathcal{L}_i \overline{u}_i \geq \overline{f}_i =: \sup_{\underline{u}_j \leq \xi_j \leq \overline{u}_j} f_i(\xi[\overline{u}_i], D_x \xi[D_x \overline{u}_i], x) \quad \text{in } \overline{Q}_T$

(iii) $\alpha_i \overline{u}_i + \beta_i \frac{\partial \overline{u}_i}{\partial n} \geq \sup_{\underline{u}_j \leq \xi_j \leq \overline{u}_j} \psi_i(\xi_1, \dots, \xi_{i-1}, \xi_{i+1}, \xi_m, x) \quad \text{in } \overline{S}_T$

(iv) $\overline{u}_i(x,0) \geq u_i^0(x)$

(v) $\mathcal{L}_i \underline{u}_i \leq \underline{f}_i =: \inf_{\underline{u}_j \leq \xi_j \leq \overline{u}_j} f_i(\xi[\underline{u}_i], D_x \xi[D_x \underline{u}_i], x) \quad \text{in } \overline{Q}_T$

(vi) $\alpha_i \underline{u}_i + \beta_i \frac{\partial \underline{u}_i}{\partial n} \leq \inf_{\underline{u}_j \leq \xi_j \leq \overline{u}_j} \psi_i(\xi_1, \dots, \xi_{i-1}, \xi_{i+1}, \xi_m, x) \quad \text{in } \overline{S}_T$

(vii) $\underline{u}_i(x,0) \leq u_i^0(x)$.

If the f_i fulfil certain additional assumptions, we can make the following statement about problems which have coupled upper-lower-solutions:

Theorem 4.1. *Let f_i in system (4.1.4) be uniformly Lipschitzian in all variables, independent of x, for bounded $\xi = (\xi_1, \dots, \xi_m) \in \mathbb{R}^m$. Additionally, assume that there exists a function $L \in C^\delta(\mathbb{R}^{m-1} \times \mathbb{R}^{n(m-1)}, \mathbb{R}^n)$, such that f_i fulfils the following condition:*

$$\begin{aligned} f_i(\xi[u_i], D_x\xi[D_x u_i], x) - f_i(\xi[\tilde{u}_i], D_x\xi[D_x \tilde{u}_i], x) \\ \leq P_i |u_i - \tilde{u}_i| + L(\xi, D_x\xi)\,(D_x \tilde{u}_i - D_x u_i)\,. \end{aligned} \tag{4.1.5}$$

If $\underline{u}$ and $\overline{u}$ are coupled upper-lower solutions of the parabolic system (4.1.4), then there exists a solution $u = (u_1, \ldots, u_m)$, where $u_i(x,t) \in C^{2+\delta,1+\delta/2}(\overline{\Omega}, [0,T])$, to the system (4.1.4), such that $\underline{u}_i \leq u_i \leq \overline{u}_i$.

Proof. We define the set

$$\begin{gathered} K := \{\theta = (\theta_1, \cdots, \theta_m) \in \bigoplus_{i=1}^{m} C^{2+\delta,1+\delta/2}(\overline{\Omega}, [0,T]) : \\ \underline{u}_i \leq \theta_i \leq \overline{u}_i, \\ \alpha_i \underline{u}_i + \beta_i \frac{\partial \underline{u}_i}{\partial n} \leq \alpha_i \theta_i + \beta_i \frac{\partial \theta_i}{\partial n} \leq \alpha_i \overline{u}_i + \beta_i \frac{\partial \overline{u}_i}{\partial n}, \\ \underline{u}_i(x,0) \leq \theta_i(x,0) \leq \overline{u}_i(x,0), \\ \|\theta_i(x,0)\|_{2+\delta,\Omega} \leq C_0, \\ \|\theta_i\|_{1+\delta} \leq C_1, \\ i = 1, \cdots, m\}. \end{gathered}$$

We will fix a value for δ later on. Additionally, we define an Operator T with $T(\theta) = v$ such that v is the solution of

$$(v_i)_t - d_i \triangle v_i + P_i v_i + L(\theta, D_x\theta) D_x v_i = P_i \theta_i + L(\theta, D_x\theta) D_x \theta_i + f_i(\theta, D_x\theta, x) \quad \text{in } Q_T \tag{4.1.6a}$$

$$\alpha_i v_i + \beta_i \frac{\partial v_i}{\partial n} = \psi_i(\theta_1, \cdots, \theta_{i-1}, \theta_{i+1}, \cdots, \theta_m) \quad \text{in } S_T \tag{4.1.6b}$$

$$v_i(x,0) = \theta_i(x,0) \quad \text{on } \Omega. \tag{4.1.6c}$$

T is well-defined, as equation (4.1.6) has a unique solution for all $\theta \in K$ (see e.g. theorem A.11). The set K has the following properties:

K is non-empty As $\underline{u}_i, \overline{u_i} \in K$, $K \neq \emptyset$.

K is closed and convex Both properties are easy to see.

$T(K) \subseteq K$ In order to show that the operator T maps K to K, we check if v has the properties required to be an element of K.

- $\underline{u}_i \leq v_i \leq \overline{u}_i \quad \forall i = 1, \ldots, m$
  From definitions 4.1.(ii) and 4.1.(iii) we have that

$$\begin{gathered} (\overline{u}_i)_t - d_i \triangle \overline{u}_i + P_i \overline{u}_i + L(\theta, D_x\theta) D_x \overline{u}_i \\ \geq P_i \overline{u}_i + L(\theta, D_x\theta) D_x \overline{u}_i + f_i(\theta[\overline{u}_i], D_x\theta[D_x\overline{u}_i], x) \quad \text{in } Q_T \\ \alpha_i \overline{u}_i + \beta_i \frac{\partial \overline{u}_i}{\partial n} \geq \psi_i(\theta_1, \cdots, \theta_{i-1}, \theta_{i+1}, \cdots, \theta_m) \quad \text{in } S_T \\ \overline{u}_i(x,0) \geq \theta_i(x,0) \quad \text{on } \Omega. \end{gathered}$$

We subtract (4.1.6a) from these equations and use definition 4.1.(ii), getting

$$\begin{aligned}(\overline{u}_i - v_i)_t - d_i \triangle(\overline{u}_i - v_i) + P_i(\overline{u}_i - v_i) + L(\theta, D_x\theta)D_x(\overline{u}_i - v_i) \\ \geq P_i(\overline{u}_i - \theta_i) + L(\theta, D_x\theta)(D_x\overline{u}_i - D_x\theta_i) \\ + f_i(\theta[\overline{u}_i], D_x\theta[D_x\overline{u}_i], x) - f_i(\theta, D_x\theta, x).\end{aligned}$$

We transform equation (4.1.5)

$$\begin{aligned} & f_i(\theta, D_x\theta, x) - f_i(\theta[\overline{u}_i], D_x\theta[D_x\overline{u}_i], x) \\ & \qquad \leq P_i|\overline{u}_i - \theta_i| + L(\theta, D_x\theta)\,(D_x\overline{u}_i - D_x\theta_i) \\ \Rightarrow \quad & f_i(\theta[\overline{u}_i], D_x\theta[D_x\overline{u}_i], x) - f_i(\theta, D_x\theta, x) \\ & \qquad \geq -P_i|\overline{u}_i - \theta_i| - L(\theta, D_x\theta)\,(D_x\overline{u}_i - D_x\theta_i)\,,\end{aligned}$$

where $|\overline{u}_i - \theta_i| = \overline{u}_i - \theta_i$, since $\theta_i \in K$. We thus have

$$\begin{aligned}(\overline{u}_i - v_i)_t - d_i \triangle(\overline{u}_i - v_i) + P_i(\overline{u}_i - v_i) + L(\theta, D_x\theta)D_x(\overline{u}_i - v_i) \\ \geq P_i(\overline{u}_i - \theta_i) - P_i(\overline{u}_i - \theta_i) \\ + L(\theta, D_x\theta)(D_x\overline{u}_i - D_x\theta_i) - L(\theta, D_x\theta)(D_x\overline{u}_i - D_x\theta_i) \\ \geq 0\end{aligned}$$

From the comparison theorem (theorem A.4) it follows that $\overline{u}_i \geq v_i$. Equivalent calculations give us $\underline{u}_i \leq v_i$, hence $\|v_i\|_0 \leq M_0 = \max_i(\|\underline{u}_i\|_0, \|\overline{u}_i\|_0)$.

- Boundary Conditions

$$\begin{aligned}\alpha_i\underline{u}_i + \beta_i\frac{\partial\underline{u}_i}{\partial n} &\leq \inf_{\underline{u}_j \leq \xi_j \leq \overline{u}_j} \psi_i(\xi_1, \ldots, \xi_{i-1}, \xi_{i+1}, \xi_m, x) \\ &\leq \psi_i(\theta_1, \cdots, \theta_{i-1}, \theta_{i+1}, \cdots, \theta_m) \\ \alpha_i\overline{u}_i + \beta_i\frac{\partial\overline{u}_i}{\partial n} &\geq \sup_{\underline{u}_j \leq \xi_j \leq \overline{u}_j} \psi_i(\xi_1, \ldots, \xi_{i-1}, \xi_{i+1}, \xi_m, x) \\ &\geq \psi_i(\theta_1, \cdots, \theta_{i-1}, \theta_{i+1}, \cdots, \theta_m) \\ \overset{(4.1.6)}{\Rightarrow} \alpha_i\underline{u}_i + \beta_i\frac{\partial\underline{u}_i}{\partial n} &\leq \alpha_i v_i + \beta_i\frac{\partial v_i}{\partial n} \leq \alpha_i\overline{u}_i + \beta_i\frac{\partial\overline{u}_i}{\partial n}\end{aligned}$$

- Initial Conditions

$$\underline{u}_i(x, 0) \leq \theta_i(x, 0) = v_i(x, 0) \leq \overline{u}_i(x, 0)$$

- Regularity
  From $P_i\theta_i + L(\theta, D_x\theta)D_x\theta_i + f_i(\theta_1, \cdots, \theta_m, x) \in C^\delta$ we immediately get that $v_i \in C^{2+\delta,1+\delta/2}(\overline{\Omega}, [0,T])$.

- Boundedness
  The first part is simple, as

$$v_i^0(x) = \theta_i^0(x) \Rightarrow \left\|v_i^0(x)\right\|_{2+\delta,\Omega} = \left\|\theta_i^0(x)\right\|_{2+\delta,\Omega} \leq C_0.$$

  For the norm in $\bar{Q}_T$, we use theorem A.9. That means we have $\|v_i\|_{1+\delta'} \leq C$, where δ', C depend only on $M_0, c, \mu, \|v_i^0(x)\|_2$ and S. As such, we can find a common δ and C_1 for which the inequality holds. This also determines the value for δ that we left open until now.

***T* is continuous** We take two solutions, $v_i = T(\theta)$ and $\tilde{v}_i = T(\tilde{\theta})$ and consider the difference. It follows that for $\delta v_i = v_i - \tilde{v}_i$ and $\delta\theta_i = \theta_i - \tilde{\theta}_i$ it holds

$$\begin{aligned}
&(\delta v_i)_t - d_i \triangle(\delta v_i) + P_i(\delta v_i) + L(\theta, D_x\theta)D_x v_i - L(\tilde{\theta}, D_x\tilde{\theta})D_x\tilde{v}_i \\
&= P_i\delta\theta_i + L(\theta, D_x\theta)D_x\theta_i - L(\tilde{\theta}, D_x\tilde{\theta})D_x\tilde{\theta}_i + f_i(\theta, D_x\theta, x) - f_i(\tilde{\theta}, D_x\tilde{\theta}, x) \\
&\delta v_i(x,0) = \delta\theta_i(x,0) \\
\alpha_i\delta v_i + \beta_i\frac{\partial\delta v_i}{\partial n} &= \psi_i(\theta_1, \cdots, \theta_{i-1}, \theta_{i+1}, \cdots, \theta_m) - \psi_i(\tilde{\theta}_1, \cdots, \tilde{\theta}_{i-1}, \tilde{\theta}_{i+1}, \cdots, \tilde{\theta}_m).
\end{aligned}$$

We aim to apply theorem A.11. To that end we reformulate some parts of the equation:

$$\begin{aligned}
L(\theta, D_x\theta)D_x v_i - L(\tilde{\theta}, D_x\tilde{\theta})D_x\tilde{v}_i &= L(\theta, D_x\theta)D_x(v_i - \tilde{v}_i) \\
&\quad + \left(L(\theta, D_x\theta) - L(\tilde{\theta}, D_x\tilde{\theta})\right) D_x\tilde{v}_i
\end{aligned}$$

and thus

$$\begin{aligned}
&(\delta v_i)_t - d_i \triangle(\delta v_i) + P_i(\delta v_i) + L(\theta, D_x\theta)D_x(\delta v_i) \\
&\quad = P_i\delta\theta_i + L(\theta, D_x\theta)D_x\theta_i - L(\tilde{\theta}, D_x\tilde{\theta})D_x\tilde{\theta}_i \\
&\quad\quad - \left(L(\theta, D_x\theta) - L(\tilde{\theta}, D_x\tilde{\theta})\right) D_x\tilde{v}_i + f_i(\theta, D_x\theta, x) - f_i(\tilde{\theta}, D_x\tilde{\theta}, x).
\end{aligned}$$

We know further that

$$\begin{aligned}
&\left\|L(\theta, D_x\theta)D_x\theta_i - L(\tilde{\theta}, D_x\tilde{\theta})D_x\tilde{\theta}_i + \left(L(\theta, D_x\theta) - L(\tilde{\theta}, D_x\tilde{\theta})\right) D_x\tilde{v}_i\right\|_\delta \\
&\leq \|L(\theta, D_x\theta)D_x\delta\theta\|_\delta + \left\|\left(L(\theta, D_x\theta) - L(\tilde{\theta}, D_x\tilde{\theta})\right)\left(D_x\tilde{\theta} - D_x\tilde{v}_i\right)\right\|_\delta,
\end{aligned}$$

using the multiplication inequality, Lipschitz continuity of L as well as the boundedness of v_i and θ, we get

$$\begin{aligned}&\leq \|L(\theta, D_x\theta)\|_\delta \|D_x\delta\theta\|_\delta + (\|\delta\theta\|_\delta + \|\delta D_x\theta\|_\delta)\, 2C_1\\ &\leq K_1\|\delta\theta\|_{2+\delta}.\end{aligned}$$

It also holds that $\|P_i\delta\theta_i\|_\delta \leq P_i\|\delta\theta\|_{2+\delta}$ and because of the Lipschitz continuity of f_i

$$\begin{aligned}\left\|f_i(\theta, D_x\theta, x) - f_i(\tilde{\theta}, D_x\tilde{\theta}, x)\right\|_\delta &\leq K_2\|\delta\theta\|_\delta + K_2\|D_x\delta\theta\|_\delta\\ &\leq K_2\|\delta\theta\|_{2+\delta},\end{aligned}$$

with a similar estimate for ψ_i. We can thus conclude from theorem A.11 that

$$\|\delta v_i\|_{2+\delta} \leq K_3\|\delta\theta\|_{2+\delta}.$$

***T* has a compact image** We use a version of Arzelà-Ascoli, defined in theorem A.7 to prove that K is compact, taking $D = \bar{\Omega} \times [0, T]$ as compact metric space. Then $T(K)$ is compact as a continuous mapping of a compact space. As we already know that K is closed, we only need to show boundedness and equicontinuity. Both can be derived from the fact that for $\theta \in K$ it holds that $\|\theta_i\|_{1+\delta} \leq C_1$. This implies on the one hand that $\|\theta_i\|_0 \leq C_1$ as well, which guarantees boundedness of K. On the other hand, the equicontinuity can be derived from the Holder continuity of all functions $\theta \in K$ with a common Holder constant.

Schauders fixed point theorem (see page 167) now guarantees a fixed point $T(v) = v \in K \subset C^{2+\delta,1+\delta/2}(\overline{\Omega}, [0, T])$, which is the desired solution. □

While this proves existence of classical solutions to equation (4.1.4), there is no statement about uniqueness as of yet. We will prove such a statement in the next section. But first we concern ourselves with the application of theorem 4.1 to our equations. To that end, we identify $u = (b, v)$. We first note the following:

Theorem 4.2. *The function*

$$f_i(u, D_x u) = \varepsilon\partial_1 G(v_i, v, b) + \frac{2d_i\nabla b_i \cdot \nabla v_i}{b_i}$$

fulfils the assumption from equation (4.1.5)*, namely*

$$\begin{aligned}\varepsilon\partial_1 G(v_i, v, b) + \frac{2d_i\nabla b_i \cdot \nabla v_i}{b_i} - \varepsilon\partial_1 G(\tilde{v}_i, \tilde{v}, b) + \frac{2d_i\nabla b_i \cdot \nabla \tilde{v}_i}{b_i}\\ \leq P_i|v_i - \tilde{v}_i| + L(b_i, \nabla b_i)\left(\nabla\tilde{v}_i - \nabla v_i\right),\end{aligned} \tag{4.1.7}$$

with

$$L(b_i, \nabla b_i) = \frac{-2d_i \nabla b_i}{b_i}$$

Holder continuous with Holder constant δ *if* $b_i \geq \gamma > 0$ *and* $b_i \in C^{1+\delta}$.

Proof. We start by proving equation (4.1.7). To that end, we recall that $\partial_1 G$ is Lipschitz continuous by assumption. If we denote the Lipschitz factor by P_i, we have

$$\begin{aligned}\varepsilon\partial_1 G(v_i, v, b) - \varepsilon\partial_1 G(\tilde{v}_i, \tilde{v}, b) &\leq |\varepsilon\partial_1 G(v_i, v, b) - \varepsilon\partial_1 G(\tilde{v}_i, \tilde{v}, b)| \\ &\leq P_i |v_i - \tilde{v}_i|.\end{aligned}$$

On the other hand,

$$\begin{aligned}\frac{2d_i \nabla b_i \cdot \nabla v_i}{b_i} - \frac{2d_i \nabla b_i \cdot \nabla \tilde{v}_i}{b_i} &= \frac{2d_i \nabla b_i}{b_i} (\nabla v_i - \nabla \tilde{v}_i) \\ &= \frac{-2d_i \nabla b_i}{b_i} (\nabla \tilde{v}_i - \nabla v_i).\end{aligned}$$

In order to show the Holder continuity, we take a look at the j-th component of L

$$\begin{aligned}L_j(b_i, \nabla b_i) &= \frac{-2d_i \partial_{x_j} b_i}{b_i} \\ \Rightarrow \quad |L_j(b_i, \nabla b_i)|^{(0)} &\leq \frac{2d_i \left|\partial_{x_j} b_i\right|^{(0)}}{\gamma}.\end{aligned}$$

The assumption $b_i \in C^{1+\delta}$ implies that $\left|\partial_{x_j} b_i\right|^{(0)}$ has a finite value. Therefore $|L_j(b_i, \nabla b_i)|^{(0)}$ has a finite value as well. Meanwhile,

$$\begin{aligned}&L_j(b_i(x,t), \nabla b_i(x,t)) - L_j(b_i(x',t), \nabla b_i(x',t)) \\ &\quad = \frac{-2d_i \partial_{x_j} b_i(x,t)}{b_i(x,t)} - \frac{-2d_i \partial_{x_j} b_i(x',t)}{b_i(x',t)} \\ &\quad = \frac{-2d_i \left(\partial_{x_j} b_i(x,t) - \partial_{x_j} b_i(x',t)\right)}{b_i(x,t)} + \frac{-2d_i \partial_{x_j} b_i(x',t)}{b_i(x,t)} - \frac{-2d_i \partial_{x_j} b_i(x',t)}{b_i(x',t)} \\ &\quad = \frac{-2d_i}{b_i(x,t)} \left(\partial_{x_j} b_i(x,t) - \partial_{x_j} b_i(x',t)\right) + \frac{-2d_i \partial_{x_j} b_i(x',t)}{b_i(x,t) b_i(x',t)} (b_i(x',t) - b_i(x,t))\end{aligned}$$

and thus

$$\langle L_j(b_i, \nabla b_i)\rangle_x^{(\delta)} \leq \frac{2d_i}{\gamma}\langle \partial_{x_j} b_i\rangle_x^{(\delta)} + \frac{2d_i\left|\partial_{x_j} b_i\right|^{(0)}}{\gamma^2}\langle b_i\rangle_x^{(\delta)}.$$

Taken together, we have shown that L is in C^δ under the given assumptions. □

We construct specific upper and lower solutions for equation (4.1.1). In order to keep thing simple, we will use homogeneous Robin boundary conditions, that means

$$\alpha_i u_i + \beta_i \frac{\partial u_i}{\partial n} = 0, \tag{4.1.8}$$

and starting conditions that fulfil

$$0 < b_i^0(x) < \frac{G_{\max}}{\mu}, \qquad 0 \leq v_i^0(x) \leq v^*. \tag{4.1.9}$$

We can then take

$$\begin{aligned} \underline{b}_i &= \inf_{x\in\Omega} b_i^0(x) \cdot \exp(-G_{\max} m t), \quad \text{if } \alpha_i \leq 0 \\ \underline{b}_i &= C\Phi(x) \cdot \exp(-(G_{\max} m + \lambda d_i)t), \quad \text{else,} \end{aligned} \tag{4.1.10a}$$

$$\overline{v}_i = v^*, \text{ see assumption (IV) on page 26} \tag{4.1.10b}$$

$$\underline{v}_i = 0, \tag{4.1.10c}$$

where $\Phi(x)$ is an eigenfunction to the eigenvalue problem

$$-\triangle\Phi = \lambda\Phi, \quad x \in \Omega \qquad \alpha\Phi + \beta\frac{\partial\Phi}{\partial n} = 0, \quad x \in \partial\Omega$$

and $C \in \mathbb{R}$ chosen in a way that $C\Phi(x) \leq b_i^0(x)$. If we take λ to be the principal eigenvalue, it is both real and nonnegative, and we can choose Φ to be positive.

We define $\overline{b}_i$ as the solution of

$$\partial_t \overline{b}_i - d_i \triangle \overline{b}_i = (G_{\max} - \mu\overline{b}_i)\cdot \overline{b}_i \quad \text{in } \Omega \tag{4.1.10d}$$

$$\alpha_i \overline{b}_i + \beta_i \frac{\partial \overline{b}_i}{\partial n} = 0 \quad \text{in } \partial\Omega \tag{4.1.10e}$$

$$\overline{b}_i(x,0) = b_i^0(x). \tag{4.1.10f}$$

Theorem 4.3. *The functions $\overline{u} = (\overline{b}, \overline{v})^T, \underline{u} = (\underline{b}, \underline{v})^T$ defined in equation* (4.1.10) *are coupled upper-lower solutions for the system* (4.1.1) *with conditions* (4.1.8) *and* (4.1.9).

Proof. We prove that the chosen functions fulfil definitions 4.1.(i) to 4.1.(vii). As constants or solutions to a semi-linear problem with smooth enough coefficients, all functions lie in $C^{2+\delta,1+\delta/2}(\overline{\Omega}\times[0,T])$.

Checking definition 4.1.(ii)

$$\begin{aligned}
\partial_t \overline{b}_i - d_i \triangle \overline{b}_i &= (G_{\max} - \mu \overline{b}_i)\overline{b}_i \\
&\geq \sup_{\underline{u}_j \leq \xi_j \leq \overline{u}_j} G(\xi_{m+i}, (\xi_{m+1}, \ldots, \xi_{2m}), (\xi_1, \ldots, \overline{b}_i, \ldots, \xi_m))\overline{b_i} \\
&= \sup_{\underline{u}_j \leq \xi_j \leq \overline{u}_j} f_i(\xi_1, \ldots, \xi_{i-1}, \overline{b}_i, \xi_{i+1}, \ldots, \xi_{2m}, x) \\
\partial_t \overline{v}_i - d_i \triangle \overline{v}_i &= 0 \\
&\geq \sup_{\underline{u}_j \leq \xi_j \leq \overline{u}_j} \underbrace{\partial_1 G(\overline{v}_i, (\xi_{m+1}, \ldots, \xi_{2m}), (\xi_1, \ldots, \xi_m))}_{\leq 0} + \frac{2\nabla \xi_i \cdot 0}{\xi_i} \\
&= \sup_{\underline{u}_j \leq \xi_j \leq \overline{u}_j} f_{m+i}(\xi_1, \ldots, \xi_{m+i-1}, \overline{v}_i, \xi_{m+i+1}, \ldots, \xi_{2m}, x),
\end{aligned}$$

where we have taken advantage of assumption (IV).

Checking definition 4.1.(iii)

$$\begin{aligned}
\alpha \overline{b}_i + \beta \frac{\partial \overline{b}_i}{\partial n} = 0 &= \sup_{\underline{u}_j \leq \xi_j \leq \overline{u}_j} \psi_i(\xi_1, \ldots, \xi_{i-1}, \xi_{i+1}, \ldots, \xi_{2m}, x) \\
\alpha \overline{v}_i + \beta \frac{\partial \overline{v}_i}{\partial n} = 0 &= \sup_{\underline{u}_j \leq \xi_j \leq \overline{u}_j} \psi_{m+i}(\xi_1, \ldots, \xi_{m+i-1}, \xi_{m+i+1}, \ldots, \xi_{2m}, x)
\end{aligned}$$

Checking definition 4.1.(iv)

$$\overline{b}_i(0, x) = b_i^0(x), \quad \overline{v}_i \geq v_i^0(x)$$

Checking definition 4.1.(v) If $\alpha_i \leq 0$, we have

$$\begin{aligned}
\partial_t \underline{b}_i - d_i \triangle \underline{b}_i &= -G_{\max} m \underline{b}_i^0 \exp(-G_{\max} m t) \\
&= -\mu \left(\sum_{j=1}^{m} \frac{G_{\max}}{\mu} \right) \underline{b}_i^0 \exp(-G_{\max} m t) \\
&\leq -\mu \left(\sum_{j=1}^{m} \overline{b}_i \right) \underline{b}_i \\
&\leq \inf_{\underline{u}_j \leq \xi_j \leq \overline{u}_j} G(\xi_{m+i}, (\xi_{m+1}, \ldots, \xi_{2m}), (\xi_1, \ldots, 0, \ldots, \xi_m)) \cdot \underline{u}_i \\
&\leq \inf_{\underline{u}_j \leq \xi_j \leq \overline{u}_j} f_i(\xi_1, \ldots, \xi_{i-1}, \underline{b}_i, \xi_{i+1}, \ldots, \xi_{2m}, x).
\end{aligned}$$

If on the other hand $\alpha_i \not\leq 0$, we have

$$\begin{aligned}\partial_t \underline{b}_i - d_i \triangle \underline{b}_i &= C\Phi(x)\exp\left(-(G_{\max}m + \lambda d_i)t\right)\left(-G_{\max}m - \lambda d_i\right)\\ &\quad + d_i C\exp\left(-(G_{\max}m + \lambda d_i)t\right)\left(-\triangle\Phi(x)\right)\\ &= C\Phi(x)\exp\left(-(G_{\max}m + \lambda d_i)t\right)\left(-G_{\max}m - \lambda d_i + \lambda d_i\right)\\ &= \underline{b}_i\left(-G_{\max}m\right)\end{aligned}$$

from which we can continue as before. For v_i it holds that

$$\begin{aligned}\partial_t \underline{v}_i - \varepsilon' \triangle \underline{v}_i = 0 &= \inf_{\underline{u}_j \leq \xi_j \leq \overline{u}_j} \partial_1 G(0, (\xi_{m+1}, \ldots, \xi_{2m}), (\xi_1, \ldots, \xi_m))\\ &= \inf_{\underline{u}_j \leq \xi_j \leq \overline{u}_j} f_{m+i}(\xi_1, \ldots, \xi_{m+i-1}, \underline{v}_i, \xi_{m+i+1}, \ldots, \xi_{2m}, x),\end{aligned}$$

where the second equality is due to assumption (IV).

Checking definition 4.1.(vi) If $\alpha_i \leq 0$, we can conclude from the positivity of $\underline{b}_i$ and its independence of x that

$$\alpha_i \underline{b}_i + \beta_i \frac{\partial \underline{b}_i}{\partial n} \leq 0 = \inf_{\underline{u}_j \leq \xi_j \leq \overline{u}_j} \psi_i(\xi_1, \ldots, \xi_{i-1}, \xi_{i+1}, \ldots, \xi_{2m}, x).$$

In the case $\alpha_i \not\leq 0$

$$\begin{aligned}\alpha_i \underline{b}_i + \beta_i \frac{\partial \underline{b}_i}{\partial n} &= C\exp\left(-(G_{\max}m + \lambda d_i)t\right)\left(\alpha_i\Phi(x) + \beta_i \frac{\partial \Phi(x)}{\partial n}\right)\\ &= 0 = \inf_{\underline{u}_j \leq \xi_j \leq \overline{u}_j} \psi_i(\xi_1, \ldots, \xi_{i-1}, \xi_{i+1}, \ldots, \xi_{2m}, x).\\ \alpha_i \underline{v}_i + \beta_i \frac{\partial \underline{v}_i}{\partial n} &= 0 = \inf_{\underline{u}_j \leq \xi_j \leq \overline{u}_j} \psi_{m+i}(\xi_1, \ldots, \xi_{m+i-1}, \xi_{m+i+1}, \ldots, \xi_{2m}, x)\end{aligned}$$

Checking definition 4.1.(vii)

$$\begin{aligned}\underline{b}_i^0 = \inf_{x\in\Omega} b_i^0(x) \leq b_i^0(x) = u_i^0(x) \quad \text{for } \alpha_i \leq 0\\ \underline{b}_i^0 = C\Phi(x) \leq b_i^0(x) = u_i^0(x) \quad \text{for } \alpha_i \not\leq 0\\ \underline{v}_i^0 = 0 \leq v_i^0(x) = u_{m+i}^0(x)\end{aligned}$$

It remains to show definition 4.1.(i), $\overline{u}_i \geq \underline{u}_i$, and that $|\overline{b}_i| < K$ for a positive constant K. But we know that $\overline{b}_i$ solves

$$\partial_t \overline{b}_i - d_i \triangle \overline{b}_i = (G_{\max} - \mu \overline{b}_i) \cdot \overline{b}_i$$

and thus has an invariant rectangle of the form $\{b_i | l_i \leq b_i \leq r_i\}$, with $b_i^0 < l_i < \frac{G_{\max}}{\mu}$ and $r_i > \frac{G_{\max}}{\mu}$ [see Smo83, Corollary 14.8]. This proves both remaining points. Additionally, for arbitrary but fixed T, $\underline{b}_i(x,t) \geq \underline{b}_i(x,T) = \gamma > 0$, which we required. □

4.1.2 Uniqueness

As before, we will simplify the boundary conditions (4.1.4b) to homogeneous Robin boundary conditions (4.1.8) when showing the uniqueness of solutions for equation (4.1.4).

f_i independent of ∇u

If f_i is independent of ∇u, as is the case for equation (4.1.1), we can proceed as follows:

As a first step, we multiply equation (4.1.4a) by a test function $\varphi_i \in C^\infty(D)$ and integrate over Ω as well as $[0,t]$

$$\int_0^t \int_\Omega \partial_t u_i \cdot \varphi_i \,\mathrm{d}x \,\mathrm{d}\tau = \int_0^t \int_\Omega d_i \triangle u_i \cdot \varphi_i \,\mathrm{d}x \,\mathrm{d}\tau + \int_0^t \int_\Omega f_i(u,x) \cdot \varphi_i \,\mathrm{d}x \,\mathrm{d}\tau.$$

We partially integrate $\partial_t u_i \cdot \varphi_i$

$$\begin{aligned}\int_\Omega u_i(x,t)\varphi_i(x,t)\,\mathrm{d}x - \int_\Omega u_i^0(x)\varphi_i(x,0)\,\mathrm{d}x - \int_0^t \int_\Omega u_i \cdot \partial_t \varphi_i \,\mathrm{d}x \,\mathrm{d}\tau \\ = \int_0^t \int_\Omega d_i \triangle u_i \cdot \varphi_i \,\mathrm{d}x \,\mathrm{d}\tau + \int_0^t \int_\Omega f_i(u,x) \cdot \varphi_i \,\mathrm{d}x \,\mathrm{d}\tau\end{aligned}$$

and apply the first Green identity to transform $\triangle u_i \cdot \varphi_i$

$$\begin{aligned}&\int_\Omega u_i(x,t)\varphi_i(x,t)\,\mathrm{d}x - \int_\Omega u_i^0(x)\varphi_i(x,0)\,\mathrm{d}x - \int_0^t \int_\Omega u_i \cdot \partial_t \varphi_i \,\mathrm{d}x \,\mathrm{d}\tau \\ &\quad = -\int_0^t \int_\Omega d_i \nabla u_i^T \cdot \nabla \varphi_i \,\mathrm{d}x \,\mathrm{d}\tau - \int_0^t \int_{\partial\Omega} d_i \alpha \varphi_i u_i \,\mathrm{d}S + \int_0^t \int_\Omega f_i(u,x) \cdot \varphi_i \,\mathrm{d}x \,\mathrm{d}\tau,\end{aligned}$$

where we used equation (4.1.8). After employing the first Green identity once again, we arrive at

$$\begin{aligned}\int_\Omega u_i(x,t)\varphi_i(x,t)\,\mathrm{d}x - \int_\Omega u_i^0(x)\varphi_i(x,0)\,\mathrm{d}x - \int_0^t \int_\Omega u_i \cdot \partial_t \varphi_i \,\mathrm{d}x \,\mathrm{d}\tau \\ = \int_0^t \int_\Omega d_i u_i \cdot \triangle \varphi_i \,\mathrm{d}x \,\mathrm{d}\tau - \int_0^t \int_{\partial\Omega} d_i u_i \cdot \frac{\partial \varphi_i}{\partial n} \,\mathrm{d}S \\ - \int_0^t \int_{\partial\Omega} d_i \alpha \varphi_i u_i \,\mathrm{d}S + \int_0^t \int_\Omega f_i(u,x) \cdot \varphi_i \,\mathrm{d}x \,\mathrm{d}\tau. \quad (4.1.11)\end{aligned}$$

We now assume that there exist two solutions, u and w, with $u(x,0) = u^0(x) = w(x,0)$. By subtracting equation (4.1.11) for u_i and w_i (and rearranging some

terms), we get

$$\begin{aligned}\int_\Omega (u_i(x,t) - w_i(x,t))\varphi_i(x,t)\,\mathrm{d}x = &\int_0^t \int_\Omega (u_i - w_i)\cdot(d_i \triangle\varphi_i + \partial_t\varphi_i)\,\mathrm{d}x\,\mathrm{d}\tau \\ &- d_i \int_0^t \int_{\partial\Omega} (u_i - w_i)\cdot\left(\frac{\partial\varphi_i}{\partial n} + \alpha\varphi_i\right)\mathrm{d}S \\ &+ \int_0^t \int_\Omega (f_i(u,x) - f_i(w,x))\cdot\varphi_i\,\mathrm{d}x\,\mathrm{d}\tau.\end{aligned}$$

This form corresponds to the one found in Anderson [And91, p. 118f], with $\Phi(x,s,u) = d_i u_i$, $g(x,s,u) = -\alpha_i d_i u_i$, $h(x,s,u) = f_i(u,x)$, $f(x,s,u) = 0$ and $\Sigma = \partial\Omega$. One can therefore construct an appropriate test function φ_i as the solution to a related PDE exactly as shown therein (even easier, given the simplicity of the functions involved). Combined with the Lipschitz continuity of f_i we obtain

$$\begin{aligned}&\int_\Omega |u_i(x,t) - w_i(x,t)|\,\mathrm{d}x \le C\int_0^t \int_\Omega \sum_{i=1}^m |u_i - w_i|\,\mathrm{d}x\,\mathrm{d}\tau \\ \Rightarrow\quad &\int_\Omega \sum_{i=1}^m |u_i(x,t) - w_i(x,t)|\,\mathrm{d}x \le mC\int_0^t \int_\Omega \sum_{i=1}^m |u_i - w_i|\,\mathrm{d}x\,\mathrm{d}\tau.\end{aligned}$$

Using Grönwall's inequality (theorem A.1)

$$\begin{aligned}&\int_\Omega \sum_{i=1}^m |u_i(x,t) - w_i(x,t)|\,\mathrm{d}x \le 0 \\ \Rightarrow\quad &\sum_{i=1}^m |u_i(x,t) - w_i(x,t)| \le 0 \qquad \forall x\in\Omega \\ \Rightarrow\quad &u_i(x,t) = w_i(x,t) \qquad \forall x\in\Omega,\end{aligned}$$

which proves the uniqueness, since t was chosen arbitrarily.

f_i dependent on ∇u

If f_i is not independent of ∇u, as is the case for equation (4.1.2), we cannot apply this method. The additional term $\nabla(u_i - w_i)$ cropping up prohibits the use of Grönwall's inequality. Instead, we can apply the mean value theorem

$$\begin{aligned}f_i(u, D_x u, x) - f_i(w, D_x w, x) = &\sum_{j=1}^m \frac{\partial f_i(\xi,\tilde{\xi},x)}{\partial u_j}(u_j - w_j) \\ &+ \sum_{j=1}^m \sum_{k=1}^n \frac{\partial f_i(\xi,\tilde{\xi},x)}{\partial (D_x u)^{jk}}\partial_{x_k}(u_j - w_j),\end{aligned}$$

where $(D_x u)^{jk} = \partial_{x_k} u_j$. This allows us to write

$$f_i(u, D_x u, x) - f_i(w, D_x w, x) = \sum_{j=1}^{m} c_j^i(t,x)(u_j - w_j) + \sum_{j=1}^{m}\sum_{k=1}^{n} b_{jk}^i(t,x)\partial_{x_k}(u_j - w_j).$$

The difference between two solutions u and w, $v = u - w$ thus follows the equation

$$\partial_t v_i - d_i \triangle v_i - \sum_{j=1}^{m} c_j^i(t,x) v_j - \sum_{j=1}^{m}\sum_{k=1}^{n} b_{jk}^i(t,x)\partial_{x_k} v_j = 0. \tag{4.1.12}$$

If we define the components of a matrix operator $\mathscr{L}$ as

$$\mathscr{L}_{ij} = -c_j^i(t,x) - \sum_{k=1}^{n} b_{jk}^i(t,x)\cdot\partial_{x_k}, \qquad i \neq j \tag{4.1.13a}$$

$$\mathscr{L}_{ii} = \partial_t - \sum_{k=1}^{n} d_i \partial_{x_k}^2 - c_i^i(t,x) - \sum_{k=1}^{n} b_{ik}^i(t,x)\cdot\partial_{x_k}, \tag{4.1.13b}$$

then we can write equation (4.1.12) for all i as

$$\mathscr{L} v|_{Q_T} = 0, \tag{4.1.14a}$$

$$\mathscr{B} v|_{S_T} = 0, \tag{4.1.14b}$$

$$\mathscr{C} v|_{t=0} = 0. \tag{4.1.14c}$$

$\mathscr{B} = \operatorname{diag}(\alpha_i + \beta_i \sum_{k=1}^{n} n_j(x)\partial_{x_j})$ is the boundary operator, with n_j the j-th component of the outer normal vector at x, while $\mathscr{C} = \mathbb{I}_{m\times m}$ gives the initial condition at $t = 0$. It is apparent from the diagonal form that these matrices fulfil the complementary condition.

We aim to prove that the so-defined operator $\mathscr{L}$ is parabolic, and thus $v = 0$ must hold. To that end, we first cite some definitions concerning when a matrix operator is called parabolic, which are taken from Petrovskii [Pet38] and Ladyzenskaja, Solonnikov, and Uralceva [LSU67].

Definition 4.2. *The* ***principal part*** *of a polynomial $L(x,t,i\xi\lambda,p\lambda^{2b})$ with degree $2br$, $r \in \mathbb{N}$, is the sum of those terms of L for which*

$$L_0(x,t,i\xi\lambda,p\lambda^{2b}) = \lambda^{2br} L_0(x,t,i\xi,p).$$

Definition 4.3. *An operator $L(x,t,\partial_x,\partial_t)$ is said to be* ***2b-parabolic*** *at a point (x,t) if for any $\xi \in \mathbb{R}^n$ the roots p_s of the polynomial $L_0(x,t,i\xi,p)$ in the variable p satisfy the condition*

$$\operatorname{Re}(p_s) \leq -\delta|\xi|^{2b} \qquad (\delta > 0).$$

Definition 4.4. *A **matrix differential operator** $\mathscr{L}(x,t,\partial_x,\partial_t)$ with elements $\mathscr{L}_{kj}(x,t,\partial_x,\partial_t)$, $(k,j=1,\dots,m)$ is said to be **parabolic** in the sense of Petrovskii if*

(i) the operator

$$L(x,t,\partial_x,\partial_t)=\det\mathscr{L}(x,t,\partial_x,\partial_t)$$

is 2b-parabolic in the sense of definition 4.3.

(ii) the degree of the polynomials $\mathscr{L}_{kj}(x,t,i\xi\lambda,p\lambda^{2b})$ in λ does not exceed $2br_j$ and

$$\mathscr{L}_{kj}(x,t,i\xi,p)=\sigma_k^j p^{r_j}+L'_{kj}(x,t,i\xi,p),$$

where L'_{kj} is a polynomial not containing p^{r_j}.

We start out by noticing that for the $\mathscr{L}$ defined in equation (4.1.13) $r_j=1$ independent of j, $b=1$ and $\sigma_j^j=1$, $\sigma_k^j=0$ if $j\neq k$. Definition 4.4.(ii) follows directly. We can also see immediately from the definition that the principal part of $L=\det\mathscr{L}$ will be the product of the diagonal elements, as all entries that do not lie on the diagonal contain at most λ^1. It follows that

$$L_0(x,t,i\xi\lambda,p\lambda^2)=\prod_{j=1}^{m}\left(p\lambda^2+d_j\lambda^2\sum_{k=1}^{n}\xi_k^2\right),$$

from which we gather that $r=m$ and $p_s=-d_j|\xi|^2$. If we define $\delta=\min_{1\leq j\leq m}\{d_j\}$, definition 4.4.(i) follows. The matrix operator $\mathscr{L}$ is therefore parabolic in the sense of Petrovskii. We can now invoke the following theorem from Ladyzenskaja, Solonnikov, and Uralceva [LSU67, Theorem VII.10.1]:

Theorem 4.4. *Suppose the coefficients of the operators $\mathscr{L}$,$\mathscr{B}$ and $\mathscr{C}$ are smooth enough. Then the problem*

$$\begin{aligned}\mathscr{L}(x,t,\partial_x,\partial_t)u|_{Q_T}&=f\\ \mathscr{B}(x,t,\partial_x,\partial_t)u|_{S_T}&=\Phi\\ \mathscr{C}(x,t,\partial_x,\partial_t)u|_{t=0}&=\Psi\end{aligned}$$

has a unique smooth solution in the class of vector functions, which is subject to the inequality

$$\sum_{j=1}^{m}\|u_j\|_{Q_T}\leq c\left(\sum_{j=1}^{m}\|f_j\|_{Q_T}+\sum_{q=1}^{b_r}\|\Phi_q\|_{S_T}+\sum_{\alpha=1}^{r}\|\Psi_\alpha\|_{\Omega}\right),$$

with appropriately chosen norms.

Theorem 4.5. *Equation* (4.1.2) *equipped with homogeneous Robin boundary conditions and appropriate initial conditions has a unique solution.*

Proof. Since $f, \Phi, \Psi = 0$ in equation (4.1.14), we can conclude that

$$\sum_{j=1}^{m} \|v_j\|_{Q_T} \leq c \cdot 0 \qquad \Rightarrow \qquad v_j = 0 \quad \forall 1 \leq j \leq m,$$

which shows the required uniqueness. □

4.1.3 Attracting sets

Theorem 4.6. *Let the following assumptions hold:*

(I) There exists a region $\mathcal{D} \subset \mathbb{R}^m$, which is compact and positively invariant.

(II) For $u_0 \in H = L^2(\Omega, \mathcal{D}) = \{v \in L^2(\Omega) | v(x) \in \mathcal{D}$ for a.e. $x \in \Omega\}$, equation (4.1.4) *possesses a unique solution u for all time, $u(t) \in H \, \forall t$, $u \in L^2(0, T; V), \forall T > 0$ with $V = H_0^1(\Omega)$ or $H^1(\Omega)$, depending on boundary conditions,*

(III) The mapping $u_0 \to u(t)$ is continuous in H. If moreover $u_0 \in V$, then $u \in L^2(0, T; H^2(\Omega)^m) \, \forall T > 0$.

(IV) f is continuous on $\bar{\Omega} \times \mathcal{D}$

Then the semigroup $S(t)$ associated with equation (4.1.4) *with Dirichlet or Neumann boundary conditions is such that*

1. *There exist absorbing sets in H and $H \cap V$.*
2. *There exists a maximal attractor $\mathcal{A}$ which is bounded in V, compact in H. $\mathcal{A}$ attracts the bounded sets of H. If furthermore $\mathcal{D}$ is convex, then $\mathcal{A}$ is connected in H.*

For a proof of theorem 4.6 see Marion [Mar87]. We know that a solution to equation (4.1.1) will lie between the upper and lower solutions constructed in equation (4.1.10). This means we have a positively invariant set for (b, v) given as $\mathcal{D} := [0, r]^n \times [0, v^*]^n$, with $r > \frac{G_{\max}}{\mu}$, for which it holds that $S(t)\mathcal{D} \subsetneq \mathcal{D}$. Furthermore, the following theorem holds:

Theorem 4.7. *If we have the assumptions of theorem 4.6 and moreover*

(I) the positively invariant region $\mathcal{D}$ is convex and

(II) $f(x,u)$ *is of class* C^2 *with respect to* u *on* $\bar{\Omega}\times\mathbb{R}^m$ *and its derivatives of order less than or equal to two are bounded on* $\bar{\Omega}\times\mathcal{D}$,

then we set

$$c = \sup_{1\le j\le m}\sup_{1\le i\le m}\sup_{(x,u)\in\bar{\Omega}\times\mathcal{D}}\left|\frac{\partial f_j}{\partial u_i}(x,u)\right|,$$
$$d_0 = \min_{1\le i\le m} d_i.$$

It follows that the maximal attractor $\mathcal{A}$ *has finite Hausdorff and fractal dimensions. Moreover, these dimensions are both bounded by*

$$\bar{c}(1+|\Omega|c^{m/2}d_0^{-m/2}),$$

where $\bar{c}$ *depends on* n, m *and the shape of* Ω.

4.1.4 Stationary solutions

In order to determine the long-term behaviour of our fully parabolic system, it is of use to take a look at the stationary solutions of equation (4.1.1). These are themselves solutions of the system

$$-D\,\triangle b_i = G(v_i,v,b)\cdot b_i \tag{4.1.15a}$$
$$-\varepsilon'\,\triangle v_i = \varepsilon\partial_1 G(v_i,v,b) \tag{4.1.15b}$$

or, depending on the choice of model,

$$-D\,\triangle v_i = \varepsilon\partial_1 G(v_i,v,b) + \frac{2D\nabla b_i\cdot\nabla v_i}{b_i} \tag{4.1.15b'}$$

with appropriate boundary conditions.

It is important to note at this point that our observations from chapter 2 remain true. This is due to the common diffusion coefficient of the equations. Such a structure makes instabilities of Turing type impossible and therefore the stability of a spatially homogeneous equilibrium is the same as for the point process, as Kronik and Cohen note in [KC09, page 71].

Coupled upper-lower solutions

Definition 4.5. *Two functions* $\overline{u}_i, \underline{u}_i \in C^{2+\delta}$ *are called* ***coupled upper-lower solutions*** *to the stationary system*

$$-d_i\,\triangle u_i = f_i(u_1,\dots,u_m,x) \quad \text{in } \Omega \tag{4.1.16a}$$
$$\alpha_i u_i + \beta_i\frac{\partial u_i}{\partial n} = \psi_i(u_1,\dots,u_{i-1},u_{i+1},\dots,u_m,x) \quad \text{in } \partial\Omega \tag{4.1.16b}$$

if it holds that

(I) $\overline{u}_i \geq \underline{u}_i$

(II) $-d_i \triangle \overline{u}_i \geq \sup_{\underline{u}_j \leq \xi_j \leq \overline{u}_j} f_i(\xi_1, \ldots, \xi_{i-1}, \overline{u}_i, \xi_{i+1}, \xi_m, x) \quad \text{in } \Omega$

(III) $\alpha_i \overline{u}_i + \beta_i \frac{\partial \overline{u}_i}{\partial n} \geq \sup_{\underline{u}_j \leq \xi_j \leq \overline{u}_j} \psi_i(\xi_1, \ldots, \xi_{i-1}, \xi_{i+1}, \xi_m, x) \quad \text{in } \partial\Omega$

(IV) $-d_i \triangle \underline{u}_i \leq \inf_{\underline{u}_j \leq \xi_j \leq \overline{u}_j} f_i(\xi_1, \ldots, \xi_{i-1}, \overline{u}_i, \xi_{i+1}, \xi_m, x) \quad \text{in } \Omega$

(V) $\alpha_i \underline{u}_i + \beta_i \frac{\partial \underline{u}_i}{\partial n} \leq \inf_{\underline{u}_j \leq \xi_j \leq \overline{u}_j} \psi_i(\xi_1, \ldots, \xi_{i-1}, \xi_{i+1}, \xi_m, x) \quad \text{in } \partial\Omega$

Theorem 4.8. *Let f_i in system* (4.1.16) *be uniformly Lipschitzian independent of x, $\psi_i \in C^2(\mathbb{R}^{m-1})$ as above. If $\underline{u}$ and $\overline{u}$ are coupled upper-lower solutions of the elliptic system* (4.1.16)*, then there exists a solution $u = (u_1, \ldots, u_m)$ to the system* (4.1.16)*, such that $\underline{u}_i \leq u_i \leq \overline{u}_i$.*

For a proof see Li, Abudiab, and Ahn [LAA08]. This theorem is only given in the absence of any dependency on the first derivatives of u, but we could generalize it as in the parabolic case before. Existence and uniqueness theorems, a priori estimates of solution as well as the comparison theorem remain valid in the elliptic case [see for example GT01, Lemma 6.30, 6.31].

We state additional lemmas before constructing coupled upper-lower solutions for our specific system.

Lemma 4.9. *The equation*

$$\begin{aligned} -\triangle u &= up(x,u) && x \in \Omega \\ \alpha(x)u + \beta(x)\frac{\partial u}{\partial n} &= 0 && x \in \partial\Omega \end{aligned}$$

has a unique strictly positive solution iff the principal eigenvalue $\lambda_1(\triangle + p(x,0)) > 0$.

A proof of this lemma can be found in Li and Liu [LL93, Lemma 2]. The next lemma is taken from Pao [Pao92, theorem 1.2].

Lemma 4.10. *Let $\mathcal{L}$ be a uniformly elliptic operator on D. We can consider the eigenvalue problem*

$$\begin{aligned} (\mathcal{L} - c(x)u + \lambda r(x))\,\Phi &= 0 && x \in \Omega \\ \left(\alpha(x) + \beta(x)\frac{\partial}{\partial n}\right)\Phi &= 0 && x \in \partial\Omega, \end{aligned}$$

where $c(x), r(x) \in C(\Omega), c \geq 0, r > 0$. Then the principal eigenvalue λ_1 is real and nonnegative, and the corresponding principal eigenfunction can be taken to be positive on Ω. Moreover, $\lambda_1 > 0$ when c and α are not both identically zero.

We now construct our upper-lower solutions in the elliptic case similar to the parabolic case (see equation (4.1.10).

$$\underline{b}_i = 0, \tag{4.1.17a}$$
$$\overline{v}_i = v^*, \text{ see assumption (IV) on page 26} \tag{4.1.17b}$$
$$\underline{v}_i = 0. \tag{4.1.17c}$$

We define $\overline{b}_i$ as the solution of

$$-d_i \triangle \overline{b}_i = (G_{\max} - \mu \overline{b}_i) \cdot \overline{b}_i \qquad \text{in } \Omega \tag{4.1.17d}$$
$$\alpha_i(x)\overline{b}_i + \beta_i(x)\frac{\partial \overline{b}_i}{\partial n} = 0 \qquad \text{in } \partial\Omega, \tag{4.1.17e}$$

where we assume homogeneous boundary conditions, that is

$$\psi_i(u_1, \ldots, u_{i-1}, u_{i+1}, \ldots, u_m, x) = 0.$$

Theorem 4.11. *The functions $\overline{u} = (\overline{b}, \overline{v})^T, \underline{u} = (\underline{b}, \underline{v})^T$ defined in equation* (4.1.17) *are coupled upper-lower solutions to the system* (4.1.15) *with the boundary condition*

$$\alpha_i u_i + \beta_i \frac{\partial u_i}{\partial n} = 0 \quad \text{in } \partial\Omega.$$

Proof. We prove that the chosen functions fulfil assumptions 4.5.(I) to 4.5.(V). As constants or solutions to a semi-linear problem with smooth enough coefficients, all functions lie in $C^{2+\alpha}(\overline{\Omega})$.

Assumption 4.5.(IV)

$$\begin{aligned}
-d_i \triangle \underline{b}_i = 0 &= \inf_{\underline{u}_j \le \xi_j \le \overline{u}_j} f_i(\xi_1, \ldots, \xi_{i-1}, \underline{b}_i, \xi_{i+1}, \ldots, \xi_{2m}, x) \\
&= \inf_{\underline{u}_j \le \xi_j \le \overline{u}_j} G(\xi_{m+i}, (\xi_{m+1}, \ldots, \xi_{2m}), (\xi_1, \ldots, 0, \ldots, \xi_m)) \cdot 0 \\
-\varepsilon' \triangle \underline{v}_i = 0 &= \inf_{\underline{u}_j \le \xi_j \le \overline{u}_j} f_{m+i}(\xi_1, \ldots, \xi_{m+i-1}, \underline{v}_i, \xi_{m+i+1}, \ldots, \xi_{2m}, x) \\
&= \inf_{\underline{u}_j \le \xi_j \le \overline{u}_j} \partial_1 G(0, (\xi_{m+1}, \ldots, \xi_{2m}), (\xi_1, \ldots, \xi_m)),
\end{aligned}$$

where the last step is due to assumption (IV).

Assumption 4.5.(V)

$$\alpha_i \underline{b}_i + \beta_i \frac{\partial \underline{b}_i}{\partial n} = 0 = \inf_{\underline{u}_j \le \xi_j \le \overline{u}_j} \psi_i(\xi_1, \ldots, \xi_{i-1}, \xi_{i+1}, \ldots, \xi_{2m}, x)$$
$$\alpha_{m+i} \underline{v}_i + \beta_{m+i} \frac{\partial \underline{v}_i}{\partial n} = 0 = \inf_{\underline{u}_j \le \xi_j \le \overline{u}_j} \psi_{m+i}(\xi_1, \ldots, \xi_{m+i-1}, \xi_{m+i+1}, \ldots, \xi_{2m}, x)$$

Assumption 4.5.(II)

$$\begin{aligned}
-d_i \triangle \overline{b}_i &= (G_{\max} - \mu \overline{b}_i)\overline{b}_i \\
&\geq \sup_{\underline{u}_j \leq \xi_j \leq \overline{u}_j} f_i(\xi_1, \ldots, \xi_{i-1}, \overline{b}_i, \xi_{i+1}, \ldots, \xi_{2m}, x) \\
&= \sup_{\underline{u}_j \leq \xi_j \leq \overline{u}_j} G(\xi_{m+i}, (\xi_{m+1}, \ldots, \xi_{2m}), (\xi_1, \ldots, \overline{b}_i, \ldots, \xi_m))\overline{b_i} \\
-d_i \triangle \overline{v}_i &= 0 \\
&\geq \sup_{\underline{u}_j \leq \xi_j \leq \overline{u}_j} f_{m+i}(\xi_1, \ldots, \xi_{m+i-1}, \overline{v}_i, \xi_{m+i+1}, \ldots, \xi_{2m}, x) \\
&= \sup_{\underline{u}_j \leq \xi_j \leq \overline{u}_j} \underbrace{\partial_1 G(\overline{v}_i, (\xi_{m+1}, \ldots, \xi_{2m}), (\xi_1, \ldots, \xi_m))}_{\leq 0} \text{ see (IV), p. 26}
\end{aligned}$$

Assumption 4.5.(III)

$$\alpha_i \overline{b}_i + \beta_i \frac{\partial \overline{b}_i}{\partial n} = 0 = \sup_{\underline{u}_j \leq \xi_j \leq \overline{u}_j} \psi_i(\xi_1, \ldots, \xi_{i-1}, \xi_{i+1}, \ldots, \xi_{2m}, x)$$

$$\alpha_{m+i} \overline{v}_i + \beta_{m+i} \frac{\partial \overline{v}_i}{\partial n} = 0 = \sup_{\underline{u}_j \leq \xi_j \leq \overline{u}_j} \psi_{m+i}(\xi_1, \ldots, \xi_{m+i-1}, \xi_{m+i+1}, \ldots, \xi_{2m}, x)$$

It remains to show assumption 4.5.(I), $\overline{u}_i \geq \underline{u}_i$. We know that $\overline{b}_i$ solves

$$\begin{aligned}
-\triangle \overline{b}_i &= \underbrace{\frac{G_{\max} - \mu \overline{b}_i}{d_i}}_{=: p_i(x, \overline{b}_i)} \cdot \overline{b}_i && \text{in } \Omega \\
\alpha_i(x) \overline{b}_i + \beta_i(x) \frac{\partial \overline{b}_i}{\partial n} &= 0 && \text{in } \partial\Omega,
\end{aligned}$$

In order to apply lemma 4.9, we need to look at the eigenvalue problem for $\triangle + p_i(x, 0)$:

$$\begin{aligned}
& \triangle \Phi + \frac{G_{\max}}{d_i} \Phi = \lambda \Phi && \text{in } \Omega \\
\Rightarrow \quad & \left(-\triangle - \frac{G_{\max}}{d_i} + \lambda \right) \Phi = 0 && \text{in } \Omega \\
& \left(\alpha_i(x) + \beta_i(x) \frac{\partial}{\partial n} \right) \Phi = 0 && \text{in } \partial\Omega,
\end{aligned}$$

which has the shape discussed in lemma 4.10, with $c(x) = \frac{G_{\max}}{d_i}$ and $r(x) = 1$. We thus have fulfilled all assumptions of lemma 4.10 and as $c(x)$ is not identically zero, we know that $\lambda_1(\triangle + p_i(x, 0)) > 0$. It follows from lemma 4.9 that $\overline{b}_i > 0 = \underline{b}_i$ and hence assumption 4.5.(I). □

4.2 Coupled ODE-PDE system

If we assume that strategies do not diffuse on their own, it is more natural to use equation (4.0.5b) and get a coupled ODE-PDE system. It can be written as

$$\partial_t b_i(x,t) = G(v_i(t), v(t), b(x,t)) \cdot b_i(x,t) + D \triangle b_i(x,t), \tag{4.2.1a}$$
$$\partial_t v_i(x,t) = \varepsilon \partial_1 G(v_i(x,t), v(x,t), b(x,t)). \tag{4.2.1b}$$

We will specifically work with a homogeneous Robin boundary condition,

$$\alpha_i b_i + \beta_i \frac{\partial b_i}{\partial n} = 0 \quad \text{in } S_T. \tag{4.2.1c}$$

4.2.1 Existence and Uniqueness of solutions

Weak solution

First we take a look at *weak solutions* of our problem, allowing for solutions that do not have the smoothness required of classical solutions. For b, we will be using the Banach space $X = C([0,T]; L^2(\Omega))$ with $\|b\|_X = \max\limits_{0\le t\le T} \|b(t)\|_{L^2(\Omega)}$ and the standard weak formulation therein.

Theorem 4.12 (Existence and Uniqueness of weak solutions)**.** *The equation* (4.2.1) *has a unique local weak solution.*

Proof. We will prove this in three steps. First we will show that equation (4.2.1b) has a unique solution v^b for b fixed. In a second step we will show that this v^b induces a unique solution $\hat{b}$. Thus we have a mapping $\mathcal{B}(b) = \hat{b}$. In a third step we will show that this mapping $\mathcal{B}$ has a unique fixed point (via Banachs contraction mapping, theorem A.5), thus showing that the original system has a unique local solution.

1st Step: Unique solution v^b for (4.2.1b) with fixed b
This result can be gained directly from the Picard-Lindelöf theorem, because $\partial_1 G$ is Lipschitz continuous by assumption. It is thus also Lipschitz continuous in the $L^2(\Omega)$-norm, and it follows that there exists a unique solution v^b which lies in X.

2nd Step: Unique solution $\hat{b}$ for (4.2.1a) with fixed v^b
We can apply the arguments from section 4.1 to the case with v^b as parameter and b as the only dependent variable. As $G \cdot b$ is Lipschitz continuous from our assumption, the same constructions lead to a unique solution $\hat{b}$ in $C^{2+\delta,1+\delta/2}$. But since Ω is bounded, that implies $\hat{b} \in X$.

3rd Step: Fixed point for $\mathcal{B} : b \mapsto \hat{b}$

The goal is to show that $\mathcal{B}$ is a contraction, meaning that

$$\left\|\delta\hat{b}\right\| := \left\|\mathcal{B}(\bar{b}) - \mathcal{B}(\underline{b})\right\| \leq C\|\delta b\| = C\left\|\bar{b} - \underline{b}\right\|,$$

with $C < 1$. To this end we first consider $\delta v = v^{\bar{b}} - v^{\underline{b}}$, where $\bar{b}$ and $\underline{b}$ are two arbitrary but fixed functions from X with $\bar{b}(x,0) = \underline{b}(x,0)$. Using equation (4.2.1b) we have

$$\partial_t \delta v = \varepsilon \cdot \begin{pmatrix} \partial_1 G(v_1^{\bar{b}}, v^{\bar{b}}, \bar{b}) - \partial_1 G(v_1^{\underline{b}}, v^{\underline{b}}, \underline{b}) \\ \vdots \\ \partial_1 G(v_m^{\bar{b}}, v^{\bar{b}}, \bar{b}) - \partial_1 G(v_m^{\underline{b}}, v^{\underline{b}}, \underline{b}) \end{pmatrix}.$$

Multiplying with δv and integrating over Ω leads to

$$\int_\Omega \partial_t \delta v \cdot \delta v \,\mathrm{d}x = \int_\Omega \varepsilon \begin{pmatrix} \partial_1 G(v_1^{\bar{b}}, v^{\bar{b}}, \bar{b}) - \partial_1 G(v_1^{\underline{b}}, v^{\underline{b}}, \underline{b}) \\ \vdots \\ \partial_1 G(v_m^{\bar{b}}, v^{\bar{b}}, \bar{b}) - \partial_1 G(v_m^{\underline{b}}, v^{\underline{b}}, \underline{b}) \end{pmatrix} \cdot \delta v \,\mathrm{d}x$$

$$\Rightarrow \quad \frac{1}{2}\frac{\mathrm{d}}{\mathrm{d}t}\|\delta v\|_{L^2}^2 \leq \varepsilon \int_\Omega \left| \begin{pmatrix} \partial_1 G(v_1^{\bar{b}}, v^{\bar{b}}, \bar{b}) - \partial_1 G(v_1^{\underline{b}}, v^{\underline{b}}, \underline{b}) \\ \vdots \\ \partial_1 G(v_m^{\bar{b}}, v^{\bar{b}}, \bar{b}) - \partial_1 G(v_m^{\underline{b}}, v^{\underline{b}}, \underline{b}) \end{pmatrix} \right| |\delta v| \,\mathrm{d}x.$$

We use the Lipschitz continuity of $\partial_1 G$ with Lipschitz factor L':

$$\begin{aligned} \frac{1}{2}\frac{\mathrm{d}}{\mathrm{d}t}\|\delta v\|_{L^2}^2 &\leq \varepsilon \int_\Omega \sqrt{m} L' \left| \begin{pmatrix} v^{\bar{b}} \\ \bar{b} \end{pmatrix} - \begin{pmatrix} v^{\underline{b}} \\ \underline{b} \end{pmatrix} \right| \cdot |\delta v| \,\mathrm{d}x \\ &\leq \varepsilon\sqrt{m} L' \int_\Omega \left(\left| v^{\bar{b}} - v^{\underline{b}} \right| + \left| \bar{b} - \underline{b} \right| \right) |\delta v| \,\mathrm{d}x \\ &= \varepsilon\sqrt{m} L' \left(\int_\Omega |\delta v|^2 \,\mathrm{d}x + \int_\Omega |\delta b||\delta v| \,\mathrm{d}x \right). \end{aligned}$$

At this point, one can apply the Cauchy-Schwartz inequality and divide by $\|\delta v\|_{L^2}$ afterwards

$$\begin{aligned} \frac{\mathrm{d}}{\mathrm{d}t}\|\delta v\|_{L^2} \cdot \|\delta v\|_{L^2} &\leq \varepsilon\sqrt{m} L' \left(\|\delta v\|_{L^2}^2 + \|\delta b\|_{L^2} \|\delta v\|_{L^2} \right) \\ \frac{\mathrm{d}}{\mathrm{d}t}\|\delta v\|_{L^2} &\leq \underbrace{\varepsilon\sqrt{m} L'}_{=:C_2} \left(\|\delta v\|_{L^2} + \|\delta b\|_{L^2} \right) \end{aligned}$$

Integration from 0 to t, where it is known that $\delta v(x,0) = 0$, gives us

$$\|\delta v\|_{L^2} \leq C_2 \int_0^t \|\delta b\|_{L^2} \,\mathrm{d}s + C_2 \int_0^t \|\delta v\|_{L^2} \,\mathrm{d}s$$

Here we apply Grönwall's inequality, with $\alpha(t) = C_2 \int_0^t \|\delta b\|_{L^2} \,\mathrm{d}s$ non-decreasing and $\beta(t) = C_2$.

$$\|\delta v\|_{L^2} \leq C_2 \mathrm{e}^{C_2 t} \int_0^t \|\delta b\|_{L^2} \,\mathrm{d}s \tag{4.2.2}$$

Now that we have an estimate of $\|\delta v\|_{L^2}$, we take a look at $\left\|\delta \hat{b}\right\|_{L^2}$. Based on equation (4.2.1a) we can state the following for $\delta \hat{b} := \hat{b} - \hat{\underline{b}}$:

$$\partial_t \delta \hat{b} = \begin{pmatrix} G(v_1^{\overline{b}}, v^{\overline{b}}, \hat{b})\hat{b}_i - G(v_1^{\underline{b}}, v^{\underline{b}}, \hat{\underline{b}})\hat{\underline{b}}_i \\ \vdots \\ G(v_m^{\overline{b}}, v^{\overline{b}}, \hat{b})\hat{b}_i - G(v_m^{\underline{b}}, v^{\underline{b}}, \hat{\underline{b}})\hat{\underline{b}}_i \end{pmatrix} + \triangle \delta \hat{b}$$

We integrate over Ω and apply the first Green identity, using equation (4.2.1c)

$$\begin{aligned} \int_\Omega \partial_t \delta \hat{b} \cdot \delta \hat{b} \,\mathrm{d}x &= \int_\Omega \begin{pmatrix} G(v_1^{\overline{b}}, v^{\overline{b}}, \hat{b})\hat{b}_i - G(v_1^{\underline{b}}, v^{\underline{b}}, \hat{\underline{b}})\hat{\underline{b}}_i \\ \vdots \\ G(v_m^{\overline{b}}, v^{\overline{b}}, \hat{b})\hat{b}_i - G(v_m^{\underline{b}}, v^{\underline{b}}, \hat{\underline{b}})\hat{\underline{b}}_i \end{pmatrix} \cdot \delta \hat{b} \,\mathrm{d}x \\ &\quad - \left\|\nabla \delta \hat{b}\right\|_{L^2}^2 + \int_{\partial\Omega} -\alpha \left(\delta \hat{b}\right)^2 \mathrm{d}S \\ \Rightarrow \quad \frac{1}{2}\frac{\mathrm{d}}{\mathrm{d}t}\left\|\delta \hat{b}\right\|_{L^2}^2 &\leq \int_\Omega \left| \begin{pmatrix} G(v_1^{\overline{b}}, v^{\overline{b}}, \hat{b})\hat{b}_i - G(v_1^{\underline{b}}, v^{\underline{b}}, \hat{\underline{b}})\hat{\underline{b}}_i \\ \vdots \\ G(v_m^{\overline{b}}, v^{\overline{b}}, \hat{b})\hat{b}_i - G(v_m^{\underline{b}}, v^{\underline{b}}, \hat{\underline{b}})\hat{\underline{b}}_i \end{pmatrix} \right| |\delta \hat{b}| \,\mathrm{d}x. \end{aligned}$$

At this point we need the Lipschitz constant L of G. As seen in lemma 2.1, it holds that $L = G_{\max} + L_1 |\hat{b}_i|$. but we know that $|\hat{b}_i| \leq \max\{b_i(x,0), \frac{G_{\max}}{\mu}\}$. Therefore we can take $b_{\max} := \max\{b_i(x,0)\,\forall i, \frac{G_{\max}}{\mu}\}$ and the Lipschitz constant is thus $G_{\max} + L_1 b_{\max}$

$$\begin{aligned} \frac{1}{2}\frac{\mathrm{d}}{\mathrm{d}t}\left\|\delta \hat{b}\right\|_{L^2}^2 &\leq \int_\Omega \underbrace{\sqrt{m}\,(G_{\max} + L_1 b_{\max})}_{C_1} \left| \begin{pmatrix} v^{\overline{b}} \\ \overline{b} \end{pmatrix} - \begin{pmatrix} v^{\underline{b}} \\ \underline{b} \end{pmatrix} \right| \cdot |\delta \hat{b}| \,\mathrm{d}x \\ &\leq C_1 \int_\Omega \left(|\delta \hat{b}| + |\delta v|\right) |\delta \hat{b}| \,\mathrm{d}x. \end{aligned}$$

Once again we use the Cauchy-Schwartz inequality, divide by $\left\|\delta \hat{b}\right\|_{L^2}$, integrate over t and subsequently use Grönwall's inequality. We can also plug in (4.2.2) for $\|\delta v\|_{L^2}$.

$$\begin{aligned} \left\|\delta \hat{b}\right\|_{L^2} &\leq C_1 \int_0^t \left\|\delta \hat{b}\right\|_{L^2} \mathrm{d}s + C_1 \int_0^t \|\delta v\|_{L^2} \,\mathrm{d}s \\ \Rightarrow \quad \left\|\delta \hat{b}\right\|_{L^2} &\leq C_1 C_2 \mathrm{e}^{C_1 t} \int_0^t \mathrm{e}^{C_2 s} \left(\int_0^s \|\delta b\|_{L^2} \,\mathrm{d}\tau\right) \mathrm{d}s \end{aligned}$$

$$\Rightarrow \quad \left\|\delta\hat{b}\right\|_{L^2} \leq C_1 C_2 \mathrm{e}^{C_1 t} \int_0^t \mathrm{e}^{C_2 s} \left(\int_0^s \|\delta b\|_X \, \mathrm{d}\tau \right) \mathrm{d}s$$

$$\Rightarrow \quad \left\|\delta\hat{b}\right\|_{L^2} \leq C_1 C_2 \mathrm{e}^{C_1 t} \int_0^t \mathrm{e}^{C_2 s} s \|\delta b\|_X \, \mathrm{d}s$$

$$\Rightarrow \quad \left\|\delta\hat{b}\right\|_{L^2} \leq C_1 \mathrm{e}^{C_1 t} \cdot \frac{\mathrm{e}^{C_2 t}(Ct-1)+1}{C_2} \cdot \|\delta b\|_X$$

If this equation holds for all t, it also holds for $\max_{0 \leq t \leq T}$

$$\left\|\delta\hat{b}\right\|_X \leq C_1 \mathrm{e}^{C_1 t} \cdot \frac{\mathrm{e}^{C_2 t}(Ct-1)+1}{C_2} \cdot \|\delta b\|_X$$

We can now take $t \to 0$, and see that the right hand side goes to 0. This means there exists a T_0 for which $\mathcal{B}$ is a contraction for $t \in [0, T_0]$.

□

Classical solution

Theorem 4.13 (Existence and Uniqueness of strong solutions)**.** *The equation* (4.2.1) *has a unique local classical solution.*

Proof. We are now interested in the space $C^{2+\delta,1+\delta/2}(\Omega \times [0,T])$ of functions whose second derivative in x is Hölder-continuous with coefficient δ and whose first derivative in t is Hölder-continuous with coefficient $\delta/2$. As estimates regarding the norm in this space are quite hard to obtain, we will not use Banachs but Schauders fixed point theorem (theorem A.6). As we already know the uniqueness of the weak solution, it follows that the classical solution must be unique as well.

The first and second step of the proof remain the same as in the proof for a weak solution. Hence we start with the mapping $\mathcal{B} : b \mapsto \hat{b}$, with $b, \hat{b}$ in $C^{2+\delta,1+\delta/2}(D)$. It maps b to the solution of

$$\partial_t \hat{b}_i(x,t) = G(v_i^b(t), v^b(t), b(x,t)) \cdot \hat{b}_i(x,t) + D \triangle \hat{b}_i(x,t) \quad \text{in } \Omega \tag{4.2.3a}$$

$$\alpha_i \hat{b}_i + \beta_i \frac{\partial \hat{b}_i}{\partial n} = 0 \quad \text{in } \partial\Omega. \tag{4.2.3b}$$

$$\hat{b}_i^0(x) = b_i^0(x) \tag{4.2.3c}$$

We take a subspace $X = \left\{ f \in C^{2+\delta,1+\delta/2}(D) \middle| \|f\|_{2+\delta} \leq K \right\}$, with K to be defined later on. This subspace is clearly non-empty, closed, bounded and convex. It remains to show that B is continuous and its image is compact.

- B continuous
  We take a convergent series $b_{n,i}$, with $\lim_{n\to\infty} b_{n,i} = b_i$. We want to show that $\hat{b}_i := \lim_{n\to\infty} B(b_{n,i}) = B(b_i)$. Defining $\hat{b}_{n,i} = B(b_{n,i})$ it solves the equation

  $$\partial_t \hat{b}_{n,i} = G(v_i^{b_n}, v^{b_n}, b_n)\hat{b}_{n,i} + D \triangle \hat{b}_{n,i}$$

  We take the limit $n \to \infty$

  $$\lim_{n\to\infty} \left(\partial_t \hat{b}_{n,i}\right) = \lim_{n\to\infty} \left(G(v_i^{b_n}, v^{b_n}, b_n)\hat{b}_{n,i} + D \triangle \hat{b}_{n,i}\right)$$

  As both the derivative operator and G are continuous it follows that

  $$\partial_t \left(\lim_{n\to\infty} \hat{b}_{n,i}\right) = \left(G(v_i^{\lim_{n\to\infty} b_n}, v^{\lim_{n\to\infty} b_n}, \lim_{n\to\infty} b_n) \lim_{n\to\infty} \hat{b}_{n,i} + D \triangle \lim_{n\to\infty} \hat{b}_{n,i}\right).$$

  We know that v is continuously dependent on b_n

  $$\partial_t \left(\lim_{n\to\infty} \hat{b}_{n,i}\right) = \left(G(v_i^b, v^b, b) \lim_{n\to\infty} \hat{b}_{n,i} + D \triangle \lim_{n\to\infty} \hat{b}_{n,i}\right)$$

  which is what we wanted to show.

- $\mathcal{B}$ maps X to X
  We use the boundary Schauder estimates (see theorem A.10):

  $$\left\|\hat{b}_i\right\|_{2+\delta} \leq \bar{K}\left(\|f\|_\delta + \|\psi\|_{1+\delta} + \left\|\hat{b}_i^0\right\|_{2+\delta}\right),$$

  where $f = 0$, $\psi = 0$ and $\hat{b}_i^0 = b_i^0$ from the definition in equation (4.2.3). Since $b_i^0 \in C^{2+\delta}(\Omega)$ with bounded Ω, we know that $\|b_i^0\|_{2+\delta} < C$ for a $C \in \mathbb{R}$. If we choose $K = \bar{K} \cdot C$ we have $\mathcal{B} : X \to X$.

- The functions in X are equicontinuous
  As stated above, we know that $\left\|\hat{b}_i\right\|_{2+\delta} \leq K$, which gives an upper limit to the Lipschitz constant for all functions in X.

This shows that all prerequisites of Arzelà-Ascoli (theorem A.7) are fulfilled, so X is compact. As a continuous mapping of a compact space, $\operatorname{Im} B$ is compact as well. We can thus apply the Schauder fixed-point theorem. □

Theorem 4.14. *The local solution can be extended in time to any arbitrary T.*

Proof. Take the values at time T_0 as the new starting values; as v and b are bounded a priori by v^* respectively $b_{\max}$, we can then repeat the arguments above to extend the existence of the solution to the interval $[0, 2T_0]$. These steps can be repeated as needed. □

4.2.2 Asymptotic Behaviour

In order to look at the long-time development of the population number, we will use an orthogonal decomposition of b_i. It is well-known that the eigenfunctions $(\psi_j)_{j\in\mathbb{N}}$ of the eigenvalue problem

$$\begin{aligned} -\triangle\psi_j(x) &= \lambda_j\psi_j(x), && x\in\Omega \\ \frac{\partial\psi_j}{\partial n} &= 0, && x\in\partial\Omega \end{aligned}$$

form a complete orthonormal system in $L^2(\Omega)$, where $\lambda_1 = 0$ with $\psi_1(x)\equiv C_\psi$ and $\lambda_j > 0$ for $j > 1$. Note that we have again simplified the boundary condition to a homogeneous Neumann condition. We can then display $b_i(x,t)$ as

$$b_i(x,t) = \sum_{j=1}^{\infty} a_j^i(t)\psi_j^i(x) = a_1^i(t)\psi_1^i(x) + \psi_\perp^i(x,t),$$

where

$$a_j^i(t) = \langle b_i(x,t), \psi_j^i(x)\rangle = \int_\Omega b_i(x,t)\psi_j^i(x)\,\mathrm{d}x.$$

We drop the superscript i in the following in order to simplify notation. First, we are interested in the behaviour of $a_1(t)$.

$$a_1(t) = \langle b_i(x,t), \psi_1(x)\rangle = C_\psi\int_\Omega b_i(t,x)\,\mathrm{d}x \tag{4.2.4}$$

$$\begin{aligned} \Rightarrow \frac{\mathrm{d}}{\mathrm{d}t}a_1(t) &= C_\psi\int_\Omega \partial_t b_i(x,t)\,\mathrm{d}x \\ &= C_\psi\int_\Omega D\triangle b_i(x,t)\,\mathrm{d}x + C_\psi\int_\Omega G(v_i,v,b)b_i(x,t)\,\mathrm{d}x \\ &= C_\psi\int_\Omega G(v_i,v,b)b_i(x,t)\,\mathrm{d}x, \end{aligned} \tag{4.2.5}$$

where the last step is due to the first Green identity and the homogeneous Neumann condition on b_i. It also follows from equation (4.2.4) and the previously established a-priori-estimations of b_i that

$$0 \le a_1(t) \le \lambda(\Omega)C_\psi\frac{G_{\max}}{\mu}. \tag{4.2.6}$$

We concentrate on the case $G(v_i,v,b)\le 0$ first, which for instance arises if $v_i = 0$ is the only ESS. Equation (4.2.5) then indicates that $a_1(t)$ is monotonously decreasing in t, while equation (4.2.6) guarantees the boundedness. Taken together,

we have shown that $a_1(t)$ converges to a constant for t to infinity. It remains to investigate the behaviour of $\psi_\perp(x,t)$. We know the following:

$$\frac{\partial \psi_\perp}{\partial n} = 0 \tag{4.2.7}$$

$$\langle \psi_1, \psi_\perp \rangle = 0 \quad \Rightarrow \quad \int_\Omega \psi_\perp \,\mathrm{d}x = 0 \tag{4.2.8}$$

$$\Rightarrow \quad \|\psi_\perp\|_{L^2} \leq C_P \|\nabla \psi_\perp\|_{L^2}, \tag{4.2.9}$$

where we have used the Generalised Poincaré inequality with $p(\psi_\perp) = |\int_\Omega \psi_\perp \,\mathrm{d}x| = 0$ in order to gain equation (4.2.9). Substituting $b_i(x,t)$ by our orthogonal decomposition, we arrive at

$$\begin{aligned} \partial_t \left(a_1(t)\psi_1(x) + \psi_\perp(x,t)\right) &= D \triangle \left(a_1(t)\psi_1(x) + \psi_\perp(x,t)\right) \\ &\quad + G(v_i, v, b) \left(a_1(t)\psi_1(x) + \psi_\perp(x,t)\right) \\ \Rightarrow \quad \frac{\mathrm{d}}{\mathrm{d}t} a_1(t)\psi_1(x) + \partial_t \psi_\perp(x,t) &= D \triangle \psi_\perp(x,t) + G(v_i, v, b) \left(a_1(t)\psi_1(x) + \psi_\perp(x,t)\right). \end{aligned}$$

Multiplying with $\psi_\perp$ and integrating over Ω leads to

$$\begin{aligned} &\frac{\mathrm{d}}{\mathrm{d}t} a_1(t) \int_\Omega \psi_1(x)\psi_\perp(x,t) \,\mathrm{d}x + \int_\Omega \partial_t \psi_\perp(x,t) \cdot \psi_\perp(x,t) \,\mathrm{d}x \\ &= D \int_\Omega \triangle \psi_\perp(x,t) \cdot \psi_\perp(x,t) \,\mathrm{d}x + \int_\Omega G(v_i, v, b) \left(a_1(t)\psi_1(x) + \psi_\perp(x,t)\right) \psi_\perp(x,t) \,\mathrm{d}x. \end{aligned}$$

Green's first identity, equations (4.2.7) and (4.2.8) allow us to simplify

$$\begin{aligned} \int_\Omega \frac{1}{2} \frac{\mathrm{d}}{\mathrm{d}t} \left(\psi_\perp(x,t)\right)^2 \mathrm{d}x &= -D \int_\Omega \langle \nabla \psi_\perp(x,t), \nabla \psi_\perp(x,t) \rangle \,\mathrm{d}x \\ &\quad + \int_\Omega G(v_i, v, b) \left(a_1(t)\psi_1(x) + \psi_\perp(x,t)\right) \psi_\perp(x,t) \,\mathrm{d}x \\ \frac{1}{2} \frac{\mathrm{d}}{\mathrm{d}t} \|\psi_\perp(t)\|_{L^2}^2 + D \|\nabla \psi_\perp(t)\|_{L^2}^2 &= \int_\Omega G(v_i, v, b) \left(a_1(t)\psi_1(x) + \psi_\perp(x,t)\right) \psi_\perp(x,t) \,\mathrm{d}x \\ \frac{1}{2} \frac{\mathrm{d}}{\mathrm{d}t} \|\psi_\perp(t)\|_{L^2}^2 + \frac{D}{C_P^2} \|\psi_\perp(t)\|_{L^2}^2 &\leq \int_\Omega G(v_i, v, b) \left(a_1(t)\psi_1(x) + \psi_\perp(x,t)\right) \psi_\perp(x,t) \,\mathrm{d}x, \end{aligned} \tag{4.2.10}$$

where the last step is due to equation (4.2.9). We aim to apply the following theorem from Eisenhofer [Eis13]:

Theorem 4.15. *Let $y(t)$ and $a(t)$ be non-negative functions with $y \in C^1([t_0, t_1])$ and $a \in C([t_0, t_1])$ for $0 \leq t_0 < t_1 \leq \infty$. If the inequality*

$$\frac{\mathrm{d}}{\mathrm{d}t} y(t) + \gamma y(t) \leq a(t) \tag{4.2.11}$$

is satisfied with $\gamma \geq 0$, then for $t_0 \leq t \leq t_1$ it holds that

$$y(t) \leq y(t_0)\mathrm{e}^{-\gamma(t-t_0)} + \int_{t_0}^{t} a(s)\mathrm{e}^{-\gamma(t-s)}\,\mathrm{d}s.$$

If in addition $\int_0^\infty a(t)\,\mathrm{d}t < \infty$,

$$y(t) \leq y(t_0)\mathrm{e}^{-\gamma(t-t_0)} + \int_{t_0}^{\infty} a(s)\,\mathrm{d}s,$$

which implies $y(t) \to 0$ for $t \to \infty$.

We set $y(t) := \|\psi_\perp(t)\|_{L^2}^2$, $a(t) := \int_\Omega G(v_i, v, b)\,(a_1(t)\psi_1(x) + \psi_\perp(x,t))\,\psi_\perp\,\mathrm{d}x$ and find that equation (4.2.10) transforms into equation (4.2.11), with $\gamma = D/C_P^2$. The next step is to take a closer look at $a(t)$, using the a-priori estimates of b_i as well as equation (4.2.1a).

$$\begin{aligned} 0 \leq \int_\Omega b_i(x,t) &= \int_\Omega b_i^0(x) + \int_0^t \partial_s b_i(x,s)\,\mathrm{d}s\,\mathrm{d}x \qquad (4.2.12)\\ &= \left\|b_i^0\right\|_{L^1} + \int_0^t \underbrace{\int_\Omega D\,\triangle b_i(x,s)\,\mathrm{d}x}_{=0}\,\mathrm{d}s + \int_0^t \int_\Omega G(v_i,v,b) b_i(x,s)\,\mathrm{d}x\,\mathrm{d}s \end{aligned}$$

So for all $t \geq 0$

$$\begin{aligned} \int_0^t \int_\Omega -G(v_i,v,b) b_i(x,s)\,\mathrm{d}x\,\mathrm{d}s &\leq \left\|b_i^0\right\|_{L^1}\\ \Rightarrow \int_0^\infty \int_\Omega -G(v_i,v,b)\,(a_1(s)\psi_1(x) + \psi_\perp(x,s))\,\mathrm{d}x\,\mathrm{d}s &\leq \left\|b_i^0\right\|_{L^1} \qquad (4.2.13) \end{aligned}$$

In order to apply equation (4.2.13) to $a(t)$ we note that

$$a(t) = \int_\Omega -G(v_i,v,b)\Big(\underbrace{a_1(t)\psi_1(x) + \psi_\perp(x,t)}_{\geq 0}\Big)\,(-\psi_\perp)\,\mathrm{d}x.$$

Since we assumed $G(v_i, v, b) \leq 0$, we can now apply the mean value theorem

$$a(t) \leq \|\psi_\perp\|_0 \int_\Omega -G(v_i,v,b)\,(a_1(t)\psi_1(x) + \psi_\perp(x,t))\,\mathrm{d}x. \qquad (4.2.14)$$

Combining equations (4.2.13) and (4.2.14), we gather that $\int_0^\infty a(t)\,\mathrm{d}t < \infty$, which lets us apply theorem 4.15. It follows that $y(t) = \|\psi_\perp\|_{L^2}^2 \to 0$, which implies $\psi_\perp \to 0$.

All in all, if $G(v_i, v, b) \leq 0\ \forall x, t$ we have

$$b_i(x,t) = a_1(t)\psi_1(x) + \psi_\perp(x,t) \to C_\psi a_1^\infty. \qquad (4.2.15)$$

A very similar calculation can be done in the case $G(v_i, v, b) \geq 0$, where we establish an upper bound in equation (4.2.12) through our a-priori estimate $G_{\max}/\mu$.

In biological terms this implies that in situations where $v_i = 0$ is the only ESS ($G \leq 0$), or there is only a positive ESS and the starting population is low ($G \geq 0$), the resulting equilibrium population is constant. If, however, that is not the case and there are for example multiple ESSs, the resulting equilibrium might well be more complex, as can be seen in chapter 6 (e.g. figure 6.10). Determining such an equilibrium analytically in the general case is quite difficult, unfortunately.

Chapter 5

Experiments

Frequently, when using mathematical models to explore biological processes, experimental evidence is required to validate certain features of a model, make reliable predictions or compute parameter values which may be used in numerical simulations. Similarly, experimental findings inspire and help shape mathematical models. The following chapter is the result of my 6-month research stay at the laboratory of Stephen Diggle, where I conducted experiments which are also used to explore some aspects of my model numerically in chapter 6.

The laboratory group itself was based at the University of Nottingham in the Centre for Biomolecular Sciences. My stay was partially supported by the Erasmus+ program, while the work was supported by a Human Frontier Science Program Young Investigators grant (RGY0081/2012) and a NERC grant (NE/J007064/1) to Stephen P. Diggle.

As evolution in bacteria is hard to measure experimentally because of the effort involved in sampling and sequencing resulting mutants, the focus of the experiments is on the role of spatiality for producer/non-producer interactions.

5.1 Experimental setup

All the experiments were conducted at the University of Nottingham at the Centre for Biomolecular Sciences in a laboratory of biosafety level 2 by myself. A FastPrep-24 5G bead beater (MP Biomedicals) and a Tecan multimode plate reader available to all laboratory users were used in these experiments.

5.1.1 General Idea

The main hypothesis of this series of experiments can be summarised as

H1 *lasI* mutants act as cheats in media with adenosine as carbon source.

H2 Higher concentrations of agar limit diffusion of the signal molecule.

H3 With limited diffusion of the signal molecule, the relative fitness of the cheat will decline.

These hypotheses are meant to explore two new ideas. The first is that, as assumed in the model itself, quorum sensing (QS) signal is already a public good in itself and can be cheated against. This has been theorised before, but it is shown conclusively in these experiments. The second point is that a reduction of cheating can be achieved by thickening the medium, thus limiting diffusion.

This simple step can already serve to make an *in vitro* experiment replicate *in vivo* conditions more realistically, for example the thick, adhesive mucus that blocks the airways of cystic fibrosis patients with chronic lung infection.

One important thing to consider when using signal as a public good is the impact of the QS regulated exoproduct. As secreted exoproducts are public goods as well, fitness benefit of mutants might be caused by those, instead of signal, thereby obscuring the role of signal.

For that reason we will use adenosine (Ad) as a carbon source. Adenosine is deaminated to form inosine, which is degraded inside the cell by a nucleoside hydrolase (Nuh) to hypoxanthine plus ribose; hypoxanthine is then metabolised to produce glyoxylate plus urea (Heurlier, Dénervaud, and Haas [HDH06], see also figure 5.1). QS is crucial to the breakdown of adenosine because the *las* system (through the regulator LasR) positively regulates Nuh. Because Nuh acts intracellularly, any fitness effect of a loss-of-function mutation in the signal gene *lasI* in this growth medium will be directly due to the lack of signal and not to any downstream effect on the production of extracellular enzymes. The signal molecules of *Pseudomonas aeruginosa* (*P. aeruginosa*) are shown in detail in figure 1.2

In order to tune the impact of QS on growth, the total available carbon will be comprised of casamino acids (CAA) as well as adenosine. CAA is available to all bacteria, regardless of QS ability.

5.1.2 Materials and Methods

The strains used were the wild-type *P. aeruginosa* laboratory strain PAO1, *lasI* mutant (lasI$^-$) and *lasR* mutant (lasR$^-$), both isogenic insertion mutants created via insertion of a gentamicin (Gm) resistance gene in the QS genes *lasI* respectively *lasR* (PAO1 lasI::Gm respectively lasR::Gm), where the latter is used as a negative control. The growth medium used in these experiments was quorum sensing medium (QSM), which is specifically designed to make maximal growth dependent upon *lasRI*-regulated proteases. As a last step, I added 0.1 % w/v of carbon sources as a mix of CAA and Ad and the medium was filter sterilised. The exact mixture of CAA and Ad depended on the experiment in question and is given there.

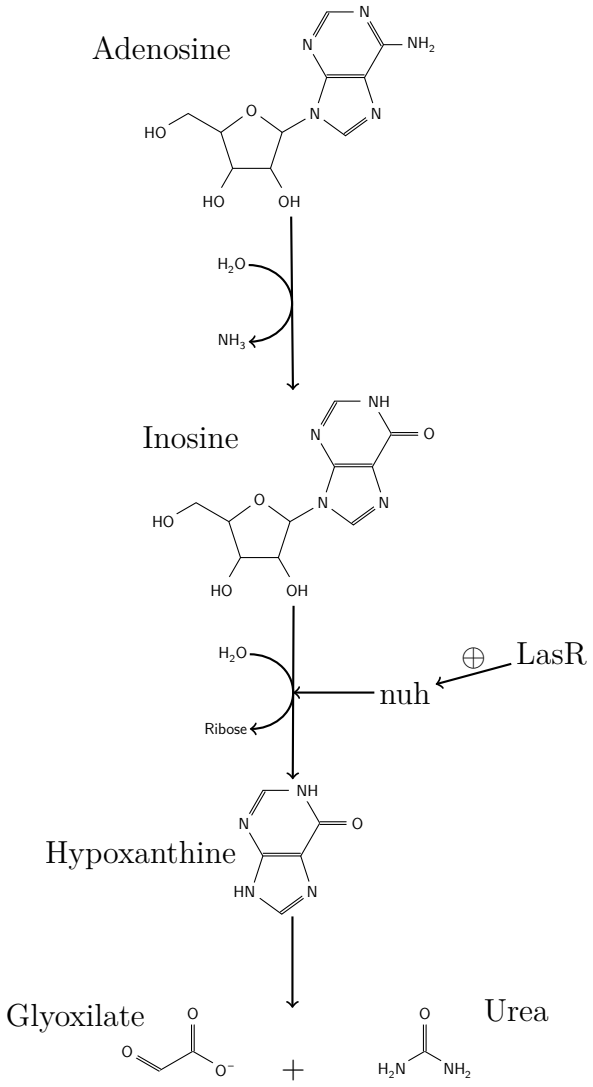

Figure 5.1: Schematic representation of adenosine metabolism.

In order to measure the concentration of QS signal N-3-oxo-dodecanoyl-l-homoserine lactone (3-oxo-C12-HSL) after 48 h of incubation, 100 µL of the culture supernatant was mixed with the same amount of a log phase culture of an *Escherichia coli* (*E. coli*) bioreporter (psB1142). This mixture was incubated for 3 h while luminescence and OD_{600} were recorded. To estimate 3-oxo-C12-HSL concentration, the luminescence of unknown samples was then compared to that of known concentrations. A *P. aeruginosa* PAO1 strain containing a chromosomal mini-CTXlux fusion to the lasB promoter (PAO1 lasI$^-$ plasB::lux) was used in order to test 3-oxo-C12-HSL diffusion in different media over the course of 8 h.

A more detailed description of the materials used can be found in Mund, Diggle, and Harrison [MDH17].

5.2 Cheating in liquid culture

The liquid culture experiments were conducted in 24-well-plates with a volume of 2 mL of media and 2 µL of mixed or pure bacteria cultures. Cultures were incubated overnight in sterile lysogeny broth (LB) medium and brought to an OD_{600} of 0.8 (lasI$^-$) respectively 0.9 (PAO1) prior to inoculation. Starting frequency of the mutant was determined by diluting and plating the starter cultures, in order to determine the colony forming units (CFU). The plates were then incubated at 37 °C with orbital shaking for 24 h or 48 h. After that time, cultures were diluted and plated on LB as well as LB + Gm(25 µg/mL), in order to count CFU of PAO1 and lasI$^-$ in pure and mixed culture.

5.2.1 *lasI* mutants act as cheats in liquid medium

Looking at the CFU count after 24 h and 48 h, one can notice that with higher adenosine levels the total CFU count declines (see figure 5.2). As the resulting CFU count was quite low for 0.1 % Ad the incubation time was chosen to be 48 h for future experiments. This effect was not as pronounced with pure PAO1 as it was with lasI$^-$. While all different cultures had a CFU count of around 1×10^8 for pure CAA, the CFU count dropped to 4.6 % of that amount for pure PAO1 and to 0.1 % for pure lasI$^-$ at 0.1 % Ad. As a result, the lasI$^-$ in pure adenosine medium grew to only 7 % of the density of pure PAO1 in the same medium, while mixed cultures have an in-between value.

From this, it is already apparent that lasI$^-$ grows poorly in an environment where QS is required for growth. We now want to investigate the growth of mixed populations in more detail. To this end we calculate the amount of doublings the bacteria undergo in 48 h for PAO1 and lasI$^-$ both in pure and mixed culture.

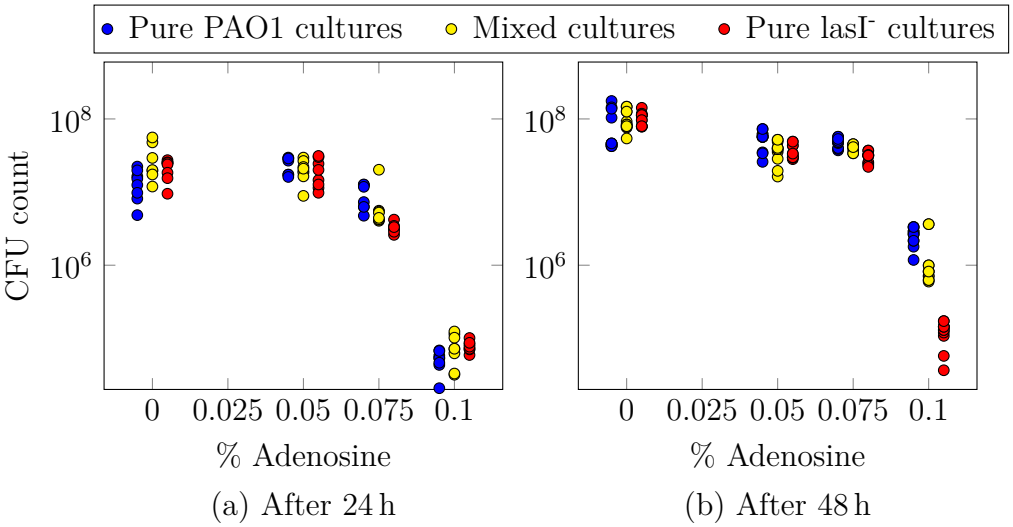

(a) After 24 h (b) After 48 h

Figure 5.2: Total CFU after incubation time for different adenosine percentages. CAA was added to reach 0.1 % carbon source in every culture. With rising Ad content, growth of cultures was retarded. This effect was more noticeable in lasI- cultures.

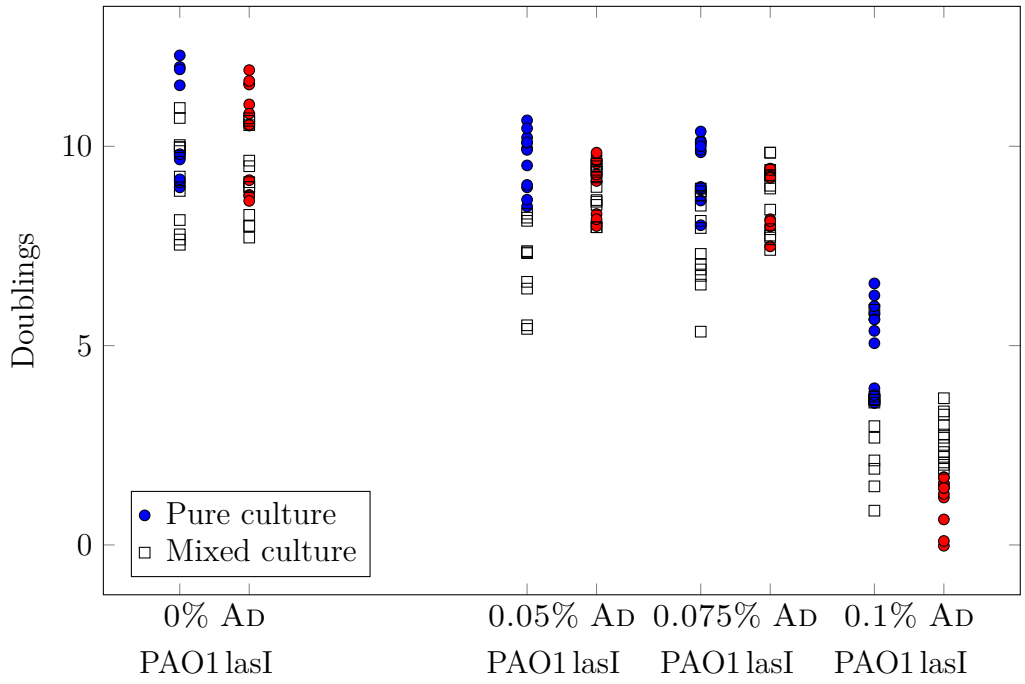

Figure 5.3: Amount of cell number doublings after 48 h incubation time for PAO1 and lasI- in pure or mixed cultures. One can see that PAO1 cultures have a higher number of doublings when in pure culture, while the reverse is true for lasI-.

As we can see in figure 5.3 PAO1 has a higher number of doublings in pure culture while lasI$^-$ tends to have a higher number of doublings in mixed culture. This implies that adding lasI$^-$ to the PAO1 bacteria has a negative impact on their growth, while the *lasI* mutants benefit.

Another measure for the relative growth rate of two populations is the relative fitness, defined as

$$\text{relFit} = \frac{f_{\text{end}}\,(1 - f_{\text{start}})}{f_{\text{start}}\,(1 - f_{\text{end}})}, \tag{5.2.1}$$

where f_{start} and f_{end} stand for start and end frequency of the focus population, calculated as the CFU of the focus population divided by the total CFU. A relative fitness of one therefore indicates $f_{\text{start}} = f_{\text{end}}$, while a value of less than one signifies relatively poorer growth and vice versa. From here on onwards, we will use lasI$^-$ respectively lasR$^-$ as focus population. We can plot the relative fitness values calculated from our experimental data for different percentages of adenosine and for pure or mixed culture with figure 5.4 as result.

One can now observe the circumstances under which lasI$^-$ grows better or worse than the PAO1 wild type by comparing the relative fitness values to 1. Looking at the pure cultures, we recover the same trend as before — with increasing adenosine, the growth of lasI$^-$ is more and more diminished. For mixed cultures, however, this trend is reversed. In media with both CAA and Ad, lasI$^-$ has a relative fitness of above 1, making it perform better than the wild type does. There is, however, a decline in relative fitness when all carbon is supplied as Ad. This is most likely attributable to the wild-type bacteria growing more slowly in the absence of carbon sources that can be exploited before QS responses are fully switched on. As we have seen in figure 5.2, CFU count is drastically decreased in pure Ad. This means the wild-type cells enter an "up-regulated" status later on, leaving less time to be exploited by the *lasI* mutant. But even though the relative fitness in mixed culture may sink below 1, it is still significantly higher than the relative fitness in pure culture. In fact, the difference between relative fitness of lasI$^-$ in pure or mixed culture is significant in all media except for pure CAA, where QS is unnecessary (Adenosine level/p-Values: $0\,\%/0.9692$, $0.05\,\%/4.4787 \times 10^{-4}$, $0.075\,\%/3.4198 \times 10^{-5}$, $0.1\,\%/0.0049$)

All these results indicate that *lasI* mutants act as cheats in media with adenosine as carbon source, with 3-oxo-C12-HSL as a public good — they have a lower growth rate when alone, which is increased in the presence of signal producing wild-type cells and in turn decrease wild-type growth.

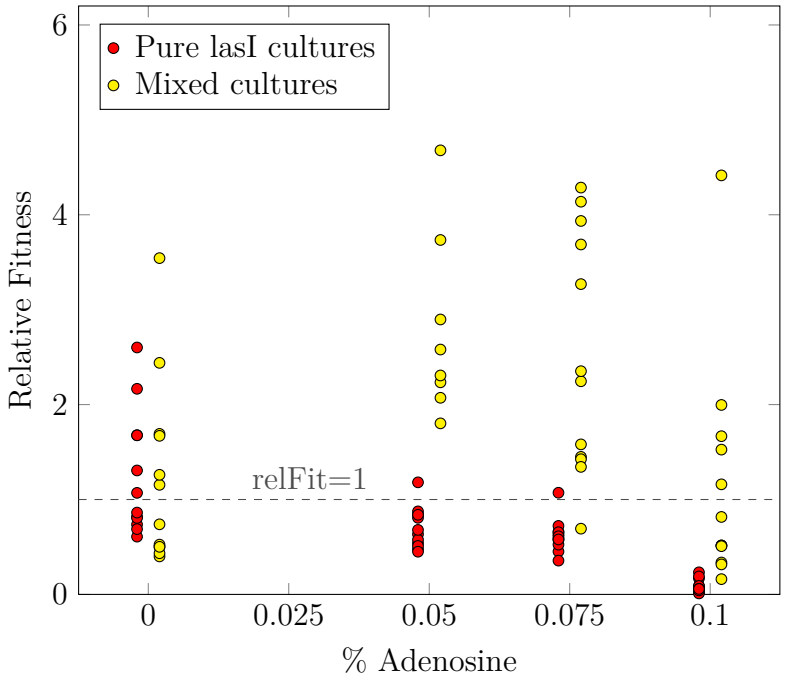

Figure 5.4: Relative Fitness of lasI$^-$ after 48 h incubation time.

5.2.2 Signal production is increased in adenosine

Signal production of wild-type cultures was measured as signal concentration in cell-free supernatant. After 48 h of growth and extraction of a small volume for counting purposes, the remaining medium was filter-sterilised to prepare for measurement.

As described in section 5.1.2, 100 µL of this supernatant as well as a series of QSM with known concentrations of 3-oxo-C12-HSL were mixed 1:1 with *E. coli* bioreporter psB1142. Both luminescence and OD_{600} of the bioreporter with the known concentrations are shown in figure 5.5. Luminescence of the bioreporter was adjusted by its OD_{600} to account for rising cell numbers during measurement. One can make out an outlier curve for 0 µM 3-oxo-C12-HSL, which has no further influence on the calculations. From the time course of luminescence for known concentrations we choose $t = 150$ min as a point in time at which the luminescence for different concentration is markedly different without the bacteria having reached exponential phase, as indicated by the OD_{600}.

Based on the luminescence of *E. coli* for our known concentrations, a linear model is fitted to the calibration curve, linking concentration of 3-oxo-C12-HSL to luminescence of the bioreporter. As the dependence seems to be parabolic in type (see figure 5.6), the squared concentration was included as predictor as well.

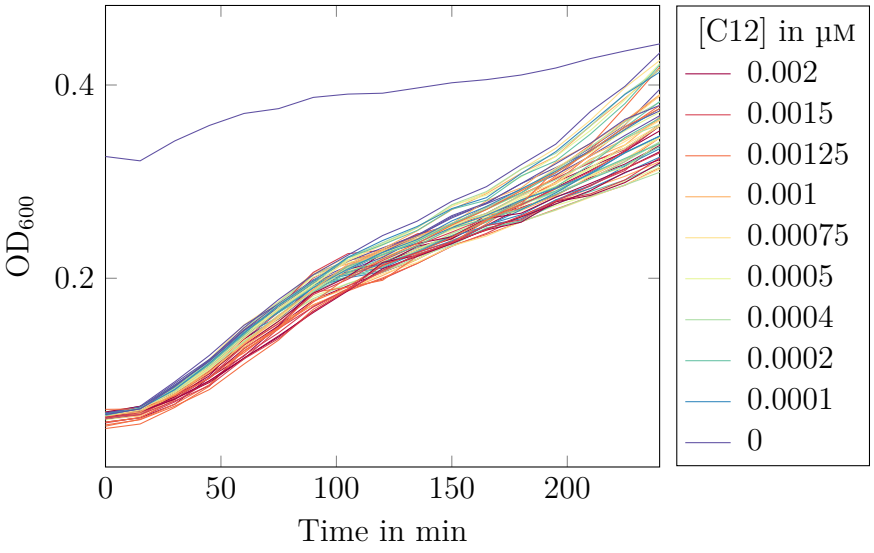

(a) OD_{600} of biosensor psB1142. After 150 min, the curves start drifting apart.

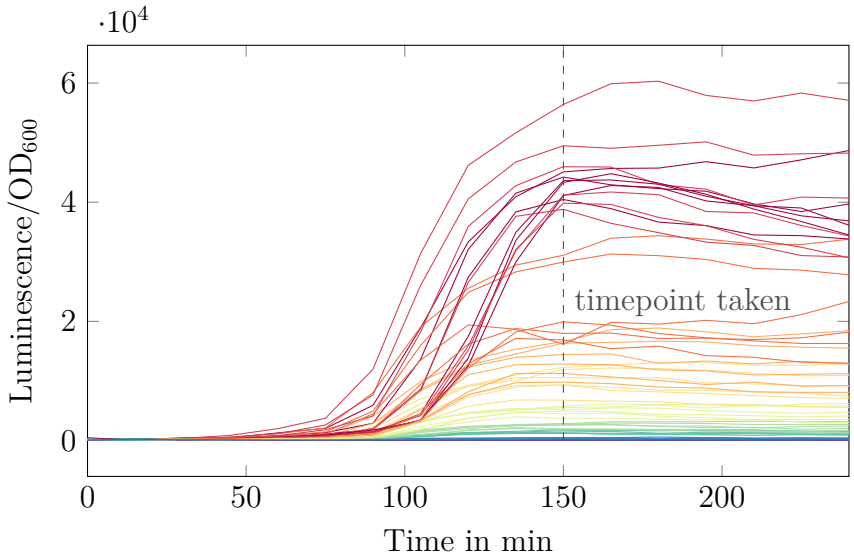

(b) Luminescence of *E. coli* biosensor, adjusted by OD_{600}. At $t = 150$ min the curves have separated.

Figure 5.5: Time course for calibration series. Different concentration of purified 3-oxo-C12-HSL are shown as different colours, while lines of the same colour indicate technical repetitions.

Table 5.1: Estimators for Luminescence

Luminescence ~ Concentration + Concentration^2					
		Estimate	Standard Deviation	t Value	p Value
Concentration		5.4×10^6	7.4×10^5	7.3	3.6×10^{-9}
Concentration^2		8.0×10^9	4.5×10^8	17.6	1.4×10^{-21}
	Degrees of Freedom	Sum of Squares	Mean of Squares	F value	p Value
Conc	1	1.3×10^{10}	1.3×10^{10}	5087.2	$<10^{-16}$
Conc^2	1	8.2×10^8	8.2×10^8	311.0	$<10^{-16}$
Residuals	44	1.2×10^8	2.6×10^6		

The values for this fit can be found in table 5.1. For this fit, two Cook's distance outliers have been removed from the data set. They can be identified visually in figure 5.6.

Having found the correlation between luminescence of the bioreporter and signal concentration, we can calculate the unknown signal concentration of the wild-type supernatant. The resulting concentration, as shown in figure 5.7a, declines with increasing adenosine. But we know from section 5.2.1 that CFU count also decreases with adenosine. We therefore divide the signal concentration by the CFU count of the culture which produced it (see figure 5.7b). We can then observe the reverse trend - signal concentration per CFU increases with Ad level. The most notable jump occurs for 0.1 % Ad, where the produced concentration jumps from around 1×10^{-12} µM/CFU to 6.5×10^{-11} µM/CFU. So even though the total 3-oxo-C12-HSL concentration is lowest at 0.1 % Ad, the per capita production is at its highest.

5.2.3 The cheating benefit is provided by the signal itself

As described in section 5.1.1, the digestion of adenosine is internal and controlled by the *las* system. Any benefit that non-producing mutants incur should therefore be due to 3-oxo-C12-HSL.

In order to check that this hypothesis holds true, two sets of control experiments have been conducted. First, the same experimental setup has been performed with lasR$^-$ instead of lasI$^-$. LasR$^-$ is a signal-blind mutant lacking the las-Receptor, meaning it cannot respond to the signal in any way. In a setup with adenosine, it should thus not be able to derive any benefit by being in proximity of PAO1 because it cannot digest adenosine even in the presence of 3-oxo-C12-HSL.

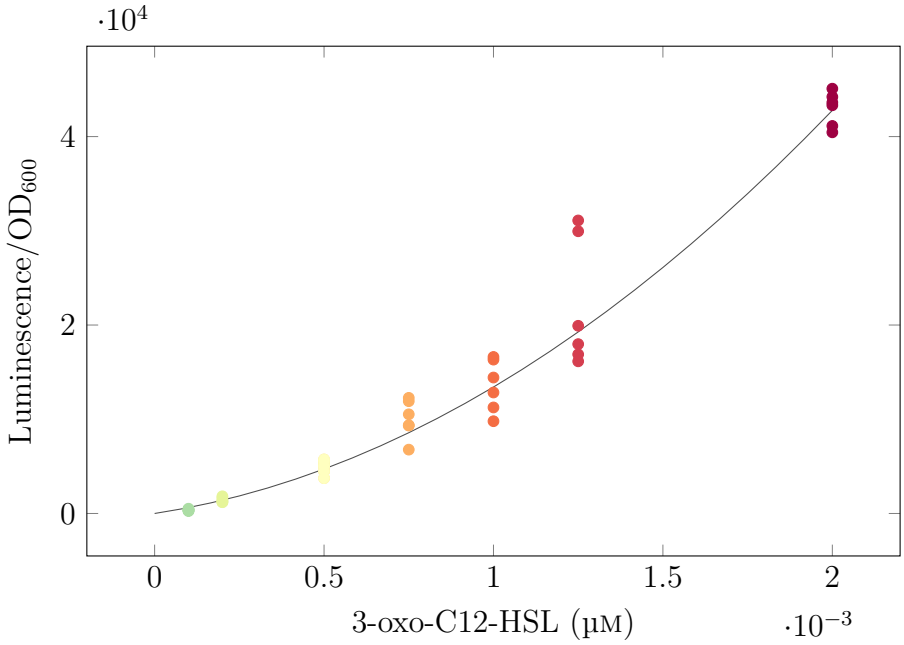

Figure 5.6: Luminescence for calibration series at $t = 150\,\text{min}$ (coloured dots), including the calculated fit (black line) from the generalised linear model.

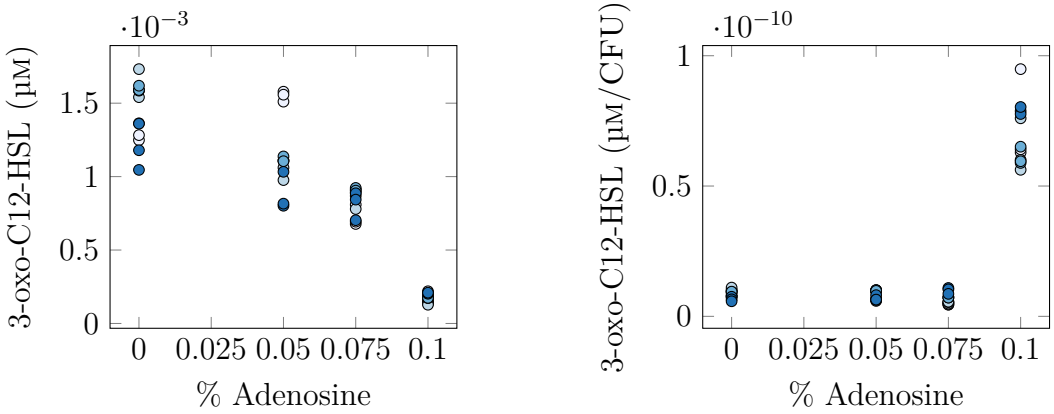

(a) Total signal concentration

(b) Adjusted for *P. aeruginosa* CFU

Figure 5.7: Calculated signal concentration in bacterial supernatant after 48 h. While total signal concentration is negatively correlated with Ad percentage, cultures in pure Ad have the highest per-capita production rate. Dots of the same colour indicate technical repetitions, while different colours indicate the biological repeats.

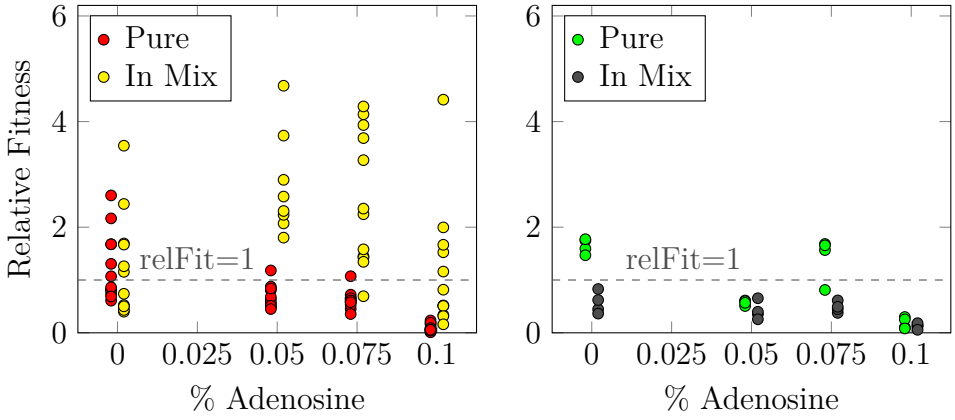

(c) Relative fitness of lasI⁻ (d) Relative fitness of lasR⁻

Figure 5.8: Comparison between the relative fitness of *lasI* and *lasR* mutant after 48 h. While lasI⁻ has a significantly higher fitness in mixed than in pure culture, there is no such effect for lasR⁻. Every dot stands for one measurement.

To simplify comparison, we use equation (5.2.1) to calculate the relative fitness of lasR⁻ in pure and mixed culture, where mixed again refers to a 1:1 mix with PAO1. We can then compare the computed values for lasI⁻ and lasR⁻. It is visually apparent from figure 5.8, that relative fitness of pure lasR⁻ cultures undergoes a similar decline with rising Ad level as pure lasI⁻ cultures. At the same time, where lasI⁻ in mixed culture has a relative fitness significantly greater than that in pure culture, lasR⁻ relative fitness shows the same trend for both mixed and pure culture. This shows that *lasR* mutants are indeed unable to cheat in this situation, confirming the hypothesis that 3-oxo-C12-HSL, and not some downstream exoproducts, acts as a public good.

To further confirm this, as a second control experiment both mutants as well as PAO1 wild-type were again cultivated for 48 h, this time only in pure culture but with the addition of 10 µM 3-oxo-C12-HSL. This should, in theory, have a similar effect as co-culturing the mutants with PAO1, as it provides a source of external signal.

The purified 3-oxo-C12-HSL was helpfully provided by Alex Truman from the University of Nottingham. As it was solved in methanol, another set of experiments with the same amount of pure methanol was conducted as proof of the fact that any changes are not due to addition of methanol. After calculating relative fitness from the results, we recover the data displayed in figure 5.9. Again we find that with increasing Ad level the relative fitness of nearly all culture types decreases, with the only exception of lasI⁻ either in mixed culture or in pure culture with

added 3-oxo-C12-HSL. Apart from some biological variation in the measurements, methanol has no effect on relative fitness of cultures, while 3-oxo-C12-HSL has the same effect as adding PAO1.

Apart from the visual interpretation of the results, one can also fit a generalised linear model to the data sets in order to assess the influence of the different culture conditions. This will be undertaken in section 5.4.

5.3 Cheating in solid culture

The experiments in solid media were conducted in 48-well plates with 1 mL culture volume. The basic QSM remained the same, but was supplemented with 1 % agar, in order to solidify the culture medium. Since QSM cannot be autoclaved while agar has to be autoclaved, stocks of doubly concentrated QSM were mixed with doubly concentrated agar solutions in equal parts. Bacterial cultures were added while this mix was around 40 °C. At this temperature the media was still warm enough to be in liquid phase and thus allow for distribution of bacterial cultures, while at the same time being cool enough to prevent hyperthermic cell killing.

In order to count CFU from these solid 1 mL agar cubes, they had to be liquefied using a bead beater. Due to volume constrains for bead beater tubes, agar cubes were divided into three parts with a sterile metal spatula and the resulting re-liquefied volumes remixed before plating out.

5.3.1 Adding agar retards diffusion

As a proof of concept that different agar concentrations have an effect on signal diffusion I conducted a "sandwich experiment", consisting of three layers: a bottom layer of purified 3-oxo-C12-HSL in 0.5 % agar (0.1 mL of 0.5 µM), a middle layer of different agar concentrations (0.8 mL of 1 % to 4 % Agar) and a top layer of PAO1 lasI$^-$ plasB::lux biosensor in LB with 0.5 % agar (0.1 mL, OD_{600}=0.2). The signal would over time diffuse trough the middle layer into the top, where it would induce the bacteria to luminescence. figure 5.10 shows a mock-up of this setup with food colouring instead of 3-oxo-C12-HSL and biosensor to better illuminate the concept as well as prove that when poured in a careful manner, the layers do not immediately mix but rather diffuse with time.

In order to check if higher luminescence was due to increased bacteria number, CFU were counted after 8 h. The results indicate that there was no large growth difference between the different agar treatments, see figure 5.10a. However, treatments with lower agar concentrations did reach higher luminescence values. Figure 5.10b shows the time curve for these treatments.

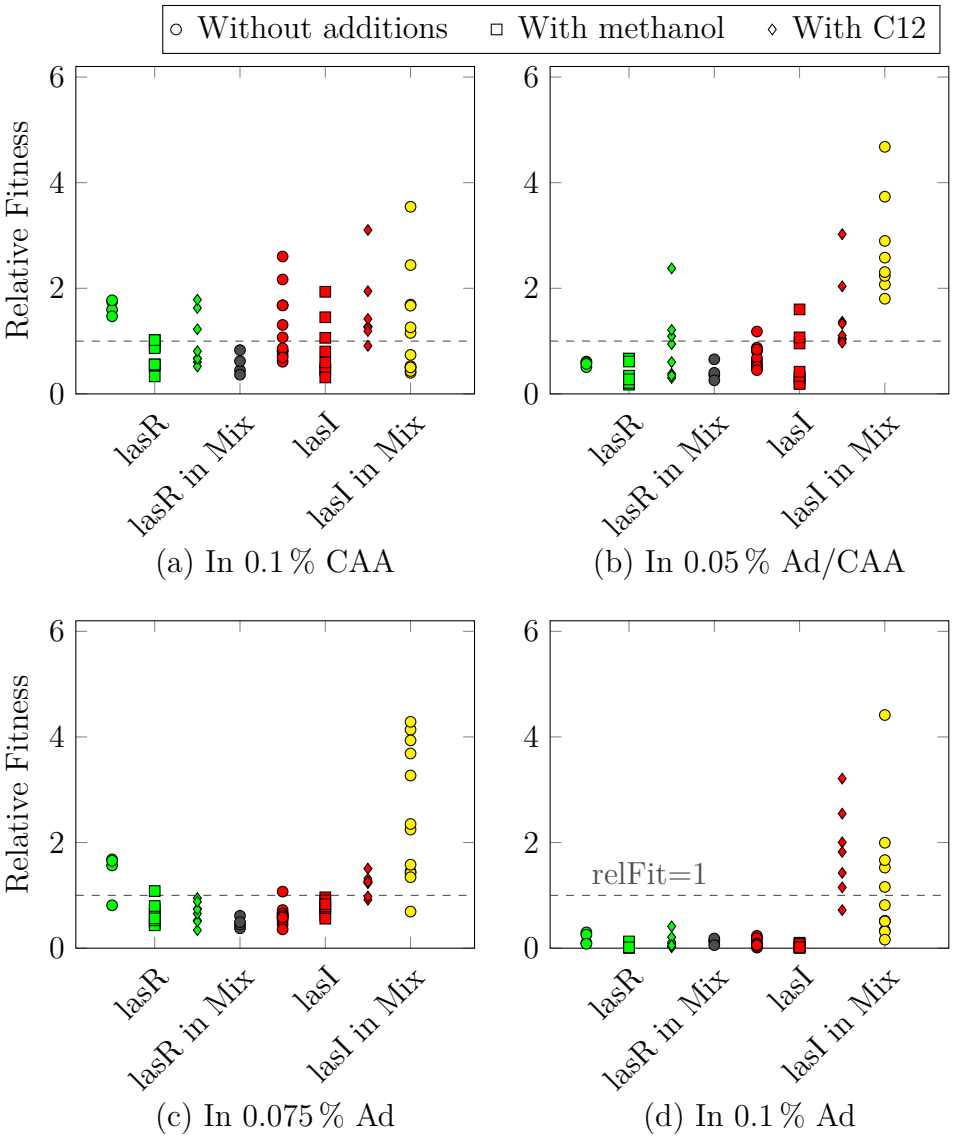

(a) In 0.1 % CAA (b) In 0.05 % Ad/CAA

(c) In 0.075 % Ad (d) In 0.1 % Ad

Figure 5.9: Relative fitness of lasI$^-$ and lasR$^-$ for varying treatments. With higher Ad concentrations, relative fitness of almost all mutant cultures declines, the only exceptions being lasI$^-$ in mixed culture or with added 3-oxo-C12-HSL.

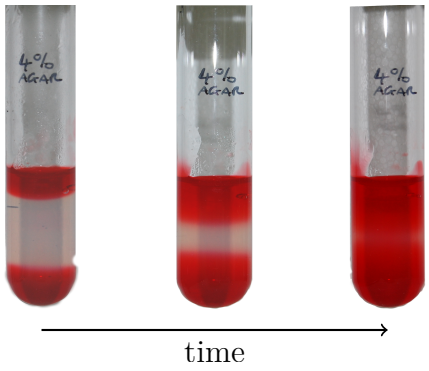

Figure 5.10: Concept of sandwich experiment, done with red food colouring. The top and bottom layers consist of 0.5 % agar, while the middle part consists of 4 % agar in these photos. When carefully poured, the layers remain separated at first and only small molecules diffuse with time.

This indicates different diffusion rates of 3-oxo-C12-HSL in different agar concentrations. Due to time constraints and difficulty working with higher agar concentrations, 1 % agar was chosen for the cheating experiments themselves.

5.3.2 Slowing diffusion reduces cheating

As our theory suggests, cheating in 1 % Agar is limited. This can be determined by comparing the relative fitness of lasI$^-$ in the solidified media with the values from the liquid experiments conducted before. The results are displayed in figure 5.12 and show that while relative fitness in pure culture does not differ much between liquid and solid media, there is a reduction of relative fitness in mixed culture when agar is added. The significance of this reduction will be shown in section 5.4.

Looking at the total CFU values after 48 h (accounting for different experiment volumes, see figure 5.13), one can see that there is not much change for 0 % to 0.075 % Ad. At 0.1 % Ad, however, we have a large increase in CFU for cultures in solid media. This increase is likely due to nutritional value of agar and thus plays a larger role in a nutrient-depraved environment such as pure adenosine when signal concentration is low. As we only compare relative fitness of cultures, this increase in total CFU does not play a role in our analysis.

5.4 Generalised linear models

In order to assess the importance of the different environmental aspects and the significance of the findings, the relative fitness values can be fitted by generalised

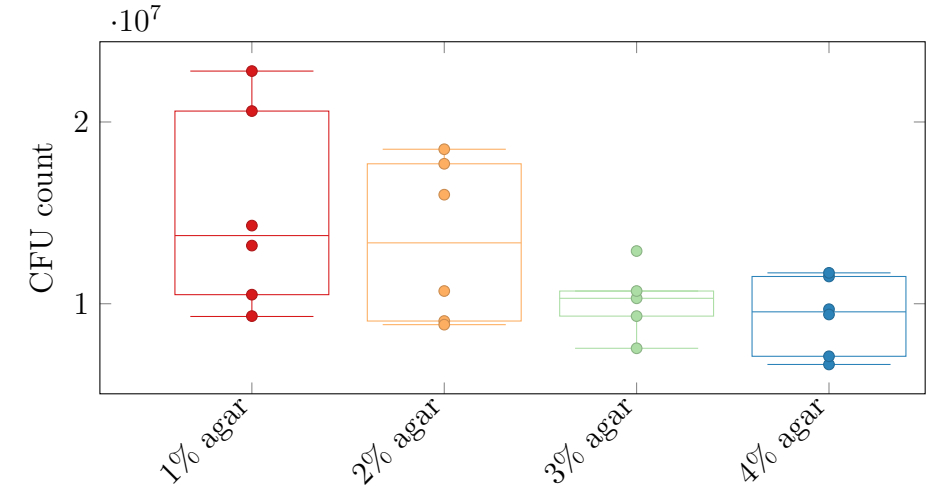

(a) CFU for different agar concentrations after 8h

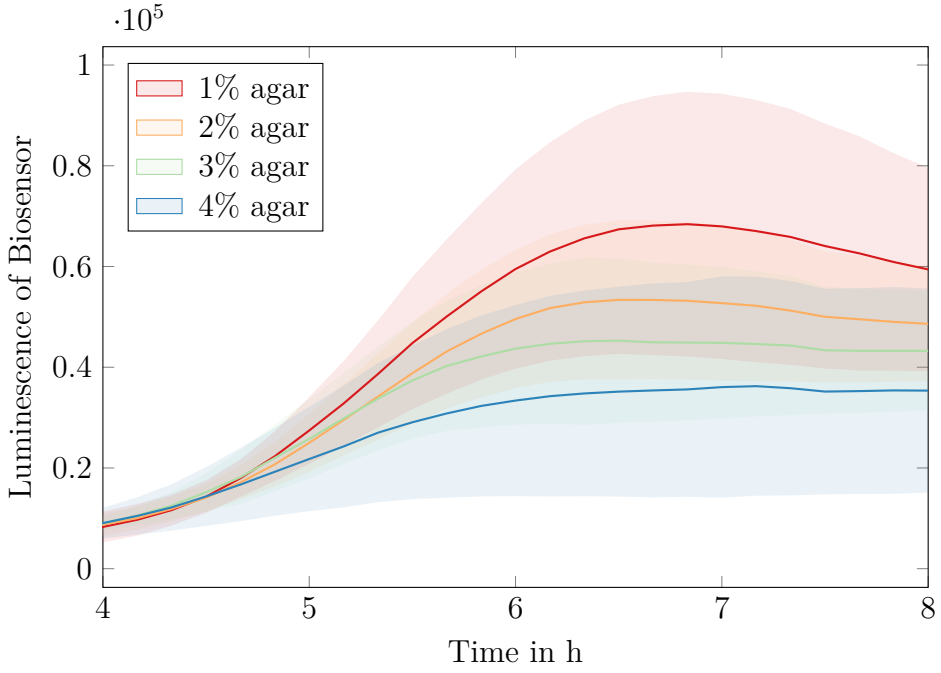

(b) Luminescence of biosensor

Figure 5.11: CFU count and luminescence of PAO1 lasI::lux in a top layer with 0.5 µM 3-oxo-C12-HSL in the bottom layer and different agar concentrations in between. Lines indicate mean values, while shaded areas indicate standard deviation around this mean. Although the data is noisy, one can see that there is a clear trend towards lower luminescence for higher agar values.

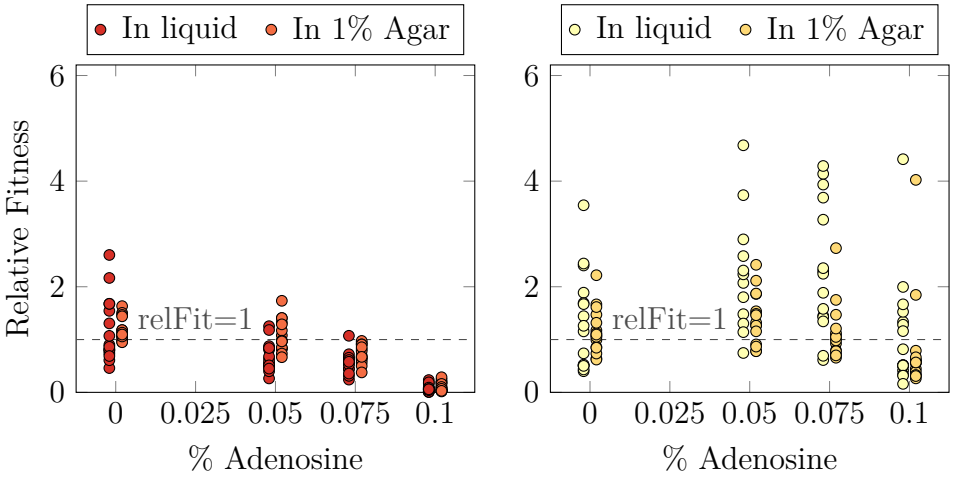

(a) Pure lasI⁻ cultures (b) Mixed cultures

Figure 5.12: Relative Fitness of lasI⁻ in mixed or pure cultures after 48 h, depending on whether or not the medium contained agar. While relative fitness of pure cultures is quite similar, it is continuously lower for 1 % agar in mixed cultures.

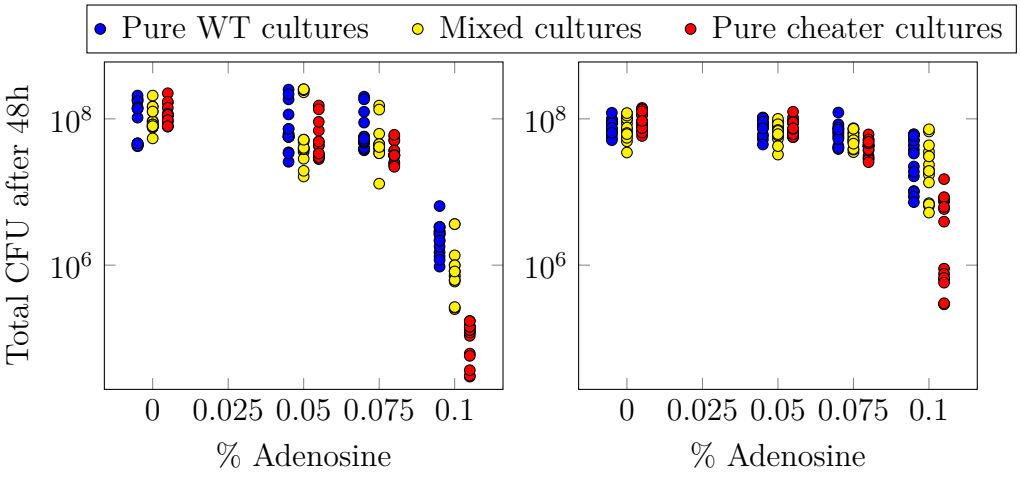

(a) In liquid culture (b) In solid culture

Figure 5.13: Comparison between CFU counts in liquid and solid culture after 48 h. The only notable difference is an increase in CFU for pure Ad in solid culture.

Table 5.2: Potential predictors for relative fitness

Description	Fitted as	Short form
How much adenosine the medium contained	continuous variable	Ad
Whether or not the mutant was grown in a coculture with PAO1	factor	Mix
Whether or not the medium was enriched with 3-oxo-C12-HSL	factor	C12
Whether or not the medium was solidified with 1 % agar	factor	Solid

linear models (GLMs). A look at the typical distribution of the relative fitness reveals that data with higher mean also shows higher variance. Hence a gamma distribution was chosen as underlying distribution for all the following GLMs. Table 5.2 shows the possible predictors for relative fitness. Depending on the situation, a subset of the possible predictors was chosen for the model. The analysis was conducted using the R package 3.2.3 and the model with or without interaction terms chosen depending on goodness of fit.

As a first dataset, we analyse the dependence of lasI$^-$ and lasR$^-$ fitness on co-culture and 3-oxo-C12-HSL addition. From figure 5.9 we expect both influences to be roughly similar. A plot of the GLM with standard deviation as shaded interval can be found in figure 5.14. We indeed find that *Mix* and *C12* have a similar influence on the relative fitness. A detailed list of all estimators and significance values can be found in appendix B. Here we just note that relative fitness declines with adenosine level for all cultures, as could be seen from the raw data points before (estimate for Ad -11.79 to -20.92). However, this is offset by the interaction term of *Ad* and *C12* respectively *Mix* for lasI$^-$ cultures (estimate for Ad:C12/Ad:Mix 25.14/22.76), leading to a positive slope for lasI$^-$ in mixed culture and with 3-oxo-C12-HSL. There is no such thing for lasR$^-$ colonies, and indeed the interaction term is not significant for them. This reinforces the statement made earlier: lasI$^-$ colonies have a growth advantage over PAO1 when external signal is supplied in some form that lasR$^-$ colonies do not achieve.

In the second analysis we want to compare relative fitness of lasI$^-$ in solid and liquid medium. The raw data in figure 5.12 suggests that for pure cultures, *Solid* should not change the behaviour, while the reverse is true for mixed cultures. And indeed we find that *Solid* does not have a big impact on pure lasI$^-$ cultures - the interaction term between *Ad* and *Solid* is not significant (Ad:Solid $p = 0.61$), while *Solid* on its own, though significant (Solid $p = 0.01$) has a very small estimator

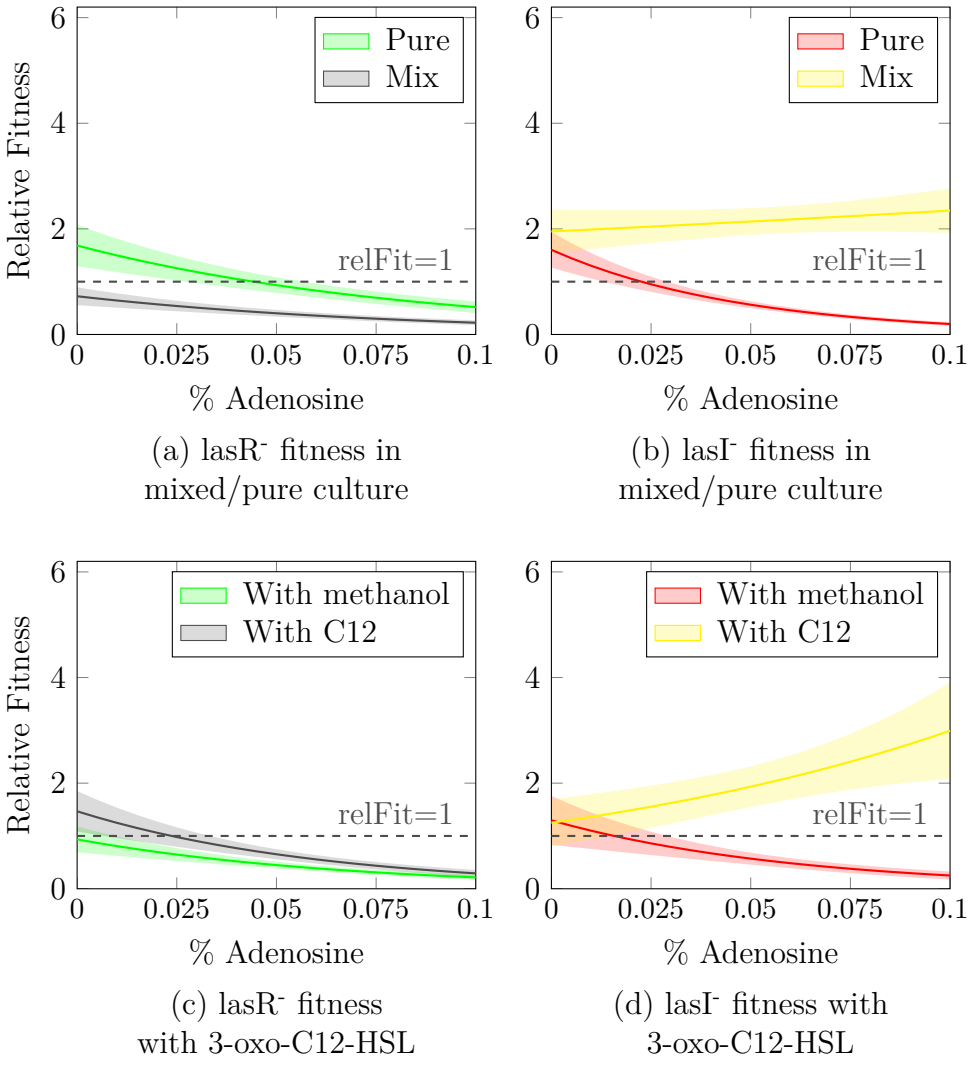

(a) lasR⁻ fitness in mixed/pure culture

(b) lasI⁻ fitness in mixed/pure culture

(c) lasR⁻ fitness with 3-oxo-C12-HSL

(d) lasI⁻ fitness with 3-oxo-C12-HSL

Figure 5.14: GLMs of lasR⁻ and lasI⁻ in pure/mixed culture and with/without 3-oxo-C12-HSL. For lasR⁻, relative fitness is negatively correlated with Ad percentage regardless of treatment. In lasI⁻, both the addition of purified 3-oxo-C12-HSL and PAO1 lead to a significant increase in relative fitness with Ad.

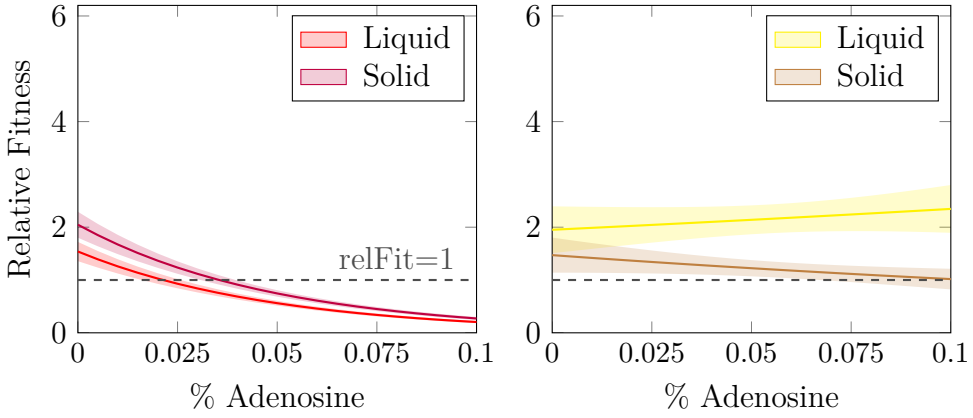

(a) lasI⁻ fitness in pure culture (b) lasI⁻ fitness in mixed culture

Figure 5.15: GLMs of lasI⁻ fitness in liquid and solid media, depending on culture condition. While there is a positive correlation between Ad concentration and relative fitness for lasI⁻ in liquid mixed culture, solidifying the media negates this effect, reverting the correlation back to a negative one as found for pure cultures. On the other hand, there is no notable difference in relative fitness when adding agar to pure cultures.

(Ad -20.20, Solid 0.28). At the same time, there is a significant decrease of relative fitness with Ad level (Ad $p < 10^{-16}$). For mixed cultures *Solid* is very significant ($p = 0.001$) and the interaction of *Ad* and *Solid* leads to a slight negative correlation of lasI⁻ fitness with Ad in solid culture in contrast to the positive correlation in liquid culture. As before, a list of all estimators and significance values can be found in appendix B. We can also visually compare the behaviour in figure 5.15.

These findings emphasise the impact of solidifying the media on relative fitness and show how important even a very simple spatial structure is. As such, they not only allow us to estimate parameters for the numerical simulations in the next chapter, but also encourage the ideas developed in chapters 3 and 4 about the importance of spatial modelling. Furthermore, our findings regarding growth rates of different cultures correspond well with the assumptions made in chapter 2 regarding costs and benefit of QS.

Chapter 6

Numerical implementation

6.1 Setting parameters

We use the experimental data from chapter 5 to derive values for the parameters in our model. Our aim here was to obtain rough estimates which replicate the general qualitative behaviour, as opposed to fit the experimental data exactly.

In the experimental set-up, there were two different *P. aeruginosa* strains investigated in different conditions: PAO1 bacteria in pure culture, further referred to as wild-type bacteria (WT), as well as *lasI* mutants (lasI$^-$) in pure culture and both WT and lasI$^-$ in mixed culture. Going back to chapter 2, we start with the simplest form of G-function, described in section 2.2.1. We note the shape of the G-function for the different culture conditions, the average number of colony forming units (CFU) as well as the amount of doublings in 0.05 % adenosine and casamino acids (CAA) after 24 h in tables 6.1 and 6.2. To this end, we assume that wild-type bacteria have a strategy $v = 1$, *lasI* mutants a strategy $v = 0$.

From these doublings, we can calculate a rough estimate of the cultures growth

Table 6.1: Averaged experimental values for 0.05 % adenosine and CAA.

Type	CFU at start	CFU after 24 h	Doublings
WT pure culture	1.2×10^5	3.7×10^7	8.26
lasI$^-$ pure culture	1.2×10^5	2.7×10^7	7.79
WT mixed culture	6.0×10^4	5.1×10^6	6.42
lasI$^-$ mixed culture	6.2×10^4	2.4×10^7	8.60

Table 6.2: Comparison of G-function shape and calculated growth rates in 0.05 % adenosine and CAA.

Type	G-function	estimated growth rate (1/h)
WT pure	$\left(B_{max} \cdot \frac{\mathrm{WT}^2}{\mathrm{WT}^2+\tau \mathrm{WT}} + B_{min}\right) \mathrm{e}^{-K} - \mu_{\mathrm{WT}}$	0.2386
lasI$^-$ pure	$B_{min} - \mu_{\mathrm{lasI^-}}$	0.2251
WT mix	$\left(B_{max} \cdot \frac{\mathrm{WT}^2}{\mathrm{WT}^2+\tau(\mathrm{WT}+\mathrm{lasI^-})} + B_{min}\right) \mathrm{e}^{-K} - \mu_{(\mathrm{WT}+\mathrm{lasI^-})}$	0.1854
lasI$^-$ mix	$\left(B_{max} \cdot \frac{\mathrm{WT}^2}{\mathrm{WT}^2+\tau(\mathrm{WT}+\mathrm{lasI^-})} + B_{min}\right) - \mu_{(\mathrm{WT}+\mathrm{lasI^-})}$	0.2484

rate (summarized in table 6.2), as

$$\begin{aligned} b(24\,\mathrm{h}) &= b_0 \cdot \mathrm{e}^{24\,\mathrm{h}\cdot r} \\ b_0 \cdot 2^{\mathrm{doublings}} &= b_0 \cdot \mathrm{e}^{24\,\mathrm{h}\cdot r} \\ r &= \frac{\mathrm{doublings}}{24\,\mathrm{h}} \cdot \ln(2). \end{aligned}$$

We can do this calculation for lasI$^-$ in pure culture, obtaining

$$r_{\mathrm{lasI^-}} = 0.2251\,\frac{1}{\mathrm{h}}.$$

The second parameter we want to calculate is μ. As we see a carrying capacity of about 10^7 CFU, we use the growth rate of lasI$^-$ in pure culture (being the lowest) to calculate μ through

$$\begin{aligned} 0.2251\,\mathrm{h}^{-1} &= \mu \cdot \frac{10^7\,\mathrm{CFU}}{20^2} \\ \mu &= 1.8 \times 10^{-6}\,\mathrm{h}^{-1}\,\mathrm{CFU}^{-1}. \end{aligned}$$

We divide by 20^2 as we will use a two-dimensional grid with 20 "spaces" in each direction in our calculations later on. The total amount of bacteria in the grid will therefore be

$$\sum_{i=1}^{20}\sum_{j=1}^{20} b_{i,j} \approx 20^2 \cdot b$$

if enough time has passed for the bacteria to distribute. As such, we will also adjust the start and end CFU of the cultures by dividing through 20^2 for the further calculations. The CFU at start will be used to calculate the population-dependent

death rate, while the CFU after 24 h is used in calculating the effect of QS, because the benefit of QS is more apparent with higher cell numbers.

We start by noting that

$$B_{\min} = 0.2251\,\mathrm{h}^{-1} + \mu \cdot \frac{1.2 \times 10^5\,\mathrm{CFU}}{20^2} = 0.2256\,\mathrm{h}^{-1}.$$

Another short calculations for the two bacteria types in mixed population gives us

$$\frac{r_{\mathrm{WT}} + \mu_{(\mathrm{WT+lasI^-})}}{r_{\mathrm{lasI^-}} + \mu_{(\mathrm{WT+lasI^-})}} = \mathrm{e}^{-K} = \frac{0.1859}{0.2489}$$
$$\Rightarrow \quad K = 0.2918.$$

In order to calculate B_{max} and τ, we compare wildtype populations growing in pure and mixed conditions. It holds that

$$\begin{aligned}
&r_{\mathrm{pure}} + \mu_{\mathrm{WT}} \\
&\quad = \left(B_{max} \cdot \frac{3.7 \times 10^7\,\mathrm{CFU}/20^2}{3.7 \times 10^7\,\mathrm{CFU}/20^2 + \tau} + 0.2256\,\mathrm{h}^{-1} \right) \cdot \mathrm{e}^{-0.2918} \\
&\quad = 0.2391\,\mathrm{h}^{-1} \\
&r_{\mathrm{mix}} + \mu_{(\mathrm{WT+lasI^-})} \\
&\quad = \left(B_{max} \cdot \frac{(1.3 \times 10^4)^2\mathrm{CFU}}{(1.3 \times 10^4)^2\mathrm{CFU} + \tau \cdot 7.3 \times 10^4} + 0.2256\,\mathrm{h}^{-1} \right) \cdot \mathrm{e}^{-0.2918} \\
&\quad = 0.1859\,\mathrm{h}^{-1} \\
\Rightarrow \quad & B_{max} \cdot \frac{9.2 \times 10^4\,\mathrm{CFU}}{9.2 \times 10^4\,\mathrm{CFU} + \tau} = 0.1363\,\mathrm{h}^{-1} \\
& B_{max} \cdot \frac{1.7 \times 10^8\,\mathrm{CFU}}{1.7 \times 10^8\,\mathrm{CFU} + \tau \cdot 7.3 \times 10^4} = 0.0699\,\mathrm{h}^{-1} \\
\Rightarrow \quad & \frac{9.2 \times 10^4}{9.2 \times 10^4\,\mathrm{CFU} + \tau} \cdot \frac{1.7 \times 10^8\,\mathrm{CFU} + \tau \cdot 7.3 \times 10^4}{1.7 \times 10^8} = 1.9499 \\
\Rightarrow \quad & \tau = 7.61 \times 10^3\,\mathrm{CFU} \\
\Rightarrow \quad & B_{max} = 0.1024\,\mathrm{h}^{-1}.
\end{aligned}$$

We now have a full set of parameters for the situation with 0.05 % adenosine and CAA. If we repeat the process for the 0.075 % adenosine, we get the parameters listed in the first two lines of table 6.3.

The situation for pure CAA and pure adenosine is a bit different. If all carbon is supplied in the form of CAA the growth rates of all our experimental setups is equal to 0.269 ± 0.006. We will therefore conclude that QS seems to have no special impact on the bacteria in this situation.

Table 6.3: Calculated parameter values for different media.

Media	B_{max} 1/h	a	B_{min} 1/h	K	μ 1/(h CFU)	τ CFU
0.05 % Ad	0.1024		0.2256	0.2918	1.8×10^{-6}	7.6×10^{3}
0.075 % Ad	0.091		0.1945	0.1978	2.2×10^{-6}	6.1×10^{3}
0.1 % Ad		0.7186	0.0181	2.459	7.2×10^{-7}	1.5×10^{5}

Table 6.4: Comparison of G-function shape and calculated growth rates in 0.1 % adenosine.

Type	G-function	estimated growth rate (1/h)
WT pure	$\left(\frac{\mathrm{WT}^2}{\mathrm{WT}^2+\tau\mathrm{WT}} + \frac{1}{1+a^2} + B_{min}\right) \mathrm{e}^{-K}$	0.0608
lasI$^-$ pure	B_{min}	0.0065
WT mix	$\left(\frac{\mathrm{WT}^2}{\mathrm{WT}^2+\tau(\mathrm{WT}+\mathrm{lasI}^-)} + \frac{1}{1+a^2} + B_{min}\right) \mathrm{e}^{-K}$	0.0474
lasI$^-$ mix	$\left(\frac{\mathrm{WT}^2}{\mathrm{WT}^2+\tau(\mathrm{WT}+\mathrm{lasI}^-)} + B_{min}\right)$	0.0384

For pure adenosine we calculate the growth rate from the doublings after 48 h. Since the bacteria have not yet reached carrying capacity in this case and exhibit very slow growth, this will give us more accurate numbers. The resulting estimates can be found in the last line of table 6.4.

It becomes apparent that it is not possible to proceed analogously in the 0.1 % Ad case, since we can find no biologically feasible parameters that fit the estimated growth rates.

Looking at the growth rates again it becomes clear that in mixed culture the wild type has a higher growth rate than lasI$^-$. For this reason, we suspect that there might be a private, non-cheatable benefit associated with QS in this medium. Table 6.4 already shows the appropriate G-function terms for the different cases if we assume a private benefit as detailed in section 2.2.1. The calculations themselves then proceed much like before; results can be found in table 6.3.

6.2 Method of lines

If we want to make numerical simulations of the coupled ODE-PDE systems developed before, the pre-programmed PDE solvers of Matlab will not suffice. In order to calculate a numerical solution, we must therefore discretise the equations

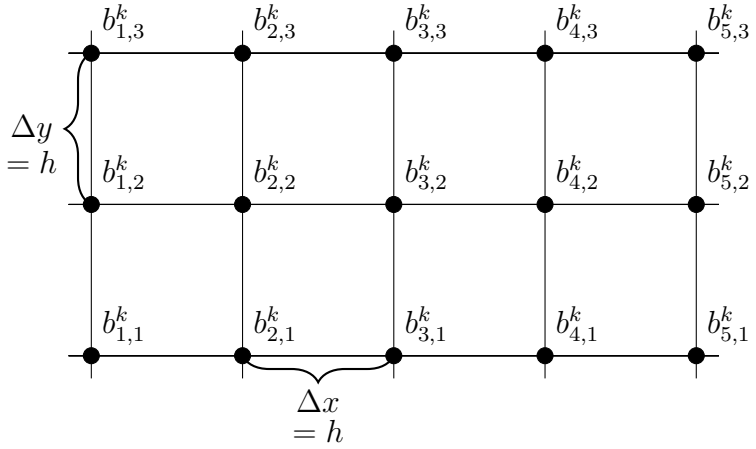

Figure 6.1: A basic representation of the method of lines

with respect to both time and space.

The method of lines is a way to discretise a PDE with respect to space, turning it into a system of coupled ODEs. This system can then be solved using standard ODE solvers, e.g. Runge-Kutta methods. It is a simple method for cases like ours, where the exact shape of Ω is not of particular interest. Schiesser [Sch91] introduced the method for many classes of PDEs in his book. In order to keep the results demonstrative, we will concentrate on space dimension 2.

The basic idea is to have an evenly spaced grid with distance h. The grid intersections will then have coordinates (x_i, y_i), where $\Delta x = x_i - x_{i-1} = h$ as well as $\Delta y = y_i - y_{i-1} = h$ for all grid points. In the following, we will assume Ω to be a square of side length L and require h to be a divider of L, s.t. $L = h \cdot (N-1)$ for an $N \in \mathbb{N}$. Without loss of generality we can assume the square to have its lower left corner in the origin. It then holds that $x_i = (i-1) \cdot h$ and thus $x_1 = 0$, $x_N = L$. Figure 6.1 shows this construction, along with the notation we will adapt, namely denoting the bacterial population of type k at the grid intersection points x_i and y_i as b^k_{ij}:

$$b^k_{ij}(t) = b_k(t, x_i, x_j).$$

In two-dimensional space, the Laplace transforms to

$$\triangle b_k(t, x, y) = \partial^2_x b_k(t, x, y) + \partial^2_y b_k(t, x, y).$$

It remains to find an approximation to the partial derivatives in the discretised system. For that, we will use the standard central finite difference schemes with

second order accuracy, e.g.

$$\partial_x b_i^k = \frac{b_{i+1}^k - b_{i-1}^k}{2h}, \tag{6.2.1}$$

$$\partial_x^2 b_i^k = \frac{b_{i+1}^k - 2b_i^k + b_{i-1}^k}{h^2}. \tag{6.2.2}$$

All in all, equation (4.2.1) transforms to a coupled ODE system for b_{ij}^k and v_{ij}^k, namely

$$\partial_t b_{ij}^k = G(v_{ij}^k, v_{ij}, b_{ij}) \cdot b_{ij}^k + D \cdot \frac{b_{i+1,j}^k + b_{i,j+1}^k - 4b_{ij}^k + b_{i-1,j}^k + b_{i,j-1}^k}{h^2}, \tag{6.2.3a}$$

$$\partial_t v_{ij}^k = \varepsilon \partial_1 G(v_{ij}^k, v_{ij}, b_{ij}). \tag{6.2.3b}$$

In order to solve the full problem, we need to take care of initial and boundary conditions. While initial conditions translate into the discretised system without further problems, one needs to take a bit more care with boundary conditions. In this case, as there is no loss of bacteria on the boundary, we will assume Neumann boundary conditions. They translate to

$$\partial_x b^k(t, 0, y) = 0, \qquad \partial_x b^k(t, L, y) = 0,$$
$$\partial_y b^k(t, x, 0) = 0, \qquad \partial_y b^k(t, x, L) = 0,$$

and can be reshaped using equation (6.2.1) to get

$$b_{i,0}^k = b_{i,2}^k, \quad b_{i,N+1}^k = b_{i,N-1}^k, \quad b_{0,j}^k = b_{2,j}^k, \quad b_{N+1,j}^k = b_{N-1,j}^k. \tag{6.2.4}$$

The system of ODEs consisting of (6.2.3) together with (6.2.4) and appropriate initial conditions is then implemented in Matlab and solved with Runge-Kutta-techniques. The explicit Matlab code for the calculations themselves can be found in appendix C.2. It makes use of an explicit Runge-Kutta-Solver inherent in Matlab, based on the Dormand-Prince method.

6.3 Changes to equation system

When going from the theoretical analysis done in chapters 2 to 4 to a numerically solvable system, a few changes are usually necessary. For our system, there are three such changes: We define concrete initial and boundary conditions and modify the definition of our cost function.

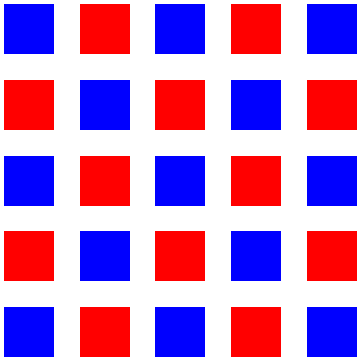

Figure 6.2: Output of the `patches` code (see appendix C.1) with 2 species (depicted in blue and red), a patch size of 4 and a separation of 2.

Initial conditions For initial conditions we will be using patches for b, as we assume that the subpopulations are mixed but not completely homogeneous in the beginning. Appendix C.1 displays the code used to create these patches, while figure 6.2 exemplarily shows the output.

Boundary conditions In chapter 4 we have often assumed homogeneous Robin boundary conditions, or even more general ones. For our numerical calculations, we will simplify the boundary conditions to homogeneous Neumann conditions in order to model the no-flux condition of the experimental system.

Modification of the cost function We also add in a feature of QS that we have neglected before: the costs of QS depend on the signal level, as QS products are only produced when the signal level is high enough. For models without abiotic components, we can achieve this by modifying the cost term from equation (2.1.3) to

$$C(v_i, v, b) = \exp\left(-K \cdot (B(v, b) \cdot v_i)^2\right), \tag{6.3.1}$$

as $B(v, b)$ is a measure for the level of QS. We have not done so before, since it does not change the analysis qualitatively, but leads to unnecessarily long and obfuscating terms.

If we already work with explicit model terms for QS signal, we can use this straight away by setting

$$C(s, v_i) = \exp\left(-K \cdot \left(\frac{s^2}{s^2 + \tau^2} \cdot v_i\right)^2\right). \tag{6.3.2}$$

Table 6.5: Comparison of relative fitness (see equation (5.2.1)) of different cultures after 48 h, from numerical simulations and experimental values

	liquid		solid	
Media	simulation	experiment	simulation	experiment
0.05 % Ad	2.39	2.68	1.29	1.48
0.075 % Ad	1.56	1.70	0.91	0.94
0.1 % Ad	0.72	0.64	0.54	0.56

6.4 Replicating experimental situations

We first run simulations based completely on the parameters calculated in section 6.1 and check if the qualitative behaviour we find is the same as in the experiments. For this part, we will use the system analysed in section 4.2, with the changes discussed in section 6.3. The equations to be solved are

$$\partial_t b_i(x,t) = G(v_i(x,t), v(x,t), b(x,t)) \cdot b_i(x,t) + D \triangle b_i(x,t), \quad x \in \Omega \tag{6.4.1a}$$

$$\frac{\partial b_i(x,t)}{\partial n} = 0, \quad x \in \partial\Omega \tag{6.4.1b}$$

$$\partial_t v_i(x,t) = \varepsilon \partial_1 G(v_i(x,t), v(x,t), b(x,t)). \quad x \in \bar{\Omega} \tag{6.4.1c}$$

The only parameter not yet determined is the diffusion coefficient D. Through a series of simulation runs, we find that simulations with $D = 0.1\,\mathrm{mm}^2/\mathrm{h}$ correspond well to the experiments done in liquid culture, while $D = 0.001\,\mathrm{mm}^2/\mathrm{h}$ lets us replicate the experimental values from solid culture. Table 6.5 gives an overview of the correspondence between simulation and experiment. The plots for 0.05 % to 0.1 % Ad can be found in figures 6.3 to 6.5. We can see that the lower diffusion rate of $D = 0.1$ leads to a fast spatial homogenisation, while $D = 0.001$ preserves the initial inhomogeneous structure longer. Consequently, lasI$^-$ cannot profit as much from being in proximity to WT when diffusion is low, which we found to be true in the experiments. Additionally, the growth advantage of lasI$^-$ is diminished by rising Ad content. This is visually most apparent when comparing the growth in liquid culture, figures 6.3a, 6.4a and 6.5a.

6.5 Comparing different *G*-functions

In chapter 2, we have examined two different categories of G-functions, with and without abiotic components. In addition, we have explored the possibilities for a private benefit to QS, in addition to public good (PG) production. We now

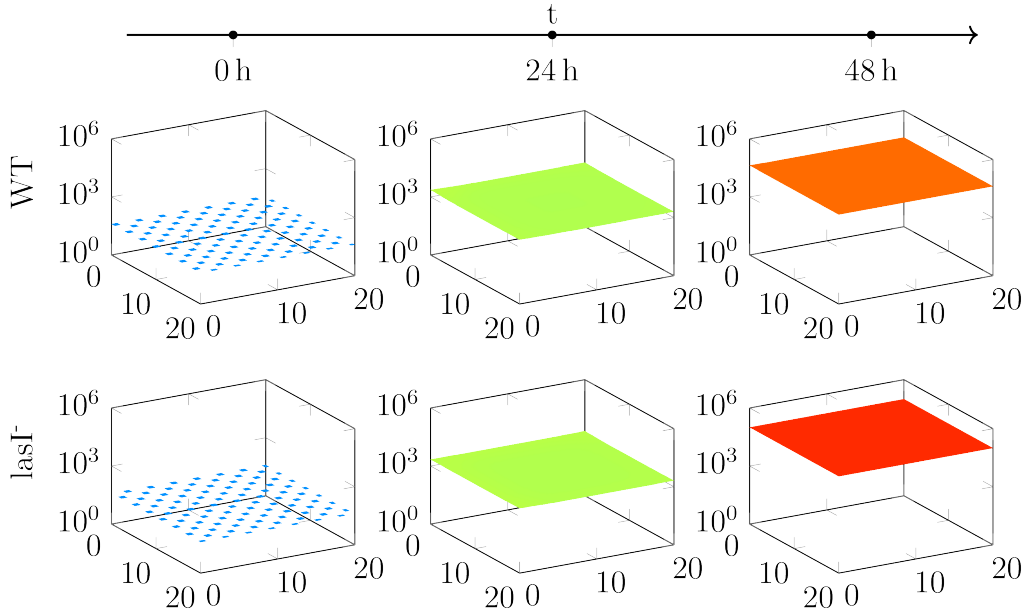

(a) Simulation results for $D = 0.1$.

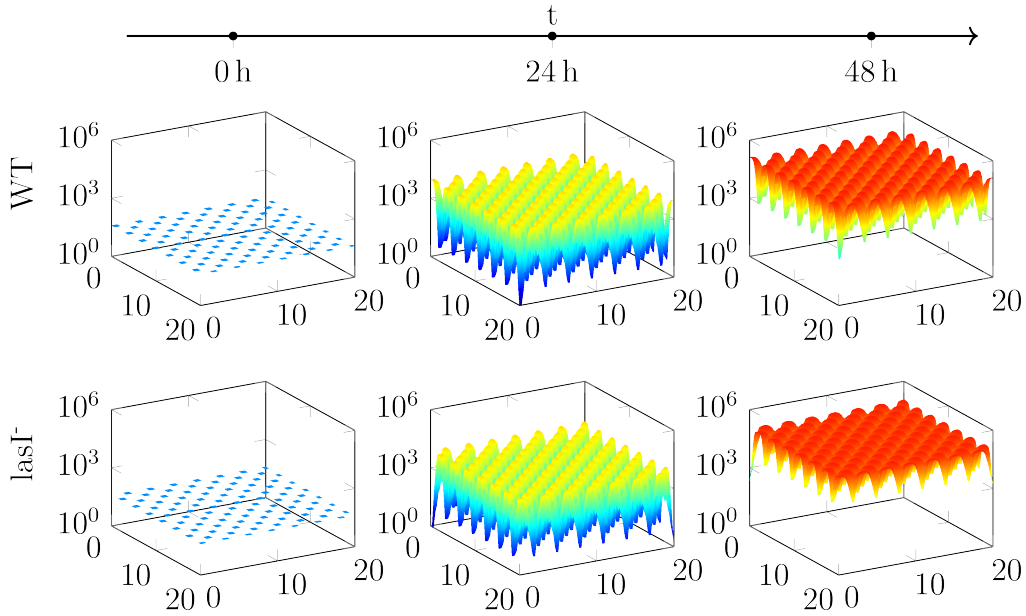

(b) Simulation results for $D = 0.001$.

Figure 6.3: Simulation results in 0.05 % Ad. Both WT and lasI- start out with the same CFU, but lasI- ends with the higher density after 48 h. This effect is more pronounced in liquid culture ($D = 0.1$), while the lower diffusion in solid culture ($D = 0.001$) preserves the initial inhomogeneous structure.

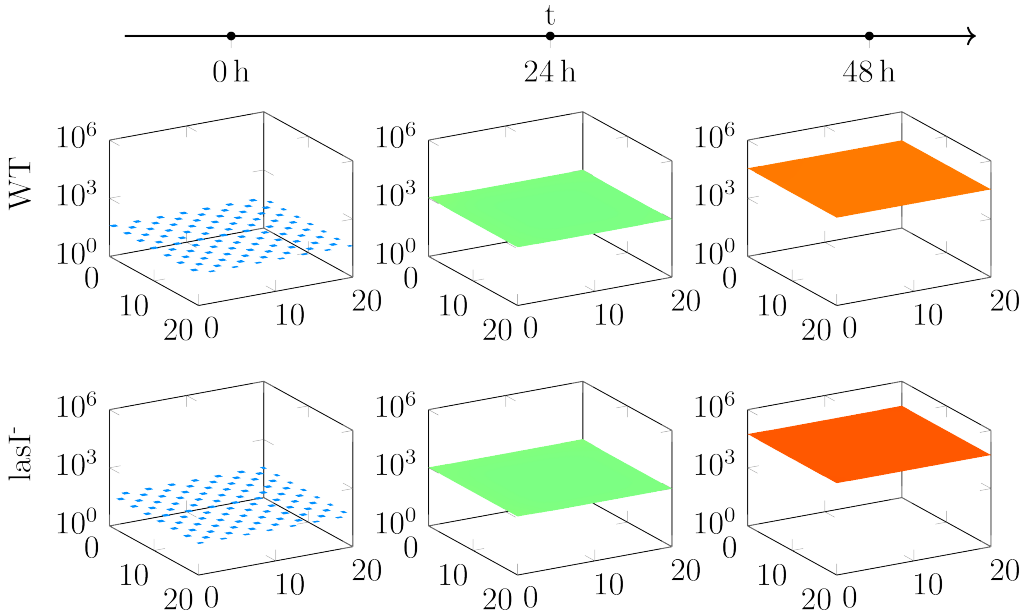

(a) Simulation results for $D = 0.1$.

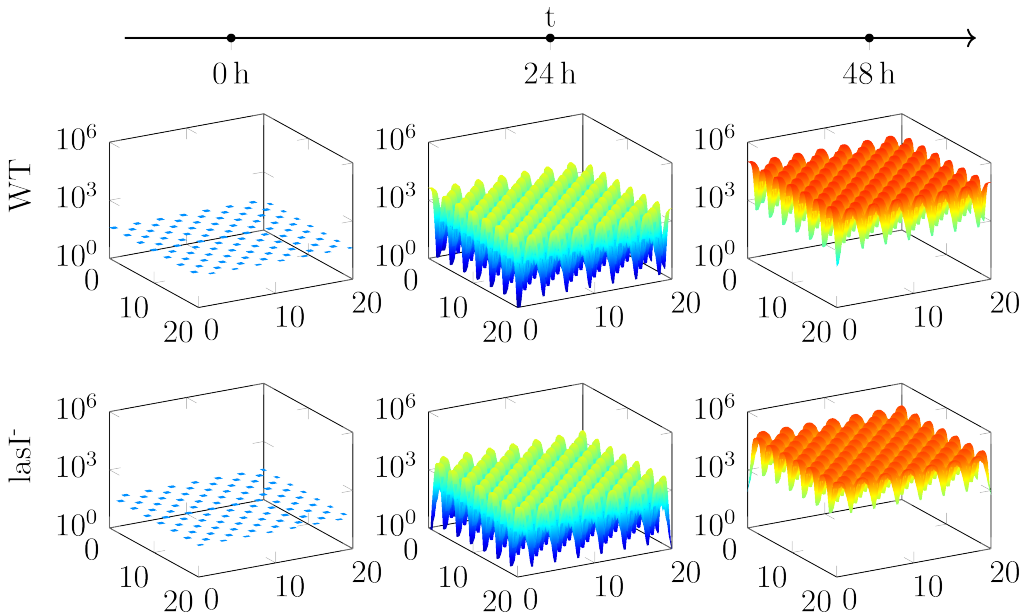

(b) Simulation results for $D = 0.001$.

Figure 6.4: Simulation results for parameter values in 0.075 % adenosine.

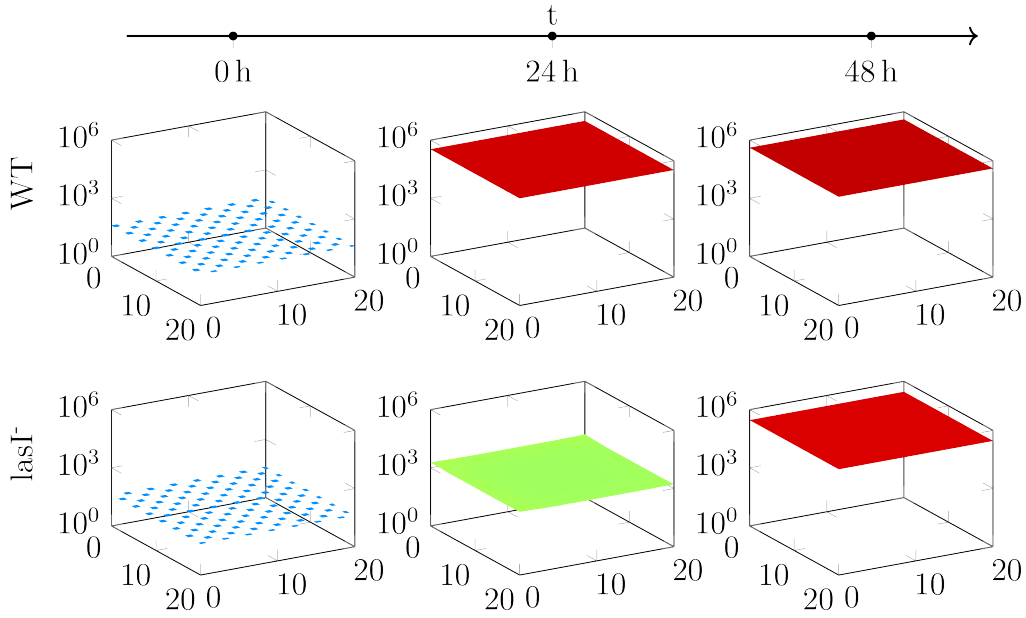

(a) Simulation results for $D = 0.1$.

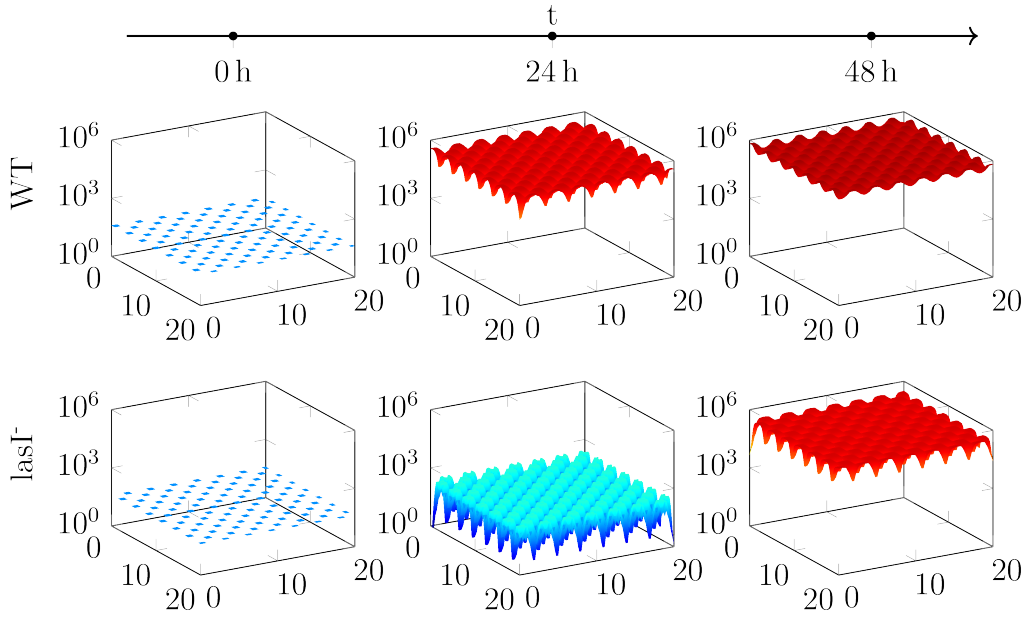

(b) Simulation results for $D = 0.001$.

Figure 6.5: Simulation results for parameter values in 0.1 % adenosine.

want to explore the behaviour in these cases numerically. In order to keep the results comparable, the underlying model will remain as before, namely a coupled ODE-PDE system.

6.5.1 G-function without abiotic components

In this case, the equation system to be solved remains exactly as in equation (6.4.1). We study the cases investigated in section 2.2.1: a case where there is only the public benefit to QS, one with private benefits $B(v_i)$ and one with a strategy-dependent death rate.

$$\boldsymbol{G(v_i, v, b) = B(v, b) \cdot C(v_i) - \mu \|b\|_1}$$

We have seen in our calculations that $v_i = 0$ is the only stable strategy in this situation. We should therefore have $v_i \to 0$, and if $B_{\min} = 0$, $b_i \to 0$. Yet, when looking at the simulation results for 3000 h as displayed in figure 6.6, we notice that this convergence is very slow indeed. A quick calculation of $\partial_1 G$ and G for our parameter values confirms that both are close to zero. So even though QS is theoretically unstable, both cheaters and producers persist alongside each other for a very long time, albeit at different densities.

$$\boldsymbol{G(v_i, v, b) = \Big(B(v, b) + B(v_i)\Big) \cdot C(v_i) - \mu \|b\|_1}$$

In section 2.2.1 we have focussed on Hill-terms for $B(v_i)$ and realized that the long-term behaviour is critically dependent on the Hill coefficient h. Figures 6.7 to 6.9 show the results for $h = 1, 2$ or 3.

As predicted, the behaviour in these cases is quite different. For $h \leq 2$ we postulated that there can only be one positive stationary point for v and if it is stable, then the zero solution is unstable. This is the case for the parameters we have calculated. Additionally, we find that for $h = 1$ the zero solution is not a stationary point. Thus both strategies converge towards the stable positive equilibrium, one from above, the other from below. Population 2, which started out as cheaters, gains QS functionality, while there is reduced production from population 1. Since reducing production is slower to reach the stable point in this parameter constellation, population 1 succumbs to the population pressure from population 2 and dies out (see figure 6.7). This happens on a rather short time frame of less than 200 h.

For $h = 2$, we can see from figure 6.8 that once again the strategies converge to a positive value. But this time the zero solution is a stationary point, although an unstable one. Hence population 2 cannot gain QS functionality by starting out

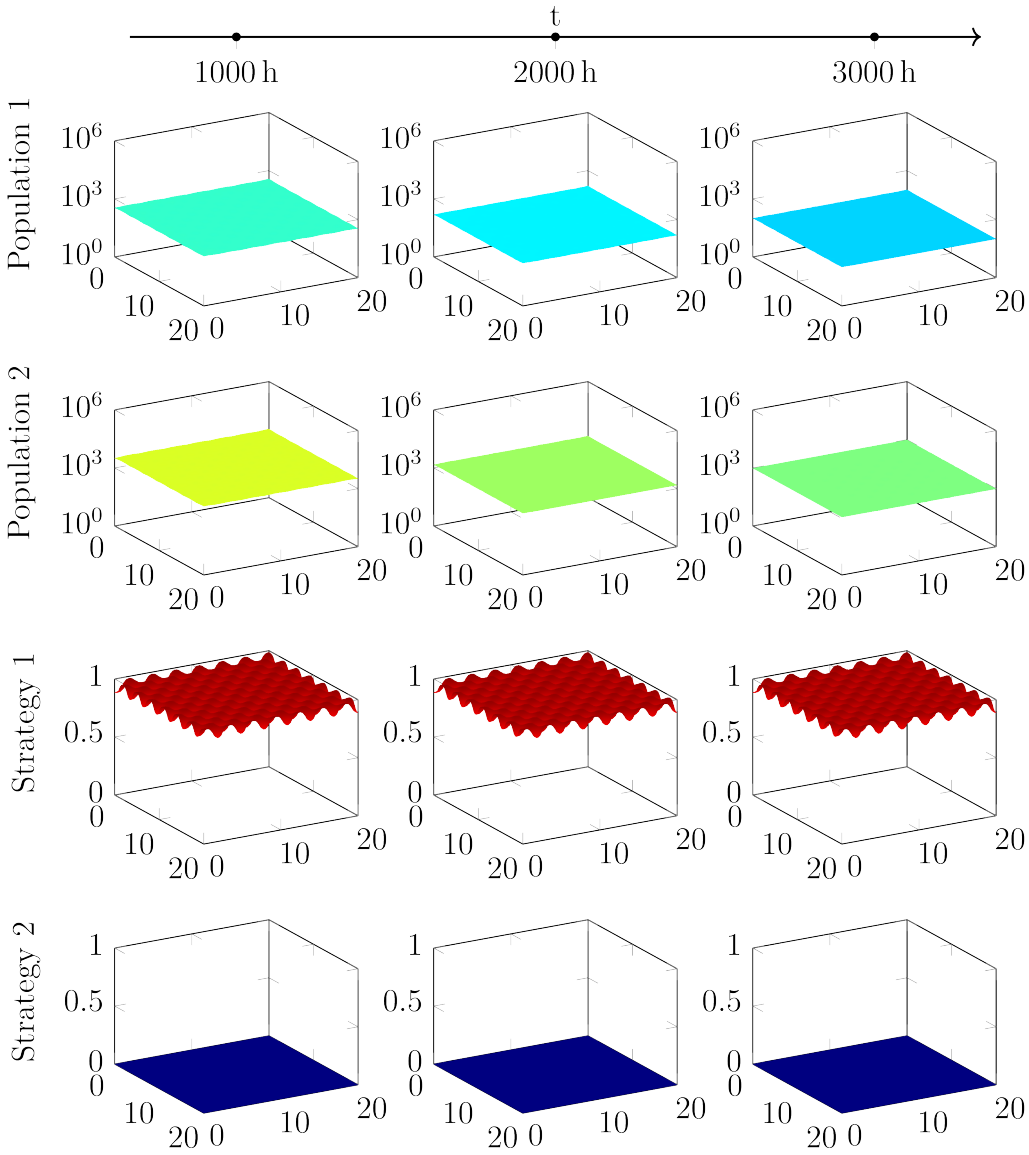

Figure 6.6: Long-term behaviour of two populations with different start strategies, using a G-function without additions. Both populations numbers are slowly converging towards zero, with WT having the lower CFU.

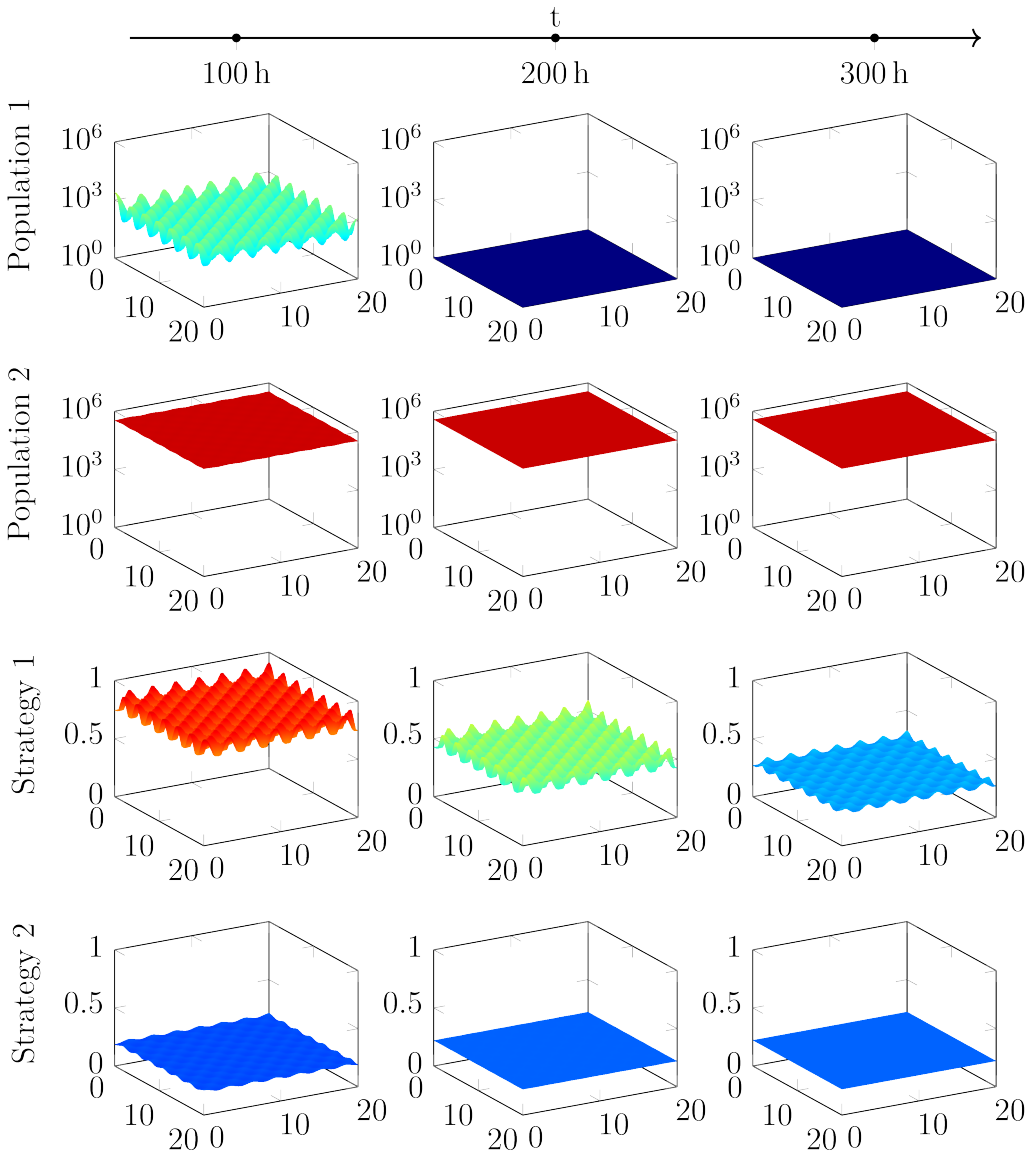

Figure 6.7: Evolution of two populations with different start strategies, using a G-function with private benefit and a hill factor of $h = 1$. Note the shorter time-scale in this plot. Population 1 dies out rather quickly, while population 2 gains the QS functionality, albeit at a low level, and remains at a stable population level.

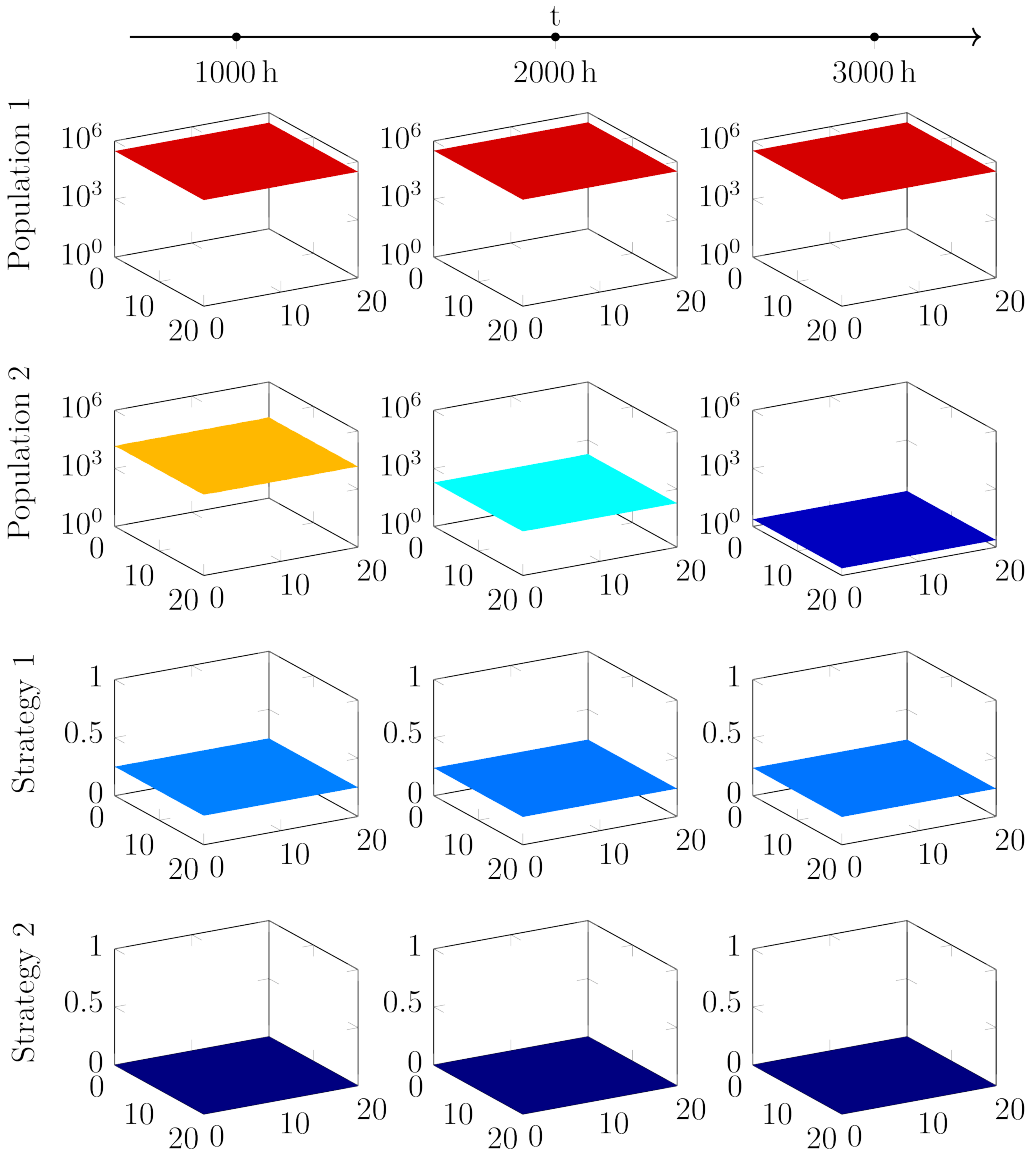

Figure 6.8: Evolution of two populations with different start strategies, using a G-function with private benefit and a hill factor of $h = 2$. In this scenario, population 1 reduces its QS strategy to a lower, but stable value. Population 2 is unable to compete and dies out.

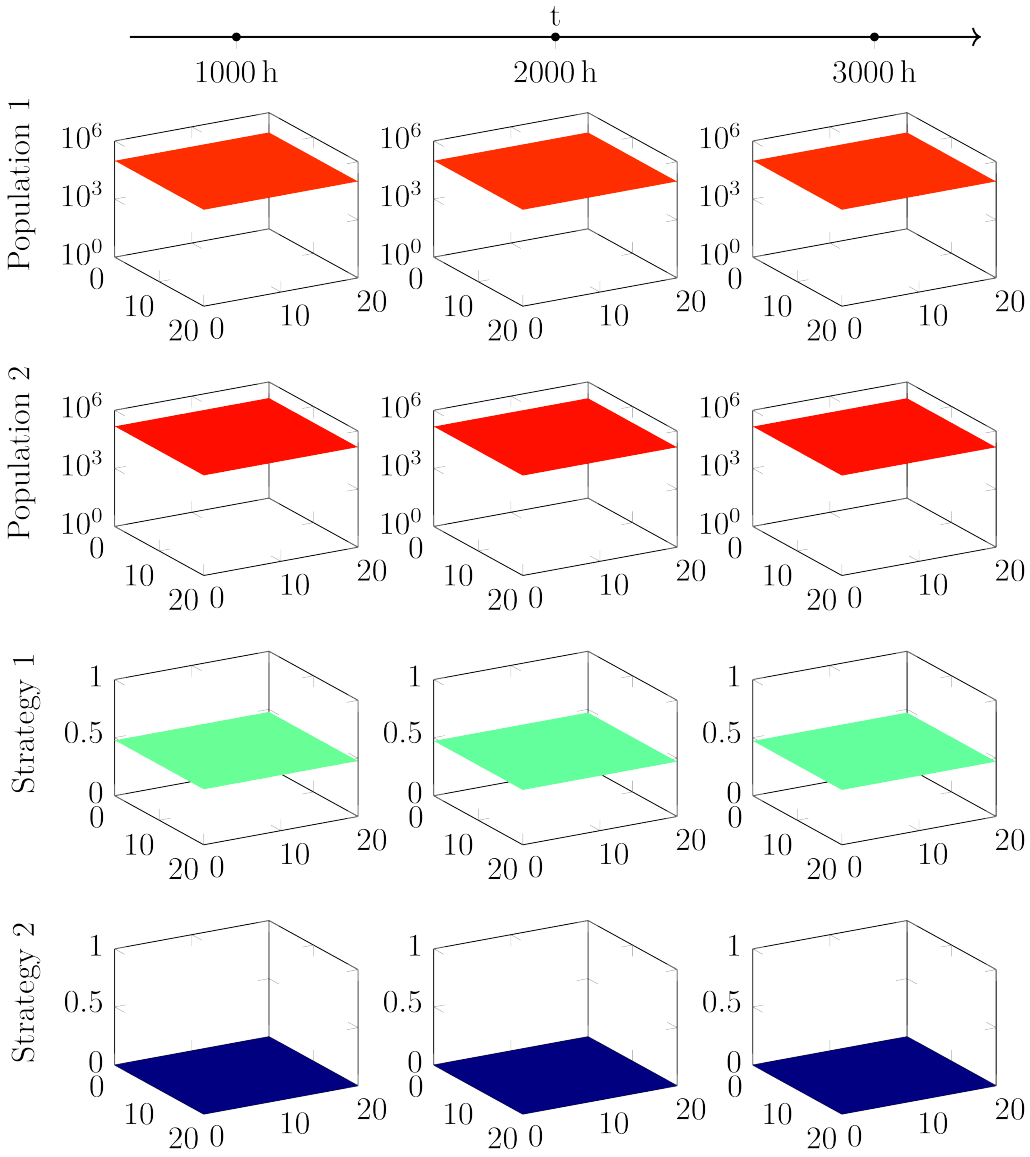

Figure 6.9: Evolution of two populations with different start strategies, using a G-function with private benefit and a hill factor of $h = 3$. Both population 1 and 2 are coexisting in a stable way with similar CFU. One population is QS active while the other is not.

with $v_2 = 0$. The end result is the extinction of population 2, while population 1 remains stable.

All in all, for $h \leq 2$ we find that one population is driven to extinction, while the other stays at a stable level with QS intact at lower levels.

When $h > 2$, we know from section 2.2.1 that there might be a stable positive strategy in addition to a stable zero solution. We find this to be the case for $h = 3$ for our parameters, as one can see in figure 6.9. This means that both population 1 and population 2 remain at stable population and strategy levels, with population 1 practising QS while population 2 consists of cheaters. In this scenario, producers and non-producers can live side-by-side indefinitely.

Additionally, for $h = 3$, there might exist unstable positive stationary strategies, depending on parameter values. For simplicity's sake, we show the effect for one population only and set $B_{\min} = 1$, $K = 0.5$ as well as disable cost dependency. As a result, when set to this unstable state both population and strategy remain constant, but tend towards either zero or the positive evolutionary stable strategy (ESS) if perturbed. If the perturbation is not spatially homogeneous, the resulting stationary state might not be homogeneous as well. One example for such an effect is shown in figure 6.10.

$\boldsymbol{G(v_i, v, b) = B(v, b) \cdot C(v_i) - \mu(v_i)\|b\|_1}$

Instead of a direct private benefit we have also discussed G-functions with strategy-dependent death rates $\mu(v_i)$ in section 2.2.1. The explicit function examined in detail was

$$\mu(v_i) = (\mu_{\max} - \mu_{\min})\, \mathrm{e}^{-dv_i^2} + \mu_{\min}.$$

We know that the behaviour largely depends on the relation between K and d and between $B(v, b)$, $\|b\|_1$, $\Delta\mu$ and K. In order to change the latter of the two relations, one would have to change some of the "main" parameters we have kept constant so far. In addition, it is difficult to calculate this value before running the simulation. It is thus easier to change the relation between K and d, even though we have raised some concerns about the case $K > d$ in section 2.2.1. Our primary concern we voiced was about the instability of the positive stationary point $\bar{v}_i$ and the subsequent divergence of the strategy value for large v_i. But in praxis, this instability hardly matters if $\bar{v}_i$ is large enough. In fact, one could even relax our initial assumption from

$$\exists v^* : \ \partial_1 G(v^*, v, b) < 0 \quad \forall v_i \geq v^*$$

to

$$\exists v^* > \max\left\{\left\|v_i^0\right\|_\infty\right\} : \ \partial_1 G(v^*, v, b) < 0$$

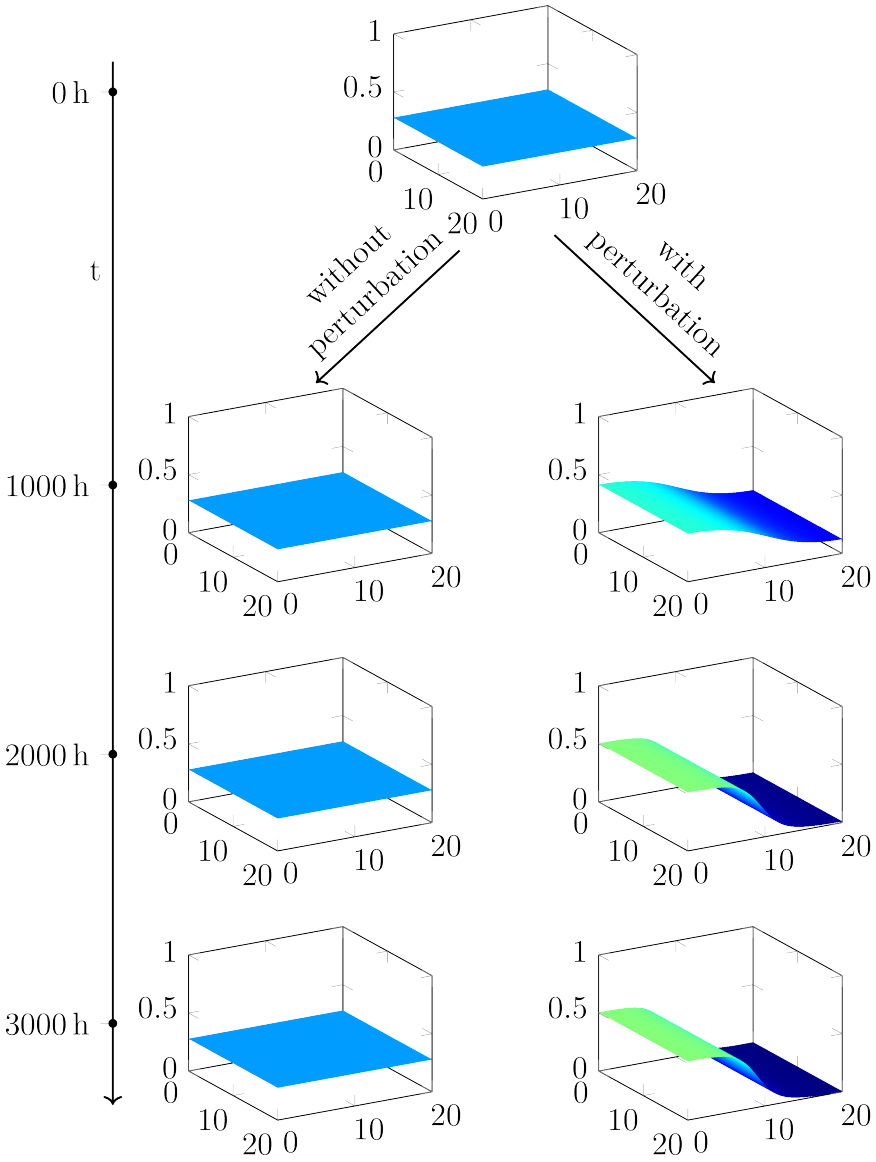

Figure 6.10: Time evolution of a strategy starting out in an unstable stationary point with and without perturbation. Without perturbation, the strategy value remains in the unstable point. With the addition of a small perturbation, it converges towards the nearest ESS. If the perturbation is sine-shaped, as in this case, the resulting strategy limit is spatially inhomogeneous.

without implications. As such, we can safely consider a parameter set with $K > d$, as long as $\bar{v}_i > \max\{\|v_i^0\|_\infty\}$.

Since we have set $K = 2.459$, the cases $d = 2$ and $d = 3$ are of particular interest. Additionally, we need to specify $\mu_{\max}$ as well as $\mu_{\min}$. We expect that the constant death rate of $\mu = 7.24 \times 10^{-7}$ is the maximal death rate for this model. For the minimal death rate we roughly assume a reduction to one tenth, so that $\mu_{\min} = 7.24 \times 10^{-8}$.

If $d = 3$, we have $K < d$ and a behaviour very similar to a private benefit with $h = 2$: There is a positive stable equilibrium point for v_i to which population 1 converges, while the strategy of population 2 is caught in the unstable zero point. In accordance with these results, population 2 dies out while population 1 remains at a stable level. The results are shown in figure 6.11.

If $d = 2$, on the other hand, we have $K > d$. Since a short calculation for our parameter values yields $\bar{v}_i = 108$, the critical point is indeed far away from the interesting strategy value domain. As expected, the populations behave as in the case without additions, with both populations declining very slowly towards extinction (see figure 6.12).

6.5.2 G-function with abiotic components

As discussed in section 2.2.2, we can also model the benefit from QS directly through the signal and enzymes produced. We take the system proposed there and add in the signal influence on costs:

$$\begin{aligned}
\dot{s} &= F_s(v, s, b) + D_s \triangle s, \\
\dot{e} &= F_e(v, s, e, b) + D_e \triangle e, \\
\dot{b_i} &= G(v_i, s, e, b) \cdot b_i + D_b \triangle b_i, \\
\dot{v_i} &= \varepsilon \partial_1 G(v_i, s, e, b),
\end{aligned}$$

with

$$\begin{aligned}
F_s(v, (s, e, b)^T) &= \alpha_s \cdot \sum_j b_j v_j^s + \beta_s \cdot \frac{s^2}{s^2 + \tau^2} \cdot \sum_j b_j v_j^s - \gamma_s s, \\
F_e(v, (s, e, b)^T) &= \beta_e \cdot \frac{s^2}{s^2 + \tau^2} \cdot \sum_j b_j v_j^e - \gamma_e e.
\end{aligned}$$

It follows that we have to set values for some additional parameters, some of which we will take from literature while we calculate the others. First, we divide the total cost for QS into signalling costs and responding costs. As we know that signalling is the less expensive step, we choose to divide them approximately $1 : 3$. The resulting costs as well as the other parameters are detailed in table 6.6. We

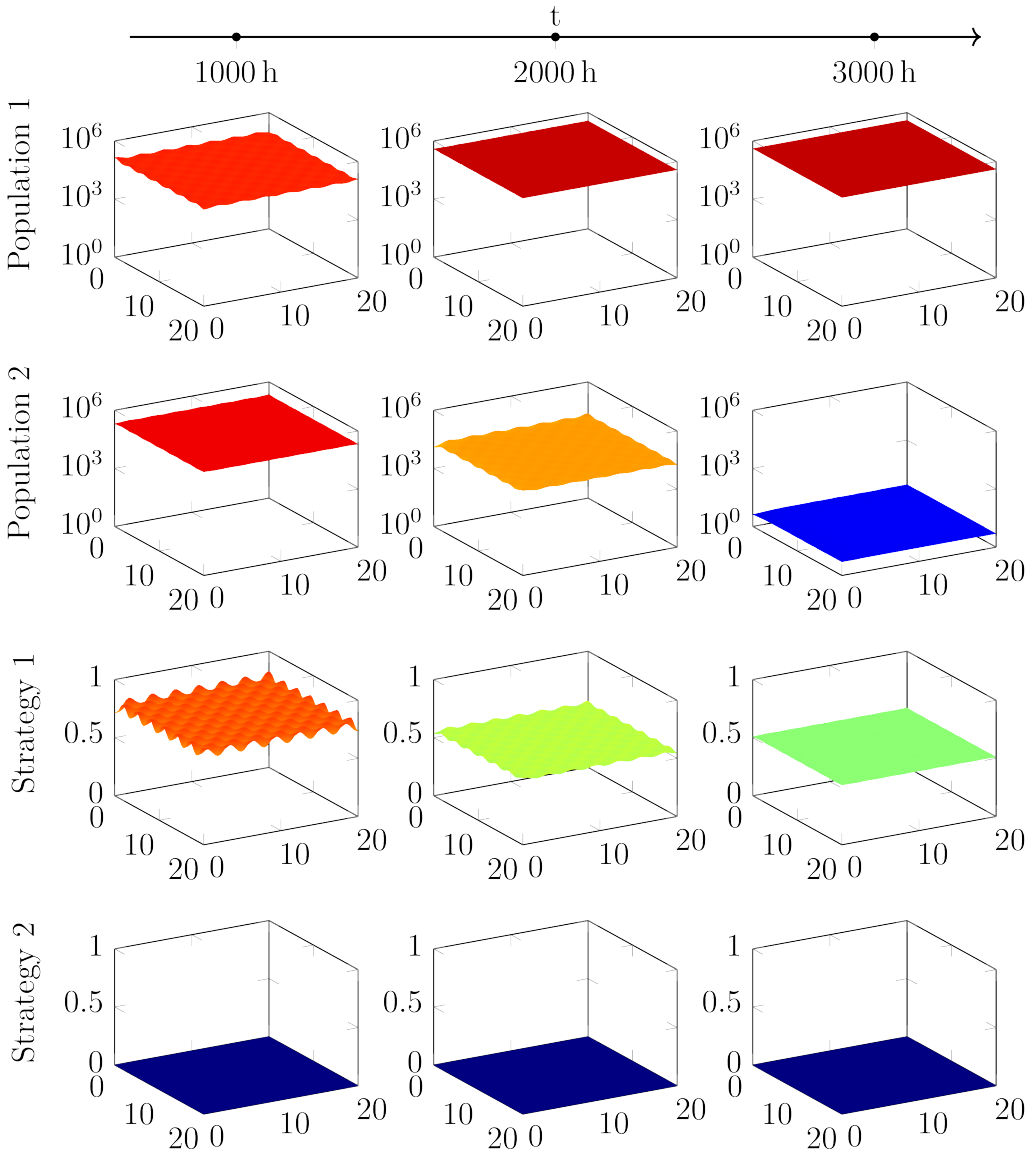

Figure 6.11: Evolution of two populations with different start strategies, using a G-function with a strategy-dependent death rate and $d = 3$. In this scenario, the reduced death rate serves to stabilize population 1 with its strategy converging towards the positive ESS, while population 2 declines towards zero.

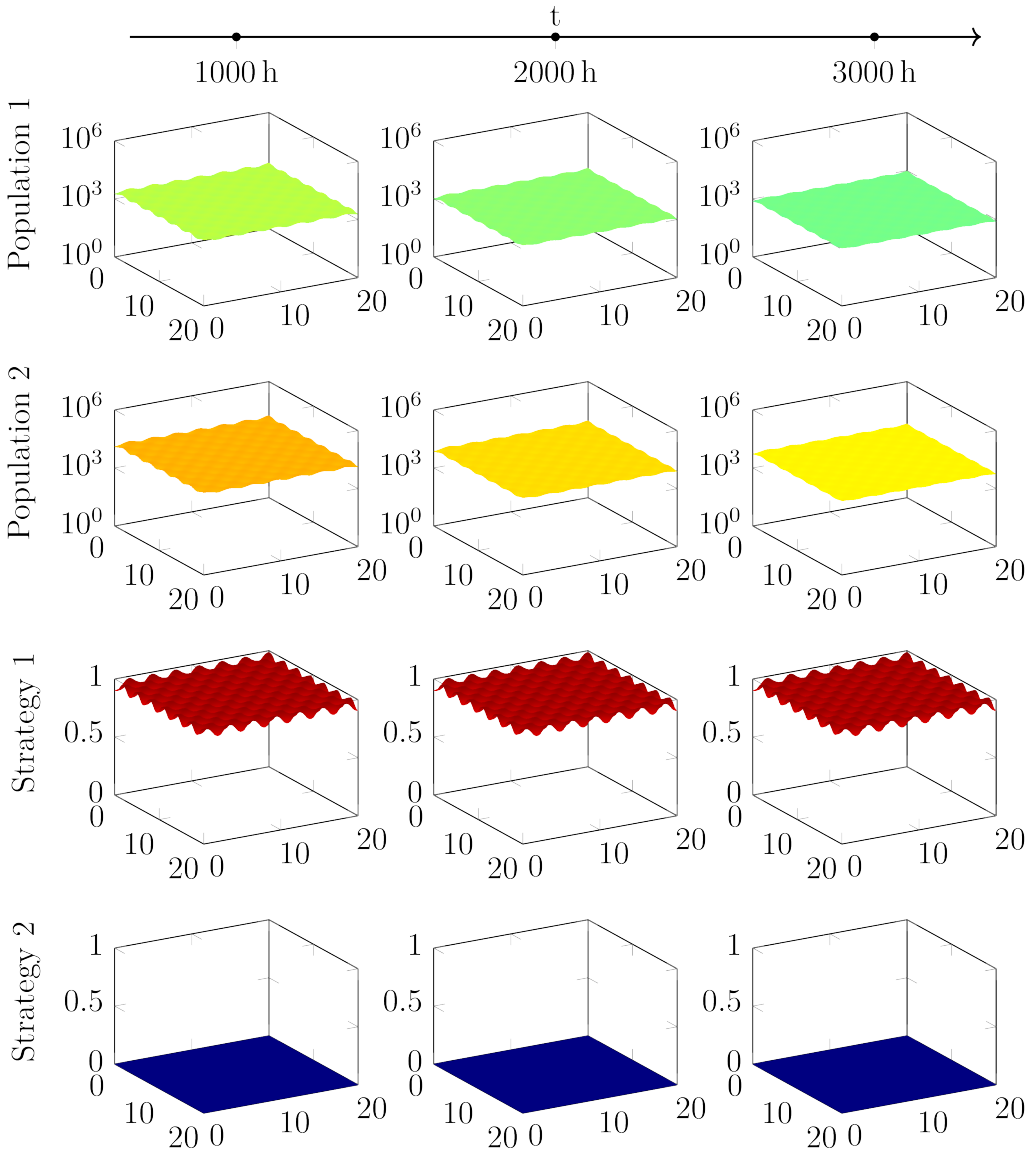

Figure 6.12: Evolution of two populations with different start strategies, using a G-function with a strategy-dependent death rate and $d = 2$. Both populations decline towards zero, albeit very slowly, with population 1 having the lower CFU.

Table 6.6: Standard parameter values for the numeric simulations with abiotic components

description	name	value			source
signal base production	α_s	9.2	$\times 10^{-5}$	nmol/(L h)	[Fek+10]
enzyme induced production	β_e	4.8	$\times 10^{5}$	mol/(CFU L h)	[Vet+98]
signal induced production	β_s	9.2	$\times 10^{-4}$	nmol/(L h)	[Fek+10]
effectiveness of enzyme	c_1	3.6	$\times 10^{4}$	1/(mol h)	[BGM95]
food intake of bacteria	c_2	1	$\times 10^{-19}$	1/(CFU h)	[Sim85]
enzyme degradation	γ_e	2.1	$\times 10^{-2}$	1/h	
nutrient degradation	γ_n	2.3	$\times 10^{-2}$	1/h	
signal degradation	γ_s	5.5	$\times 10^{-3}$	1/h	[Eng+07]
enzyme cost	K_e	0.14		1	
signal cost	K_s	5.78	$\times 10^{-2}$	1	
replenishment of nutrients	$\bar{n}_0$	4	$\times 10^{-13}$	mol/(L h)	
signal threshold	τ	70		nmol/L	[Fek+10]

choose to measure the signal s in nmol/L, the enzyme e and nutrients n in mol/L. Since the production rates for QS products are usually given as an amount of moles in the literature, we need to reformulate it. To that end we note that we want our total area to represent 1 mL, as in the experiments from chapter 5. Like before, we divide this total volume by the amount of spaces in our grid, getting

$$V = \frac{1\,\mathrm{mL}}{20^2} = 2.5 \times 10^{-3}\,\mathrm{mL}$$
$$\Rightarrow V^{-1} = 4 \times 10^{5}\,\frac{1}{\mathrm{L}}.$$

In order to transform our two-dimensional space into three-dimensional volume, we can continue to think about the spaces in our grid as 1 mm long and imagine a "height" of 2.5 mm.

$\boldsymbol{G(v_i, s, e, b) = B(e, b) \cdot C(s, v_i) - \mu\|b\|_1}$

If the G-function is structured in this way, signal and enzyme are freely available to bacteria in the vicinity. We have noted before that this leads to the demise of cooperators in the long term. Inspired by equation (2.2.30a), we take

$$n(e, b) = \frac{c_1 e}{c_2\|b\|_1 + \gamma_n} \cdot \frac{n_0}{c_1 e + \gamma_n},$$
$$B(e, b) = B_{\max} \cdot n(e, b).$$

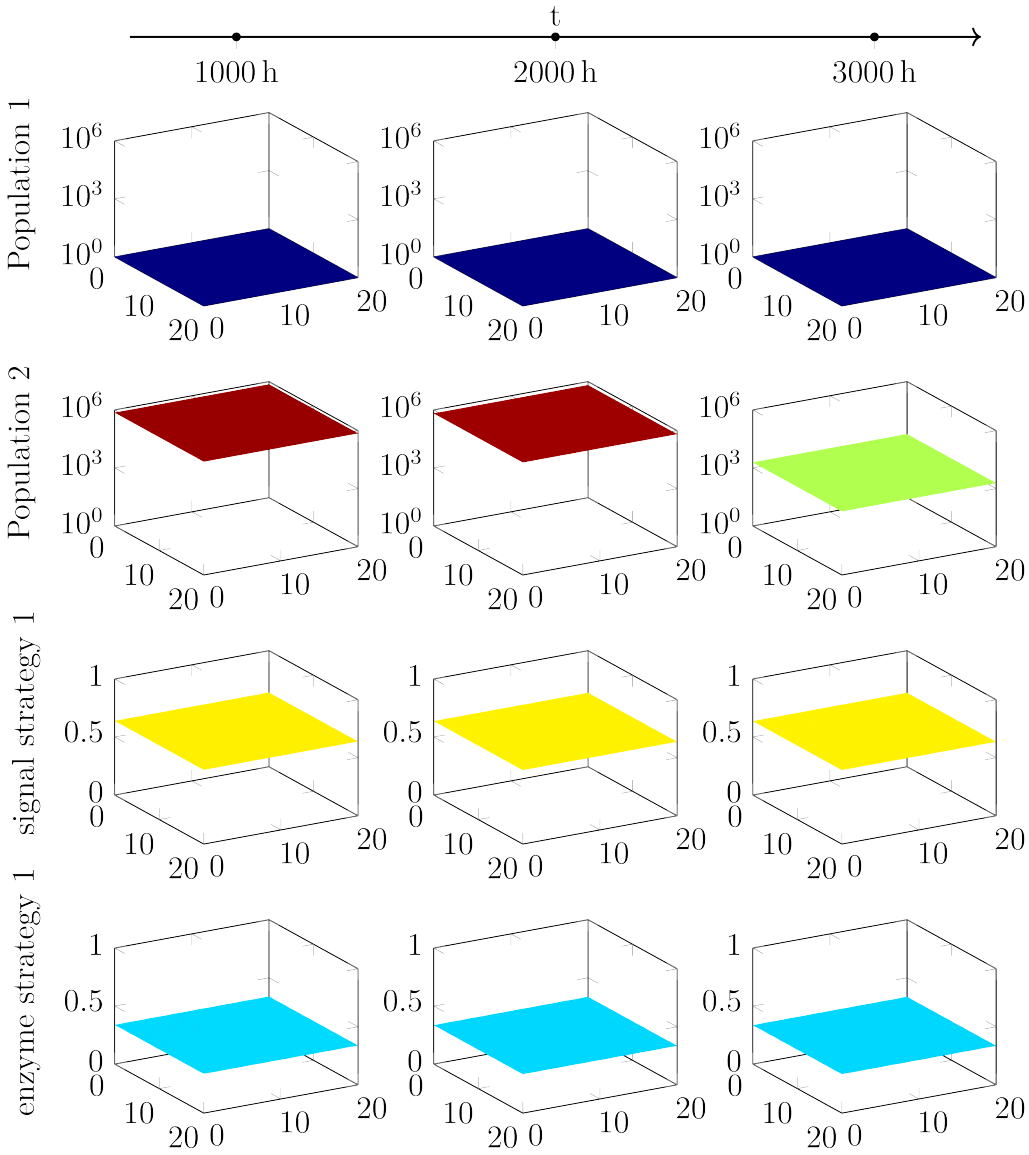

Figure 6.13: Evolution of two populations with different start strategies, using a G-function dependent on explicit abiotic components without private benefits. The strategy of population 2 is constantly zero and not shown here. Population 1 dies out right away, lowering both strategy values in the process. Population 2 remains stable as long as there are abiotic components left and starts to decline quickly afterwards.

The results are shown in figure 6.13. As expected, the cooperators decline after the initial growth spurt, which leads to lower enzyme concentrations and, ultimately, to the extinction of both populations. It is notable that after the remaining enzyme is degraded, this extinction is much quicker than the one predicted by the G-function without abiotic components (see figure 6.6), though both share the same ultimate fate.

Private Compartments

In order to model the behaviour of *P. aeruginosa* when one considers private compartments, we revisit section 2.2.3. We want to include private compartments for both signal (s_i) and enzyme (e_i). From equation (2.2.31) we have

$$e_i = \frac{\beta_e}{\theta^- + \gamma_e} \cdot v_i^e \cdot \frac{s_i^2}{s_i^2 + \tau^2} + \frac{\theta^+}{\theta^- + \gamma_e} \cdot e =: E(v_i^e, v_i^s, e),$$

where s_i is the solution of equation (2.2.36):

$$\begin{aligned} 0 &= -s_i^3(1 + \gamma_s\theta^{-1}) + \Big((\alpha_s + \beta_s)\omega + s\Big)s_i^2 - \tau^2(1 + \gamma_s\theta^{-1})s_i + \Big(\alpha_s\omega + s\Big)\tau^2 \\ \Leftrightarrow \quad 0 &= \alpha_s v_i^s + \beta_s v_i^s \cdot \frac{s_i^2}{s_i^2 + \tau^2} + \theta(s - s_i) - \gamma_s s_i. \end{aligned}$$

While it is possible to solve equation (2.2.36) for s_i, doing so involves calculating the root of a cubic polynomial and thus requires a lot of computing time if done often. For that reason, instead of using a Hill function for activation, we use a step function, reducing the equation to

$$0 = \alpha_s v_i^s + \beta_s v_i^s \cdot 1_{\geq\tau} + \theta(s - s_i) - \gamma_s s_i.$$

For practical purposes, we calculate s_i by

$$\underline{s}_i := \frac{\alpha_s v_i^s + \theta s}{\theta + \gamma_s}, \qquad s_i = \begin{cases} \underline{s}_i & \text{if } \underline{s}_i < \tau \\ \underline{s}_i + \frac{\beta_s v_i^s}{\theta + \gamma_s} & \text{if } \underline{s}_i \geq \tau \end{cases}. \tag{6.5.1}$$

This leads to a slight underestimation of the actual signal concentration, as the step function only admits a higher signal production once the base production is sufficient in order to reach the threshold τ, while a Hill-function term already admits a partial activation. Figure 6.14 shows a comparison of both versions. There is however little actual difference in the simulations when using any one of the activation terms for our parameter values.

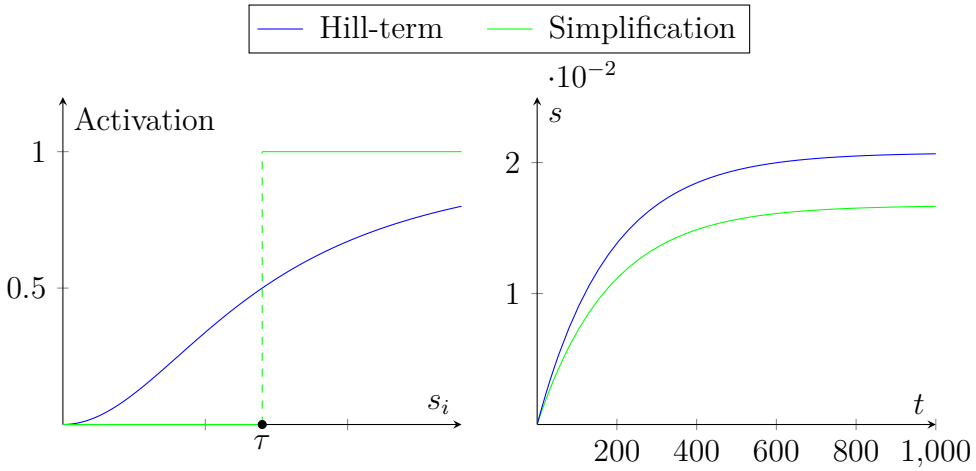

(a) Activation of QS, as regulated by intracellular signal concentration

(b) Resulting extracellular concentration

Figure 6.14: Comparison between the actual activation function using a Hill term and a step function simplification.

The system to be solved is based on equation (2.2.33) and can be written as

$$\begin{aligned}
\dot{s} &= \lambda\theta \cdot \sum_j \left(b_j(s_j - s)\right) + D_s \triangle s - \gamma_s s \\
\dot{e} &= \lambda \sum_j \left(b_j \left(\theta^- e_j - \theta^+ e\right)\right) + D_e \triangle e - \gamma_e e \\
\dot{b_i} &= \underbrace{\left(\left(r_n n(v_i, v, e, b)\right) C(v_i) - \mu \|b\|_1\right)}_{G(v_i,e,b)} \cdot b_i + D_b \triangle b_i \\
\dot{v_i} &= \varepsilon \partial_1 G(v_i, v, e, b)
\end{aligned}$$

with

$$n(v_i, v, e, b) = \left(\frac{c_1 e}{c_2 \|b\|_1 + \gamma_n} + \frac{c_1 E(v_i^e, v_i^s, e)}{c_2 + \gamma_n}\right) \cdot \frac{n_0}{c_1 \left(e + \sum_j (b_j E(v_j^e, v_j^s, e))\right) + \gamma_n}.$$

It remains to calculate $\partial_1 G(v_i, v, e, b)$. We have

$$\begin{aligned}
\partial_1 G(v_i, v, e, b) &= r_n n(v_i, v, e, b) \cdot \partial_{v_i} C(v_i) + r_n \partial_{v_i} n(v_i, v, e, b) \cdot C(v_i) \\
\partial_{v_i} C(v_i) &= \begin{pmatrix} \partial_{v_i^s} C(v_i) \\ \partial_{v_i^e} C(v_i) \end{pmatrix} = -2 \left(\frac{s_i^2}{s_i^2 + \tau^2}\right)^2 C(v_i) \begin{pmatrix} K_s v_i^s \\ K_e v_i^e \end{pmatrix}
\end{aligned}$$

Table 6.7: Adjusted parameter values for the numeric simulations with private compartments

name	value	
α_s	2.3×10^5	nmol/(L h)
β_e	1.2×10^{15}	mol/(CFU L h)
β_s	2.3×10^6	nmol/(L h)
λ	4×10^{-10}	1
θ	2.6×10^4	1/h
θ^+	$10^{-5} \cdot \theta^-$	1/h

$$\partial_{v_i} n(v_i, v, e, b) = \frac{c_1}{c_2 + \gamma_n} \cdot \frac{n_0}{c_1 \left(e + \sum_j (b_j E(v_j^e, v_j^s, e)) \right) + \gamma_n} \cdot \begin{pmatrix} \partial_{v_i^s} E(v_i^e, v_i^s, e) \\ \partial_{v_i^e} E(v_i^e, v_i^s, e) \end{pmatrix}$$

$$\partial_{v_i^e} E(v_i^e, v_i^s, e) = \frac{\beta_e}{\theta^- + \gamma_e} \cdot \frac{s_i^2}{s_i^2 + \tau^2}$$

$$\partial_{v_i^s} E(v_i^e, v_i^s, e) = \frac{\beta_e}{\theta^- + \gamma_e} v_i^e \cdot \frac{2 s_i \tau^2}{(s_i^2 + \tau^2)^2} \cdot \partial_{v_i^s} s_i$$

$$\partial_{v_i^s} s_i = \frac{(\alpha_s + \beta_s) s_i^2 + \alpha_s \tau^2}{\theta \left(3 s_i^2 (1 + \frac{\gamma_s}{\theta}) - 2 s_i \left((\alpha_s + \beta_s) \frac{v_i^s}{\theta} + s \right) + (1 + \frac{\gamma_s}{\theta}) \tau^2 \right)}$$

where the last equation is gained by deriving equation (2.2.36) with respect to v_i^s.

Due to the shift from extra- to intracellular production of QS products, we need to recalculate some parameters that depend on volume. We assume that a bacterial cell has an inside volume of 1×10^{-15} L and recalculate the values of $\alpha_s, \beta_s, \beta_e$ based on this number. Additionally, we have

$$\lambda = \frac{V_{\text{intracellular}}}{V_{\text{extracellular}}} = \frac{1 \times 10^{-15}\,\text{L}}{2.5 \times 10^{-6}\,\text{L}}.$$

For θ, we take a rather high value to model the high permeability of the bacterial cell membrane for QS signal found in experiments. A summary of the new parameter values can be found in table 6.7.

The result depends on the magnitude of θ^-, as might be expected. For θ^- small, a large part of the QS enzymes produced remain with the producing bacteria and provide private benefits. Accordingly, cheating bacteria die out (figure 6.15). Again, this process happens faster than when modelling the behaviour without explicit abiotic terms.

If on the other hand θ^- is large, more enzyme is freely available to all bacteria, which leads to coexistence (figure 6.16). It is however noticeable that non-producing

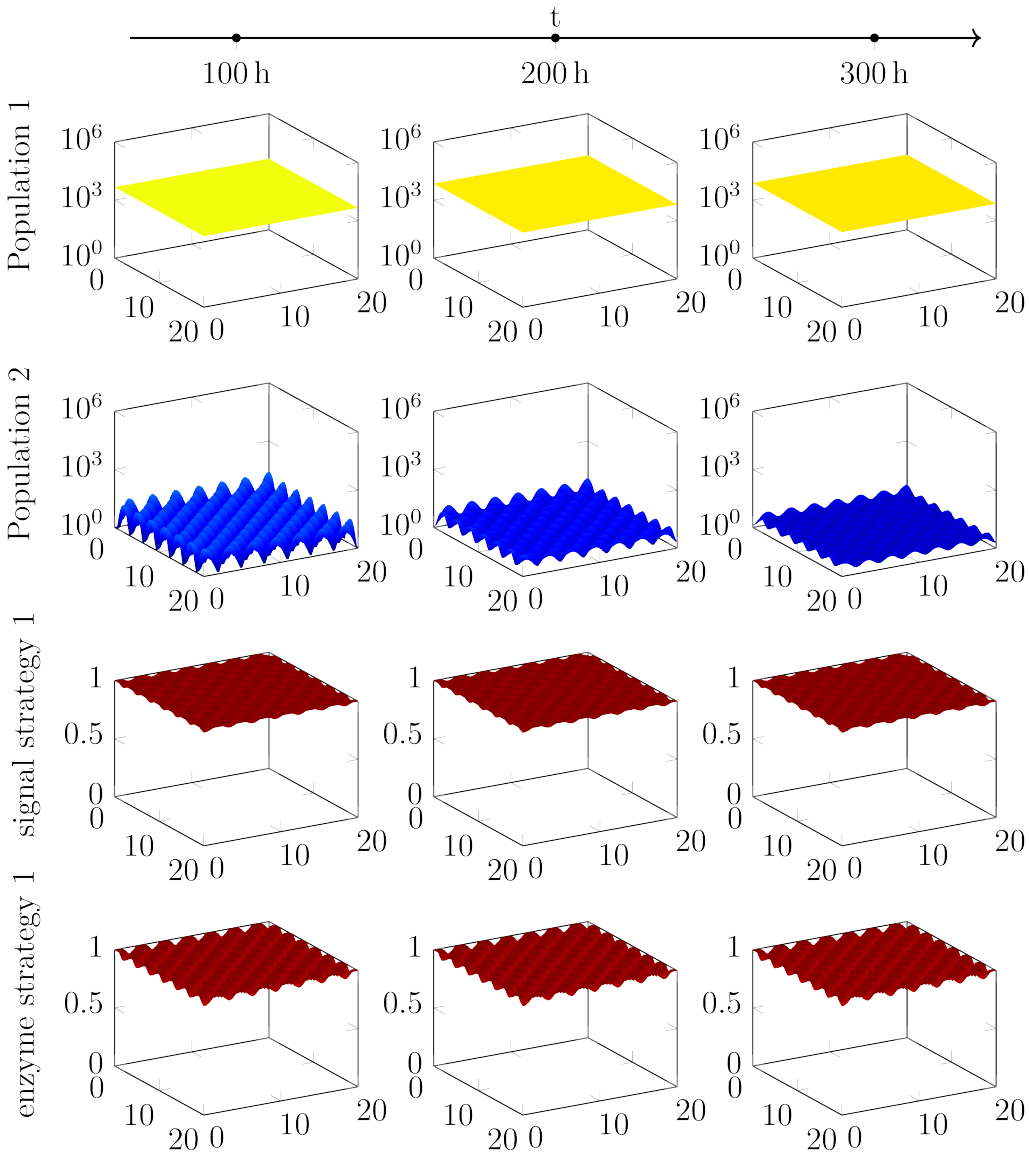

Figure 6.15: Evolution of two populations with different start strategies, using a G-function dependent on explicit abiotic components with private benefits and $\theta^- = 2.6$. The strategy of population 2 is constantly zero and not shown here. Note the short time-scale. QS strategy as well as population numbers of population 1 remain stable, while population 2 dies off.

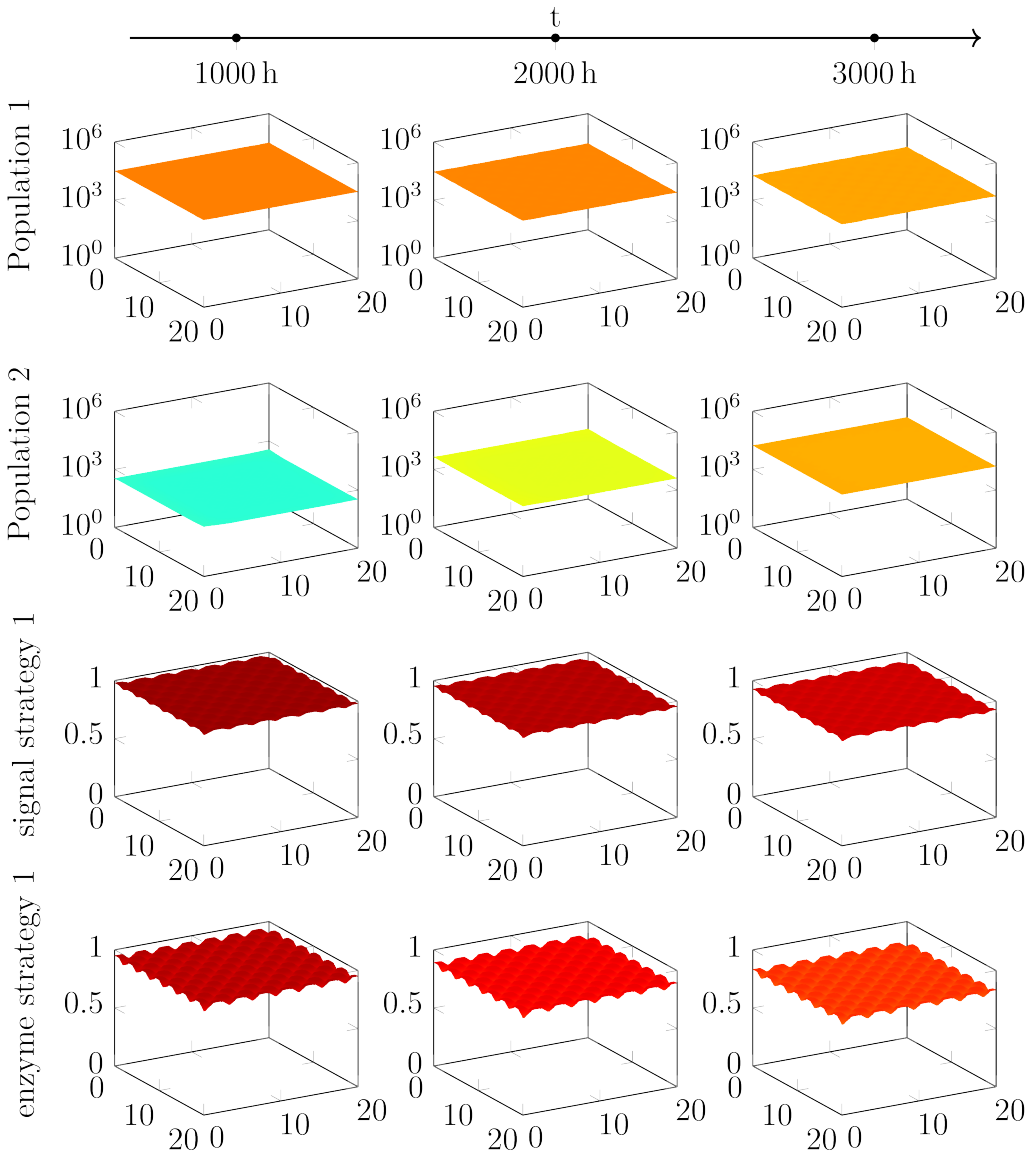

Figure 6.16: Evolution of two populations with different start strategies, using a G-function dependent on explicit abiotic components with private benefits and $\theta^- = 2.6 \times 10^4$. The strategy of population 2 is constantly zero and not shown here. With this higher exchange rate, population 1 reaches a high number of CFU quickly, while population 2 takes longer to grow but eventually surpasses the other.

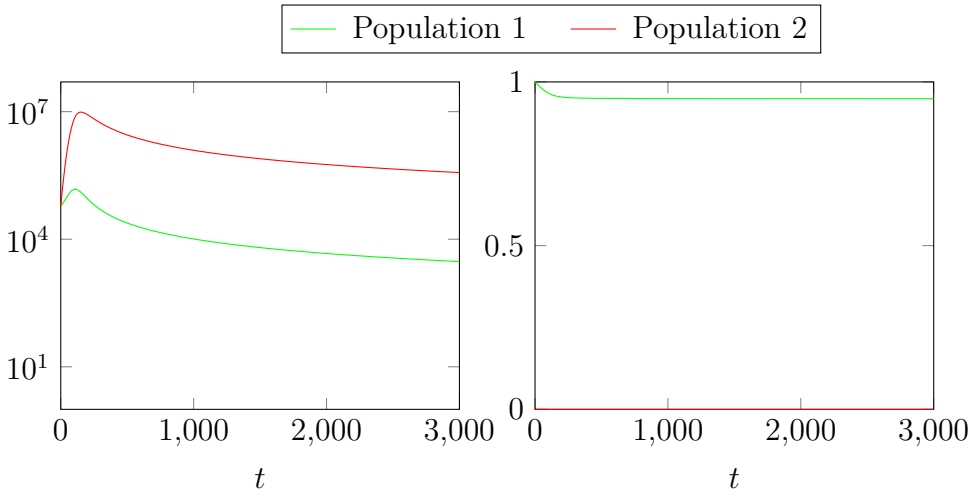

(a) Population count (b) Strategies

Figure 6.17: Simulation results for an ODE system with a plain G-function and two populations. Both populations decline after the initial growth spurt.

bacteria grow more slowly, as it takes time for QS enzymes to diffuse from the producing bacteria. But in the long term they are able to reach the same number or even outgrow the cooperators.

6.6 Comparing different equation systems

Having seen how the shape of the G-function influences the competition outcome between cooperators and QS-Cheaters, we now ask how the choice of equation system influences said outcome. In chapters 3 and 4, we have seen a variety of equation systems that could describe the QS interactions. We will restrict ourselves to a basic G-function without additions in these cases, so as to keep the results comparable.

6.6.1 ODE system

When passing from a PDE system with explicit spatial variables to an ODE system, we need to adjust the death rate μ. As we have divided the total amount of bacteria by 20^2 before, we now gain the adjusted death rate μ by dividing our former rate by 20^2. This gives a value of $\mu = 1.81 \times 10^{-9}$.

As we already expect from our analytical results in section 3.1, there is no stable strategy different from zero and both populations as well as strategies are on

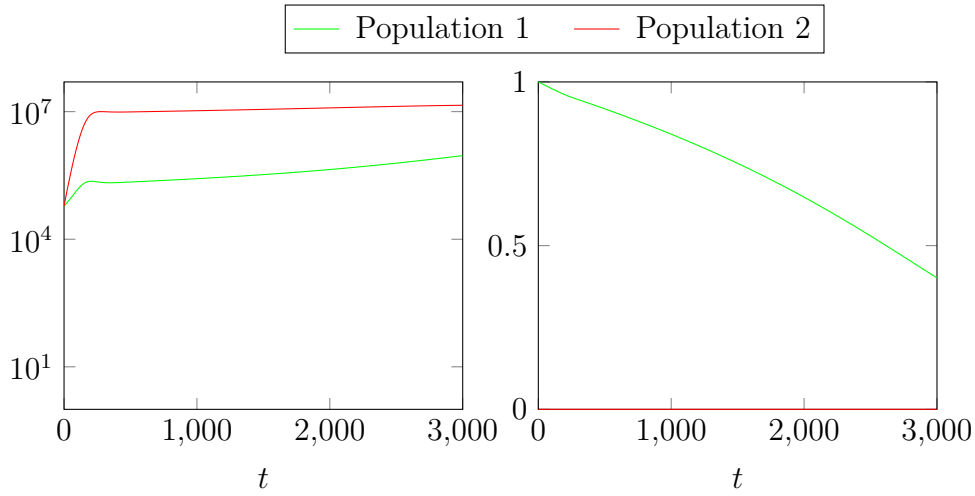

(a) Population count (b) Strategies

Figure 6.18: Simulation results for an ODE system with a mixing term of $m = 0.5$ and two populations. We can see that the strategy of population 1 declines towards zero, while both populations are growing.

a decline (see figure 6.17). The speed of this decline is comparable to the coupled system from section 6.5.1, shown in figure 6.6.

6.6.2 ODE system with mixing

One way to achieve spatial effects with ODEs is to introduce a mixing parameter m, as detailed in section 3.3 and Appel [App16]. While Appel investigates the behaviour for many different values of the mixing parameter, m, we will just exemplarily pick $m = 0.5$ and $m = 0$.

For $m = 0.5$, we find that population 1, starting out with a strategy of 1 and thus a full producer, is able to increase in population (see figure 6.18). The "cheater" population 2 still has a growth advantage, but on a much lower level. This is mainly due to the decline in strategy value that population 1 undergoes in this scenario — m is large enough to allow growth and subsequent evolution of the population, but too small for a positive value of v_i to be stable.

For $m = 0$, the situation is quite different. Here, the non-producer population 2 is unable to derive any benefit from being in close contact with the producer population 1, while they in turn gain the entire benefit from QS. This leads to a sharp decline for population 2, whereas population 1 grows towards a stable population size. At the same time, the strategy values remain stationary, as displayed in figure 6.19.

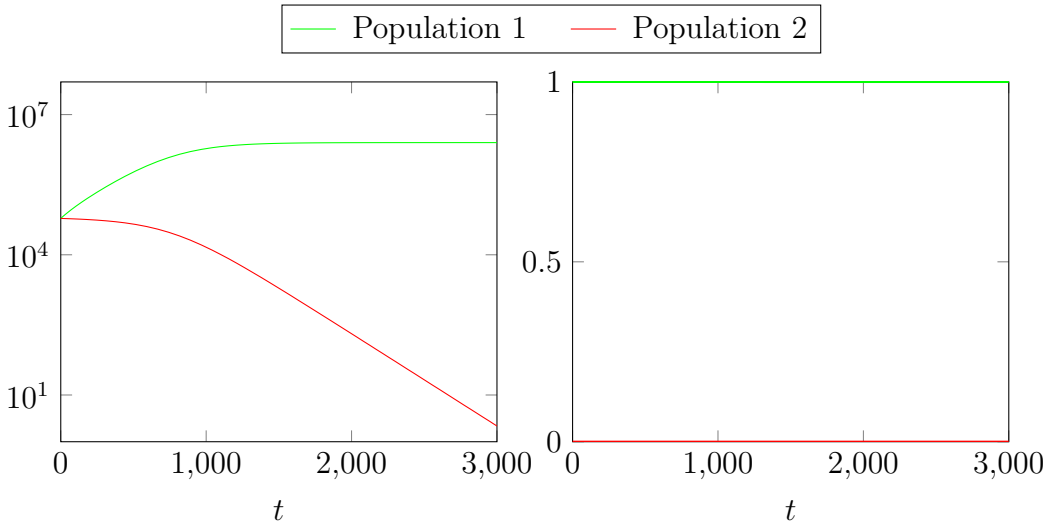

(a) Population count (b) Strategies

Figure 6.19: Simulation results for an ODE system with a mixing term of $m = 0$, i.e. a separated system. In this scenario, the non-producer population 2 cannot survive, while population 1 remains QS active and converges towards a stable population level. Both strategies remain unchanged.

6.6.3 ODE system with external influence

We implement the simplified influx term as specified in equation (3.2.2), and solve the corresponding ODE system. At first, the behaviour resembles the one without additions, as seen in figure 6.20. But when looking at a longer time scale, the strategy value of population 1 declines until quite close to zero, while the population itself is able to stabilize. At the same time, the rise and evolution of population 1 sparks the extinction of population 2.

6.6.4 Coupled ODE-PDE system

We have already seen the results of this system in section 6.5.1. They are quite comparable to the results from an unmodified ODE system, as shown in section 6.6.1.

6.6.5 Fully parabolic PDE system

In this version, not only the bacteria, but also the strategies underlie diffusion. Numerically, it is quite simple to implement diffusion via method of lines for the strategies as well.

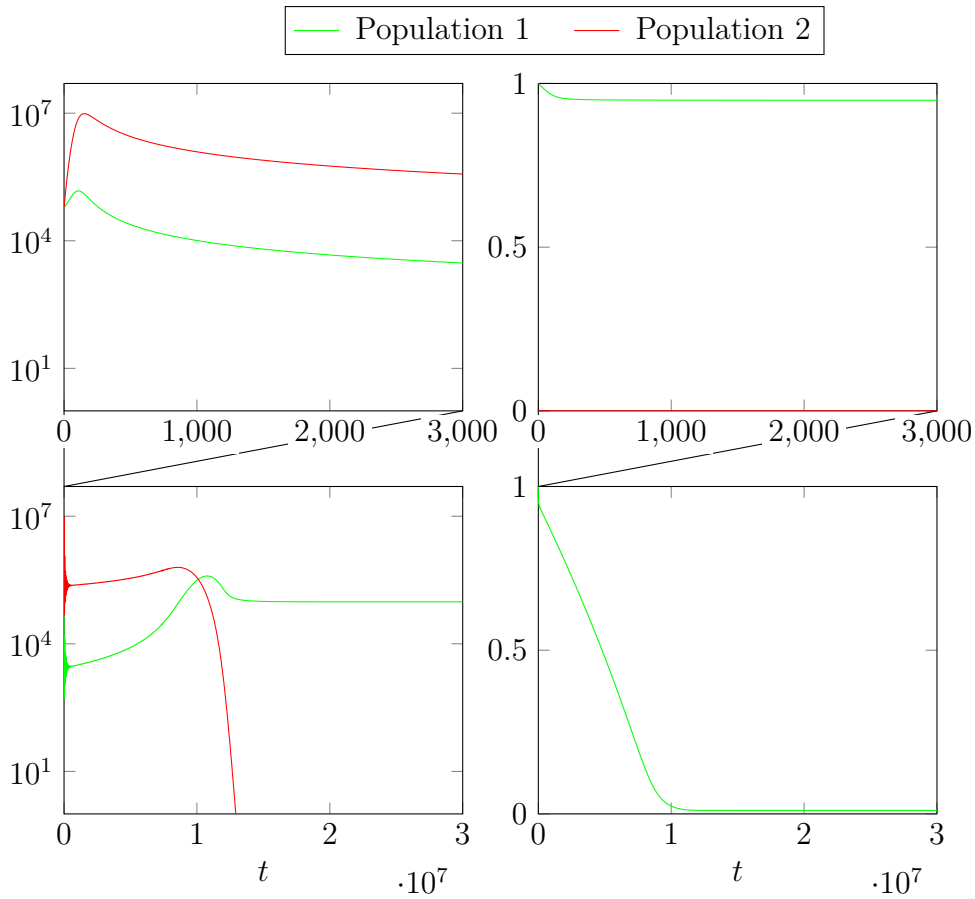

(a) Population count (b) Strategies

Figure 6.20: Simulation results for an ODE system with external influence, on two different time scales. Population 1 very slowly reduces their strategy to a near-zero level, where it stabilises. At the same time, population 2 dies off after dominating the other initially. After this event, the population count of population 1 remains constant.

The behaviour is very similar, too. When taking a G-function without additions, both strategies as well as populations decline as they did for the coupled system, with no discernible differences in population numbers. We can gather from figure 6.21 that the only notable difference is the "smoothness" of the strategy data.

The magnitude of strategy diffusion has no strong influence on this behaviour. Changing D_v from $0.01 \cdot D_b$ to $100 \cdot D_b$ results in a deviation of only 1.5 %.

6.6.6 Quasilinear PDE system

In contrast to section 6.6.5, we forgo the autonomous strategy diffusion, using the same diffusion constant as the bacterial population, but add an advection term. The resulting equation for v_i has been described in equation (4.1.2b):

$$\partial_t v_i(x,t) = \varepsilon \partial_1 G\Big(v_i(x,t), v(x,t), b(x,t)\Big) + D \triangle v_i(x,t) + \frac{2D \nabla b_i(x,t) \cdot \nabla v_i(x,t)}{b_i(x,t)}. \tag{4.1.2b revisited}$$

By using the central finite difference scheme proposed in equation (6.2.1), we can write

$$\begin{aligned}
\frac{2D \nabla b^k \cdot \nabla v^k}{b^k} &= \frac{2D}{b^k}\left(\partial_x b^k \partial_x v^k + \partial_y b^k + \partial_y v^k\right) \\
&= \frac{2D}{b^k_{ij}}\left(\frac{b^k_{i+1,j} - b^k_{i-1,j}}{2h} \cdot \frac{v^k_{i+1,j} - v^k_{i-1,j}}{2h} + \frac{b^k_{i,j+1} - b^k_{i,j-1}}{2h} \cdot \frac{v^k_{i,j+1} - v^k_{i,j-1}}{2h}\right) \\
&= \frac{D}{2h^2 b^k_{ij}}\left((b^k_{i+1,j} - b^k_{i-1,j})(v^k_{i+1,j} - v^k_{i-1,j}) + (b^k_{i,j+1} - b^k_{i,j-1})(v^k_{i,j+1} - v^k_{i,j-1})\right).
\end{aligned}$$

In this way, our quasilinear system can be solved by the method of lines as well. As one can see when comparing PDE systems in figure 6.22, the results do not differ from those without advection, except for a minor drop in strategy value.

One can however find a slight difference in strategy evolution when looking at a different start situation. To that end we define the function

$$\psi(x,y) = \begin{cases} \varepsilon + 1 + \cos\left(\frac{\pi}{r} \cdot \sqrt{(x-a)^2 + (y-a)^2}\right) & \text{if } (x,y) \in B_r(a) \\ \varepsilon & \text{if } (x,y) \notin B_r(a) \end{cases},$$

where r and a are parameters defining the centre and radius of the resulting "hump" and $B_r(a)$ the ball around a with radius r. We scale ψ so that the overall starting CFU remains the same and fix different centres for two populations in order to observe the spatial behaviour better. With this starting condition, we regain the same overall behaviour as before, namely a cheater population whose growth is

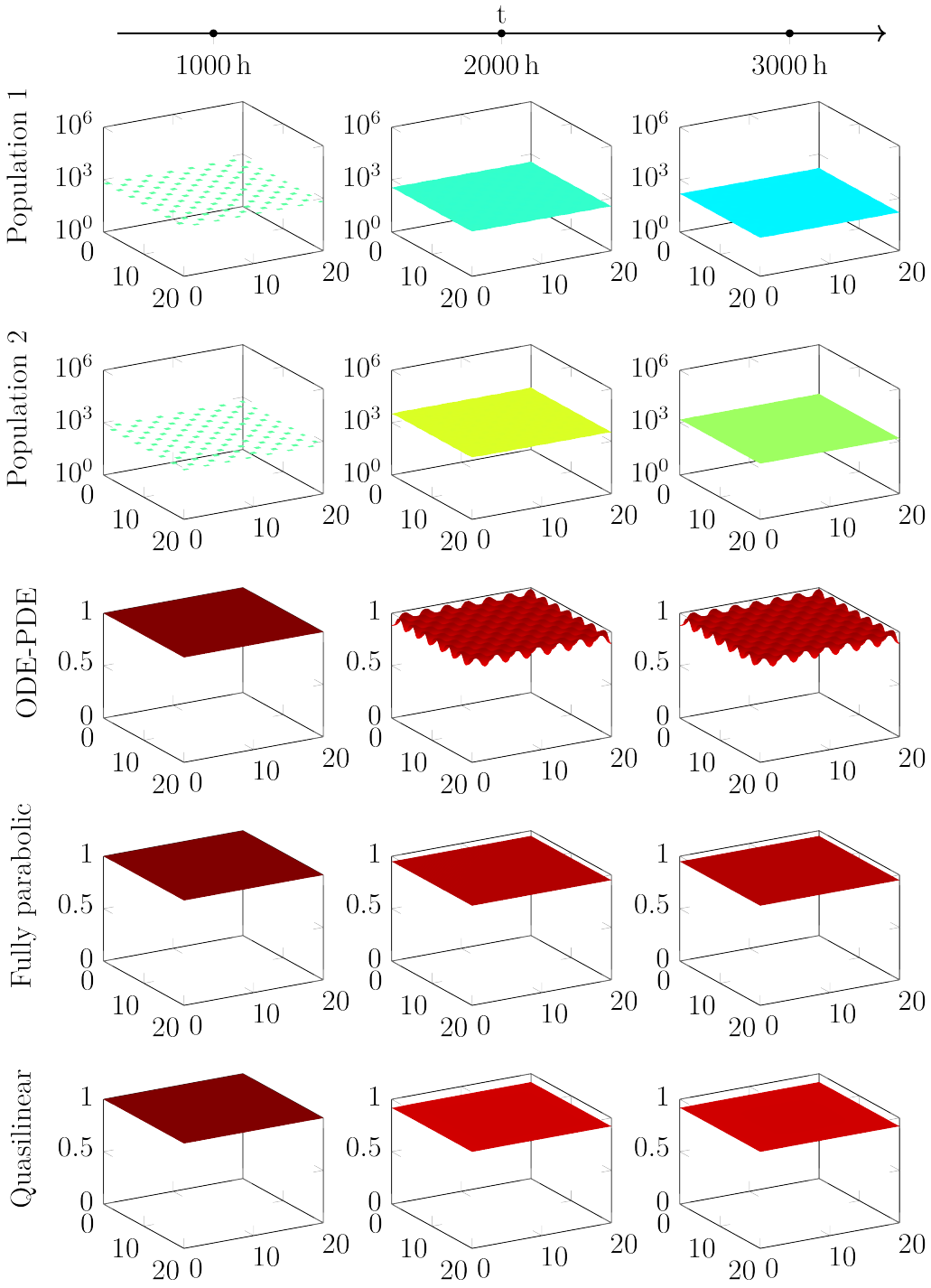

Figure 6.21: Simulation of three different PDE systems with the `patches` start. Population numbers (first 2 rows, blue/yellow) remain the same across the different systems, strategy evolution (last 3 rows, red) deviates slightly.

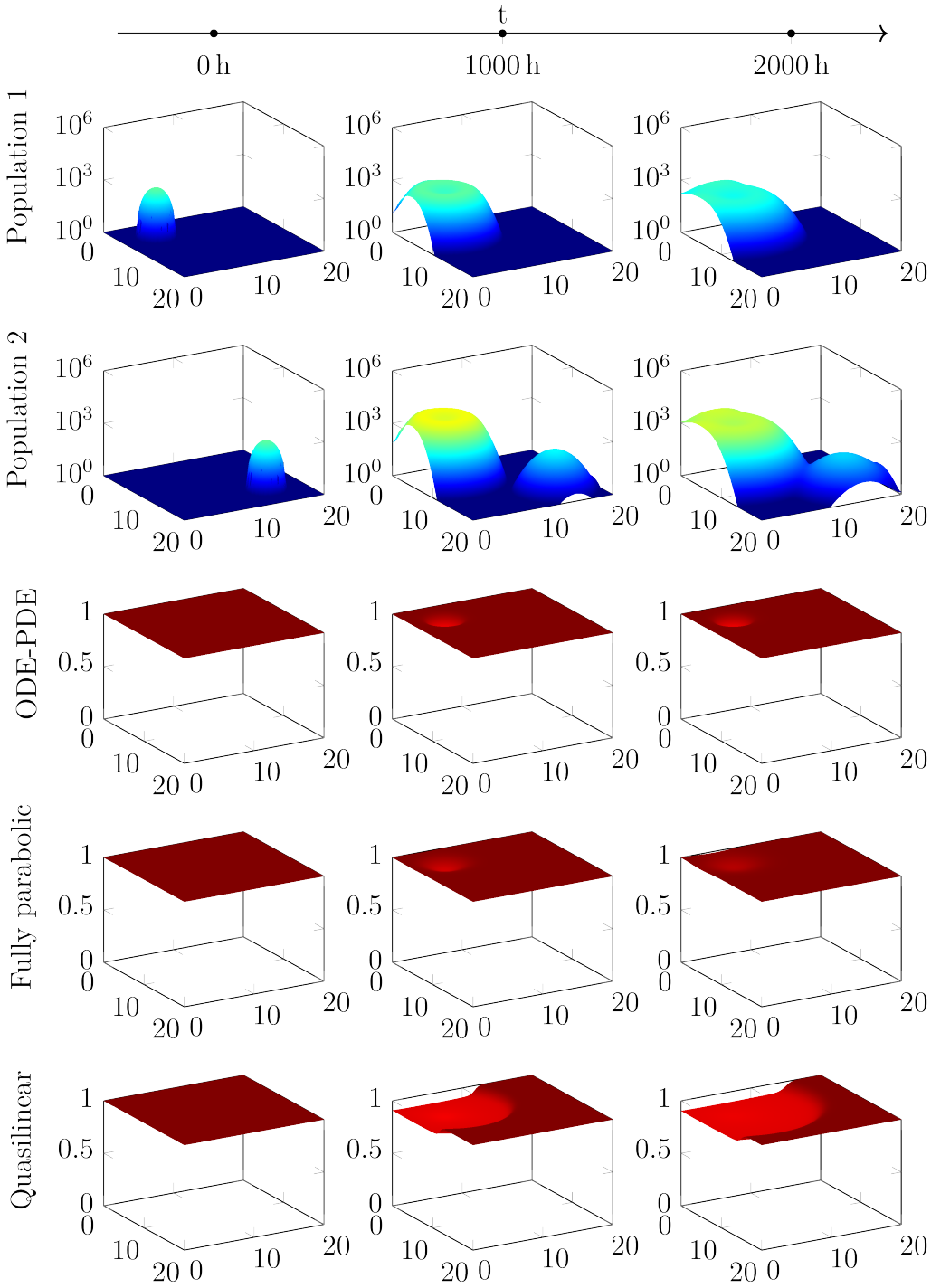

Figure 6.22: Simulation of three different PDE systems with $\psi(x, y)$ as start. Population numbers (first 2 rows, blue/yellow) remain the same across the different systems, but the strategy evolution (last 3 rows, red) differs.

dependent on a declining WT population. But there is a difference in the evolution of strategy between the three PDE systems.

This difference is quite small between the coupled ODE-PDE and the fully parabolic system, consisting mostly of a difference in "smoothness" caused by the smoothing properties of the Laplacian. The added advection term in the quasilinear system, on the other hand, influences the strategy evolution perceptively. That is especially apparent with low bacteria numbers, since

$$\partial_1 G(v_i, v, b) = C'(v_i)B(v, b),$$

where $B(v, b)$ scales with the amount of producing bacteria. Thus, when bacteria numbers are low, the rate of change for the strategy goes to zero. But the quasilinear system mitigates this behaviour by introducing an advection term which is not negatively dependent on the bacteria numbers. All in all, it follows that the strategy value in populations with low CFU count is more subject to change in quasilinear systems than it is in coupled or fully parabolic systems. This effect can be seen in figure 6.22.

Chapter 7

Conclusion

In this thesis, we have developed several models to investigate quorum sensing in *P. aeruginosa*, focussing on evolutionary forces and population development in spatially organised communities. Previous studies [Bro07; CMF12; CRL09; Mel+10; Rum+12; DCG12] had indicated that both assortment and private benefits might help stabilise cooperation through QS and we have indeed found correlations between these effects and ESSs.

We have considered simplified models at first, using ODE systems as basis and foregoing explicit modelling of QS molecules. We found that when QS has a purely public benefit without any assortment, QS is evolutionary unstable, as has been shown experimentally [Rum+09; MDH17]. But we have also shown that this instability persists both when changing the underlying system to a PDE or coupled ODE-PDE model as well as when modelling abiotic terms explicitly. We established that in order to stabilise cooperation, it was necessary to introduce some kind of external separation.

This separation could take the form of a mixing factor which determines the strength of interaction between bacteria. In systems with a low mixing factor, QS serves more as a self-inducing mechanism than as a group behaviour and there exist positive ESSs. We have found evidence of such behaviour in our experiments, where a reduced diffusion led to less cheating behaviour and higher relative fitness for the QS-active subpopulation [MDH17].

Another variant is a process of segregation and re-mixing, modelled by external influxes. It represents migration of bacteria from a well-mixed, planktonic state into segregated micro-colonies and back again. Depending on parameter values, such a system can admit a positive ESS [Mun+16].

If we do not enforce spatial effects through such mechanisms, but work directly with spatial variables in a PDE system, the stability of QS is dependent on the G-function we apply. G-functions that admit a private benefit for QS-active bacteria, either directly or by reducing cell death, allow for the existence of positive ESSs.

For a certain class of benefit terms subpopulations engaging in QS can even coexist indefinitely with non-producers.

Besides consideration of long-term behaviour, we have also explored existence and uniqueness of solutions to the systems. Proving and applying a theorem about the existence of coupled upper-lower solutions has established the existence of strong solutions to a broad class of PDE systems, ours included, provided the functions involved fulfil certain smoothness assumptions. In the case of coupled ODE-PDE systems, we have successfully applied fixed point theorems to gain existence and uniqueness results. We were also able to demonstrate the asymptotic behaviour for some special cases of G-functions, including all systems with only zero for ESS.

We have also employed numerical methods to showcase the behaviour and confirm our results. This allowed us to explore the systems in a range of conditions. While we have not found much difference between simulations of different PDE systems, changing G-functions as well as certain key parameters had a profound impact on both evolutionary and population dynamics, as we had predicted.

Naturally, there are still open questions. For all our models, we have assumed that bacteria that share a genotype also exhibit the same phenotype. This might not hold true for QS: bacteria may have intact QS genes while not participating in the QS process. Such a mechanism changes the dynamics of the cooperation, as the fitness benefit of this kind of "cheating" bacteria results in an increased reproduction rate of bacteria with *intact* QS genes [HS15]. There are also other mechanisms that might help stabilize QS that we have not explored, such as policing or kin selection [for an overview, see RGK14].

Furthermore, it has been reported that QS plays a role in antibiotic resistance, both directly [Lih+13] and indirectly by regulating biofilm formation [Dav+98]. While we have made some approaches to this topic by considering a strategy-dependent death rate, integrating these dynamics in more detail could be of further interest, as the complex interplay between QS, biofilm formation and antibiotic resistance has a profound impact upon medical treatment strategies.

From a mathematical point of view, another interesting expansion would be a strategy-dependent diffusion rate. This would require an in-depth look at the foundations of the G-function ansatz but would potentially allow for Turing-type perturbations in PDE systems.

Bibliography

[AAL11] M. Abudiab, I. Ahn, and L. Li. "Upper–lower solutions for nonlinear parabolic systems and their applications". In: *Journal of Mathematical Analysis and Applications* 378.2 (2011), pp. 620–633. DOI: 10.1016/j.jmaa.2011.01.003.

[And91] J. R. Anderson. "Local existence and uniqueness of solutions of degenerate parabolic equations". In: *Communications in Partial Differential Equations* 16.1 (1991), pp. 105–143. DOI: 10.1080/03605309108820753.

[Ang+04] K Anguige et al. "Mathematical modelling of therapies targeted at bacterial quorum sensing". In: *Mathematical Biosciences* 192.1 (2004), pp. 39–83. DOI: 10.1016/j.mbs.2004.06.008.

[App16] S. Appel. "Einfluss des Durchmischungsgrades auf die evolutionäre Dynamik von Quorum Sensing". Master's thesis. TU München, 2016.

[Ban22] S. Banach. "Sur les opérations dans les ensembles abstraits et leur application aux équations intégrales". In: *Fundamenta Mathematicae* 3.1 (1922), pp. 133–181.

[BB08] A Buckling and M. Brockhurst. "Kin selection and the evolution of virulence". In: *Heredity* 100.5 (2008), pp. 484–488. DOI: 10.1038/sj.hdy.6801093.

[Bel43] R. Bellman. "The stability of solutions of linear differential equations". In: *Duke Mathematical Journal* 10.4 (Dec. 1943), pp. 643–647. DOI: 10.1215/S0012-7094-43-01059-2.

[BGM95] B. Boeckle, B. Galunsky, and R. Mueller. "Characterization of a keratinolytic serine proteinase from *Streptomyces pactum* DSM 40530." In: *Applied and Environmental Microbiology* 61.10 (1995), pp. 3705–3710.

[BJ01] S. P. Brown and R. A. Johnstone. "Cooperation in the dark: signalling and collective action in quorum-sensing bacteria". In: *Proceedings of the Royal Society B* 268 (2001), pp. 961–965. DOI: 10.1098/rspb.2001.1609.

[BJF13] Å. Brännström, J. Johansson, and N. von Festenberg. "The hitchhikers guide to adaptive dynamics". In: *Games* 4.3 (2013), pp. 304–328. DOI: 10.3390/g4030304.

[Bro+09] S. P. Brown et al. "Social evolution in micro-organisms and a Trojan horse approach to medical intervention strategies". In: *Philosophical Transactions of the Royal Society B: Biological Sciences* 364.1533 (2009), pp. 3157–3168. ISSN: 0962-8436. DOI: 10.1098/rstb.2009.0055.

[Bro07] M. A. Brockhurst. "Population bottlenecks promote cooperation in bacterial biofilms". In: *PLoS One* 2.7 (2007), e634. DOI: 10.1371/journal.pone.0000634.

[Bul+80] M. G. Bulmer et al. *The mathematical theory of quantitative genetics.* Oxford: Clarendon Press., 1980. ISBN: 0198575300.

[CG13] Y. Cohen and G. Galiano. "Evolutionary distributions and competition by way of reaction-diffusion and by way of convolution". In: *Bulletin of Mathematical Biology* 75.12 (2013), pp. 2305–2323. DOI: 10.1007/s11538-013-9890-x.

[Cho+02] D. L. Chopp et al. "A mathematical model of quorum sensing in a growing bacterial biofilm". In: *Journal of Industrial Microbiology and Biotechnology* 29.6 (2002), pp. 339–346. DOI: 10.1038/sj.jim.7000316.

[CMF12] J. Cremer, A. Melbinger, and E. Frey. "Growth dynamics and the evolution of cooperation in microbial populations". In: *Scientific Reports* 281.2 (2012). DOI: 10.1038/srep00281.

[CPV00] Y. Cohen, J. Pastor, and T. L. Vincent. "Evolutionary strategies and nutrient cycling in ecosystems". In: *Evolutionary Ecology Research* 2 (2000), pp. 719–743.

[CRL09] J. S. Chuang, O. Rivoire, and S. Leibler. "Simpson's paradox in a synthetic microbial system". In: *Science* 323.5911 (2009), pp. 272–275. DOI: 10.1126/science.1166739.

[CVB99] Y. Cohen, T. Vincent, and J. Brown. "A G-function approach to fitness minima, fitness maxima, evolutionary stable strategies and adaptive landscapes". In: *Evolutionary Ecology Research* 1 (1999), pp. 923–942.

[Dav+98] D. G. Davies et al. "The involvement of cell-to-cell signals in the development of a bacterial biofilm". In: *Science* 280.5361 (1998), pp. 295–298. DOI: 10.1126/science.280.5361.295.

[DCG12] A. A. Dandekar, S. Chugani, and E. P. Greenberg. "Bacterial quorum sensing and metabolic incentives to cooperate". In: *Science* 338.6104 (2012), pp. 264–266. ISSN: 0036-8075. DOI: 10.1126/science.1227289.

[Dig+07] S. P. Diggle et al. "Cooperation and conflict in quorum-sensing bacterial populations". In: *Nature* 450 (2007), pp. 411–414. DOI: 10.1038/nature06279.

[DK01] J. D. Dockery and J. P. Keener. "A mathematical model for quorum sensing in *Pseudomonas aeruginosa*". In: *Bulletin of Mathematical Biology* 63.1 (2001), pp. 95–116. DOI: 10.1006/bulm.2000.0205.

[DS07] K. Duan and M. G. Surette. "Environmental regulation of *Pseudomonas aeruginosa* PAO1 las and rhl quorum-sensing systems". In: *Journal of Bacteriology* 189.13 (2007), pp. 4827–4836. DOI: 10.1128/JB.00043-07.

[Efe13] M. Efendiev. *Attractors for degenerate parabolic type equations*. Vol. 192. American Mathematical Society, 2013. ISBN: 978-1-4704-0985-2.

[Eis13] S. Eisenhofer. "A coupled system of ordinary and partial differential equations modeling the swelling of mitochondria". PhD thesis. Technische Universität München, 2013.

[EK04] L. Edelstein-Keshet. *Mathematical Models in Biology*. Vol. 46. Classics in Applied Mathematics. Siam, 2004. ISBN: 978-0-89871-554-5.

[Eng+07] M. Englmann et al. "The hydrolysis of unsubstituted N-acylhomoserine lactones to their homoserine metabolites: analytical approaches using ultra performance liquid chromatography". In: *Journal of Chromatography A* 1160.1 (2007), pp. 184–193. DOI: 10.1016/j.chroma.2007.05.059.

[Eva10] L. C. Evans. *Partial Differential Equations: Second Edition*. Graduate Series in Mathematics. American Mathematical Society (AMS), 2010. ISBN: 978-0-8218-4974-3.

[Fek+10] A. Fekete et al. "Dynamic regulation of N-acyl-homoserine lactone production and degradation in *Pseudomonas putida* IsoF". In: *FEMS Microbiology Ecology* 72.1 (2010), pp. 22–34. DOI: 10.1111/j.1574-6941.2009.00828.x.

[FR11] E. Frey and T. Reichenbach. "Bacterial games". In: *Principles of Evolution: From the Planck Epoch to Complex Multicellular Life*. Ed. by H. Meyer-Ortmanns and S. Thurner. Berlin, Heidelberg: Springer Berlin Heidelberg, 2011, pp. 297–329. ISBN: 978-3-642-18137-5.

[Fra10] S. A. Frank. "Microbial secretor–cheater dynamics". In: *Philosophical Transactions of the Royal Society of London B: Biological Sciences* 365.1552 (2010), pp. 2515–2522. DOI: 10.1098/rstb.2010.0003.

[Fri64] A. Friedmann. *Partial Differential Equations of Parabolic Type*. Prentice Hall, 1964.

[FS13] K. Fujimoto and S. Sawai. "A design principle of group-level decision making in cell populations". In: *PLoS Computational Biology* 9.6 (2013), pp. 1–13. DOI: 10.1371/journal.pcbi.1003110.

[FWG94] W. C. Fuqua, S. C. Winans, and E. P. Greenberg. "Quorum sensing in bacteria: the LuxR-LuxI family of cell density-responsive transcriptional regulators." In: *Journal of bacteriology* 176.2 (1994), p. 269. DOI: 10.1146/annurev.micro.50.1.727.

[FWG96] W. C. Fuqua, S. C. Winans, and E. P. Greenberg. "Census and consensus in bacterial ecosystems: the LuxR-LuxI family of quorum-sensing transcriptional regulators". In: *Annual Review of Microbiology* 50.1 (1996), pp. 727–751. DOI: 10.1146/annurev.micro.50.1.727.

[GBDM14] T. Garcia, L. G. Brunnet, and S. De Monte. "Differential adhesion between moving particles as a mechanism for the evolution of social groups". In: *PLoS Computational Biology* 10.2 (2014), e1003482. DOI: 10.1371/journal.pcbi.1003482.

[Ger+97] S. A. Geritz et al. "Dynamics of adaptation and evolutionary branching". In: *Physical Review Letters* 78.10 (1997), p. 2024. DOI: 10.1103/PhysRevLett.78.2024.

[GT01] D. Gilbarg and N. S. Trudinger. *Elliptic partial differential equations of second order*. Vol. 224. Classics in Mathematics. Springer Verlag, 2001. ISBN: 978-3-540-41160-4.

[HCB10] N. Høiby, O. Ciofu, and T. Bjarnsholt. "*Pseudomonas aeruginosa* biofilms in cystic fibrosis". In: *Future Microbiology* 5.11 (2010), pp. 1663–1674. DOI: 10.2217/fmb.10.125.

[HDH06] K. Heurlier, V. Dénervaud, and D. Haas. "Impact of quorum sensing on fitness of *Pseudomonas aeruginosa*". In: *International Journal of Medical Microbiology* 296.2 (2006), pp. 93–102. DOI: 10.1016/j.ijmm.2006.01.043.

[Hen+07] B. A. Hense et al. "Does efficiency sensing unify diffusion and quorum sensing?" In: *Nature Reviews Microbiology* 5.3 (2007), pp. 230–239.

[HN77] J. Hastings and K. Nealson. "Bacterial bioluminescence". In: *Annual Reviews in Microbiology* 31.1 (1977), pp. 549–595. DOI: 10.1146/annurev.mi.31.100177.003001.

[Hor+12] T. Horino et al. "Clinical characteristics and risk factors for mortality in patients with bacteremia caused by *Pseudomonas aeruginosa*". In: *Internal Medicine* 51.1 (2012), pp. 59–64. DOI: 10.2169/internalmedicine.51.5698.

[HS15] B. A. Hense and M. Schuster. "Core principles of bacterial autoinducer systems". In: *Microbiology and Molecular Biology Reviews* 79.1 (2015), pp. 153–169. DOI: 10.1128/MMBR.00024-14.

[JKW12] S. Jabbari, J. R. King, and P. Williams. "Cross-strain quorum sensing inhibition by *Staphylococcus Aureus*. Part 2: a spatially inhomogeneous model". In: *Bulletin of Mathematical Biology* 74.6 (2012), pp. 1326–1353. ISSN: 1522-9602. DOI: 10.1007/s11538-011-9702-0.

[KC09] N Kronik and Y Cohen. "Evolutionary games in space". In: *Mathematical Modelling of Natural Phenomena* 4.6 (2009), pp. 54–90. DOI: 10.1051/mmnp/20094602.

[Koe+02] A. J. Koerber et al. "A mathematical model of partial-thickness burn-wound infection by *Pseudomonas aeruginosa*: quorum sensing and the build-up to invasion". In: *Bulletin of Mathematical Biology* 64.2 (2002), pp. 239–259. ISSN: 1522-9602. DOI: 10.1006/bulm.2001.0272.

[KRG14] R. Kümmerli and A. Ross-Gillespie. "Explaining the sociobiology of pyoverdin producing *Pseudomonas*: a comment on Zhang and Rainey (2013)". In: *Evolution* 68.11 (2014), pp. 3337–3343. DOI: 10.1111/evo.12311.

[KS06] L. Keller and M. G. Surette. "Communication in bacteria: an ecological and evolutionary perspective". In: *Nature Reviews Microbiology* 4.4 (2006), pp. 249–258. DOI: 10.1038/nrmicro1383.

[Kön92] K. Königsberger. *Analysis 1*. Springer-Lehrbuch. Springer Berlin Heidelberg, 1992. ISBN: 978-3-540-55116-4.

[Küm+14] R. Kümmerli et al. "Habitat structure and the evolution of diffusible siderophores in bacteria". In: *Ecology letters* 17.12 (2014), pp. 1536–1544. DOI: 10.1111/ele.12371.

[LAA08] L. Li, M. Abudiab, and I. Ahn. "A theorem on upper–lower solutions for nonlinear elliptic systems and its applications". In: *Journal of Mathematical Analysis and Applications* 340.1 (2008), pp. 175–182. DOI: 10.1016/j.jmaa.2011.01.003.

[Lee+13] J. Lee et al. "A cell-cell communication signal integrates quorum sensing and stress response". In: *Nature Chemical Biology* 9.5 (2013), pp. 339–343. DOI: 10.1038/nchembio.1225.

[Lie86] G. M. Lieberman. "Mixed boundary value problems for elliptic and parabolic differential equations of second order". In: *Journal of Mathematical Analysis and Applications* 113.2 (1986), pp. 422–440. DOI: 10.1016/0022-247X(86)90314-8.

[Lih+13] L. Lihua et al. "Effects of allicin on the formation of *Pseudomonas aeruginosa* biofilm and the production of quorum-sensing controlled virulence factors". In: *Polish Journal of Microbiology* 62.3 (2013), pp. 243–251.

[LL93] L. Li and Y. Liu. "Spectral and nonlinear effects in certain elliptic systems of three variables". In: *SIAM Journal on Mathematical Analysis* 24.2 (1993), pp. 480–498. DOI: 10.1137/0524030.

[LSU67] O. Ladyzenskaja, V. Solonnikov, and N. Uralceva. "Linear and quasilinear equations of parabolic type (Russian). Translated from the Russian by S. Smith. Translations of mathematical monographs 23". In: *American Mathematical Society, Providence RI* (1967).

[LWH09] P. D. Lister, D. J. Wolter, and N. D. Hanson. "Antibacterial-resistant *Pseudomonas aeruginosa*: clinical impact and complex regulation of chromosomally encoded resistance mechanisms". In: *Clinical Microbiology Reviews* 22.4 (2009), pp. 582–610. DOI: 10.1128/CMR.00040-09.

[Mar87] M. Marion. "Attractors for reaction-diffusion equations: existence and estimate of their dimension". In: *Applicable Analysis* 25.1-2 (1987), pp. 101–147. DOI: 10.1080/00036818708839678.

[MDH17] A. Mund, S. P. Diggle, and F. Harrison. "The fitness of *Pseudomonas aeruginosa* quorum sensing signal cheats is influenced by the diffusivity of the environment". In: *mBio* 8.3 (2017). DOI: 10.1128/mBio.00353-17.

[Mel+10] P. Melke et al. "A cell-based model for quorum sensing in heterogeneous bacterial colonies". In: *PLoS Computational Biology* 6.6 (2010), e1000819. DOI: 10.1371/journal.pcbi.1000819.

[Met+95] J. A. Metz et al. "Adaptive dynamics: a geometrical study of the consequences of nearly faithful reproduction". In: (1995).

[MP12] A. McKendrick and M. K. Pai. "XLV.–The rate of multiplication of micro-organisms: a mathematical study." In: *Proceedings of the Royal Society of Edinburgh* 31 (1912), pp. 649–653. DOI: 10.1017/S0370164600025426.

[Mun+16] A. Mund et al. "An age-dependent model to analyse the evolutionary stability of bacterial quorum sensing". In: *Journal of Theoretical Biology* (2016). DOI: 10.1016/j.jtbi.2015.12.021.

[MY15] T. Maire and H. Youk. "Molecular-level tuning of cellular autonomy controls the collective behaviors of cell populations". In: *Cell systems* 1.5 (2015), pp. 349–360. DOI: 10.1016/j.cels.2015.10.012.

[NFX10] C. D. Nadell, K. R. Foster, and J. B. Xavier. "Emergence of spatial structure in cell groups and the evolution of cooperation". In: *PLoS Computational Biology* 6.3 (2010), e1000716. DOI: 10.1371/journal.pcbi.1000716.

[NPH70] K. H. Nealson, T. Platt, and J. W. Hastings. "Cellular control of the synthesis and activity of the bacterial luminescent system". In: *Journal of bacteriology* 104.1 (1970), pp. 313–322.

[Pao92] C. V. Pao. *Nonlinear parabolic and elliptic equations*. New York: Plenum Press, 1992. ISBN: 0-306-44343-0.

[Pet38] I. G. Petrovskii. "On the cauchy problem for systems of linear partial differential equations in the domain of non-analytic functions". In: *Bull. MGU, Sect. A* 1 (1938).

[PK15] A. I. Psarras and I. G. Karafyllidis. "Simulation of the dynamics of bacterial quorum sensing". In: *IEEE Transactions on Nanobioscience* 14.4 (2015), pp. 440–446. DOI: 10.1109/TNB.2014.2385109.

[Pol+14] E. J. Pollitt et al. "Cooperation, quorum sensing, and evolution of virulence in *Staphylococcus aureus*". In: *Infection and Immunity* 82.3 (2014), pp. 1045–1051. DOI: 10.1128/IAI.01216-13.

[Poo04] K Poole. "Efflux-mediated multiresistance in Gram-negative bacteria". In: *Clinical Microbiology and Infection* 10.1 (2004), pp. 12–26. DOI: 10.1111/j.1469-0691.2004.00763.x.

[Pop+12] R. Popat et al. "Quorum-sensing and cheating in bacterial biofilms". In: *Proceedings of the Royal Society of London B: Biological Sciences* (2012). DOI: 10.1098/rspb.2012.1976.

[PPI97] J. P. Pearson, E. C. Pesci, and B. H. Iglewski. "Roles of *Pseudomonas aeruginosa* las and rhl quorum-sensing systems in control of elastase and rhamnolipid biosynthesis genes." In: *Journal of Bacteriology* 179.18 (1997), pp. 5756–5767. DOI: 10.1128/jb.179.18.5756-5767.1997.

[PVGGC16] J. Pérez-Velázquez, M. Gölgeli, and R. García-Contreras. "Mathematical modelling of bacterial quorum sensing: a review". In: *Bulletin of Mathematical Biology* 78.8 (2016), pp. 1585–1639. DOI: 10.1007/s11538-016-0160-6.

[RB12] S. T. Rutherford and B. L. Bassler. "Bacterial quorum sensing: its role in virulence and possibilities for its control". In: *Cold Spring Harbor Perspectives in Medicine* 2.11 (2012), a012427. DOI: 10.1128/jb.179.18.5756-5767.1997.

[Red] "*Pseudomonas aeruginosa*". In: *Encyclopedia of Genetics, Genomics, Proteomics and Informatics*. Springer Netherlands, 2008, pp. 1594–1594. ISBN: 978-1-4020-6754-9. DOI: 10.1007/978-1-4020-6754-9_13745.

[Red02] R. J. Redfield. "Is quorum sensing a side effect of diffusion sensing?" In: *Trends in microbiology* 10.8 (2002), pp. 365–370. DOI: 10.1016/S0966-842X(02)02400-9.

[REJ16] T. Rasamiravaka and M. El Jaziri. "Quorum-sensing mechanisms and bacterial response to antibiotics in *P. aeruginosa*". In: *Current Microbiology* 73.5 (2016), pp. 747–753. ISSN: 1432-0991. DOI: 10.1007/s00284-016-1101-1.

[RGK14] A. Ross-Gillespie and R. Kümmerli. "Collective decision-making in microbes". In: *Frontiers in microbiology* 5 (2014), p. 54. DOI: 10.3389/fmicb.2014.00054.

[Rum+09] K. P. Rumbaugh et al. "Quorum sensing and the social evolution of bacterial virulence". In: *Current Biology* 19 (2009), pp. 341–345. DOI: 10.1016/j.cub.2009.01.050.

[Rum+12] K. P. Rumbaugh et al. "Kin selection, quorum sensing and virulence in pathogenic bacteria". In: *Proceedings of the Royal Society of London B: Biological Sciences* 279.1742 (2012), pp. 3584–3588. DOI: 10.1098/rspb.2012.0843.

[Rup+16] A. Ruparell et al. "The fitness burden imposed by synthesizing quorum sensing signals". In: *bioRxiv* (2016), p. 050229. DOI: 10.1038/srep33101.

[Sch+13] M. Schuster et al. "Acyl-homoserine lactone quorum sensing: from evolution to application". In: *Annual Review of Microbiology* 67 (2013), pp. 43–63. DOI: 10.1146/annurev-micro-092412-155635.

[Sch30] J Schauder. "Der Fixpunktsatz in Funktionalräumen". In: *Studia Mathematica* 2 (1930), pp. 171–180.

[Sch91] W. Schiesser. *The Numerical Method of Lines: Integration of Partial Differential Equations*. Academic Press, 1991. ISBN: 9780126241303.

[Sim85] M. Simon. "Specific uptake rates of amino acids by attached and free-living bacteria in a mesotrophic lake". In: *Applied and Environmental Microbiology* 49.5 (1985), pp. 1254–1259.

[Sio+06] C. F. Sio et al. "Quorum quenching by an N-acyl-homoserine lactone acylase from *Pseudomonas aeruginosa* PAO1". In: *Infection and immunity* 74.3 (2006), pp. 1673–1682. DOI: 10.1128/IAI.74.3.1673-1682.2006.

[Smi82] J. M. Smith. *Evolution and the Theory of Games*. Cambridge University Press, 1982. ISBN: 9780521288842.

[Smo83] J. Smoller. *Shock waves and reaction-diffusion equations*. Vol. 258. Comprehensive Studies in Mathematics. Springer Verlag, 1983. ISBN: 978-1-4612-6929-8.

[SMS07] K. M. Sandoz, S. M. Mitzimberg, and M. Schuster. "Social cheating in *Pseudomonas aeruginosa* quorum sensing". In: *Proceedings of the National Academy of Sciences* 104.40 (2007), pp. 15876–15881. DOI: 10.1073/pnas.0705653104.

[SPI95] P. C. Seed, L. Passador, and B. H. Iglewski. "Activation of the *Pseudomonas aeruginosa* lasI gene by LasR and the *Pseudomonas* autoinducer PAI: an autoinduction regulatory hierarchy." In: *Journal of Bacteriology* 177.3 (1995), pp. 654–659. DOI: 10.1128/jb.177.3.654-659.1995.

[Tem97] R. Temam. *Infinite-Dimensional Dynamical Systems in Mechanics and Physics*. Vol. 68. Applied Mathematical Sciences. Springer New York, 1997. ISBN: 978-1-4612-0645-3.

[VCB93] T. L. Vincent, Y. Cohen, and J. S. Brown. "Evolution via strategy dynamics". In: *Theoretical Population Biology* 44.2 (1993), pp. 149–176. DOI: 10.1006/tpbi.1993.1023.

[Vet+98] Y. Vetter et al. "A predictive model of bacterial foraging by means of freely released extracellular enzymes". In: *Microbial Ecology* 36 (1998), pp. 75–92. DOI: 10.1007/s002489900095.

[VVG96] T. L. Vincent, M. Van, and B. Goh. "Ecological stability, evolutionary stability and the ESS maximum principle". In: *Evolutionary Ecology* 10 (1996), pp. 567–591.

[Wan+15] M. Wang et al. "Quorum sensing and policing of *Pseudomonas aeruginosa* social cheaters". In: *Proceedings of the National Academy of Sciences* 112.7 (2015), pp. 2187–2191. DOI: 10.1073/pnas.1500704112.

[WB03] S. A. West and A. Buckling. "Cooperation, virulence and siderophore production in bacterial parasites". In: *Proceedings of the Royal Society of London B: Biological Sciences* 270.1510 (2003), pp. 37–44. DOI: 10.1098/rspb.2002.2209.

[WDS11] C. N. Wilder, S. P. Diggle, and M. Schuster. "Cooperation and cheating in *Pseudomonas aeruginosa*: the roles of the las, rhl and pqs quorum-sensing systems". In: *The ISME Journal* 5.8 (2011), pp. 1332–1343. DOI: 10.1038/ismej.2011.13.

[Wer07] D. Werner. *Funktionalanalysis*. Springer Verlag, 2007. ISBN: 978-3-642-21017-4.

[YL14] H. Youk and W. A. Lim. "Secreting and sensing the same molecule allows cells to achieve versatile social behaviors". In: *Science* 343.6171 (2014), p. 1242782. DOI: 10.1126/science.1242782.

[R C15] R Core Team. *R: A Language and Environment for Statistical Computing*. R Foundation for Statistical Computing. Vienna, Austria, 2015.

Appendix A

Theorems

A.1 Norms, spaces and properties

Definition A.1 (Sum of derivatives)**.** *The symbol $D_x^j u$ denotes any derivative of a function $u(x)$ with respect to x of order j, and we denote the summation over all possible such derivatives of order j by*

$$\sum_{(j)} D_x^j u.$$

Definition A.2 (Norms for $\boldsymbol{C^{l,l/2}}$)**.** *Let l be a positive, non-integral number. For the Banach space $C^{l,l/2}$ of functions $u(x,t)$ that are continuous in $Q_T = \Omega \times [0,T]$, together with all derivatives of the form $D_t^r D_x^s$, for $2r+s<l$ and have finite norm $\|u\|_{l,Q_T}$, we define the following norms in the style of Ladyzenskaja, Solonnikov, and Uralceva [LSU67]:*

(i) $\|u\|_{l,Q_T} = \langle u \rangle_{Q_T}^{(l)} + \sum_{j=0}^{\lfloor l \rfloor} \langle u \rangle_{Q_T}^{(j)},$

(ii) $\langle u \rangle_{Q_T}^{(0)} = |u|_{Q_T}^{(0)} = \max_{Q_T} |u|,$

(iii) $\langle u \rangle_{Q_T}^{(j)} = \sum_{(2r+s=j)} |D_t^r D_x^s u|_{Q_T}^{(0)},$

(iv) $\langle u \rangle_{Q_T}^{(l)} = \langle u \rangle_{x,Q_T}^{(l)} + \langle u \rangle_{t,Q_T}^{(l/2)},$

(v) $\langle u \rangle_{x,Q_T}^{(l)} = \sum_{(2r+s=\lfloor l \rfloor)} \langle D_t^r D_x^s u \rangle_{x,Q_T}^{(l-\lfloor l \rfloor)},$

(vi) $\langle u \rangle_{t,Q_T}^{(l/2)} = \sum_{0<l-2r-s<2} \langle D_t^r D_x^s u \rangle_{t,Q_T}^{(\frac{l-2r-s}{2})},$

(vii) $\langle u \rangle^{(\alpha)}_{x,Q_T} = \sup_{\substack{(x,t),(x',t)\in Q_T \\ |x-x'|\le\rho_0}} \dfrac{|u(x,t)-u(x',t)|}{|x-x'|^\alpha},\ 0<\alpha<1,$

(viii) $\langle u \rangle^{(\alpha)}_{t,Q_T} = \sup_{\substack{(x,t),(x,t')\in Q_T \\ |t-t'|\le\rho_0}} \dfrac{|u(x,t)-u(x,t')|}{|t-t'|^\alpha},\ 0<\alpha<1.$

Definition A.3 (Norms for $\boldsymbol{C^l}$)**.** *Let l be a positive, non-integral number. For the Banach space C^l of continuous functions $u(x)$ that have continuous derivatives up to order $\lfloor l \rfloor$ in $\overline{\Omega}$ and finite norm $\|u\|_{l,\Omega}$, we define the following norms in the style of Ladyzenskaja, Solonnikov, and Uralceva [LSU67]:*

(i) $\|u\|_{l,\Omega} = \langle u \rangle^{(l)}_\Omega + \sum_{j=0}^{\lfloor l \rfloor} \langle u \rangle^{(j)}_\Omega,$

(ii) $\langle u \rangle^{(0)}_\Omega = |u|^{(0)}_\Omega = \max_\Omega |u|,$

(iii) $\langle u \rangle^{(j)}_\Omega = \sum_{(j)} \left| D^j_x u \right|^{(0)}_\Omega,$

(iv) $\langle u \rangle^{(l)}_\Omega = \sum_{(\lfloor l \rfloor)} \langle D^{(\lfloor l \rfloor)}_x u \rangle^{(l-\lfloor l \rfloor)}_\Omega,$

(v) $\langle u \rangle^{(\alpha)}_\Omega = \sup_{\substack{x,x'\in\Omega \\ |x-x'|\le\rho_0}} \dfrac{|u(x)-u(x')|}{|x-x'|^\alpha},\ 0<\alpha<1.$

Definition A.4 (Norms for $\boldsymbol{L^p}$)**.** *Let $1 \le p < \infty$. We define the Banach space L^p of integrable functions $u(x)$ that have finite norm $\|u\|_{L^p}$, with the norm defined in the usual way:*

$$\|u\|_{L^p} = \left(\int_\Omega u(x)^p \, \mathrm{d}x \right)^{1/p}.$$

Definition A.5 (analytic)**.** *A map $f : U \subset X \to Y$, with U open, is* ***analytic*** *in U if f is infinitely often differentiable at each point of U and if, for each $x \in U$, there exists $\delta = \delta(x) > 0$ so that whenever $\|h\|_X \le \delta$,*

$$f(x+h) = \sum_{k=0}^{\infty} \frac{1}{k!} f^{(k)}(x)(h^k),$$

the series converging in Y-norm uniformly in $\|h\|_X \le \delta$.

An equivalent condition is that, for some $\delta > 0$, there exists a constant $M = M(x,\delta)$ so that

$$\frac{1}{k!} \left\| f^{(k)}(x) \right\| \delta^k \le M < \infty, \quad \forall k \ge 0.$$

A.2 Inequalities

Theorem A.1 (Grönwall's inequality)**.** *Let I denote an interval of the real line of the form $[a, \infty)$ or $[a, b]$ or $[a, b)$ with $a < b$. Let α, β and u be real-valued functions defined on I. Assume that β and u are continuous and that the negative part of α is integrable on every closed and bounded subinterval of I.*

(a) If β is non-negative and if u satisfies the integral inequality

$$u(t) \leq \alpha(t) + \int_a^t \beta(s)u(s)\,\mathrm{d}s, \qquad \forall t \in I,$$

then

$$u(t) \leq \alpha(t) + \int_a^t \alpha(s)\beta(s)\exp\left(\int_s^t \beta(r)\,\mathrm{d}r\right)\mathrm{d}s, \qquad t \in I.$$

(b) If, in addition, the function α is non-decreasing, then

$$u(t) \leq \alpha(t)\exp\left(\int_a^t \beta(s)\,\mathrm{d}s\right), \qquad t \in I.$$

[see Bel43]

Theorem A.2 (Generalised Poincaré inequality)**.** *Let Q be a bounded and Lipschitz set in $\mathbb{R}^n$, and let p be a continuous seminorm on $H^1(Q)$ which is a norm on the constants ($p(a) = 0, a \in \mathbb{R} \Rightarrow a = 0$). Then there exists a constant c depending only on Q such that*

$$\|u\|_{L^2} \leq c(\Omega)\left(\|\nabla u\|_{L^2} + p(u)\right), \quad \forall u \in H^1(\Omega).$$

[see Tem97, p.51f]
Examples for p are

$$p(u) = \left|\int_\Omega u(x)\,\mathrm{d}x\right|,$$
$$p(u) = \|u\|_{L^2(\omega)}, \quad \omega \subset \Omega, \operatorname{meas}\omega > 0$$
$$p(u) = \left(\int_\Gamma |\gamma_0 u|^2\,\mathrm{d}t\right)^{1/2}.$$

Theorem A.3 (Poincaré inequality)**.** *Let p, so that $1 \leq p \leq \infty$ and Ω a subset with at least one bound. There then exists a constant C, depending only on Ω and p , so that, for every function u of the $W_0^{1,p}(\Omega)$ Sobolev space,*

$$\|u\|_{L^p(\Omega)} \leq C\|\nabla u\|_{L^p(\Omega)}.$$

[see Eva10, Theorem 3, p.279f]

Theorem A.4 (Comparison theorem)**.** *Let $v(x,t)$ and $w(x,t)$ be continuous functions in $\bar{Q}_T$, and let the first two x-derivatives and the first t-derivative be continuous in $\bar{Q}_T$. Let $F(x,t,p,p_i,p_{ij})$ be a continuous function together with its first derivative with respect to the p_{hk} in a domain E containing the closure of the set of points (x,t,p,p_i,p_{ij}) where*

$$(x,t) \in Q_T, \quad p \in (v(x,t), w(x,t)),$$
$$p_i \in \left(\frac{\partial v(x,t)}{\partial x_i}, \frac{\partial v(x,t)}{\partial x_i}\right), \quad p_{ij} \in \left(\frac{\partial^2 v(x,t)}{\partial x_i \partial x_j}, \frac{\partial^2 v(x,t)}{\partial x_i \partial x_j}\right)$$

here (a,b) denotes the interval connecting a to b. Assume also that $\frac{\partial F}{\partial p_{hk}}$ is a positive semi-definite matrix. If

$$\frac{\partial v}{\partial t} > F\left(x,t,v,\frac{\partial v}{\partial x_i},\frac{\partial^2 v}{\partial x_i \partial x_j}\right) \qquad \text{in } Q_T, \tag{A.2.1}$$
$$\frac{\partial w}{\partial t} \leq F\left(x,t,w,\frac{\partial w}{\partial x_i},\frac{\partial^2 w}{\partial x_i \partial x_j}\right) \qquad \text{in } Q_T, \tag{A.2.2}$$

and if either

$$v > w \qquad \text{on } B + S_T, \tag{A.2.3}$$

or

$$v > w \qquad \text{on } B, \tag{A.2.4}$$
$$\frac{\partial v}{\partial n} + \beta(x,t,v) < \frac{\partial w}{\partial n} + \beta(x,t,w) \qquad \text{on } S_T. \tag{A.2.5}$$

then also $v > w$ in Q_T.

[see Fri64, Theorem 16, p.52f]

A.3 Fixed point theorems

Theorem A.5 (Banach fixed-point theorem)**.** *Let (X, d) be a non-empty complete metric space with a contraction mapping $T : X \to X$. Then T admits a unique fixed point x^* in X.*

[see Ban22, p. 160]

Theorem A.6 (Schauder fixed-point theorem)**.** *Let X be a non-empty closed convex subset of a Banach Space V. If $T : X \to X$ is continuous with a compact image, then T has a fixed point.*

[see Sch30]

Theorem A.7 (Arzelà-Ascoli)**.** *Let (X, d) be a compact metric space, and let $M \subset C(X)$, where C denotes as usual the space of continuous functions equipped with the supremum. If M fulfils*

(i) M is bounded,

(ii) M is closed,

(iii) M is equicontinuous, i.e.

$$\forall \varepsilon > 0 \exists \delta > 0 \forall x \in M : \qquad d(s,t) \leq \delta \Rightarrow |x(s) - x(t)| \leq \varepsilon$$

then M is compact.

[see Wer07, theorem II.3.4]

A.4 Uniqueness, Existence

Theorem A.8 (Rolle's theorem)**.** *Let $f \in C([a,b])$ be a real-valued function, that is differentiable on the open interval (a,b).If $f(a) = f(b)$, then there exists at least one $c \in (a,b)$ such that*

$$f'(c) = 0.$$

Königsberger [see Kön92, p.134]
The following theorems are concerned with norms of the solution u of

$$\mathcal{L}u(x,t) = f(x,t) \qquad \text{in } D, \tag{A.4.1a}$$

$$u(x,0) = u^0(x) \qquad \text{on } \bar{B}, \tag{A.4.1b}$$

$$\frac{\partial u(x,t)}{\partial n(x,t)} + \beta(x,t)u(x,t) = \psi(x,t) \qquad \text{on } S, \tag{A.4.1c}$$

Theorem A.9. *Assume that $u(x,t) \in C^{2,1}(D)$ is a solution of*

$$\begin{aligned} u_t - \sum_{i,j} a_{ij}(x,t,u)\partial_{x_i}\partial_{x_j}u + b(x,t,u,u_x) = 0 \qquad & \text{in } D \\ \frac{\partial u}{\partial_n} + \varphi(x,t,u) = 0 \qquad & \text{in } S \\ u(x,0) = u^0(x) \qquad & \text{in } B \end{aligned}$$

where the functions a_{ij}, b, φ are subject to the following conditions for $|u| \le M$, $(x,t) \in D$

$$\hat{\mu}\xi^2 \le \sum_{i,j} a_{ij}(x,t,u)\xi_i\xi_j \le \mu\xi^2 \quad \forall \xi \in \mathbb{R} \tag{A.4.2a}$$

$$|\partial_u a_{ij}|, |\partial_x a_{ij}|, |\partial_t a_{ij}|, \left|\partial_u^2 a_{ij}\right|, |\partial_u\partial_x a_{ij}|, |\partial_u\partial_t a_{ij}|, |\partial_x\partial_t a_{ij}| \le \mu \tag{A.4.2b}$$

$$|b(x,t,u,p| \le \mu(1+p^2) \tag{A.4.2c}$$

$$|\partial_p b|(1+|p|) + |\partial_u b| + |\partial_t b| \le \mu(1+p^2) \tag{A.4.2d}$$

$$|\varphi|, |\partial_u\varphi|, |\partial_x\varphi|, |\partial_t\varphi|, \left|\partial_u^2\varphi\right|, |\partial_u\partial_x\varphi|, |\partial_u\partial_t\varphi| \le \mu \tag{A.4.2e}$$

and $S \in C^2$. Then, if $\sup_D |u| \le M$ it holds that

$$\sup_D |u_x| \le M_1, \qquad \|u\|_{1+\delta} \le C,$$

where M_1, δ, C depend only on $M, c, \mu, \|u^0(x)\|_2$ and S.

For a proof of this statement, see Ladyzenskaja, Solonnikov, and Uralceva [LSU67, Theorem 7.2].

Theorem A.10 (boundary Schauder estimates)**.** *Let $\mathcal{L}$ be defined as before. If the following conditions hold:*

1. *The coefficients of $\mathcal{L}$ are locally Hölder continuous with coefficient $\alpha \in (0,1)$.*
2. *For any $(x,t) \in D$ and for any real vector ξ:*

$$\sum_{i,j=1}^{n} a_{ij}(x,t)\xi_i\xi_j \ge K|\xi|^2,$$

3. *$\beta(x,t) \in H_{1+\alpha}$,*
4. *$f(x,t) \in H_\alpha, \psi(x,t) \in H_{1+\alpha}, u^0(x) \in H_{2+\alpha}$,*
5. *$S \in H_{2+\alpha}$,*

then there exists a unique solution $u(x,t)$ *of equation* (A.4.1) *and a constant* C *such that*

$$\|u\|_{2+\alpha} \leq C\left(\|f\|_{\alpha} + \|\psi\|_{1+\alpha} + \left\|u^0\right\|_{2+\alpha}\right)$$

[see Lie86, Theorem 5]

Theorem A.11 (Schauder estimates)**.** *Let* $\mathcal{L}$ *be defined as before. If the following conditions hold:*

1. *The coefficients of* $\mathcal{L}$ *are locally Hölder continuous with coefficient* $\alpha \in (0,1)$*,*
2. $\beta(x,t) \in H_{1+\alpha}$*,*
3. $f(x,t) \in H_{\alpha}, \psi(x,t) \in H_{1+\alpha}, \phi(x) \in H_{2+\alpha}$*,*
4. $S \in H_{2+\alpha}$*,*

then there exists a unique solution $u(x,t)$ *of*

$$\begin{aligned} \mathcal{L}u(x,t) &= f(x,t) && \text{in } \Omega \times (0,\tau), \\ \frac{\partial u(x,t)}{\partial n(x,t)} + \beta(x,t)u(x,t) &= \psi(x,t) && \text{on } S, u(x,0) = \phi(x) && \text{in } \Omega, \end{aligned}$$

and a constant C *such that*

$$\|u\|_{2+\alpha,\bar{Q}_T} \leq C\left(\|f\|_{\alpha,\bar{Q}_T} + \|\psi\|_{1+\alpha,S_T} + \|\phi\|_{2+\alpha,\Omega}\right).$$

If $u(x,t)$ *satisfies a Dirichlet condition instead, i.e. solves*

$$\begin{aligned} \mathcal{L}u(x,t) &= f(x,t) && \text{in } \Omega \times (0,\tau), \\ u(x,t) &= \psi(x,t) && \text{on } S, u(x,0) = \phi(x) && \text{in } \Omega, \end{aligned}$$

then it holds that

$$\|u\|_{2+\alpha,\bar{Q}_T} \leq C\left(\|f\|_{\alpha,\bar{Q}_T} + \|\psi\|_{2+\alpha,S} + \|\phi\|_{2+\alpha,\Omega}\right).$$

[see LSU67, Theorem 5.2,5.3, p.322]

A.5 Asymptotic behaviour

Definition A.6 (dissipative)**.**

$$\|S(t)u_0\|_\Phi \leq Q(\|u_0\|_\Phi)\mathrm{e}^{-\alpha t} + C_* \qquad\qquad u_0 \in \Phi$$

Where $\|\cdot\|_\Phi$ is a norm in the function space Φ and the positive constants α and C_* and the monotonic function Q are independent of t and u_0.

Efendiev [see Efe13, p.19]

Definition A.7 (Global attractor)**.** *A set $\mathcal{A} \subset \Phi$ is a global attractor for the semigroup $S(t)$ if*

1. *$\mathcal{A}$ is compact in Φ;*
2. *$\mathcal{A}$ is strictly invariant: $S(t)\mathcal{A} = \mathcal{A} \quad \forall t \geq 0$;*
3. *$\mathcal{A}$ is an attracting set for the semigroup $S(t)$: $\lim\limits_{t\to\infty} \mathrm{dist}_H(S(t)B, \mathcal{A}) = 0$ with $\mathrm{dist}_H(X, Y) := \sup\limits_{x\in X} \inf\limits_{y\in Y} d(x, y)$.*

Definition A.8 (Exponential attractor)**.** *A set $\mathcal{M}$ is an exponential attractor for $S(t)$ in H if*

1. *it is compact in H*
2. *it is positively invariant, i.e. $S(t)\mathcal{M} \subset \mathcal{M}$, $\forall t \geq 0$*
3. *it has finite fractal dimension,*
4. *it attracts exponentially fast the bounded sets of initial data in the following sense: there exists a monotonic function Q and a constant $\alpha > 0$ such that*

$$\forall B \subset H \text{ bounded, } \mathrm{dist}_H(S(t)B, \mathcal{M}) \leq Q(\|B\|_H)\mathrm{e}^{-\alpha t}, t \geq 0$$

If $S(t)$ possesses an exponential attractor $\mathcal{M}$, then it also possesses the global attractor $\mathcal{A} \subset \mathcal{M}$ and $\mathcal{M}$ is a compact attracting set.

Efendiev [see Efe13, p. 27]

Appendix B

Generalised Linear Models

Table B.1: Estimators for lasR$^-$ ∼ Ad + Mix

Relative Fitness ∼ Adenosine + Mix						
			Estimate	Standard Deviation	t Value	p Value
(Intercept)			0.52	0.23	2.24	3.3×10^{-2}
Adenosine			−11.79	3.03	−3.89	5.4×10^{-4}
Mix			−0.84	0.22	−3.77	7.5×10^{-4}
	DoF	Deviance	Res. DoF	Residual Deviance	F value	p Value
NULL			31	23.39		
Ad	1	5.67	30	17.72	14.09	7.8×10^{-4}
Mix	1	5.54	29	12.18	13.76	8.7×10^{-4}
AIC	21.64					

Table B.2: Estimators for lasR$^-$ ∼ Ad + C12

Relative Fitness ∼ Adenosine + C12						
			Estimate	Standard Deviation	t Value	p Value
(Intercept)			−0.03	0.21	−0.12	9.0×10^{-1}
Adenosine			−15.43	2.74	−5.63	4.9×10^{-7}
C12			0.37	0.20	1.81	7.5×10^{-2}
	DoF	Deviance	Res. DoF	Residual Deviance	F value	p Value
NULL			63	70.14		
Ad	1	15.37	62	54.77	23.36	9.4×10^{-6}
C12	1	2.15	61	52.62	3.27	7.6×10^{-2}
AIC	42.197					

Table B.3: Estimators for lasR$^-$ ∼ Ad * C12

Relative Fitness ∼ Adenosine * C12						
			Estimate	Standard Deviation	t Value	p Value
(Intercept)			−0.07	0.26	−0.26	8.0×10^{-1}
Adenosine			−14.71	3.89	−3.78	3.6×10^{-4}
C12			0.45	0.37	1.22	2.3×10^{-1}
Ad:C12			−1.46	5.50	−0.27	7.9×10^{-1}
	DoF	Deviance	Res. DoF	Residual Deviance	F value	p Value
NULL			63	70.14		
Ad	1	15.37	62	54.77	23.24	1.0×10^{-5}
C12	1	2.15	61	52.62	3.25	7.6×10^{-2}
Ad:C12	1	0.03	60	52.59	0.05	8.3×10^{-1}
AIC	44.155					

Table B.4: Estimators for lasI$^-$ ∼ Ad * Mix

Relative Fitness ∼ Adenosine * Mix						
			Estimate	Standard Deviation	t Value	p Value
(Intercept)			0.47	0.21	2.24	2.7×10^{-2}
Adenosine			−20.92	3.12	−6.70	6.9×10^{-10}
Mix			0.20	0.30	0.66	5.1×10^{-1}
Ad:Mix			22.76	4.42	5.15	1×10^{-6}
	DoF	Deviance	Res. DoF	Residual Deviance	F value	p Value
NULL			125	164.95		
Ad	1	1.78	124	163.17	2.09	1.5×10^{-1}
Mix	1	59.44	123	103.73	69.63	1.3×10^{-13}
Ad:Mix	1	14.83	122	88.91	17.37	5.8×10^{-5}
AIC	254.92					

Table B.5: Estimators for lasI$^-$ ∼ Ad * C12

Relative Fitness ∼ Adenosine * C12						
			Estimate	Standard Deviation	t Value	p Value
(Intercept)			0.26	0.36	0.72	4.7×10^{-1}
Adenosine			−16.40	5.31	−3.08	3.1×10^{-3}
C12			−0.04	0.51	−0.07	9.4×10^{-1}
Ad:C12			25.14	7.51	3.35	1.4×10^{-3}
	DoF	Deviance	Res. DoF	Residual Deviance	F value	p Value
NULL			63	92.90		
Ad	1	2.37	62	90.53	1.92	1.7×10^{-1}
C12	1	23.61	61	66.93	19.12	5.0×10^{-5}
Ad:C12	1	11.98	60	54.95	9.70	2.8×10^{-3}
AIC	139.07					

Table B.6: Estimators for pure cultures, lasI$^-$ ∼ Ad + Solid

Relative Fitness ∼ Adenosine + Solid						
			Estimate	Standard Deviation	t Value	p Value
(Intercept)			0.43	0.12	3.64	4.0×10^{-4}
Adenosine			−20.20	1.55	−13.03	$<10^{-16}$
Solid			0.28	0.11	2.49	1.4×10^{-2}
	DoF	Deviance	Res. DoF	Residual Deviance	F value	p Value
NULL			125	125.27		
Ad	1	48.81	124	76.45	118.41	$<10^{-16}$
Solid	1	2.55	123	73.91	6.18	1.4×10^{-2}
AIC	92.89					

Table B.7: Estimators for mixed cultures, lasI$^-$ ~ Ad * Solid

Relative Fitness ~ Adenosine * Solid						
			Estimate	Standard Deviation	t Value	p Value
(Intercept)			0.67	0.23	2.94	3.9×10^{-3}
Adenosine			1.84	3.35	0.55	5.8×10^{-1}
Solid			−0.28	0.32	−0.88	3.8×10^{-1}
Ad:Solid			−5.53	4.74	−1.17	2.5×10^{-1}
	DoF	Deviance	Res. DoF	Residual Deviance	F value	p Value
NULL			125	86.38		
Ad	1	0.02	124	86.36	0.02	8.8×10^{-1}
Solid	1	10.95	123	75.41	11.13	1.1×10^{-3}
Ad:Solid	1	0.96	122	74.45	0.98	3.3×10^{-1}
AIC	357.75					

Appendix C

Numerical code

C.1 Auxiliary code

```
function matrix = patchmatrix(e,pS,N,K,k)

% Start out with one 'unit'
unitsize = (pS+e)*K;
unit = zeros(unitsize);
unitnr = ceil(N/unitsize);

% Fill the one unit appropriately
patch = ones(pS);
for j = 1:K
   lo = (j-1)*(pS+e)+1;
   unit(lo:lo+(pS-1),lo:lo+(pS-1)) = patch;
end

% Repeat units as needed, shifting appropriate for subpop nr
matrix = repmat(unit,unitnr);
matrix = circshift(matrix,(pS+e)*(k-1),2);
matrix = matrix(1:N,1:N);
end
```

```
function z = smoothsquare(X,Y,a,r,scale)

eps = 1e-4;

more = ((X-a).^2+(Y-a).^2 < r^2);
z = more.*(cos(pi/r*sqrt((X-a).^2+(Y-a).^2))+1) + eps;
z = scale*z;
end
```

C.2 Calculations for PDE systems

```
function dt = TwoDApprox_Vectorized(t,in,N,K,h,const,Gfunction,...
    dGfunction,tend)
%% unpacking of v and b
% i are the discretisations in x-direction, j in y-direction; v ...
    and b are
% given as vectors. We define accordingly that i will be unpacked ...
    first,
% before j and k; for N = 3, for example, it would hold that
% v(4): i=1, j=2, k=1, v(10): i=1, j=1, k=2 and so on.
braw = in(1:end/2);
vraw = in(end/2+1:end);

v = reshape(vraw,[N,N,K]);
b = reshape(braw,[N,N,K]);

dvdt = zeros(N,N,K);
dbdt = zeros(N,N,K);

%% Calculation of dt
% In order to calculate the diffusion, calculate shifted matrices;
% Neumann boundary = mirrored borders
bl = circshift(b,1,2);
bl(:,1,:) = bl(:,3,:);

br = circshift(b,-1,2);
br(:,end,:) = br(:,end-2,:);

bu = circshift(b,-1,1);
bu(end,:) = bu(end-2,:);

bo = circshift(b,1,1);
bo(1,:) = bo(3,:);

vl = circshift(v,1,2);
vl(:,1,:) = vl(:,3,:);

vr = circshift(v,-1,2);
vr(:,end,:) = vr(:,end-2,:);

vu = circshift(v,-1,1);
vu(end,:) = vu(end-2,:);

vo = circshift(v,1,1);
vo(1,:) = vo(3,:);
```

```
%Calculate the diffusion
diffb = const.D/h^2 * (bl+br+bu+bo-4*b);
diffv = const.D/h^2 * (vl+vr+vu+vo-4*v);

%Calculate the gradient term
gradv = const.D/h^2 * ((bu-bo).*(vu-vo)+(bl-br).*(vl-vr))./(2*b);
%NaN values are artifacts of starting conditions; igore them
gradv(isnan(gradv)) = 0;

% Calculate the reaction term
for k = 1:K
     dbdt(:,:,k) = Gfunction(v(:,:,k),v,b).*b(:,:,k);
     dvdt(:,:,k) = const.eps * dGfunction(v(:,:,k),v,b);
end

dbdt = dbdt + diffb;
dvdt = dvdt + diffv +gradv;

%% Reshape the matrices back into vectors
dvdtend = reshape(dvdt,[N^2*K,1]);
dbdtend = reshape(dbdt,[N^2*K,1]);
dt = [dbdtend;dvdtend];

%% Progress bar
persistent wait;

if (isempty(wait))
   wait=waitbar(0,'processing...');
else
   waitbar(t/tend,wait);
end

if (t>=tend && ~isempty(wait))
   close(wait);
   wait=[];
end

end
```